DEPARTMENT OF CIVIL ENGINEERING
UNIVERSITY OF CAPE TOWN

THE EFFECT OF AGGREGATE ON THE AGE AT CRACKING OF BONDED CONCRETE OVERLAYS SUBJECTED TO RESTRAINED DEFORMATION

Submitted in partial fulfilment of the requirements for the degree of

MASTER OF SCIENCE IN CIVIL ENGINEERING

November 2013

Prepared by:

Thomas James Dittmer

Supervisor:

A/Prof. Hans Beushausen

Co-supervisor:

Prof. Pilate Moyo

Plagiarism declaration

I know the meaning of plagiarism and I declare that all of the work in this document, save for that which is properly acknowledged, is my own. I also affirm that this work has not been submitted in this, or any other university for examination, or for any other purposes.

Signature…Signed by candidate….. Date: **19/11/2013**

Acknowledgements

The author would like to acknowledge the following people:

A/Prof. Hans Beushausen, for his help and guidance throughout the duration of this project, and for always providing me with the inspiration and motivation to produce work that meets his high expectations and standards.

Prof. Pilate Moyo and Prof. Mark Alexander for their invaluable input, expertise and advice.

The UCT Civil Engineering Laboratory staff for their long hours of physical work and assistance. A special mention must also be noted for Nooredien Hassen, for his continued assistance and excellent management of the Civil Engineering Laboratory.

Elly Yelverton for her tireless work and committed help.

The Department of Civil Engineering, CoMSIRU and the National Research Foundation (NRF) for providing the platform, opportunity and financial assistance for this work.

Finally, my family and friends for their unwavering support and encouragement through the highs and lows of this project.

Abstract

The need for effective and comprehensive repair techniques is increasing throughout the world as existing concrete structures continue to age. The bonded concrete overlay method, where a new repair material layer is cast over an existing damaged substrate, is the most commonly utilized method of repair. However, this repair technique is prone to failure due to differential volume changes between the newly cast repair material and the existing substrate. These volume changes can be attributed to thermal and shrinkage differences, with drying shrinkage being identified as they key source of the volume change.

When the resulting induced stress form the differential volume changes exceeds the intrinsic tensile strength of the repair material, cracking failure occurs. This can be detrimental to the effectiveness of the repair and its durability. Overlay crack resistance has been found to be dependent on specific material properties, namely: tensile strength, elastic modulus and shrinkage. The effect of tensile relaxation on overlay performance is also significant, with the resulting 'stress relief' cause by this relaxation prolonging the time to cracking failure.

In this investigation, the influence of the inclusion of coarse aggregate in the repair material is investigated. The study focuses on the specific impact of coarse aggregate volume content and size on the performance of bonded overlay materials, and the material properties that influence this performance. Two laboratory concrete mixes, with a w:c = 0.45 and 0.6, and a commercial repair product were tested with varying coarse aggregate volume contents. Further testing was conducted with w:c = 0.6 laboratory mixes with different nominal sized coarse aggregates.

The impact of coarse aggregate volume and size on individual material properties, which included tensile strength, tensile relaxation, free drying shrinkage and elastic modulus, were tested separately for the various mixes. In conjunction with this, direct restrained shrinkage tests were conducted using ring tests to measure the influence of coarse aggregate volume and size on the time to cracking failure and crack intensity of the repair materials.

The results for the material property tests were used as inputs for an analytical model that was proposed and predictions were made based on the separate material properties. The predicted outputs from the model were compared with the direct, restrained shrinkage, test results from the ring tests.

The results of the experimental component of the study showed that coarse aggregate volume content and size had a direct effect on some of the key material properties that influence overlay cracking. An increase in coarse aggregate volume content was shown to have a negligible influence on tensile strength, decrease tensile relaxation properties, increase elastic stiffness and reduce free drying shrinkage. Furthermore, it was found that an increase in coarse aggregate volume resulted in a prolonged time to first cracking of overlay material and a reduction in crack intensity. An increase in coarse aggregate size was shown to have a negligible effect on tensile strength at younger ages, increase tensile relaxation, increase elastic stiffness and reduce free drying shrinkage. A similar trend was observed in the direct test results that was noted for coarse aggregate volume, with an increase in aggregate size being shown to prolong the time to first cracking and reduce the crack intensity.

The results showed that the proposed material property analytical model was not effective, and did not account for the influence of coarse aggregate volume and size on overlay performance. This was significant, as this model had been shown to effectively predict the performance of various overlay repair mortars, and this inaccuracy was therefore attributed to factors associated with the crack mechanics of the failure of materials with coarse aggregate inclusions that were not accounted for by the model.

Table of contents

List of figures

List of tables

Chapter 1: Introduction

1.1 Background and scope of research

There is a growing need for improved methods and understanding of concrete repairs and retrofitting. This is the result of a number of different factors that result in existing concrete structures not reaching their intended service lives (Beushausen & Alexander, 2009, Mangat & O'Flaherty, 2000 and Banthia & Gupta, 2006). The economic implications of these unplanned concrete repairs are vast and can have a profound effect on the continued feasibility and upkeep of major structures (Beushausen & Alexander, 2009 and Banthia & Gupta, 2006). However, it is also noted that the economic implications of poorly conducted concrete repairs can be even greater than those associated with the original repair (Beushausen & Alexander, 2009).

There are currently very limited specifications and design methods available for concrete repair and many of the mechanisms of failure are not well understood. Many of the current methods that are used are based on very broad practices that are simply applied to any repair situation as a standard procedure (Bissonette *et al.,* 2013). This lack of understanding and specialised specifications is the direct cause of the failure of many of these repairs.

This investigation will focus on the cracking of bonded concrete overlays. The bonded concrete overlay repair technique is the most commonly used method for concrete repair and is used extensively around the world (Bissonette *et al.,* 2013). The method, which involves casting a new layer of concrete over an existing substrate, can be used for structural repairs where the overlay is loaded and fulfils a structural role or simply for non-structural repairs to cover and protect exposed reinforcing or damaged concrete (Mangat & O'Flaherty, 2000, Hassan *et al.*, 2000 and Bissonette *et al.,* 2013).

The research will focus on the concept of restrained deformation and the resulting tensile stresses that this induces on the overlay. This concept of differential volume changes between the substrate and overlay is based on the idea that the overlay is subjected to shrinkage and thermal movement, while the substrate's movements are usually assumed to be completed or minimal. The deformation of the overlay is therefore restrained at the interface to the substrate, which will cause tensile stresses and may result in failure by cracking or debonding (Beushausen & Alexander, 2009, Mangat & O'Flaherty, 2000, Hassan *et al.*, 2000, Banthia & Gupta, 2006 and Beushausen & Alexander, 2006a).

This investigation will focus particularly on overlay cracking as the mode of failure and will not consider overlay debonding. The factors that have been shown to have an effect on the bonding properties and bond strength between the overlay and substrate will therefore be omitted from the investigation. However, there are a number of factors that are directly linked and contribute to both forms of failure and therefore will be considered.

Overlay cracking is very difficult to control and the mechanisms and factors associated with this crack propagation are not well understood (Banthia & Gupta, 2006). As a result of this, there are currently very limited practical design methods or prediction models that can be used by designers to predict and prevent overlay cracking.

There are a number of specific, time-dependant, material properties that have been identified as contributing directly to overlay crack resistance, namely: tensile strength, shrinkage, tensile relaxation and elastic modulus. These properties can be directly linked to repair material mix design parameters such as: water:cement ratio, cement type and content, aggregate type, size, content and grading, as well as the use of admixtures.

This research will therefore be limited to investigating and understanding the link between coarse aggregate size and content, and the effect that this will have on the performance of overlay materials and the key overlay properties that affect cracking.

The experimentation component of the investigation will focus firstly, on indirectly testing and establishing a link between course aggregate size and content, and the resulting overlay material properties and secondly, directly testing the influence of varying coarse aggregate parameters on overlay material performance. Two laboratory concrete repair mixes, with a w:c = 0.45 and 0.6, and one commercial repair mix with varying aggregate sizes and contents were tested. These tests involved small scale testing on small specimens to test material properties and direct testing of restrained shrinkage using the ring test method.

An analytical model has been proposed, based on work done by Gilbert (1988), and has been successfully used by Chilwesa (2012) to predict the time to cracking failure of different repair mortars with an acceptable degree of accuracy. This analytical model will be applied to this investigation and the effectiveness of predicted outputs will be compared to direct test results.

1.2 Significance of research

The investigation makes a relevant contribution to continuing work on overlay performance, where new methods for understanding, improving and predicting the performance of overlays are the subject of extensive research. The use of coarse aggregate to improve the performance of overlay materials and the ability to use existing analytical prediction methods to model this improvement will add greatly to this field of research.

1.3 Problem statement

The first question that this research seeks to answer is what influence the effect of coarse aggregate volume content and size will have on the crack resistance of bonded concrete overlay repair materials, and what influence these coarse aggregate parameters will have on the individual material properties that directly influence the performance of the bonded concrete overlay material.

The second question that this research seeks to answer is whether the analytical model that has been successfully used by Chilwesa (2012) to predict the time to cracking failure of different repair mortars with an acceptable degree of accuracy can be used to account for the influence of coarse aggregate volume content and size on overlay material performance with the same level of accuracy.

1.4 Research aim

The aim of the research is to investigate the influence of varying coarse aggregate volume contents and sizes on the performance with respect to cracking of bonded concrete overlay repair materials. The research also aims to use the influence of these varying aggregate parameters on the specific material properties, which have been identified as influencing the crack resistance of repair materials, to analyse and predict the performance of overlay materials.

1.5 Research hypothesis

The research proposes that coarse aggregate volume content and size will have the following influence on the performance of bonded concrete overlays:

1. Coarse aggregate volume content will influence cracking behaviour of overlay repair materials with an increase in aggregate volume content resulting in an increasing age for overlay cracking failure.
2. Coarse aggregate size will have a noticeable influence on the cracking of overlay repair materials.

Furthermore, the research proposes that the performance of bonded overlay materials, with regard to cracking failure, can be analysed by examining the individual, time dependant, material properties of the repair material. Therefore the influence of coarse aggregate volume content and size on these material properties can be used to predict and analyse the effect that these varying aggregate parameters will have on overall overlay performance and resistance to cracking.

1.6 Objectives of the research

The following objectives have been determined to achieve the research aims for this investigation:

1. To identify and test the influence of varying aggregate volume contents and sizes on the material properties of repair materials.
2. To directly test the influence of varying aggregate volume contents and sizes on the crack resistance of bonded concrete overlay repair materials.
3. To model and predict this influence using inputs from tests conducted on the material properties of the repair material.

1.7 Plan of development

The investigation will begin with a detailed literature review presented in Chapter 2. The experimental details and procedures that were used for the experimental component of the study are given in Chapter 3 and the experimental results are presented and discussed in Chapter 4. The analytical modelling component of the investigation is presented and evaluated in Chapter 5. A detailed discussion, final conclusions and recommendations are presented in Chapter 6.

Chapter 2: Literature review

2.1 Background

Many sources have described the growing demand for the repair and protection of existing concrete structures (Beushausen & Alexander, 2009, Mangat & O'Flaherty, 2000 and Banthia & Gupta, 2006). It is suggested that the key reasons for the degradation of these structures is the result of poor design, workmanship, materials and environmental conditions during construction and service life, as well as the forces that the structures are exposed to (Beushausen & Alexander, 2009). The main contributing factors for this degradation are an insufficient cover depth to reinforcing steel and poor concrete cover quality. It is also shown that reinforcing corrosion is caused by disruptions and the deterioration of the cover zone as well as defects in the concrete itself (Mangat & O'Flaherty, 2000).

Many of these repairs and rehabilitation requirements were not planned or budgeted for by the design engineers. There are high costs associated with these concrete repairs and the significant economical implications that these costs can cause have a profound effect on the maintenance and upkeep of existing concrete structures (Beushausen & Alexander, 2009 and Banthia & Gupta, 2006).

Poorly conducted and executed repairs can result in financial costs far greater than the initial repair costs incurred (Beushausen & Alexander, 2009). There are a large number of different repair techniques and methods available and used by industry and it is therefore vitally important that the mechanisms and modes of failure of these different concrete repairs are understood (Mangat & O'Flaherty, 2000).

2.2 Bonded overlay repair method

There are many different types and approaches to concrete repair that address a number of different forms of deterioration. These forms of deterioration are either defects in the concrete or reinforcement corrosion. Extensive information on what causes this deterioration is known (Beushausen & Alexander, 2009). It is suggested that bonded concrete overlays are the most common form of concrete repair, and are also known as 'patch repairs' for smaller overlay repairs According to Bissonette *et al.* (2013), the purpose of the bonded concrete overlay repair method is to extend the life of the concrete slabs or pavements. This additional thickness due to the overlay can also result in an increase in flexural stiffness. Bonded overlays are widely used for the repair, rehabilitation and strengthening of concrete members (Mangat & O'Flaherty, 2000 , Hassan *et al.*, 2000 and Bissonette *et al.,* 2013).

Bonded concrete overlays can be used for structural and non-structural repairs, which usually dictate the size and strength requirements of the repair. However, Bissonette *et al.* (2013) suggest that the bonded overlay technique is particularly effective in the case of structures and members with large surface areas such as slabs and pavements.

There are a number of key factors that contribute to the success or failure of these repairs (Beushausen & Alexander, 2009 and Bissonette *et al.,* 2013) and are discussed in this section.

2.2.1 Substrate surface preparation

Surface preparation refers to all of the processes, measures and circumstances that influence the interface contact between the substrate and the overlay.

Bissonette *et al.* (2013) and Beushausen (2010) identify surface preparation factors such as integrity of the substrate, prevention of microcracks, surface roughness, cleanliness, the removal of the laitance layer, prewetting and bonding agents as having a significant effect on overlay bond strength. Edging conditions and rebar preparation such as cleaning and coating should also be considered.

2.2.2 Choice of overlay materials and material properties

There have been significant advances in the choice and design of overlay repair materials. The traditional method of "repair like with like" has been shown to be relatively ineffective and prone to failure (Bissonette *et al.*, 2013). Bissonette *et al.* (2013) and Mangat & O'Flaherty (2000) explain how the performance of the overlays can be directly linked to the dimensional compatibility of the repair material and the substrate. Other issues that must be considered when selecting the overlay material relate to the permeability compatibility, and chemical and electrochemical compatibilities of the overlay material (Bissonette *et al.*, 2013).

Differential volume changes and compatibility between the substrate and overlay are identified as the key influence on the crack resistance of bonded concrete overlays. This is directly linked to the time dependant material properties of the overlay, which dictate how the repair material will react to the resulting stresses. According to Emmons & Vaysburd (1993), this dimensional compatibility is dependent on the degree of restraint, the magnitude of shrinkage, the modulus of elasticity, the creep/relaxation characteristics and the tensile strength of the overlay material.

The American Concrete Pavement Association (ACPA, 1990) guidelines for overlay material selection are relatively flexible with mix designs, suggesting that plain concrete mixes are usually adequate for most repair situations. Suggestions are also made for fast-setting repair mixtures known as "fast-track" mixes which allow for quicker repair times.

The ACI C325 (2006) committee recommendations also discuss the use of plain concrete and "fast-track" repair mixes. It is specified that overlay concrete mixtures typically have constituents and proportions that are similar to conventional concrete, but suggest that shrinkage and shrinkage cracking can be minimized by minimizing the total amount of water and maximizing the volume proportion of aggregate in the mixes.

Banthia & Gupta (2006) and the ACI C325 (2006) committee also detail the use of fibre-reinforced concrete to control cracking of the repair overlays. Fibre materials that are suggested include: steel, polypropylene, polyester and polyolefin fibres.

Both the (ACPA, 1990) guidelines and the ACI C325 (2006) committee recommendations stress the importance of meeting the different compatibility requirements between the repair material and the substrate. ACI C325 recommendations for plain concrete mixes used for bonded overlays are presented in Table 2.1.

Table 2.1: ACI C325 recommendations of materials for plain concrete mixes used for bonded overlays (ACI C325, 2006, as cited by Bissonette *et al*., 2013)

Components/characteristics	Recommendation
Binders	- Type I, II; Type III for high early strength (ASTM C 150) - Fly ash (type C or F)
Aggregates	- Good quality aggregates, non-reactive - Common max. coarse aggregate size: 19–25 mm - Larger max. sizes considered by some agencies - Lower max. size for thinner overlays - Largest and most practical maximum coarse aggregate size should be used to minimize paste content, reduce shrinkage, minimize costs, and improve mechanical interlock properties at joints and cracks - $d_{max} \leq (h_{overlay}/3)$
Commonly used admixtures	- Air-entraining agent - Accelerator (non-chloride if steel reinforcement is present) - Water reducer
Water/binding ratio	- W/B ≤ 0.45 (humidity & freeze/thaw conditions) - Lower W/B ratios recommended for thin overlays
Fibres	- Steel, polypropylene, polyester, and polyolefin fibres
Typical mixtures	- Cement: 295–415 kg/m^3 - Air content: 4–6 % - fc_{28}-d ≥ 28 MPa - $MOR_{28\text{-}d} \geq 4.5$ MPa
"Fast-track" mixtures	- Cement ≥ 385 kg/m^3 - Type III cement, rapid-setting cement or set-accelerating admixture - W/B ≤ 0.43
Bonding agent	- No bonding agent required according to many specialists

2.2.3 Application and curing procedures

The application process used for bonded overlay repairs can have a profound effect on the durability and effectiveness of the repair. Bissonette *et al.* (2013) emphasise the importance of having an adequate placement capacity to mitigate the influence of cold joints during placement. The effective compaction of the repair material is also emphasised, especially for repairs with rough and uneven substrates to ensure a uniform bond.

Bissonette *et al.* (2013) and Naderi & Ghodousian (2012) also suggest that more desirable overlay placement can be achieved through the use of self-compacting concrete (SCC).

Curing procedure also play a key role as this contributes directly to the development of the material properties of the overlay and the effects of differential volume changes (Beushausen & Alexander, 2009, Bissonette *et al.*, 2013 and Hassan *et al.*, 2000). Bissonette *et al.* (2013) state that the key function of effective curing is to reduce early moisture loss and associated plastic and drying shrinkage. This is a particular problem noted with overlays which are susceptible to rapid early drying as they have large surface areas in relation to their volume. Curing can also help to effectively manage the influence of temperature variations.

2.2.4 Environmental conditions

The influence of environmental conditions on bonded concrete overlay performance relates specifically to moisture loss and temperature variations of the repair material and can be substantial.

Banthia & Gupta (2006) suggest that environmental factors such as relative humidity, temperature and wind velocity have a profound influence on the performance of overlay repairs. In a study conducted by Hassan *et al.* (2000), it was found that a hot and dry environment adversely affected the shrinkage and performance related properties of conventional repair materials.

These effects, which relate specifically to moisture loss and temperature variation, can be effectively addressed through appropriate curing procedures discussed by Bissonette *et al.* (2013) in the previous point.

2.2.5 Summary

The following figure (Figure 2.1) summarises these key factors that influence the success or failure of bonded concrete overlays. The key focus of this investigation will be on the influence and interaction of the overlay material properties on the performance of overlay repairs. However, the interaction of all overlay factors must be considered to gain a more comprehensive understanding of the failure mechanisms involved.

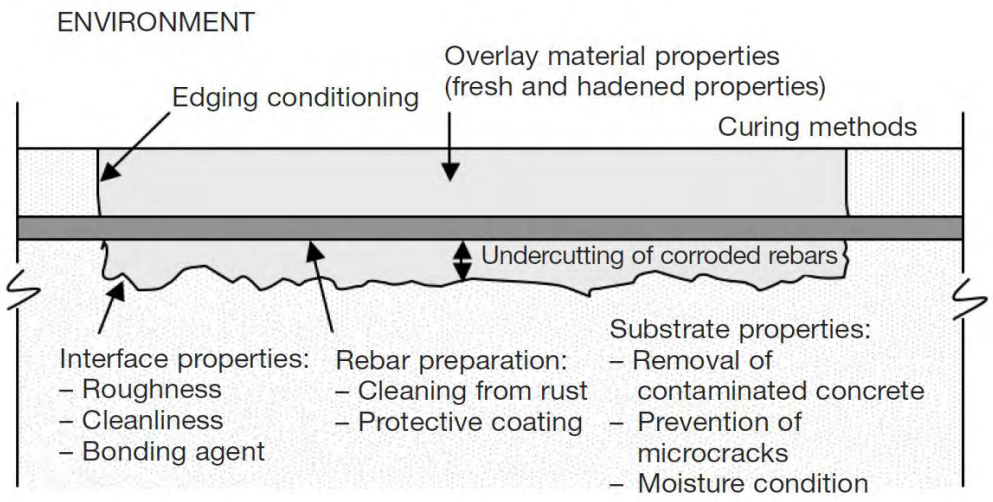

Figure 2.1: Overview of factors to be considered in the design and application of bonded overlays (Beushausen & Alexander, 2009)

2.3 Failure of overlays

Differential volume changes and the resulting induced tensile stresses are deemed to be the key factor contributing to the failure of bonded concrete overlays (Beushausen & Alexander, 2009, Mangat & O'Flaherty, 2000, Hassan *et al.*, 2000, Banthia & Gupta, 2006 and Beushausen & Alexander, 2006a). Carlswärd (2006) explains how these volume changes in the newly cast overlay cause tensile stress to develop as the contracting movement is restrained by the substrate. If this induced stress exceeds the intrinsic tensile strength of the repair material, failure in the form of cracking or debonding will occur. In some cases, a stress field is induced near the free edge of the overlay, which tends to lift. This type of failure is known as curling or edge lifting. These overlay failure mechanisms are illustrated in Figure 2.2.

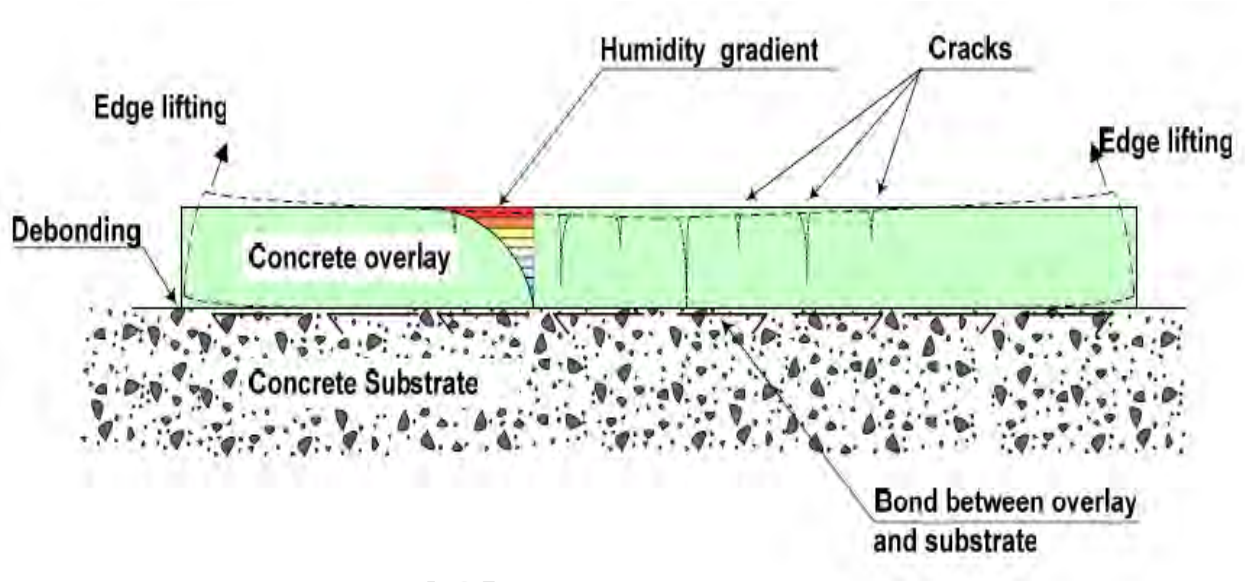

Figure 2.2: Failure mechanisms of bonded concrete overlays (Carlswärd, 2006)

Shin & Lange (2012) attribute these volume changes in overlay concrete to autogeneous and external drying shrinkage, and temperature variations caused by internal hydration and external ambient conditions. They go on to explain that the greatest volume changes in concrete occur within the first few days after placement. Denarié & Silfwerbrand (2004) also attribute shrinkage and temperature variations as causing these volume changes, but also suggest substrate settlement and externally applied loads can also influence these changes.

Beushausen & Alexander (2006b) suggest that differential shrinkage is considered the most critical influencing factor on the long term performance of bonded concrete overlay repairs. This is supported by Granju *et al.* (2004), Rahman *et al.* (2000), Weiss *et al.* (1998) and Yuan *et al.* (2002).

There are a number of different types of shrinkage mechanisms associated with overlay performance which will be discussed in more detail later on. However, consensus among experts suggests that the influence of drying shrinkage can be considered as the critical mechanism for the performance of bonded concrete overlays.

Drying shrinkage is the time-dependant reduction in volume due to moisture losses from the concrete to the environment. As the overlay concrete is restrained by the substrate or steel, these compressive strains can result in tensile stresses (Mangat & O'Flaherty, 2000 and Banthia & Gupta, 2006)

Although there may be some minor volume changes in the substrate, it is widely accepted by numerous sources that the volume changes of the substrate and reinforcing steel that are in contact with the overlay, can be assumed to be negligible. The failure of the overlay can therefore be attributed to volumetric changes in the overlay material which is restrained by the substrate or steel that has a constant volume (Mangat & O'Flaherty, 2000).

However, Beushausen & Alexander (2006a) do not agree entirely with this outlook and stress the importance of considering substrate creep strains and elastic deformations when considering the deformation of bonded concrete overlays

2.3.1 Overlay failure mechanisms

2.3.1.1 Debonding

Debonding is directly related to the strength of the bond between the overlay and substrate and can occur as a direct result of differential volume stresses or as the result of the breakdown of the bond strength caused by aggressive chemical attacks that are able to penetrate through failure cracks in the overlay (Beushausen & Alexander, 2009).

Substrate preparation is vital to prevent debonding and is discussed in detail by Júlio *et al.* (2006), Bissonette *et al.* (2013) and Beushausen (2010). These sources stress the importance of the removal of contaminated concrete from the substrate, removal of the laitance layer, the prevention of micro cracks and regulated moisture conditions as important factors contributing to the prevention of debonding.

The importance of interfacial properties such as roughness and cleanliness, as well as the use of different types of bonding agents to improve the ultimate bond strength of the repair overlay are also discussed with respect to the prevention of debonding (Beushausen & Alexander, 2009).

There is a significant link between debonding failure and restrained shrinkage cracking and it can be noted from the literature that the factors that contribute to the debonding of overlays are far better understood than the mechanisms and factors controlling restrained shrinkage cracking.

2.3.1.2 Cracking and crack failure mechanisms

Cracking failure of overlays is the key failure mechanism that this investigation focusses on. An in-depth understanding of the internal and external mechanisms involved with cracking failure was therefore required to effectively analyse and evaluate the factors that result in this type of overlay failure.

Cracking failure of overlays is a result of the tensile stresses, caused by differential volume changes, exceeding the tensile stress capacity of the overlay material (Banthia & Gupta, 2006).

Chiaia *et al.* (1998) explains how, in heterogeneous materials such as concrete, failure will generally occur along the weakest link. This weak link is represented by the interfacial zone between two dissimilar materials. In the case of concrete, the bond zone between the (mortar or cement) matrix and the aggregate particle is considered to be the weakest element in the material. This zone is referred to as the interfacial transition zone (ITZ).

However, Chiaia *et al.* (1998) also explains the importance of the combination of interface strength and the level of stress, where the material is most likely to fail at the location with the highest stress relative to the interface strength. These higher stresses are located where two different materials with different elastic properties meet, at the interface between the matrix and the aggregate, resulting in stress concentrations. These stress concentrations play a key role in crack initiation and propagation.

The concept of strain softening is discussed by Chiaia *et al.* (1998) and Wittmann (2002). This process involves the formation and nucleation of microcracks at the stress concentration zones and pre-existing microdefects which become "attractors" for the subsequent macrocracking development. The process of macrocracking is characterised by the growth and expansion of interfacial cracking through the matrix. During the strain softening stage, this macrocracking will remain discontinuous and is characterised by "crack face bridges" which provide stress transfer. Complete cracking failure is only observed when macrocracking becomes continuous through the matrix.

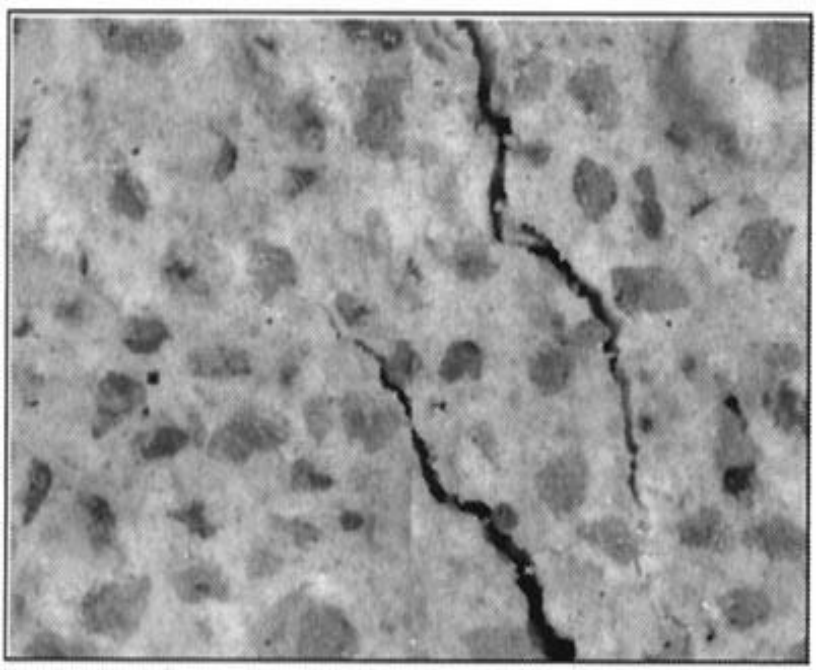

Figure 2.3: Crack face bridge (Chiaia *et al*., 1998)

As crack characteristics and propagation can be directly linked to the ITZ, the influence of aggregate properties and characteristics have a direct influence on cracking.

Giaccio & Zerbino (1998) describe how crack propagation in concrete in general starts at the interfaces, with the coarse aggregate particles arresting crack growth, producing meandering and branching cracks. This influence of coarse aggregate on crack propagation is dependent on aggregate characteristics such as surface texture, shape and stiffness. As previously highlighted, the difference in elastic properties of the matrix and the aggregate will have a profound influence on crack propagation. Giaccio & Zerbino (1998) suggest that aggregate surface texture is one of the most important factors that affect matrix-aggregate bond strength, with rougher aggregates having superior bonds.

Fracture energy is discussed by Wittmann (2002) as the specific energy required for cracking to occur. The influence of maximum aggregate size on the specific fracture energy is presented (Figure 2.4) and it was observed that fracture energy required for cracking increases as aggregate size was increased. This is supported by Hillerborg (1985) who also concluded that there is a directly proportional relationship between fracture energy and aggregate size. Wittmann (2002) attributes this to the idea that in a fine mortar, a crack can develop and run along a plane with the small strong particles only imposing minor deviations from the ideal fracture path. However, when a larger aggregate is included, the crack is forced to run around the stronger inclusions, resulting in an increase in specific energy required for cracking to occur. An increase in the presence of these aggregate inclusions, associated with an increase in aggregate volume, has also been shown to increase the fracture energy by increasing the abundance of microcracking and further extending the length of crack propagation paths.

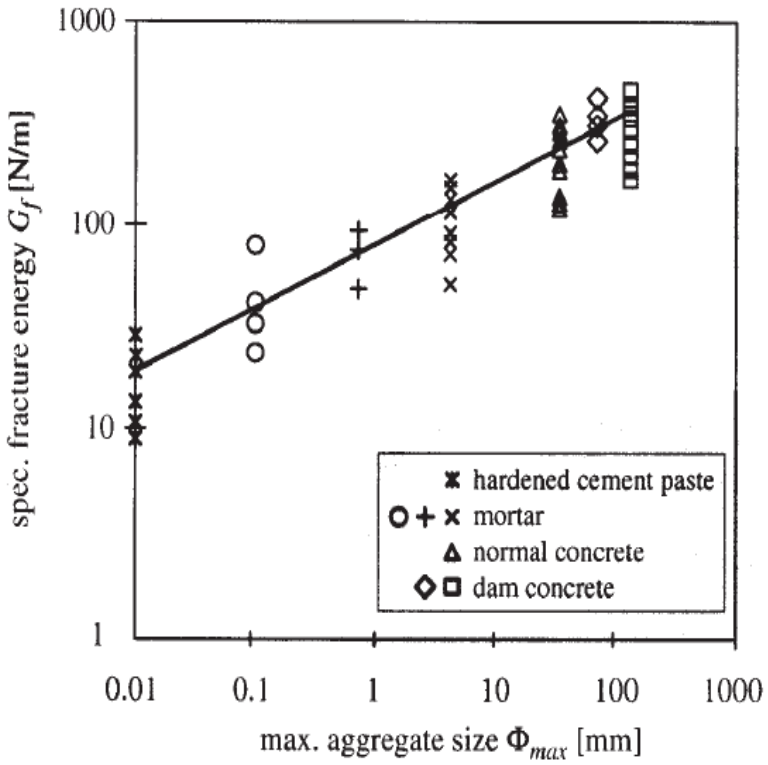

Figure 2.4: Specific fracture energy of cement-based materials as a function of maximum aggregate size (Wittmann, 2002)

The influence of concrete strength on cracking was investigated by Wittmann (2002) and Kovler & Bentur (2009). It was found that the energy consuming cracking in normal strength concrete (NC) was not observed in the cracking of high strength concrete (HSC). Due to the increased strength of the matrix associated with HSC, crack formations were observed to run through the inclusions (aggregate) and form a plane similar to that observed for fine mortars. It was deduced that mechanisms of mechanical interaction (strain softening) between the inclusions and the HSC matrix had not occurred resulting in the more brittle failure of the HSC.

The influence of microcracking due to drying shrinkage and thermal changes is also discussed by Giaccio & Zerbino (1998). It is suggested that the volume changes associated with drying shrinkage and thermal movements result in different stress concentrations along the bond between the aggregate and the matrix, resulting in microcracking and the eventual propagation of cracking failure. This reiterates the concept of strain softening discussed by Chiaia *et al.* (1998) and shows its specific relevance to the mechanisms associated with differential volume changes of bonded concrete overlays.

With regard to bonded concrete overlays, the effect of the interaction between the repair material and the substrate with respect to volume changes resulting in shrinkage cracking is not well understood (Mangat & O'Flaherty, 2000). Furthermore, it is noted that standards and specifications for bonded concrete overlays are generally deficient in information about the effects of differential volume changes on cracking (Beushausen & Alexander, 2009).

2.3.2 Factors influencing overlay cracking

As previously discussed, the cracking failure of bonded concrete overlays is dictated by the level of residual stress induced by restrained shrinkage and the tensile strength of the repair material. If this induced stress exceeds the tensile strength of the material, cracking failure will occur. There are a number of time developing material properties that directly affect the magnitude and repair concrete's resistance to elastic stresses induced by restrained shrinkage, namely:

- Shrinkage
- Tensile relaxation
- Elastic modulus

The influence of shrinkage on bonded concrete overlay cracking has been discussed in this chapter. Beushausen & Alexander (2006b) explain how tensile relaxation due to creep has been identified as a key property that can help to alleviate some of the tensile stress through 'stress relief'. Tensile stresses are also significantly affected by elastic properties of the overlay material, with an increase in repair material stiffness resulting in greater tensile stresses.

The interactions between the factors influencing overlay crack resistance are illustrated in Figure 2.5. The figure shows how the time of cracking should occur when the predicted elastic tensile stress, exceeds the tensile stress.

However, the figure also illustrates the effect of tensile relaxation and the resulting 'stress relief' which is shown to prolong the time to cracking.

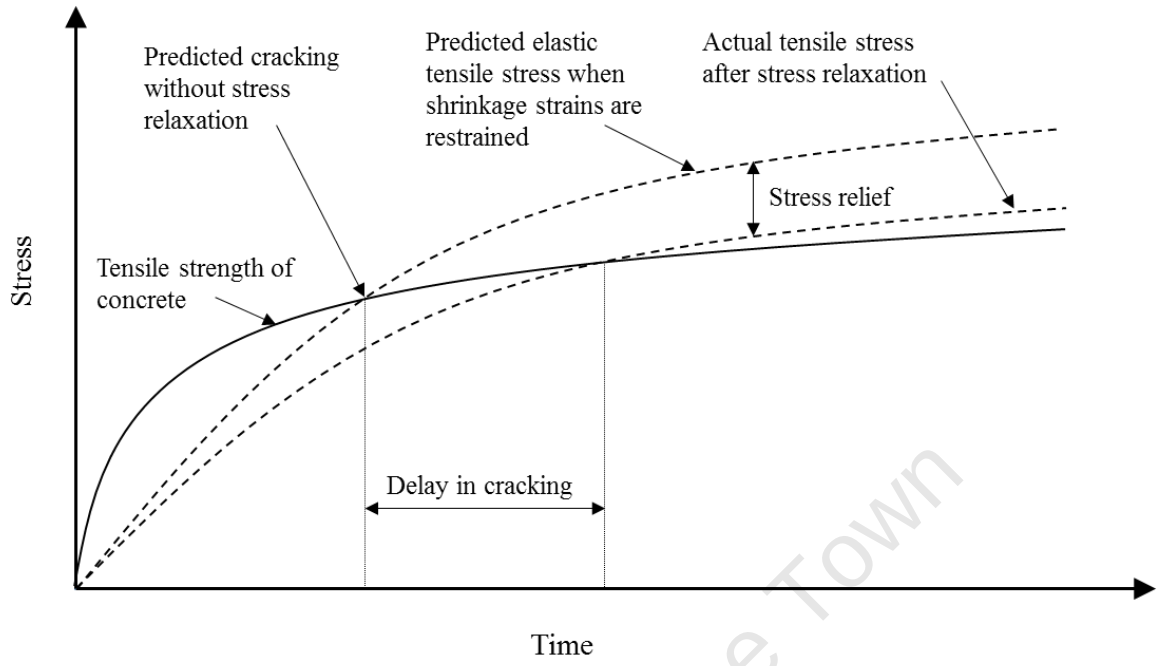

Figure 2.5: Influence of induced elastic tensile stress on the cracking failure of concrete (adapted from Chilwesa, 2012)

Many of these properties can be linked to material parameters and used to analyse and improve repair materials. These specific time dependant material properties will be analysed and discussed in detail in this chapter.

2.4 Tensile strength

The tensile strength properties of the repair concrete will dictate the point of failure (cracking) of the overlay. As previously discussed, this will occur at the point where induced residual stresses from volume changes exceed the intrinsic tensile strength of the repair material. It is therefore important that the factors that influence the magnitude and development of this property are understood to gain a more comprehensive understanding of overlay cracking.

2.4.1 Factors influencing tensile strength

Concrete strength has been shown to be dependent on the nature of the concrete itself and certain intrinsic and extrinsic factors (Perrie, 2009). The nature of concrete includes the composite heterogeneity of the concrete in its hardened state and the porosity and flaws that are present. Intrinsic factors such as water:cement ratio, aggregate, aggregate-paste interface and cement type and content influence the microstructure and have a direct influence on concrete strength. Extrinsic factors such as curing, the direction and rate of loading and specimen shape and geometry have also been shown to directly influence concrete strength in both tension and compression (Perrie, 2009).

According to Grieve (2009), concrete strength in tension and compression is dependent on the strength of the binder phase, aggregate phase and the interfacial bond. The coarse aggregate properties that affect concrete strength are surface texture, stiffness, shape, strength and toughness and grading (Alexander & Mindess, 2005). The effect of surface texture, shape and grading will indirectly affect strength by influencing plastic concrete properties through water requirement, but will also have a direct effect on stress concentrations, micro-cracking, roughness at interfaces and bonded surface area of aggregate (Alexander & Mindess, 2005).

The particular importance of coarse aggregate shape with respect to flexural strength is highlighted by Alexander & Mindess (2005). Angular particles are considered to improve concrete strength, and in particular flexural strength, over rounded particles.

The effect of coarse aggregate size on concrete tensile strength was investigated by Zhang *et al*. (2005) and it is shown that for a given aggregate content, smaller coarse aggregate size leads to an increase in tensile strength for normal strength concrete (approx. 40 MPa). Zhang *et al*. (2005) explains that this increase in tensile strength can be attributed to the greater number of coarse aggregate particles associated with smaller aggregate size, which provide better bridging restraint during tensile cracking. It was also noted that the tensile stress drop-off after the peak was much steeper for smaller coarse aggregates.

An investigation by Ozturan & Cecen (1997) compared the tensile strengths of concretes made with crushed basalt and limestone with concrete made using conventional gravel aggregate. It was shown that higher tensile strengths were obtained for the stronger basalt and limestone mixes. This was supported by the findings from Zhou *et al.* (1998) who showed that flexural and splitting tensile strengths of concrete made with a normal coarse aggregate (crushed limestone) was higher than those made using a weaker lightweight coarse aggregate (sintered fly ash).

It can therefore be deduced that concrete tensile strength is directly affected by coarse aggregate content, size, surface texture, stiffness, shape, strength and toughness and grading.

Repair concrete tensile strength has been shown to be affected by the type and design of repair mortars used and will also be affected by curing conditions (Hassan *et al.*, 2000). The effect of different types of repair mortar materials and curing methods on the tensile strength was studied by Hassan *et al.* (2000).

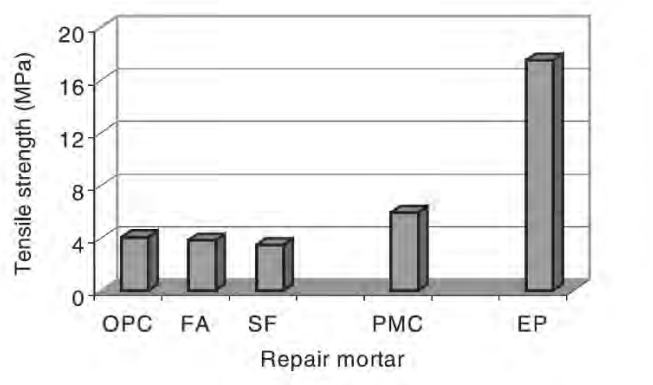

OPC - Ordinary Portland Cement Mortar

FA - Fly-ash Mortar (30%)

SF - Silica Fume Mortar (10%)

PMC - Polymer-modified Mortar (Fibre Reinforced)

EP - Epoxy Resin Mortar

Figure 2.6: 28 day tensile strength of different repair mortars (Hassan et al., 2000)

The investigation tested five different repair mortars that made use of a number of different cementitious admixtures. A mortar with fibre reinforcing and an epoxy resin mortar was also tested. The different repair materials were tested under adverse, warm and dry, curing conditions. The tensile strength results for this investigation are shown in Figure 2.6.

The investigation showed that the use of some cementitious admixtures (in particular, fly-ash) and warm-dry curing conditions can be detrimental to tensile strength. Reinforcing methods such as fibre-reinforced mortars were shown to be effective with respect to tensile strength and this is supported by findings from Banthia & Gupta (2006). The investigation also highlighted the link between compressive strength and tensile strength, with the results indicating a directly proportional relationship for overlay repair materials.

2.4.2 Modelling tensile strength

Conversion equations for determining tensile strength of concrete based on specific specimen test results have been developed and are used extensively.

The direct testing of the uniaxial tensile strength of concrete is complex and involves specialised testing apparatus. Therefore, a number of simpler, indirect testing methods have been developed and are more commonly used. The most common of these indirect tests are the splitting tests and the flexural (rupture) tests, illustrated in Figure 2.7.

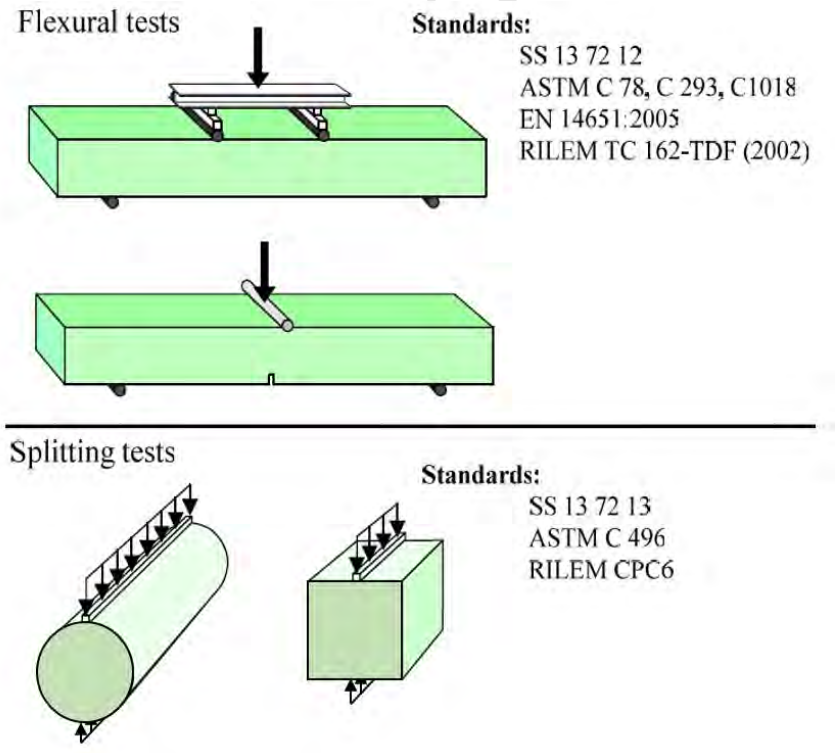

Figure 2.7: Indirect tensile strength tests (adapted from Carlswärd, 2006)

A number of conversion functions are proposed to convert these indirect tensile results to a uniaxial tensile strength value.

The tensile strength determined by the splitting test is believed to be relatively close to the direct uniaxial tensile strength, generally being only 5 – 12% higher (Neville, 1995). However, Neville (1995) suggests that for mortars and lightweight aggregate concretes, the splitting tensile strength test yields results that are significantly lower than the uniaxial tensile strength. The presence of larger aggregate particles near the surface where the splitting load is applied has also been shown to influence the results of this test method (Lee *et al*. 2004). The BS EN 1992 standard suggests an approximate relationship between uniaxial tensile strength ($f_{ct,ax}$) and splitting tensile strength ($f_{ct,sp}$):

$$f_{ct,ax} = 0{,}9\,.\,(f_{ct,sp}) \tag{2.1}$$

The BS EN 1992 standard also suggests a relationship between flexural tensile strength ($f_{ct,fl}$) and uniaxial tensile strength ($f_{ct,ax}$):

$$f_{ct,ax} = 0{,}5.\,(f_{ct,fl}) \tag{2.2}$$

A more comprehensive relationship is given in the CEB/FIP Model Code 90: 1993 which accounts for the depth (h) of the beam used for the flexural testing:

$$f_{ct,ax} = \frac{2.(\frac{h}{100})^{0,7}}{1+2.(\frac{h}{100})^{0,7}} \cdot f_{ct,fl} \tag{2.3}$$

A number of prediction formulas have also been developed that are based on a relationship between concrete tensile strength and concrete compressive strength. The BS EN 1992 suggests the following relationship between tensile strength (f_{ct}) and cylinder compressive strength (f_{ck}):

$$f_{ct} = 0{,}3.\,(f_{ck})^{2/3} \tag{2.4}$$

While, Perrie (2009) suggests a slightly different relationship between tensile strength and cylinder compressive strength based on work done by Loedolff & Chambers (1994):

$$f_{ct} = 0{,}185.\,(f_{ck})^{0{,}783} \tag{2.5}$$

Due to the varying nature of these indirect tests and prediction models it was decided that direct uniaxial testing should be used for the experimental component of this investigation to ensure accurate results.

2.4.1 Testing tensile strength

The impracticality of measuring tensile strength has been emphasised in detail. Testing tensile strength can be done in a number of ways using a number of methods. Common indirect test methods are specified which include the beam or flexural test and the splitting test. The relationships between compressive strength, flexural, splitting and direct tensile strength are given in the form of conversion equations, and have been discussed previously in the review. However, these indirect tests are insufficiently accurate or suited to the tensile testing required to evaluate concrete repair materials.

In the investigation conducted by Hassan *et al*. (2000), direct tensile strain was measured using bobbin–shaped specimens and an Instron 8500 Series Digital testing machine. This method provided accurate results, with the bobbin-shape of the specimens allowing a uniform tensile stress to be applied across the specimen.

A similar method was effectively used by Beushausen *et al*. (2012) to test tensile relaxation and tensile strength using dog-bone specimens and a Zwick Roel Universal testing machine.

2.4.2 Influence of tensile strength on bonded concrete overlay performance

As discussed previously, overlay shrinkage cracking will occur when the tensile stresses caused by shrinkage of the overlay material become greater than the intrinsic tensile strength of the overlay.

It is therefore an important factor to consider when developing repair materials that are resistant to cracking and will dictate the magnitude of residual stresses, induced by differential volume changes, which will cause this cracking failure. It therefore has a profound effect on overlay performance.

2.5 Shrinkage

Shrinkage deformation is the time-dependant decrease in volume of both fresh and hardened concrete and is generally associated with moisture loss within and outward from the concrete due to the surrounding environment and the hydration process (Alexander & Beushausen, 2009). It has been identified as the key factor contributing to volume changes that result in bonded concrete overlay cracking. However, the shrinkage of concrete, in general, is highly complex and is influenced by a number of different mechanisms and factors.

2.5.1 Types of shrinkage

There are a number of different types of shrinkage that are associated with concrete. Some of these types are more relevant than others to the shrinkage associated with bonded concrete overlays.

2.5.1.1 Plastic shrinkage

Plastic shrinkage is the result of rapid evaporation of water from the surface of young concrete, which results in concrete volume changes. This occurs during the first few hours after casting.

Carlswärd (2006) explains how early age plastic shrinking contributes to the early cracking of overlays as it occurs when the strain capacity of the fresh overlay concrete is low and therefore the shrinkage induced strains exceed this low strain capacity of the material.

Plastic shrinkage is influenced by bleeding as some water lost from the surface can be replenished by bleed water that rises from within the concrete. However, if sufficient surface moisture is lost it will cause a drop in the capillary pressure, which will lead to the development of lateral compressive strains and plastic shrinkage cracking (Mangat & O'Flaherty, 2000).

Plastic shrinkage, by nature, is particularly susceptible to environmental conditions such as high wind velocities, low humidity and warm temperatures (Grzybowski & Shah, 1990). The use of a superplasticiser or retarding agent has been shown to increase the risk of plastic shrinkage cracking, while shrinkage reducing admixtures (SRA) that lower the surface tension of the water have been shown to drastically reduce the magnitude of plastic shrinkage (Holt & Leivo, 2004).

Plastic shrinkage can easily be prevented and reduced through the correct curing methods, to ensure that surface moisture loss is kept to a minimum during the first few hours after casting.

2.5.1.2 Autogeneous shrinkage

Autogeneous shrinkage is also called basic shrinkage and is a reduction in volume caused by the internal consumption of water during the hydration process. It can therefore occur in sealed conditions and is not affected by a moisture exchange between the concrete and the environment. As autogeneous shrinkage is the result of the hydration reaction it occurs rapidly after casting with approximately 40% of autogeneous shrinkage occurring in the first 24 hours (Alexander & Beushausen, 2009).

Carlswärd (2006) explains how autogeneous shrinkage is dependent on the type and quantity of cement in the concrete. A study by Baroghel-Bouny & Godin (2001) showed that autogeneous shrinkage magnitude increases linearly with decreasing w:c ratio. It is generally accepted that autogeneous shrinkage for mixes with a w:c that exceeds 0.4 can be considered negligible (Alexander & Beushausen, 2009).

As autogeneous shrinkage is not influenced by environmental conditions, it is difficult to manage and mitigated through curing. Some success has been noted with the inclusion of a shrinkage reducing admixture (SRA). A study conducted by Rongbing & Jian (2005) showed that autogeneous shrinkage can be reduced by up to 50% with the inclusion of a SRA.

2.5.1.3 Carbonation shrinkage

Carbonation shrinkage is characterised by a reaction between carbon dioxide in the atmosphere and the constituents of hardened cement. It occurs over an extended period of time and can have a significant magnitude (Alexander & Beushausen, 2009).

Carbonation shrinkage is associated with relative humidity and Alexander & Beushausen (2009) suggest that carbonation shrinkage is greatest at intermediate humidities (around 50%), with higher and lower humidities showing reduced carbonation levels.

Although carbonation shrinkage under normal conditions is slow, it can cause irreversible volume changes that are additional to drying shrinkage. This is illustrated in Figure 2.8.

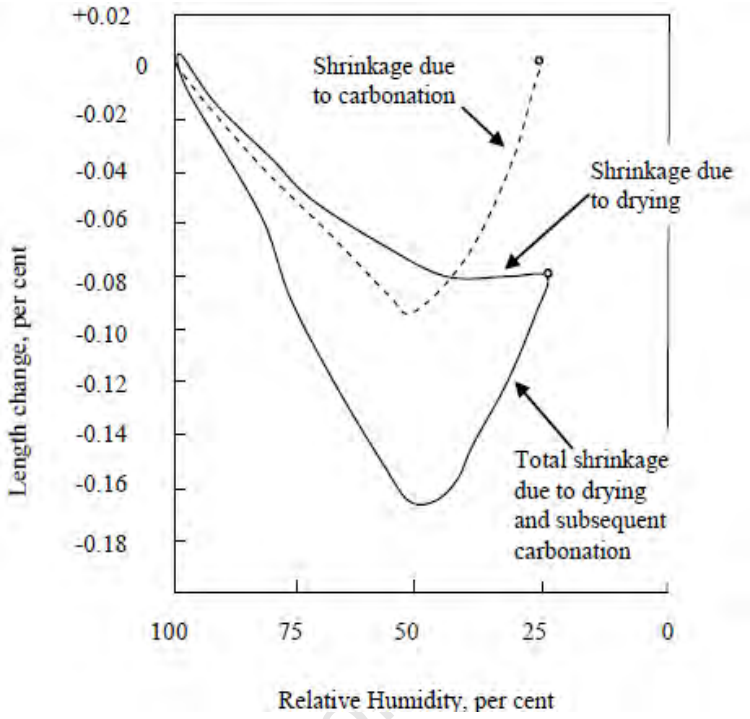

Figure 2.8: Combined influence of relative humidity on carbonation and drying shrinkage (Verbeck, 1958)

2.5.1.4 Thermal shrinkage

Thermal shrinkage is usually associated with 'massive' concrete structures that are exposed to specific climatic conditions. If poor heat dissipation conditions occur then heat generated during hydration can result in significant concrete temperatures soon after placement. (Mehta & Monteiro 2006). Thermal shrinkage occurs as the concrete cools and its volume reduces, which can lead to cracking.

Alexander & Beushausen (2009) suggest that this thermal movement is affected by factors such as moisture content, aggregate type and aggregate volume and can be controlled through appropriate mix designs and curing techniques.

2.5.1.5 Drying shrinkage

Drying shrinkage is a time-dependant reduction of concrete volume that is caused by moisture loss to the environment (Alexander & Beushausen, 2009). Asad *et al*. (1997) suggests that drying shrinkage is caused specifically by volume changes of calcium silicate hydrate (C-S-H) gel in the hardened cement paste. Three mechanisms of drying shrinkage are discussed, namely: capillary stress, disjoining pressure and surface tension.

Carlswärd (2006) explains how capillary stress is generated in the capillary pores of the cement, where the surface tension of the water as it evaporates is transferred to the walls of these pores. This form of drying shrinkage is usually the most dominant and occurs when the relative humidity is anywhere between 45% to almost 100%. It is also highly dependent on the capillary pore size.

Asad *et al*. (1997) explains disjoining pressure as the pressure caused by the removal of adsorbed water that is confined within the capillary pores. When this water is present it provides a restraining force that separates the cement particles on the sides of the capillary space. However, when this adsorbed water is removed, the cement particles are drawn closer together resulting in a decrease in volume.

The influence of surface tension on drying shrinkage is discussed by Mindess *et al*. (2003) who explain how, as adsorbed water is removed from the system, the last remaining layers of water molecules are located around the cement particles and are the most strongly adsorbed. The surface tension of these molecules exerts a compressive force on the cement particles and results in an overall decrease in volume. This form of drying shrinkage usually only occurs at relative humidities lower than 45%.

2.5.2 Factors influencing shrinkage

As previously mentioned, the general consensus among experts is that drying shrinkage is considered the key shrinkage type that must be considered when analysing the cracking of bonded concrete overlays. This consensus is based on the idea that plastic shrinkage can be effectively managed with appropriate curing, autogeneous shrinkage is considered negligible for mixes with a w:c greater than 0.4, carbonation shrinkage is very slow under normal conditions and thermal shrinkage is only an issue for ‘massive’ concrete structures.

Therefore, the factors that influence the drying shrinkage of repair concrete will be discussed. The key factors that influence drying shrinkage are the amount and composition of the cement paste, the structural geometry of the concrete and the drying conditions.

2.5.2.1 Intrinsic factors

From literature, it can be seen that there are a number of properties that have been identified as important contributing factors to drying shrinkage. The significant effect of cement paste content was investigated by Bissonnette *et al.* (1999) who found that the extent of shrinkage was directly proportional to the amount of the cement paste in the concrete.

Alexander & Beushausen (2009) emphasise the importance of the influence of w:c ratio and the degree of hydration. Stronger pastes, with lower w:c ratios, will be stiffer by nature and experience less contraction strain than weaker pastes. This also relates to the impervious nature of these stronger pastes which hinder the free movement of moisture from the paste microstructure. This influence is shown in Figure 2.9.

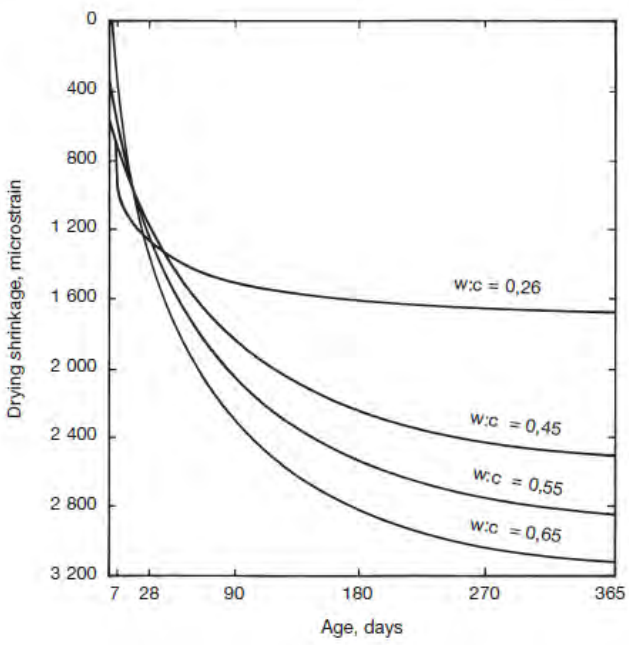

Figure 2.9: Effect of w:c ratio on the shrinkage of cement pastes (Haller, 1940)

A number of investigations considered the use of cementitious admixtures and their effect on restrained and unrestrained shrinkage.

Bloom & Bentur (1995) found that the effect of silica fume was shown to increase plastic shrinkage, but it was concluded that ultimate shrinkage was influenced very little by the presence of silica fume. It has been noted by Alexander & Beushausen (2009) that the dense microstructure caused by the silica fume does reduce the rate of moisture loss and therefore slows the rate of shrinkage. However, this is contradicted by the findings by Hassan *et al*. (2000) which show that silica fume increased shrinkage values.

The effect of fly-ash on shrinkage is a hotly debated subject and there are many different views with regard to its effectiveness.

From the literature it can be seen that there are a number of conflicting findings on the effect of fly-ash on shrinkage. In some cases it has been found to reduce shrinkage (Atis, 2003, Atis *et al.* 2003, Gesoglu *et al.*, 2006 and Naik *et al.,* 1995). Another study found that fly-ash had more of an effect on autogeneous shrinkage, and had no effect on drying shrinkage (Subramanian, 2005). This is contradicted by work done by Li *et al*. (1999) which concluded that fly-ash was observed to increase shrinkage. These controversial findings with regard to the influence of fly-ash make achieving a definitive answer from the literature reviewed very difficult.

The use of a shrinkage reducing admixture (SRA) was investigated by Banthia & Gupta (2008) and was shown to significantly reduce shrinkage and restrained shrinkage cracking. This is supported by work done by Folliard & Berke (1997) who showed that the use of a SRA can reduce drying shrinkage by 35 to 50% and can be used to effectively manage shrinkage induced cracking.

Coarse aggregates have been shown to have two key effects on paste shrinkage, namely, dilution and restraint (Alexander & Beushausen, 2009 and Alexander & Mindess, 2005). This refers to the fact that the amount of paste will reduce as aggregate content is increased and the effect of aggregate stiffness on its ability to restrain shrinkage in the concrete paste. The nature of the aggregate will also dictate the water content of the concrete and the relevant aggregate surface area that needs to be wetted. This has been shown to have an effect on drying shrinkage (Alexander & Mindess, 2005).

The effect of aggregate volume content is discussed by Alexander & Mindess (2005) and is illustrated in Figure 2.10. It is stipulated that for concretes with a total aggregate content of between 65 -75%, the concrete shrinkage will be approx. 20% of the equivalent cement paste shrinkage. These findings are supported by Banthia & Gupta (2008) who show that an increase in the aggregate/cement (a/c) ratio was highly effective in reducing shrinkage cracking of bonded concrete overlays.

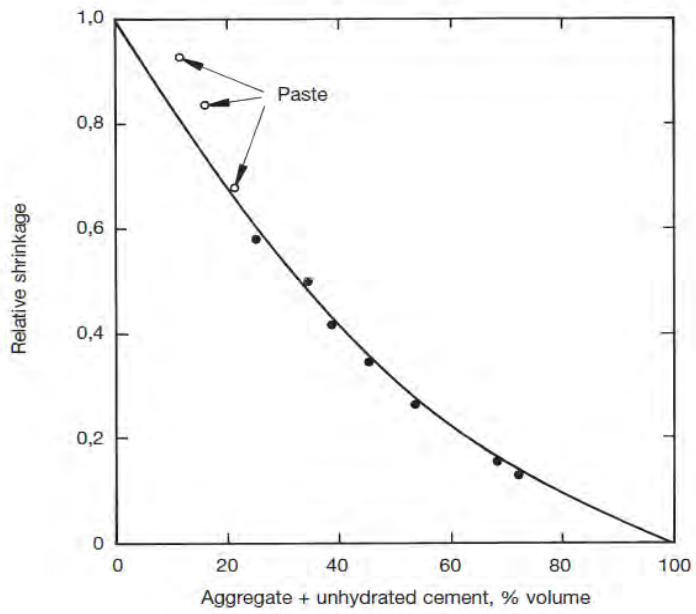

Figure 2.10: Effect of aggregate volume content on shrinkage on concrete (Alexander & Mindess, 2005)

A well graded coarse aggregate will reduce the presence of voids between the aggregate particles and will therefore ultimately reduce the volume of shrinking cement paste required Powers (1971). Furthermore, texture, size and stiffness will have a direct effect on the restraint that the aggregate will provide, with stiffer, rougher and larger coarse aggregates providing better restraint (Alexander & Beushausen, 2009).

An investigation by Troxell *et al.* (1958) studied the effect of different aggregates on concrete shrinkage and found the most important influence to be aggregate stiffness. It was found that stiffer aggregates such as quartz, limestone and granite produced lower levels of shrinkage while aggregates with a lower stiffness such as basalt, gravel and sandstone had higher levels of shrinkage. The porosity of the aggregate is also shown to have an effect on drying shrinkage in these tests.

The possible effects of shrinking aggregates are highlighted by Alexander & Mindess (2005). Certain aggregate types are not dimensionally stable and can become dimensionally unstable on wetting and drying. This can severely worsen the effects of drying shrinkage.

It can therefore be deduced that concretes that contain higher volumes of coarse aggregates with a good grading, larger size, rougher texture and higher stiffness will have lower levels of shrinkage. Shrinkage is therefore shown to be dependent on coarse aggregate content, type, size and grading.

2.5.2.2 Extrinsic factors

The effect of curing conditions and the drying environment have been investigated and emphasised extensively in the literature.

While moist curing tends to delay the onset of drying shrinkage, the influence of curing on normal concretes has been shown to be minimal (Alexander & Beushausen, 2009). In some cases, prolonged moist curing (greater than a month) has been shown to have some success in reducing shrinkage, but it is generally accepted that the length of the curing period is not an important factor with regard to drying shrinkage.

The influence of the drying environment, and in particular, the ambient relative humidity has been shown to be quite significant. A study by Baroghel-Bouny and Godin (2001) found that there was a linier relationship between relative humidity and shrinkage strain, with shrinkage strains decreasing as relative humidity levels increased. Alexander & Beushausen (2009) also suggest that elevated temperatures during drying will increase shrinkage.

One of the key extrinsic properties that relates to drying shrinkage is the size and shape of the concrete members. As drying takes place from the exposed surfaces, this generates moisture-content differentials within the sample resulting in internal strain gradients (Alexander & Beushausen, 2009). An increased drying surface area can also increase the susceptibility of the concrete to carbonation shrinkage. However, this is usually offset by the longer curing times that are associated with these larger surface areas. The influence of larger drying surface areas on shrinkage is particularly relevant for bonded concrete overlays which usually have a significant drying surface with respect to their vertical depth.

2.5.3 Modelling shrinkage

There are a number of different prediction models that have been developed to estimate the magnitude of shrinkage of different kinds of concrete. Alexander & Beushausen (2009) warn that due to the significant number of factors that influence shrinkage, the accuracy of these predicted values will vary.

The SANS 10100-1:2000 only considers shrinkage predictions that are to be used in the calculation of prestressing losses. Shrinkage values are given for pre and post-tensioning at 3 to 5 days and 7 to 14 days. These values are based on different humidity conditions in South Africa. No considerations are made for the influence of coarse aggregate content.

The BS 8110 uses a slightly more involved graphical method that relates exposure conditions to the effective section thickness and relative area of reinforcing steel. This method is based on the assumption of a water content of 8% by mass and it is assumed that a high quality, high density aggregate is used. Further provisions are made for the shrinkage of symmetrically reinforced concrete, but again no considerations are made for the influence of coarse aggregate content.

The BS EN 1992 details an in-depth shrinkage model that distinguishes between drying and autogeneous shrinkage components, with the total predicted shrinkage being the addition of these two components. Although this model is highly involved, it does not account for the influence of coarse aggregate volume.

Inputs:

f_{cm} = 28 day cylinder compressive strength (MPa)
f_{ck} = characteristic value of the compressive strength (MPa)
RH = Relative Humidity (%)
t = time (days)
t_0 = age of concrete at initiation of drying (days)
α_{ds1} = equals 3 for slowly hardening, 4 for normal or rapid hardening and 6 for rapid hardening, high strength cement
α_{ds2} = equals 0.13 for slowly hardening, 0.11 for normal or rapid hardening and 0.12 for rapid hardening high strength cement
h_0 = notional size = $2A_c/u$ (mm)
A_c = Concrete cross section (mm^2)
u = perimeter of concrete in contact with air (mm)

Drying Shrinkage $\varepsilon_{cd}(t) = \beta_{ds}(t).\varepsilon_{cd\infty}$ (2.6)

$$\beta_{ds}(t) = \left(\frac{(t-t_s)}{350.\left(\frac{h_0}{100}\right)^2+(t-t_s)}\right)^{0,5} \quad (2.7)$$

$$\varepsilon_{cd\infty} = \left((220+110.\alpha_{ds1}).e^{\left(-\alpha_{ds2}.\frac{f_{cm}}{10}\right)}\right).10^{-6}.\beta_{RH} \quad (2.8)$$

$$\beta_{RH} = -1{,}55.\left(1-\left(\frac{RH}{100}\right)^3\right) \quad (2.9)$$

Autogeneous Shrinkage $\varepsilon_{ca}(t) = \beta_{as}(t).\varepsilon_{ca\infty}$ (2.10)

$$\varepsilon_{ca\infty} = 2{,}5.(f_{ck}-10).10^{-6} \quad (2.11) \qquad \beta_{as}(t) = 1-e^{-0,2.\sqrt{t}} \quad (2.12)$$

Total Shrinkage $\varepsilon_{cs}(t) = \varepsilon_{cd}(t) + \varepsilon_{ca}(t)$ (2.13)

The ACI 209 Code Model suggests the following equation for shrinkage strain ($\varepsilon_{sh}(t, t_{sh,0})$) which is based on time (t), time at the start of drying ($t_{sh,0}$) and ultimate shrinkage strain ($\varepsilon_{sh\infty}$). It relates specifically to moist cured concrete:

$$\varepsilon_{sh}(t, t_{sh,0}) = \frac{(t-t_{sh,0})}{35+(t-t_{sh,0})}.\varepsilon_{sh\infty} \quad (2.14)$$

The RILEM Model B3 is based on the Bazant B3 Model (Bazant, 1995) and develops a shrinkage prediction that considers factors such as w:c, cement type and cement content. No considerations are made for the influence of coarse aggregate content.

Inputs:

$\varepsilon_{sh}(t,t_0)$ = shrinkage strain (in./in.)
$\varepsilon_{sh\infty}$ = ultimate shrinkage strain (in./in.)
α_1 and α_2 = 1.0
w = water content of concrete (lb/ft^3)
K_h = cross-section shape factor
h = Relative Humidity (%)
t = age of concrete (days)
t_0 = age of concrete at the beginning of shrinkage (days)
$S(t)$ = time function for shrinkage
f'_c = 28 day cylinder strength (MPa)

$$\varepsilon_{sh}(t,t_0) = -\varepsilon_{sh\infty}.K_h.S(t) \quad (2.15)$$

$$\varepsilon_{sh\infty} = -\alpha_1.\alpha_2\left(26(w)^{2,1}(f'_c)^{-0,28} + 270\right).10^{-6} \quad (2.16)$$

$$K_h = 1 - h^3 \quad (2.17)$$

$$S(t) = \tan(h).\sqrt{\frac{t-t_0}{T_{sh}}} \quad (2.18)$$

Further prediction models have been developed, such as the CEB 90 Code Model, the Gardener/Lockman Model and the Sakata Model. Mokarem *et al.* (2005) conducted an investigation to test the accuracy of these three models, as well as the ACI 209 Code Model and the Bazant B3 Model and found that the error percentage of the predicted values was generally within 15 to 30% of the tested results for all of the prediction models tested. Barr *et al* (2003) investigated the accuracy of the ACI 209 Code Model and found that it was relatively accurate for lower strength concrete, but became less accurate as the concrete strength was increased. Carlswärd (2006) makes successful use of the BS EN 1992 Model for the investigation of shrinkage cracking of fibre reinforced self-compacting concrete overlays.

It is evident that there are a number of shrinkage prediction models that have been developed, that vary with regard to their complexity and the influencing factors that are considered. However, it is noted that none of these models make specific allowances for the important influence of coarse aggregate, and specifically coarse aggregate content. Research has shown that the influence of coarse aggregate on shrinkage is profound and therefore it should be considered when attempting to model and predict shrinkage. The varying level of accuracy of these prediction models must be considered when utilizing these predicted values.

2.5.4 Testing shrinkage and factors associated with shrinkage

There are a number of methods that have been developed to effectively test and evaluate shrinkage. Some of these test methods test free shrinkage and make use of unrestrained specimens and testing techniques. Testing restrained shrinkage is slightly more complex and a number of different methods have been proposed by researchers.

There are also a number of factors that are associated with shrinkage that can be individually analysed to evaluate shrinkage.

2.5.4.1 Unrestrained shrinkage

Standard test methods for unrestrained shrinkage involve measuring the one-dimensional (linear) contraction of a prismic or cylinder specimen (Beushausen & Alexander, 2009). Some standard tests, including the BS EN 1367-4:1998, BS 1881-209:1990 and SANS Method 6085, involve using accelerated drying conditions such as an oven or low humidity environment, while the ASTM C 157-06 and RILEM: CPC 9 (1975) methods suggest a less extreme environment, that is likable to general laboratory conditions. However, a study by Goodman (1991) showed that it was inaccurate to base long-term shrinkage predictions on tests conducted using accelerated drying conditions.

The investigation conducted by Almusallam *et al*. (1998) was designed to test shrinkage of large, unrestrained, specimens that were designed to represent the surface area to volume ratio of a typical slab. Forms were made water-tight to ensure a one-dimensional water movement during curing. Shrinkage was evaluated by examining crack area and time to first crack.

This differs from the method used by Bloom & Bentur (1995) which uses a simple rig with recording instruments to measure the free shrinkage of a 1000 x 40 x 40 mm horizontal sample cast directly into the rig. The same rig could also be used for testing restrained shrinkage, see Section 2.5.4.2.

Another method used by Hassan *et al.* (2000) and described in detail in the ACI 209R-92 tests unrestrained shrinkage of repair mortars by casting cylindrical specimens (75 mm diameter and 365 mm height) and attaching Demec points to monitor shrinkage movements in the specimens. This is a very simple method that has been shown to provide accurate results.

Demec points were also used effectively by Beushausen & Alexander (2006a) and Chilwesa (2012) to measure the free shrinkage of specimens with the same cross-sectional dimensions as the overlays being tested.

2.5.4.2 Restrained shrinkage

Investigations conducted by Banthia & Gupta (2006 and 2008) used overlays cast onto substrates to evaluate restrained shrinkage. Substrate bases (40 x 95 x 325 mm) were cast with 18.5 mm, semi-circular, protuberances to enhance the substrate roughness and impose uniform restraint on the overlay.

The substrates were cast using high-strength concrete with reinforcing bars and allowed to completely cure before being stored for 60 days (Figure 2.11). This would ensure that there would be little or no volume changes in the substrate caused by shrinkage.

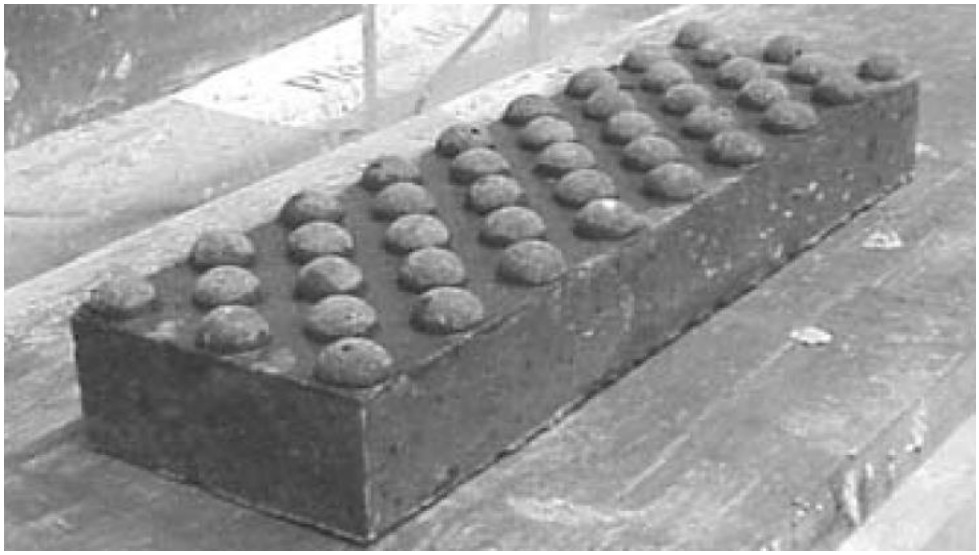

Figure 2.11: Substrate with protuberances (Banthia & Gupta, 2006)

The overlay cast onto the substrate was 60 mm deep and was then cured in an environmental chamber for 20 h, to ensure constant curing conditions. Shrinkage was then analysed by recording crack area and intensity and measuring the time to first crack.

A similar method was used by Beushausen & Alexander (2006a) with substrate beams being cast 30 months in advance to ensure that most of the shrinkage in the substrate had taken place. In this case, substrate surfaces were sandblasted and kept moist for 24 h prior to overlay casting to achieve a good bond with the repair material. Specimens were left uncovered in the laboratory after curing and exposed to varying temperatures and humidity. Shrinkage was analysed by calculating strains on the overlay and the substrate in a number of directions and distances from the interface. This was done using Demec points positioned at specific points on the overlay and substrate. Chilwesa (2012) followed this same procedure, but shrinkage was analysed by recording time to first crack and crack intensity.

The investigation presented by Bloom & Bentur (1995) uses a longitudinal testing method and apparatus to test restrained shrinkage. A specimen, 40 x 40 mm in cross-section and 1000 mm long, is cast into the rig. Each end of the specimen is wider to allow it to be gripped. The grip on one end is fixed, while the other grip is free to move. A gage monitors the movement of the free grip as the concrete shrinks. The rig also has a screw that allows the free grip to be returned to its starting position and therefore measure the load exerted on the concrete by the shrinkage. This allows the load (and calculated stress) stress under full restraining conditions to be monitored.

A ring method was used successfully by Gesoglu *et al.* (2006) and Chilwesa (2012) to test restrained shrinkage. This method is widely accepted as the most common test that is used to estimate cracking potential and intensity of repair materials. The ring-type specimens are cast around a steel ring which provides a constant restraint on the specimen. It can therefore be assumed that the specimen is subject to a uniform, uniaxial, tensile stress caused by the internal restraint of the steel ring. Shrinkage was analysed by measuring time to first crack and crack widths on the specimens.

Chilwesa (2012) explains that there are two American standards that provide specifications for the ring test, namely: the American Association of State Highways and Transportation Officials (AASHTO) standard and the American Society for Testing and Materials (ASTM) standard.

Both standards are very similar and vary only with regard to the specified dimensional sizes for the steel ring wall thickness, outer diameter and height. The dimensions specified in the ASTM standard are shown in Figure 2.12. Different inside diameters for the outer rings are also specified. A required testing environment of 23 ± 2.0º C and 50 ± 4 % relative humidity is detailed and the standards specify that four strain gauges are mounted on the inner surface of the steel ring at equal distances. These are monitored every 30 minutes and a noticeable strain decrease will indicate ring specimen failure.

It must be noted that the ring test has been shown to provide an effective and easy indication of the nature of different repair materials, but does not represent actual service life characteristics (Chilwesa, 2012).

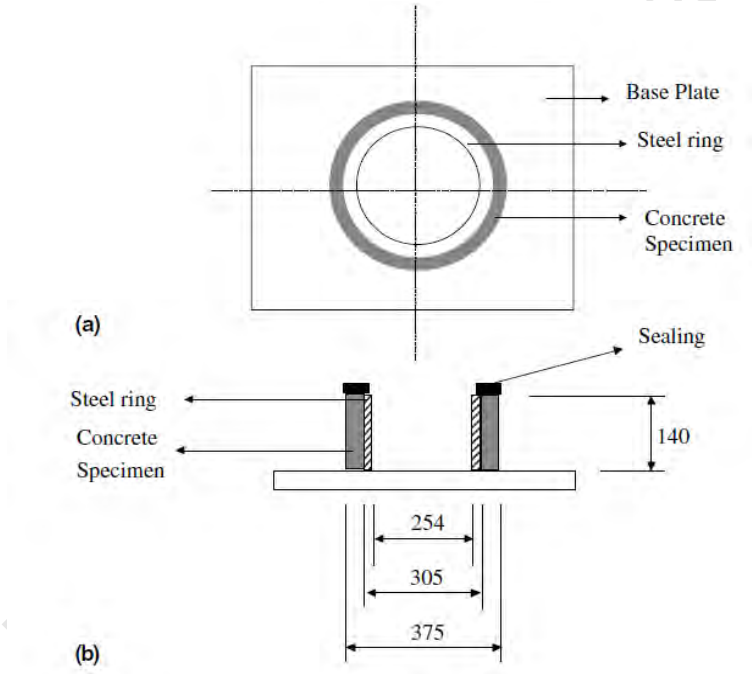

Figure 2.12: Dimensions (mm) of restrained shrinkage ring-shaped test apparatus according to the ASTM standard: (a) plan view (b) section view (Gesoglu *et al.,* 2006)

2.5.4.3 Factors associated with shrinkage

There are a number of factors and properties that can be measured and observed to evaluate and predict shrinkage and shrinkage induced cracking of concrete repair overlays.

Evaporation

The rate of evaporation has a direct effect on shrinkage with an increase in evaporation resulting in higher shrinkage values. Moisture loss of specimens is measured by calculating the change in mass of the specimen over a period of time (Banthia & Gupta, 2008, Almusallam *et al*., 1998 and Topcu & Elgun, 2003).

Bleeding

Bleeding occurs as mix water rises to the surface of the concrete. This mechanism has been shown to directly affect plastic shrinkage by replenishing moisture that is lost to the environment form the surface of the material, and therefore delaying the onset of plastic shrinkage cracking. Bleeding can be tested by casting the specimen in a bleeding bucket according to the specifications in the ASTM C232. This allows bleed water to be collected and measured until bleeding has stopped (Almusallam *et al*., 1998)

Bleeding can also be tested using a napkin, which is pre-weighed and then used to absorb water on the surface of the concrete before it is then weighed again. Bleeding is calculated by measuring the difference in weight of the napkin (Topcu & Elgun, 2003)

Early age strain

Early age strain values for concrete overlays can provide direct measurements of the resulting tensile strains that cause cracking. Strain measurements can be conducted using strain gauges that are cast within the specimens. However, these readings have been shown to be unreliable as the bond between the fresh concrete and the strain gauge is not always consistent and results in a varying accuracy of results (Banthia & Gupta, 2008).

Cracking

Crack analysis and time to first crack are methods of analysing the effects and magnitude of shrinkage that have been used extensively in the literature.

Crack analysis is based on measuring one or more of the following crack characteristics at regular time intervals (Banthia & Gupta, 2008):

- Crack area
- Average crack width
- Maximum crack width
- Number of cracks
- Time to first crack

This analysis is done by intensive observations and with the aid of specialised equipment such as high magnification microscopes (Banthia & Gupta, 2008, Almusallam *et al*., 1998 and Gesoglu *et al.*, 2006). Specialised image analysis software can also be used to constantly monitor crack propagation and development over time (Banthia & Gupta, 2008)

2.5.5 Influence of shrinkage on bonded concrete overlay performance

The volume changes in the overlay repair material that are associated with shrinkage, and in particular drying shrinkage are considered the key source of deformation associated with bonded concrete overlay failure (Beushausen & Alexander, 2006b, Granju *et al.*,2004, Rahman *et al.*,2000, Weiss *et al.*, 1998 and Yuan *et al.* 2002).

These deformations are restrained by the substrate, resulting in residual stresses in the repair material. If these induced stresses are sufficient to overcome the tensile strength of the overlay repair material, this will result in the development and propagation of cracks. This process has been discussed in detail in 2.3.

It is important to note that the intrinsic and extrinsic factors discussed in this section, which relate to drying shrinkage deformation, are usually limited to examining the effects of this volume change on the total strain of concrete specimens and samples as a whole. With regard to the performance of bonded concrete overlays, addressing drying shrinkage on this 'global' scale can be effectively used to analyse the mechanisms associated with debonding failure, as this occurs as a result of 'global' volume changes in the entire bonded overlay. However, as cracking failure occurs on a very 'local' scale within the concrete matrix, it is important to consider shrinkage strain within the cement paste around the area of cracking failure, and how the inclusion of coarse aggregate particles affects the localised stress development.

Sufficient understanding of the different mechanisms and factors that influence the shrinkage of repair materials on a 'global' and 'local' scale is therefore imperative to understand and determine the success or failure of bonded concrete overlay repair materials.

2.6 Creep and tensile relaxation

The effects of creep have been shown to reduce the stress induced by shrinkage in bonded concrete overlays. However, Carlswärd (2006) and Alexander & Beushausen (2009) suggest that this effect on overlay materials is rather directly linked to a reduction in stress associated with tensile relaxation.

Creep is defined as the time dependant increase in strain of a particular body under a sustained stress. Tensile relaxation is defined by Alexander & Beushausen (2009) as the time dependant decrease in the stress of the body under sustained strain (Figure 2.13). Chilwesa (2012) explains that both creep and relaxation are functions of the visco-elasticity of the material sourced in the cement paste and therefore tend to be addressed by researchers as the same mechanism, despite the obvious difference.

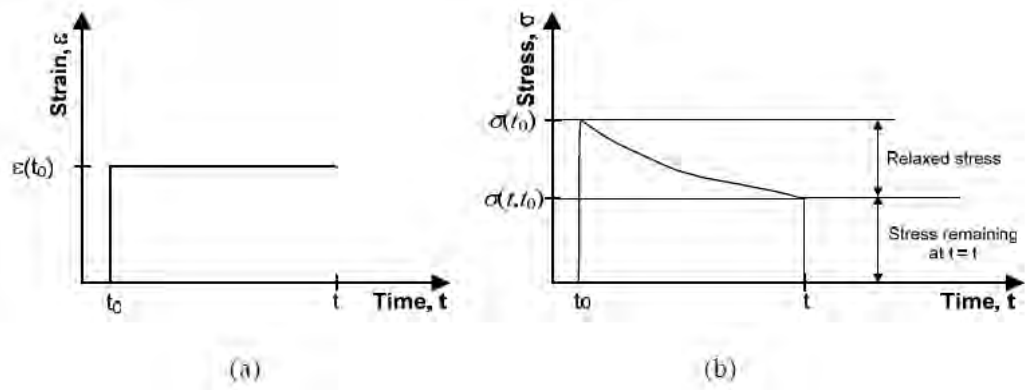

Figure 2.13: Relaxation of concrete stress under constant strain (Carlswärd, 2006)

There are number of different views on the actual internal mechanisms that influence tensile relaxation and creep.

Chilwesa (2012) reviewed a number of these theories, with Powers (1968) suggesting that creep is linked to the movement of load bearing water through diffusion mechanisms while Feldman & Sereda (1968) rather attribute creep and relaxation to movement of interlayer water within the cement gel.

In general, most experts agree that creep in tension is approximately equal to creep in compression for similar stress/shrinkage ratios (Gutch, 2002 and Yuan & Marsszeky, 1994). However, Kordina *et al*. (2000) found that tensile stress relaxation was significantly greater, when compared to compressive stress relaxation. This was attributed to the influence of microcracking, which forms when restrained stress conditions reach a magnitude close to the tensile strength of the concrete. This is supported by work done by Pigeon & Bissonnette (1999) who also highlighted the importance of the influence of microcracking when dealing with tensile relaxation.

In tensile relaxation tests conducted by Morimoto & Koyanagi (1995) it took only 2 to 3 hours to reach ultimate tensile relaxation values, with the relaxation rate decreasing with age. This was found to be irrespective of the stress to strength ratio which was varied in this investigation. However, work by Kordina *et al.* (2000) suggests that ultimate relaxation can take up to 2 days to achieve.

The magnitude of tensile relaxation has been investigated extensively (Kordina *et al.*, 2000, Morimoto & Koyanagi, 1995, Beushausen & Alexander, 2005 and Gutsch & Rostasy, 1995). Findings from these investigations suggest that tensile relaxation can relieve between 35 to 60% of the initial tensile stress. This can therefore have a profound effect on the performance of restrained repair materials.

2.6.1 Factors influencing tensile relaxation

2.6.1.1 Intrinsic factors

Tensile relaxation has been shown to be significantly dependent on the w:c ratio of the concrete. Work by Beushausen *et al*. (2009) and Masuku (2009) investigated the influence of varying w:c ratios on the tensile relaxation of cementitious mortars, and it was shown that an increase in the w:c ratio will result in an increased magnitude of relaxation (Figure 2.14).

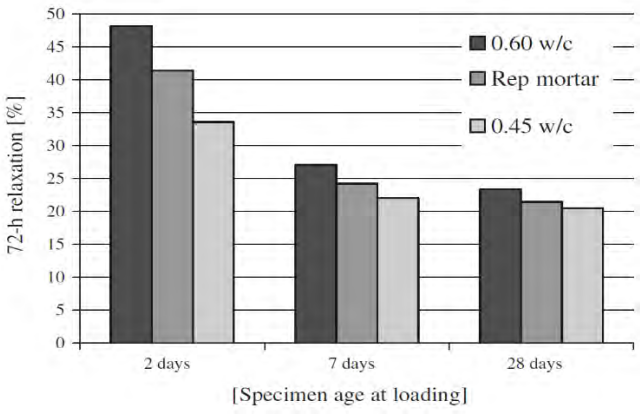

Figure 2.14: Summary of 72 hour tensile relaxation values for all specimens (Beushausen *et al*., 2009)

This influence of w:c ratio on the tensile relaxation of concrete was attributed to the reduced pore structure associated with lower w:c mixes. Beushausen *et al*. (2009) explains how lower w:c mixes are stiffer by nature and therefore more resistant to relaxation mechanisms.

Alexander & Beushausen (2009) also highlight the important influence of moisture content on creep and relaxation. As has been discussed previously, creep is associated with the presence of mobile water in the cement paste which is directly influenced by the moisture content and the drying conditions of the concrete. Creep of cement paste has also been shown to be influenced by cement composition, with higher creep levels being associated with low C_3S content and higher C_3A contents (Mindess & Young, 1981). There are varying views on the influence of extenders and admixtures on creep, with no definitive outlook being presented.

The view of many researchers is that, as the mechanisms associated with creep are the same for relaxation, it will therefore also be affected by the function of dilution and restraint provided by coarse aggregates. This is discussed by Troxell *et al.* (1958) who suggests that the effect of aggregate on concrete creep is the same as that on drying shrinkage. This would confirm findings by Alexander & Beushausen (2009) and Alexander & Mindess (2005) which show that an increase in coarse aggregate volume, size and stiffness will also reduce concrete creep and relaxation. The effect of aggregate stiffness on concrete creep is shown in Figure 2.15.

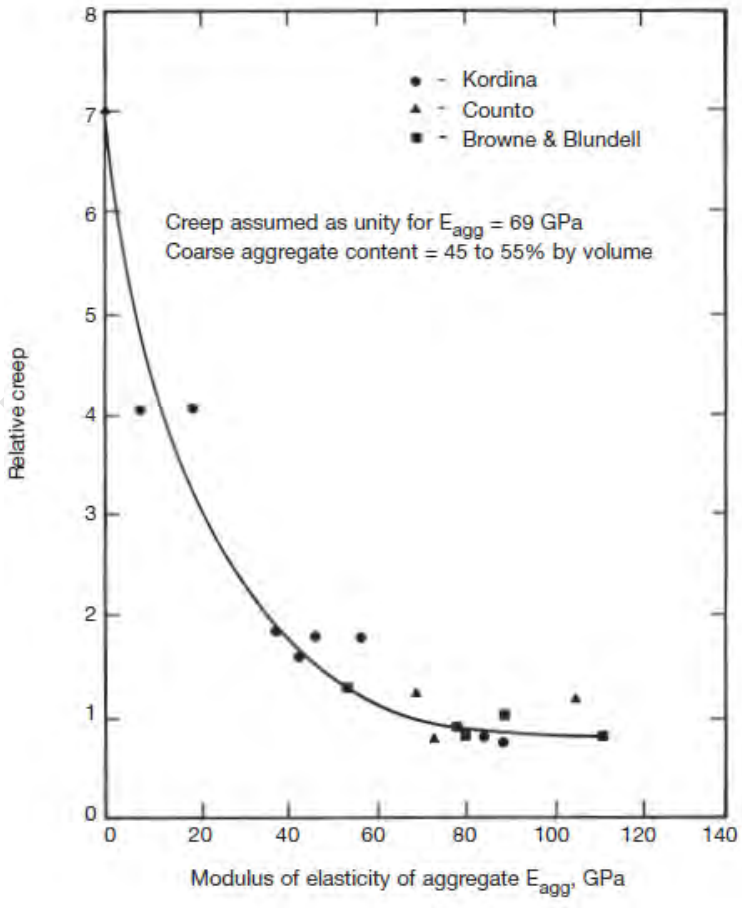

Figure 2.15: The effect of aggregate stiffness on the creep of concrete (Alexander & Beushausen, 2009)

However, as previously discussed with regard to the influence of coarse aggregate on volume changes caused by drying shrinkage, it is noted that the influence of dilution and restraint of coarse aggregate on creep and relaxation is also only examined on a 'global' scale that considers the creep or relaxation strains on the concrete specimens and samples as a whole. As cracking failure occurs on a 'local' scale within a small portion of the concrete matrix, it is important to consider the effect of paste creep or relaxation strains on this more specific level.

It is on this 'local' level that a definitive difference between creep and tensile relaxation is noted by Kordina *et al*. (2000), which pertains to the development of microcracks, resulting in an overall increase in tensile relaxation. Kordina *et al*. (2000) explains that this phenomenon does not occur during concrete creep or compressive relaxation, suggesting that it is specific to tensile relaxation.

This ties in with the concepts of tensile strain softening as a result of microcracking around aggregate inclusions discussed by Chiaia *et al.* (1998) and Wittmann (2002), who suggest a direct relationship between coarse aggregate size and content and the level of strain softening. It is therefore suggested that the influence of coarse aggregate on tensile relaxation relates to both the degree and magnitude of microcracking, on a very 'local' scale within the aggregate/paste matrix, and the functions of dilution and restraint to the concrete as a whole on a 'global' scale.

As higher levels of tensile relaxation have been shown to induce 'stress relief' and prolong time to first cracking of bonded concrete overlays, the complex effect of coarse aggregate on the magnitude of tensile relaxation is profound.

2.6.1.2 Extrinsic factors

The research by Beushausen *et al*. (2009) and Masuku (2009) also investigated the influence of the age at loading on the magnitude of tensile relaxation. Specimens were tested at either 2 or 7 days and it was found that the specimens loaded at 2 days had 15% more relaxation than those loaded at 7 days. Relaxation was therefore found to reduce as the age at loading was increased. Chilwesa (2012) explains that this is attributed to the influence of the degree of hydration on the level of tensile relaxation of concrete. This is supported by work done by Neville (1996).

Carlswärd (2006) suggests that the rate of creep will also decrease as the rate of drying increases, which is particularly relevant to bonded concrete overlays due to their geometry (volume:surface ratio). This is linked to the idea that a decrease in moisture content in the concrete will result in a decrease in the magnitude of creep.

Therefore, creep is influenced by the environmental surroundings of the concrete, as creep deformations have been shown to increase with an increase in temperature and an increase in relative humidity. For concrete loaded at younger ages, this is usually offset by an increased rate of strength development that is also associated with higher temperatures.

2.6.2 Modelling creep and tensile relaxation

A vast number of prediction models have been developed for creep. Alexander & Beushausen (2009) warn that due to the complexity of factors that influence creep it is very difficult to achieve a prediction model that will provide accurate predictions for all situations. The BS 8110 and SANS10100-1:2000 Models are highly simplistic and produce a predicted final (30 year) creep strain based on elastic strain and the modulus of elasticity at the age of loading. The ACI 209R-92 Model is also relatively simplistic and based on coefficients that cover the major factors that influence creep.

This level of accuracy is usually found to be appropriate for the majority of concrete structures, but is too broad for the level of accuracy required for this investigation. More advanced Models are presented in the CEB-FIP Code 90, the BS EN 1992:2001 and the RILEM Model B3 which are based on a more thorough synthesis of contributing factors.

The Models proposed in the CEB-FIP Code 90 and the BS EN 1992:2001 are based on the work done by Westman (1999) and have been shown to have a high level of accuracy (approx. 15%).

In this Model, an initial creep coefficient $\psi(t, t_0)$ is calculated which is based on factors that consider compressive strength, the age of concrete at loading and the duration of the load. Environmental factors such as relative humidity and temperature are also considered to improve accuracy:

Inputs:

f_{cm} = 28 day cylinder compressive strength (MPa)
RH = Relative Humidity (%)
T = Temperature (°C)
t = time from load application (days)
t_0 = age of concrete at load application
h_0 = notional size (m) = $2A_c/u$
A_c = concrete cross section (m^2)
u = perimeter of concrete in contact with the air (m)

Creep coefficient $\psi(t, t_0) = \psi_0 . \beta_c(t - t_0)$ (2.19)

Notional creep coefficient $\psi_0 = \psi_{RH} . \beta(f_{cm}) . \beta(t_0)$ (2.20)

$$\psi_{RH} = 1 + \left(\frac{1 - RH/100}{(0{,}1.h_0)^{1/3}}\right) \quad \text{for } f_{cm} \leq 35 \text{ MPa} \quad (2.21)$$

$$\psi_{RH} = \left(1 + \left(\frac{1 - \frac{RH}{100}}{(0{,}1.h_0)^{\frac{1}{3}}}\right) . \alpha_1\right) . \alpha_2 \quad \text{for } f_{cm} \geq 35 \text{ MPa} \quad (2.22)$$

$$\alpha_1 = \left(\frac{35}{f_{cm}}\right)^{0,7} \quad (2.23) \qquad \alpha_2 = \left(\frac{35}{f_{cm}}\right)^{0,2} \quad (2.24)$$

Factor to consider compressive strength $\beta(f_{cm}) = \frac{5{,}3}{\sqrt{f_{cm}}}$ (2.25)

Factor to consider the age of concrete at loading $\beta(t_0) = \frac{1}{0,1+{t_0}^{0,2}}$ (2.26)

Factor to consider the duration of the load $\beta_c(t - t_0) = (\frac{(t-t_0)}{\beta_H+(t-t_0)})^{0,3}$ (2.27)

$\beta_H = 1{,}5.h_0.(1 + (1{,}2.\frac{RH}{100})^{18}) + 250 \leq 1500$ for $f_{cm} \leq 35$ MPa (2.28)

$\beta_H = 1{,}5.h_0.(1 + (1{,}2.\frac{RH}{100})^{18}) + 250.\alpha_3 \leq 1500.\alpha_3$ for $f_{cm} \geq 35$ MPa (2.29)

$\alpha_3 = (\frac{35}{f_{cm}})^{0,5}$ (2.30)

Once the creep coefficient has been determined, a creep function $J(t, t_0)$ can be determined using the equation developed by Westman (1999). This equation relates the creep coefficient to the elastic deformation at 28 days $E_c(28d)$ and the modulus of elasticity at the time of loading $E_c(t_0)$:

$$J(t, t_0) = \frac{1}{E_c(t_0)} + \frac{\psi(t,t_0)}{E_c(28d)} \quad (2.31)$$

However, the function $J(t, t_0)$ that has been determined relates specifically to concrete creep. It has been previously discussed that, although concrete relaxation is the result of the same mechanical process within the concrete paste, it will be different in magnitude and nature. The 'effective modulus method' provides a simple conversion from a creep function $J(t, t_0)$ to a relaxation function $R_c(t, t_0)$:

$$R_c(t, t_0) = \frac{1}{J(t,t_0)} \quad (2.32)$$

According to Carlswärd (2006) this method has been shown to give acceptable results, specifically when loads are applied to more mature concretes. More detailed conversion methods have been developed such as the 'age adjusted effective modulus approach', but require complex computer software to be effectively utilized.

The RILEM Model B3 is similar in nature to the CEB-FIP Code 90 and the BS EN 1992:2001 and also incorporates both extrinsic and intrinsic variables that affect creep. However, research reviewed by Alexander & Beushausen (2009) suggests that the RILEM Model B3 was shown to significantly under predict creep strains for 30MPa concretes and only showed a moderate accuracy for 50 MPa concretes.

2.6.3 Testing relaxation

A method for testing concrete relaxation directly is described by Beushausen *et al.* (2012) and Chilwesa (2012). The method uses test specimens that are dog-bone shaped prisms with a cross-sectional area of 40x40 mm. Testing was conducted using a Zwick Roell Universal Testing Machine with a maximum capacity of 20 kN. See Figure 2.16.

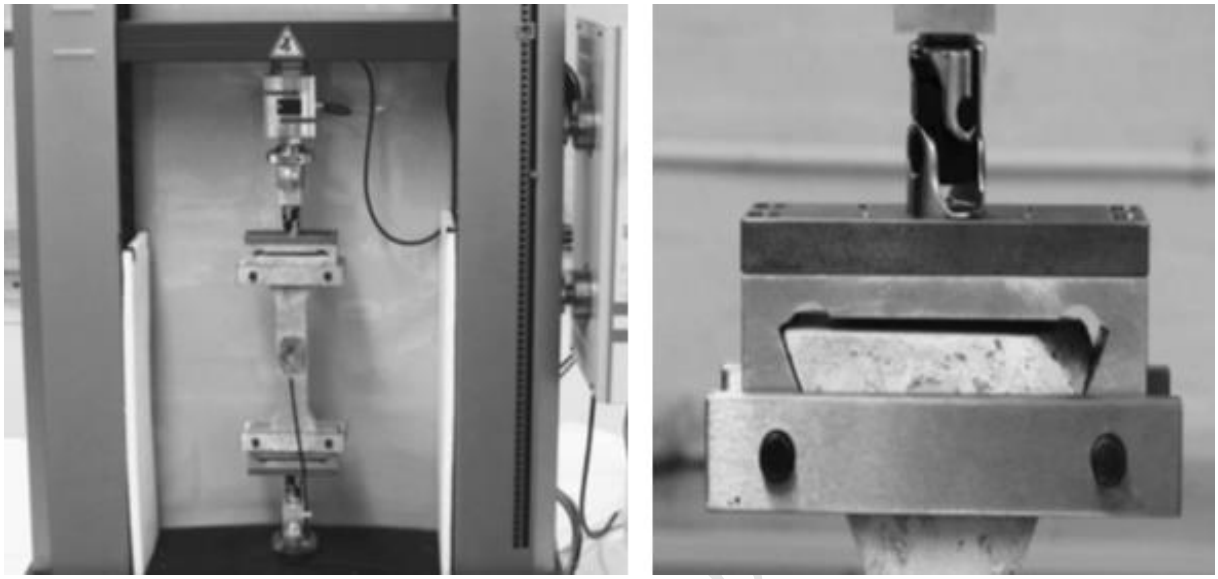

Figure 2.16: Specimen in Universal Testing Machine and detail of gripping arrangement (Beushausen *et al*., 2012)

A constant deformation was applied to the specimen, which corresponded to roughly 80% of the tensile strength of the mortar at the beginning of the test. Specimen geometry and test apparatus configuration were designed to ensure that the load passed directly through the centre of the specimen. The gripping jaws at each end were also braced to mitigate the effects of deformation and jaw widening. A swivel bearing was also used to minimize the effect of eccentricity on the applied load.

The investigation by Beushausen *et al.* (2012) measured tensile relaxation by using the Zwick Roell Universal Testing Machine to record the decay in stress exerted on the specimen. External electronic strain gauges were attached to the specimens used to monitor the imposed strain in a more accurate manner than the output provided by the test machine.

2.6.4 Influence of tensile relaxation on bonded concrete overlay performance

There are a number of key time-dependant properties that play an important role in the generation of restrained stresses in bonded concrete overlays. Tensile stress relaxation has been shown to be one of the most important influencing properties that affect stress development in concrete repair material subjected to these restrained deformations.

The resulting 'stress relief' that is associated with tensile relaxation, and is illustrated in Figure 2.5, can significantly reduce the residual shrinkage tensile stresses that are caused by restrained volume changes. This 'stress relief' can significantly extend the time taken for the residual shrinkage tensile stresses to exceed the intrinsic tensile strength of the repair material and therefore prevent of prolong the time to overlay cracking failure.

Improved bonded concrete overlay performance is therefore associated with repair materials that are characterised by a higher level of tensile relaxation.

2.7 Elastic modulus

Alexander & Beushausen (2009) define concrete elastic modulus as the ratio of uniaxial stress to the resultant axial strain. This represents the materials stiffness. This stress-strain relationship is linear for the first 30 to 40% of ultimate strength, before microcracking in the paste and ITZ result in non-linear behaviour.

The stiffness (elastic modulus) of the repair material is an important property that must be considered, as it directly affects the load-sharing capacity of the concrete overlay and can influence the degree and magnitude of restraint exerted on the repair material.

2.7.1 Factors influencing elastic properties

The elastic modulus of concrete is highly dependent on factors that influence the individual stiffness of the three concrete phases, namely: the paste phase, the aggregate phase and the interfacial transition zone (ITZ) between the paste and the aggregate (Alexander & Beushausen, 2009 and Alexander & Mindess, 2005).

As the elastic modulus of concrete is directly proportional to the stiffness of the individual phases, it is proposed by Alexander & Beushausen (2009) and Alexander & Mindess (2005) that the greater the volume concentration of the stiffer phase, which is usually the aggregate, the greater the resulting concrete elastic modulus. It has been shown that actual concrete strength has a relatively minor contribution to the concrete elastic modulus, with the aggregate stiffness having the major contribution. The nature of the interfacial transition zone (ITZ) between the hardened cement paste and the aggregate will also have a significant effect on the stress-strain relationship of the concrete (Alexander & Mindess, 2005).

A study was conducted by Alexander & Davis (1991) to determine the effect of coarse aggregate and fine aggregate on the elastic behaviour of concretes and mortars. It was shown that some coarse aggregates such as granites have very little stiffness-enhancing effect while other, stiffer, coarse aggregates such as andesite and dolerite have a significant effect and increase the elastic modulus considerably.

It can therefore be seen that the elastic deformation of concrete is highly dependent on the specific aggregate elastic properties and will therefore be significantly affected by changes in aggregate content and type.

Alexander & Beushausen (2009) explains that the influence of cement type and the use of extenders on elastic modulus is complex and no significant influence is noted.

2.7.2 Modelling elastic modulus

Many simple, more commonly used, prediction models for elastic modulus are based on a relationship between elastic modulus and compressive strength. However, Alexander & Beushausen (2009) and Alexander & Mindess (2005) have suggested that many of the factors that influence the modulus of elasticity of concrete do not always have the same influence on concrete strength.

This is supported by work by Kaplan (1959) who showed that different aggregate and mix proportions will have varying effects on concrete strength and elastic properties. Some of these compressive strength based prediction models have included components that partially account and adjust the outputs to include the influence of aggregate.

The SANS 10100-1:2000 prediction model is based on the BS 8110 which relies on a relationship between cube compressive strength ($f_{cu,28}$) and elastic modulus. The model does accounts for the major influence of aggregate through the inclusion of an aggregate stiffness factor (K_0) based on the particular aggregate elastic modulus and a coefficient (α) based on aggregate type.

$$E_{c,28} = K_0 + \alpha . f_{cu,28} \tag{2.33}$$

The ACI 318M-05 and the BS EN 1992:2004 prediction models are also based on a compressive strength to elastic modulus relationship, but account for the influence of aggregate through the inclusion of a density term and percentage adjustments respectively.

The CEB-FIP Model makes no allowance for the influence of aggregate on the elastic properties of the concrete.

Another method that is discussed by Baalbaki *et al.* (1992) is the use of composite material formulas that have been developed to estimate the elastic modulus of concrete based on the individual characteristics of its components. A number of these formulas have been developed and combine the modulus of elasticity of the coarse aggregate (E_a) and the mortar (E_m), as well as the volumetric percentages of the coarse aggregate (g_a) and the mortar (g_m).

The Voigt Model and Reuss Model are grounded on the continuum micromechanics of composites and based on the idea that strains and stresses are constant in a composite respectively (Dantu, 1957).

$$E_{c_{Voigt}} = E_m . g_m + E_a . g_a \tag{2.34}$$

$$1/E_{c_{Reuss}} = \frac{g_m}{E_m} + \frac{g_a}{E_a} \tag{2.35}$$

These models are also referred to as Dantu‘s upper and lower bound theorems with the Voigt Model giving the highest predicted elastic values and the Reuss Model giving the lowest predicted values (Dantu, 1957). It is suggested that the upper bound model is more relevant to a hard aggregate in a soft paste matrix, while the lower bound model is more accurate for a softer aggregate in a stiffer paste matrix.

The Hirsch-Dougill Model was developed and combined the upper and lower bound theorems. However, both the Hirsch-Dougill Model and the Reuss Model predict an $E_c = 0$ when $E_a = 0$. Counto (1964) was able to overcome this problem and developed the Counto Model which provided an effective combination of the upper and lower bound theorems.

$$1/E_{c_{Hirsh}} = 0{,}5.\left(\frac{1}{E_{c_{Voigt}}} + \frac{1}{E_{c_{Reuss}}}\right) \tag{2.36}$$

$$1/E_{c_{Counto}} = \frac{1-\sqrt{g_a}}{E_m} + \left(\frac{1-\sqrt{g_a}}{\sqrt{g_a}}.E_m + E_a\right)^{-1} \tag{2.37}$$

An even more involved composite model is proposed by Zheng *et al*. (2006), that attempts to model the three phases of concrete (aggregate, paste and ITZ) at a mesoscopic level. A three-phase composite model for the elasticity of concrete was developed. This model was shown to be accurate, but is highly complex.

It can be noted that the range of accuracy and level of complexity of elastic modulus prediction models is widespread. The combination of accuracy and practicality must therefore be considered when selecting an appropriate elastic modulus prediction model.

2.7.3 Testing elastic modulus

It is suggested that most elastic modulus values are derived from static tests (Alexander & Beushausen, 2009).

No SABS test methods exist to determine the static elastic modulus, however the method outlined in BS 1881-121:1983 or the ASTM C 469-02 is generally used. These tests allow the initial tangent modulus (Young's) and the secant modulus corresponding to one third of the compressive failure stress to be calculated (Alexander & Beushausen, 2009). The tests involve loading a standard sample cylinder or prism at a constant rate, while measuring the load and deformation. A number of cycles are carried out, stressing the concrete to one third of its ultimate load for two to five minutes. This reduces the effects of creep and small shrinkage cracks (Alexander & Beushausen, 2009). A similar procedure is used for the ASTM C 469-02 method, except that the concrete sample is stressed to 40% of its ultimate stress and an extensometer is used to record deformation.

A stress strain curve can then be obtained and used to calculate the modulus of elasticity.

The use of vibrating wire strain gauges to monitor the long-term performance of concrete repairs can also be used effectively. These readings can then be combined with loading information to calculate the elastic modulus (Mangat & O'Flaherty, 2000).

2.7.4 Influence of elastic properties on bonded concrete overlay performance

The influence of elastic properties on bonded concrete overlay performance is often overlooked by researchers.

It has been found that many standards and specifications for the elastic modulus of repair materials do not properly take into account the structural interaction between the substrate and repair materials with regard to elastic properties (Mangat & O'Flaherty, 2000). The compatibility between repair and substrate concrete elastic properties is considered a key factor contributing to the prevention of overlay cracking.

A number of different views are held with regard to the preferred relationship between substrate elastic modulus (E_s) and the repair material elastic modulus (E_r). Work by Emberson & Mays (1990) suggests that the elastic properties of the repair material and the substrate must be within 10 GPa of one another. However, a more recent study by Mangat & O'Flaherty (2000) has shown that effective repairs are achieved when $E_r \gg E_s$. This is attributed to the stiffer repair material achieving a better strain transfer to the substrate during the shrinkage period and therefore reducing restrained shrinkage tension in the repair material. However, these findings may be influenced by reduced shrinkage levels that are associated with the stiffer repair mixes.

The influence of the elastic properties of the repair material must also be considered with regard to the residual stresses induced by restrained shrinkage. Repair materials that are more elastic have shown to reduce this induced residual stress and therefore prevent or prolong the time to first cracking. This influence is evident and accounted for in the overlay prediction models examined in this chapter.

2.8 Analytical modelling of overlay cracking

A number of different systems have been developed to model and predict shrinkage cracking of concrete overlay materials.

Many of these systems are based on using different methods to model stresses and strains in the repair material which can then be used to predict and analyse shrinkage cracking.

2.8.1 Evaluation of existing analytical models

In the investigation presented by Beushausen & Alexander (2006a), existing analytical models for predicting strains and stresses in bonded overlays were analysed and evaluated. Experimental work was conducted to aid in this evaluation by providing comparative measured results.

Beushausen & Alexander (2006a) explain that the analytical theories and models presented by Evans & Chung (1967), Klopfer (1987), Haardt (1991), Yuan & Marsszeky (1994), Alonso (1997) Yuan et al. (2002), Bernard (2000) and Denarié & Silfwerband (2004) are all based on simple beam theory which was originally conceptualised by Birkeland (1960). These models attempt to model differential shrinkage stresses between the overlay and the substrate based on the concept of a constant direct strain.

This constant direct strain that is assumed in the composite member is based on the following fundamental concepts: the behaviour of composite members adheres to Bernoulli's hypothesis of plane sections remaining plane, an infinite substrate depth combined with a finite overlay depth results in complete overlay restraint and interface shear stresses only develop at the member ends (Beushausen & Alexander, 2006a).

The investigation showed that these existing models based on beam theory are ineffective in modelling overlay strains realistically. It was found that overlay deformations depend less on relative cross-sectional dimensions of the substrate and overlay than was originally assumed, and that the assumptions used in these models do not formulate the correct application of forces to the member.

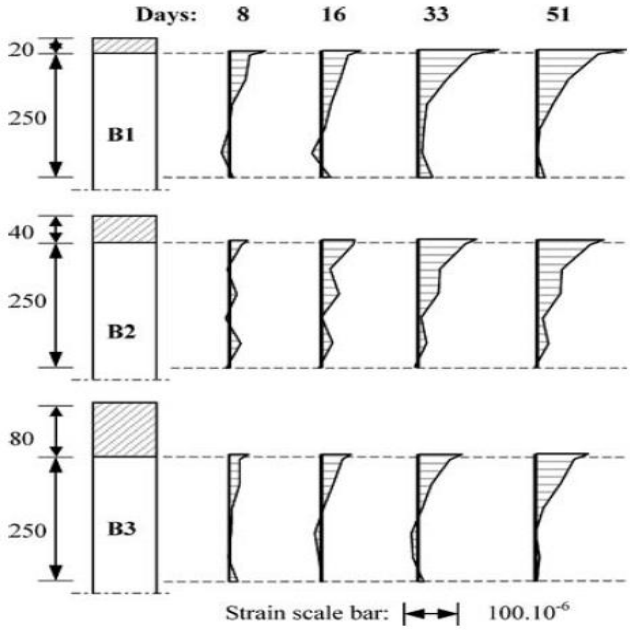

Figure 2.17: Strain distribution across substrate depth (Beushausen & Alexander, 2006a)

This is illustrated in the findings of tests conducted by Beushausen & Alexander (2006a) on overlays of varying depths. The strain distributions shown in Figure 2.17 show that the distribution of strain in the substrate, caused by overlay shrinkage, is in fact non-linear and the effect of overlay thickness is minimal.

A new analytical method is presented by Beushausen & Alexander (2006a) based on localised strain conditions at the interface between the substrate and the overlay.

2.8.2 Localised strain analytical model

The investigation by Beushausen & Alexander (2006a) proposes a new analytical model based on fundamental aspects concerning the localised strain characteristics of bonded overlays. This model is based on the idea that localised strain at the interface between the repair material and the substrate will be at a maximum. Constant shrinkage is assumed throughout the overlay depth and the bond between the overlay and substrate is assumed to be perfect. Curvature, which is also associated with the direct stresses cause by restrained shrinkage, is not considered.

The analytical model developed by Beushausen & Alexander (2006a) is based on the idea that measured strains at the overlay to substrate interface represent the sum of direct elastic strains, strain reduction related to overlay relaxation and substrate creep strains. Each of these strain components is individually modelled and a final combined, time dependant, prediction function is presented:

Inputs:

E_s = Substrate elastic modulus
E_o = Overlay elastic modulus
C_ε = Empirical constant describing the combined influences of member dimensions and strain profiles in the substrate and overlay
ε = Strain
ε_{FSS} = Free shrinkage strain of overlay
ε_{creep} = Creep strain
$\varepsilon_{inst.}$ = Instantaneous strain: strain producing stress in the substrate
$\varphi_s(t, t_0)$ = Creep factor
$\psi(t, t_0)$ = Coefficient expressing visco-elastic stress relaxation

$$\varepsilon_{total,I}(t) = \varepsilon_{inst.,I}(t) + \varepsilon_{creep,S,I}(t) \quad (2.38)$$

$$\varepsilon_{total,I}(t) = \psi(t, t_0).\varepsilon_{FSS}.\frac{1}{1+\frac{E_S}{E_O(t)}.C_\varepsilon+0{,}8.\varphi_s(t,t_0)}.(1 + 0{,}8.\varphi_s(t, t_0)) \quad (2.39)$$

This model was shown to predict results that were reasonably close to those predicted through experimental testing (Figure 2.18) and therefore can be deemed to be effective.

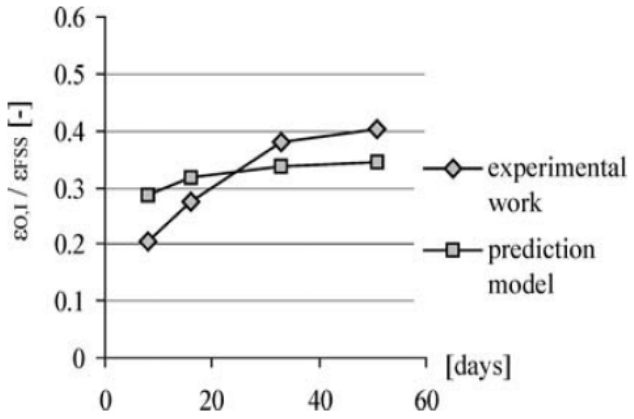

Figure 2.18: Comparison of experimental results and predicted model outputs (Beushausen & Alexander, 2006a)

2.8.3 Material property analytical model

This analytical modelling approach, which was used successfully by Chilwesa (2012), uses the time development of relevant material properties of the overlay to predict time of cracking. Tensile strength is plotted with predicted elastic stress, which is governed by shrinkage, elastic modulus and tensile relaxation, against time to determine the age at which cracking will develop in the overlay. This is illustrated in Figure 2.19.

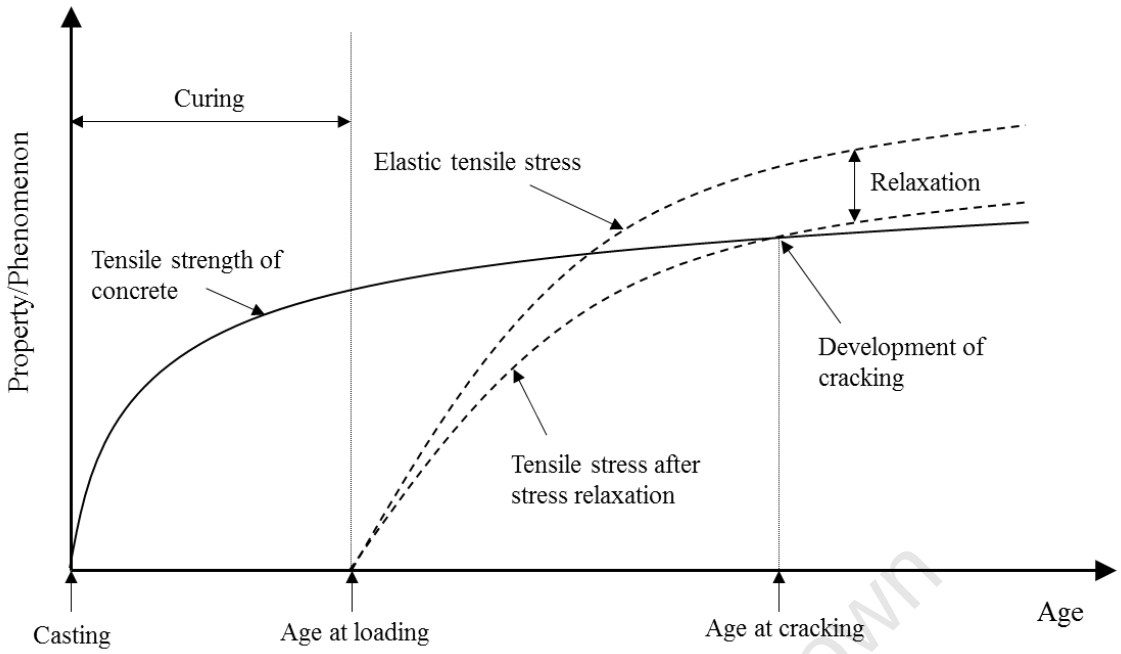

Figure 2.19: Prediction of age at cracking of bonded concrete overlay (adapted from Chilwesa, 2012)

There is no direct method of measuring the elastic stress in a bonded concrete overlay, but it can be accurately estimated from the product of the restrained shrinkage strains and the elastic modulus of the repair concrete (Gilbert, 1988 and Chilwesa, 2012). This can be applied by calculating stress increments using the principle of superposition outlined by Gilbert (1988) and Ghali *et al* (2006).

This method can be further adapted to account for the 'stress relief' due to the effect of tensile relaxation. This is achieved through the introduction of a relaxation factor (ψ). This allows the final remaining stress to be calculated for each increment (Chilwesa, 2012). The final expression for elastic stress increments is shown below:

Inputs:

$\ddot{\sigma}_i$ = Remaining stress at time t_i
$\ddot{\sigma}_{i-1}$ = Remaining stress at time t_{i-1}
$\Delta\varepsilon_i$ = Change in shrinkage in the interval $t_{i-1} - t_i$
E_i = Mean elastic modulus in the interval $t_{i-1} - t_i$
ψ_i = Factor accounting for the magnitude of mean relaxation in the interval $t_{i-1} - t_i$

$$\ddot{\sigma}_i = \ddot{\sigma}_{i-1} + \Delta\varepsilon_i . E_i . \psi_i \qquad (2.40)$$

In the investigation conducted by Chilwesa (2012) parameters used in the analytical model were recorded at 2, 7, 14, 21and 28 days. Regression functions were therefore needed to interpolate the values for the properties on the days when they were not tested. A number of different regression functions were reviewed by Chilwesa (2012) and it was found that logarithmic based regression functions showed the best fit with the experimental results.

A number of key assumptions were made when applying the material property analytical model used by Chilwesa (2012), and are as follows:

The effect of autogenous shrinkage during curing was assumed to be negligible and it was therefore assumed that shrinkage would only occur during the time after curing. However, it was suggested that a more sophisticated approach should consider the effects of autogenous shrinkage.

It has been shown in a number of previous studies that large amounts of tensile stress relaxation develop rapidly after initial loading. This was confirmed by the findings by Chilwesa (2012). As this stress relaxation develops at a much faster rate than the stresses caused by overlay shrinkage, it was assumed, for analytical modelling purposes that the tensile stress relaxation occurs instantaneously after loading. The 72 hour relaxation value was taken as the 'ultimate' value and applied to the model.

Work by Beushausen (2005) showed that the restrained shrinkage of bonded concrete overlays was roughly 60% of the overlay free shrinkage value. It was therefore assumed that the value for restrained shrinkage of the overlay used in the model was 0.6 times the value of free shrinkage measured.

The predicted results from the analytical model used by Chilwesa (2012) were compared with the results from actual overlay specimens that were tested and the model was shown to be highly effective. However, it must be noted that the investigation only compared the prediction outputs with tests conducted on repair mortars. The accuracy of these prediction models with regard to repair concretes that include coarse aggregates has still not been tested and forms a key component of this investigation.

2.9 Conclusion

From the literature it can be seen that there are varying and contradicting views on the links between specific mix design parameters and the resulting overlay properties. A number of parameters have been identified as key aspects of the mix design that contribute directly to overlay cracking. Certain curing and environmental conditions have also been identified as being directly relevant to overlay cracking.

The effects of coarse aggregate size, shape, surface texture, grading and content have been shown to have a significant effect on a number of properties that contribute to overlay crack resistance. It is noted that some of these influences can have a positive effect on one property, but have a negative effect on another with respect to crack resistance. A thorough investigation of their influence is therefore required.

The accuracy of existing prediction models is shown and a number of different analytical models have been examined. A material property analytical model has been proven to be highly effective in predicting overlay cracking for repair mortars using measurable overlay material properties.

This provides a sound literature base for of the experimental plan and research approach presented in the next chapter.

Chapter 3: Experimental details and procedures

3.1 Introduction

Extensive literature has been examined in Chapter 2 with regard to bonded concrete overlays and the concept of cracking due to restrained deformation. Key concrete properties have been identified that pertain to the susceptibility of these overlays to cracking, which relate specifically to the relationship between the tensile stress due to restrained deformation and the tensile strength of the repair concrete. A number of test methods for these relevant concrete properties have been identified in the literature, as well as methods for testing restrained shrinkage cracking directly. As proposed in the Introduction in Chapter 1, the key focus of the experimental component of this investigation is focused on the influence of coarse aggregate volume content and size on the performance of bonded concrete overlay repair concretes. An exhaustive experimental programme has therefore been conducted and is detailed in this chapter.

3.2 Experimental outline

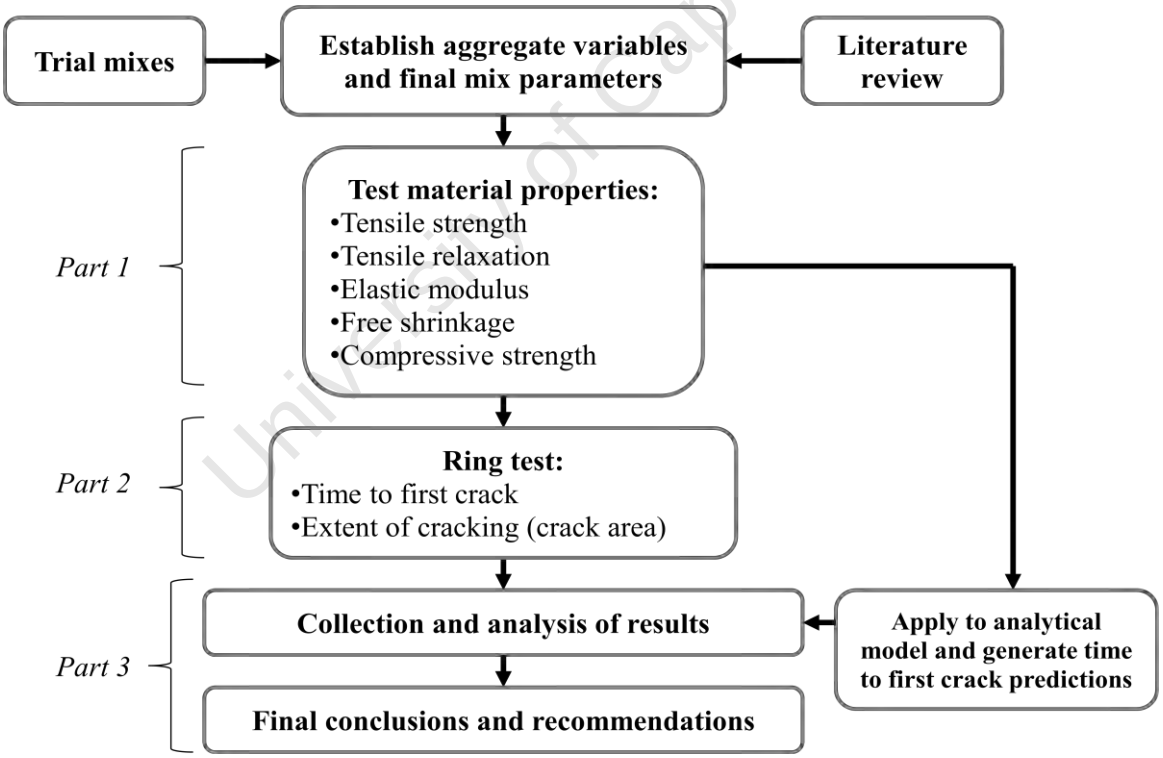

Figure 3.1: Experimental outline

Figure 3.1 provides an outline for the experimental procedure, and illustrates how the components of this experimental program are constructed. Due to the volume of the work and the complexity involved with the scale of testing, it was necessary to divide the program into a number of parts that could be addressed and tested separately before being combined in the form of final results and conclusions. These parts are discussed in detail below.

3.2.1 Defining variables and preparation

The initial component of the experimental program was to establish the key variables that would be investigated. As the focus of this research was aimed at investigating the influence of coarse aggregate on the performance of bonded concrete overlays, specific coarse aggregate variables needed to be selected.

It was determined that the volume of experimental work associated with testing all coarse aggregate variables would be too great for this single investigation and therefore it was decided that this investigation would focus specifically on the influence of coarse aggregate volume content and coarse aggregate size. This decision was based on sound literature findings which cited these two aggregate variables as being highly influential on concrete properties relevant to the crack resistance of concrete overlays.

The next step was to develop mix designs that would provide accurate representations of those commonly used for concrete overlay repairs. It was decided that two laboratory repair mixes and one commercial repair product would be used for this investigation.

Trial mixes

In order to establish specific mix parameters, it was necessary to conduct a number of trial mixes.

The laboratory mixes would be based on mortar mixes used in the investigation conducted by Chilwesa (2012) and had a w:c ratio of 0.45 and 0.6 respectively. However, these mix designs were for repair mortars and the inclusion of a coarse aggregate would have a direct influence on their workability. Modifications were therefore made to these mix designs by applying the following procedure:

- A mortar mix was made based on Chilwesa's (2012) mix designs.
- An appropriate volume content of coarse aggregate was then added to the mortar.
- Cement and water was then added in specific quantities to ensure that there was no change in the w:c ratio of the mix.
- This was done until the mix achieved a satisfactory slump for a repair mortar (approx. 50 mm)

The commercial repair grout had specific instructions from the manufacturer with regard to the inclusion of a coarse aggregate, and therefore no trial mixes were required.

Part 1: Testing repair concrete properties

The first part of the experimental program involved testing specific concrete material properties that have been identified in the literature as dictating the performance of bonded concrete overlays, namely: tensile relaxation, tensile strength, elastic modulus, drying shrinkage and compressive strength.

This allowed the influence of coarse aggregate content and size on specific concrete properties to be compared, as well as providing the necessary data that was used for analytical modelling in Part 3 and is discussed in detail in Chapter 5.

Part 2: Direct testing

Direct testing of overlay concrete cracking using ring tests to test restrained shrinkage formed the basis of Part 2 of the experimental program. This allowed direct parameters such as time to first crack and crack intensity to be measured and then compared with material properties (Part 1) and analytical predictions (Part 3).

Part 3: Analytical modelling and analysis

This part of the study incorporated the analysis of experimental outputs and results, combined with the comparison of analytical prediction outputs with the results of direct testing. Components of this part of the experimental program are presented in Chapter 4, 5 and 6.

3.3 Test materials, conditions and mix designs

The repair materials and practices that were used for the investigation were representative of those available primarily in the Western Cape Province of South Africa.

3.3.1 Coarse aggregate

As discussed above, the key variables tested in this investigation were coarse aggregate volume content and size. Mix designs were therefore constructed with varying coarse aggregate contents and varying maximum aggregate sizes. The same type of aggregate was used for all tests to ensure an accurate comparison. The selection of specific coarse aggregate parameters was therefore fundamentally important for the investigation.

3.3.1.1 Type

One of the key effects of aggregate type that has been identified in the literature is aggregate stiffness, and the influence that this has on the elastic and shrinkage behaviour of concrete. To a certain degree, the effect of coarse aggregate type on particle shape and texture must also be considered, but as the same aggregate type was used for all mixes, this did not affect the comparative value of the results.

It was therefore decided that an aggregate with a mid-range stiffness would be used for this investigation. A crushed Greywacke was selected as an appropriate aggregate type. More commonly known in the Western Cape as Malmesbury Shale, this is a metamorphic rock that has been used extensively as a coarse aggregate for concrete in the region (Grieve, 2009). Greywacke was selected over Granite, which has a similar stiffness, because it generally has a more consistent aggregate quality than Granite. The quality of Granite is significantly affected by the effects of weathering and can be highly variable. Greywacke has an aggregate elastic modulus (Ea) of approx. 72 GPa and a relative density (RD) of 2.71 (Alexander *et al*., 1995).

3.3.1.2 Size

For the purpose of this investigation two maximum coarse aggregate sizes were used to test the effect of aggregate size on the crack resistance of overlays.

A 19 mm and 9.5 mm maximum size aggregate was used in this investigation, as this allowed the influence of aggregate size to be effectively tested.

3.3.1.3 Volume

The volume of coarse aggregate formed the key variable for this investigation. Aggregate volume has been shown in the literature to have a profound effect on all concrete material properties and has been shown to have a significant effect on overlay crack resistance.

Mixes with 25%, 35% and 45% coarse aggregate volume are cast for both maximum aggregate sizes specified above. Mixes with a 0% coarse aggregate volume were also cast for comparison as a control.

3.3.1.4 Grading

Grading has been shown in the literature to have a direct influence on shrinkage, creep, tensile strength, tensile relaxation and the plastic properties of concrete. It was therefore decided that graded coarse aggregate would be used for both the 19 mm and 9.5 mm aggregates.

The SANS 1083 code only provides suggested gradings for nominally single-sized aggregates for maximum sizes ranging from 6.7 mm to 75 mm. The BS 812 code does provide specifications for graded aggregates. However, these specified gradings are only given for grading envelopes for 5 - 20 mm and 5 - 14 mm graded aggregates.

It was therefore decided to use grading envelopes from the ASTM C33 code. A 4.75 - 19 mm grading envelope was used for the larger aggregate size, while a 1.18 - 9.5 mm grading envelope was used for the smaller aggregate size. Figure 3.2 and 3.3 show the respective grading envelopes for each aggregate size and the actual gradings that were used. The grading curve used for the mixes was an average of the specified grading envelope for each aggregate size.

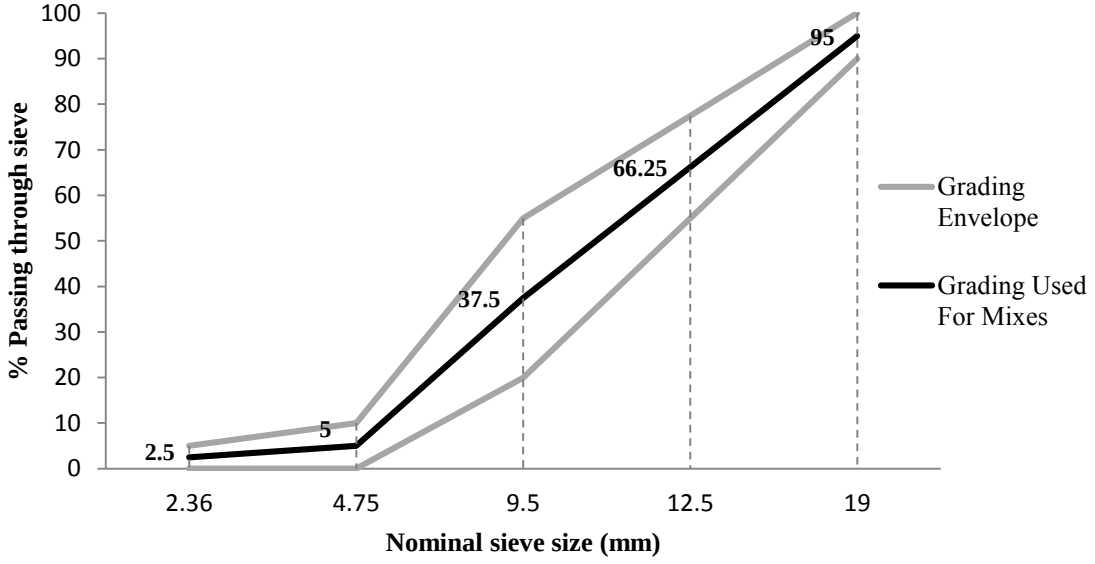

Figure 3.2: 19.0 mm to 4.75 mm Grading Envelope (ASTM C33)

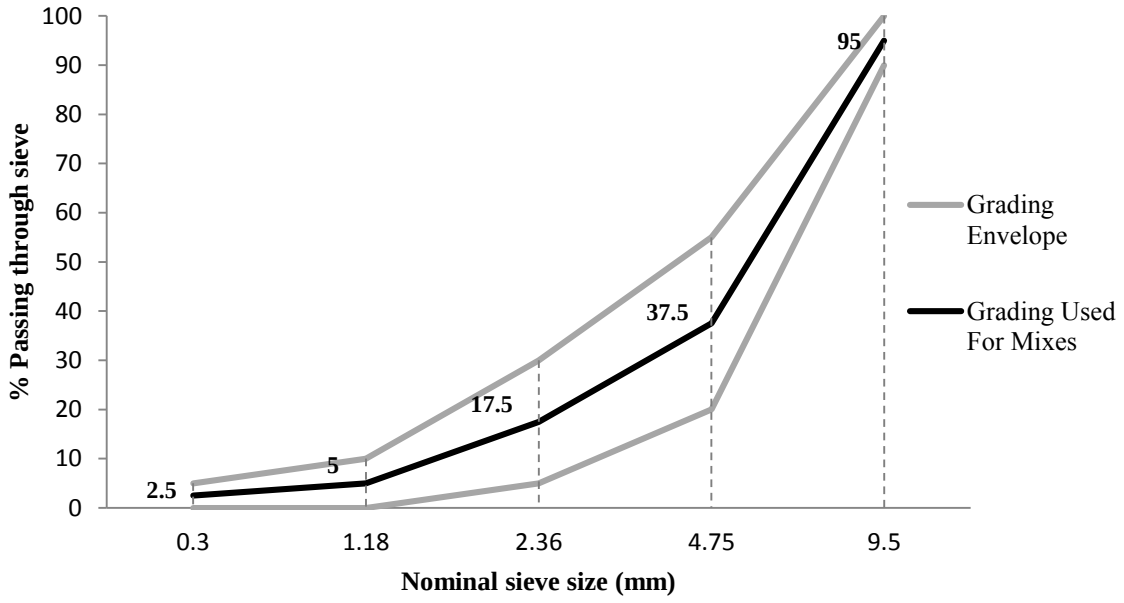

Figure 3.3: 19.0 mm to 4.75 mm Grading Envelope (ASTM C33)

3.3.2 Laboratory mixes

Two laboratory made mix designs were used in this investigation with a w:c ratio of 0.6 and 0.45 respectively. As previously mentioned, these mixes were based on the laboratory mortar mix designs used by Chilwesa's (2012), which represent the normal range of concrete mortars that are commonly used for overlay repairs. The mixes were modified by adding coarse aggregate and reducing the paste content, while ensuring that the w:c ratio remained constant. This allowed for the effective comparison of the effects of the inclusion of varying volume contents and sizes of coarse aggregate. Coarse aggregate and water content for the respective aggregate volume contents were kept constant for both w:c ratio mixes, which are shown in Table 3.1 below.

Table 3.1: Final laboratory mix designs

	Laboratory Mix (w:c = 0.45)				**Laboratory Mix (w:c = 0.6)**			
Aggregate Volume Content (%)	0	25	35	45	0	25	35	45
Water (L/m³)	**250**	**229**	**206**	**180**	**250**	**229**	**206**	**180**
Cement (kg/m³)	556	508	458	400	418	380	343	300
Fine Aggregate (kg/m³)	1490	1034	851	647	1605	1145	950	729
Coarse Aggregate (kg/m³)	**0**	**582**	**865**	**1193**	**0**	**582**	**865**	**1193**
Superplasticiser (L/m³)	1.0	1.0	1.0	1.0	1.0	0.5	0.5	0.5
Paste content (%)	43	39	35	30	38	34	31	27
Mortar content (%)	100	75	65	55	100	75	65	55
Fine aggregate content in mortar (%)	56	50	47	44	60	55	53	49
Slump (mm)	50 ± 10				50 ± 10			

A CEM II/B-M (L-S) 42,5 N with a 20 – 35% limestone and blast furnace slag extender was used for the laboratory mixes. Although literature findings on the influence of extenders on the performance of bonded concrete overlays do contain many contradicting views, this did not affect the experimental results as the same cement type was used for all mixes.

A 50/50 combination of Klipheuwel sand and Philipi dune sand was used as the fine aggregate for the concrete mixes. The Klipheuwel sand is better graded, but more coarse than the Philipi dune sand. The combination of the two fine aggregate types therefore combined to provide a very well graded fine aggregate with a good range in particle size.

Sikament – NN liquid superplasticiser was used for both mixes to ensure that they were able to achieve an acceptable workability with a slump of approx. 50 mm. Although the workability requirements for overlay repair materials can vary considerably, depending on the nature of the repair and the placement method that will be used, it was decided that a slump of approx. 50 mm was required for the repair mixes tested in this investigation.

3.3.3 Commercial product mixes

To enhance the relevance of this investigation to current practices in the concrete repair industry, it was decided that a commercially available repair product would be used for comparison with the laboratory mixes. SikaGrout-212 was selected as the most suitable product for this investigation. It is marketed as a high performance cementitious grout that can be used for concrete overlays to grout cavities, gaps and voids in concrete. SikaGrout-212 is specified as having very high final strengths in both compression and tension, with limited shrinkage, making it an ideal choice for bonded concrete overlays (Sika Product Data Sheet, 2012). The bulking of SikaGrout-212 with coarse aggregates for overlays that exceed 100 mm in depth is suggested by the supplier. Details about the constituents of the SikaGrout-212 are not specified and are therefore unknown.

SikaGrout-212 was mixed according to the manufacturer's instructions that are specified in the Sika Product Data Sheet (2012). The data sheet specified a range for the water content, and as grout is usually flowable, the lowest suggested water content was used to ensure that the mixes would come close to achieving the desired slump. Mixes with varying volumes (0%, 25%, 35% and 45%) of graded 19 mm coarse aggregates were made and compared with the results for the laboratory mixes. SikaGrout-212 mix designs are shown in Table 3.2.

Table 3.2: Commercial mix designs

	Commercial Product Mix			
Aggregate Volume Content (%)	0	25	35	45
Water (L/m³)	261	203	175	143
Premix SikaGrout-212 (kg/m³)	2174	1695	1465	1195
Coarse Aggregate (kg/m³)	**0**	**582**	**865**	**1193**
Mortar content (%)	100	75	65	55
Slump (mm)	60 ± 10			

3.3.4 Curing and test conditions

Specimens were cured for 7 days after demoulding. During this curing time they were covered in wet hessian and plastic sheets to ensure that any moisture loss was kept to a minimum.

The influence of curing conditions on bonded overlay material properties has been highlighted extensively in the literature and it was therefore vitally important that temperature and relative humidity were kept constant for all specimens throughout the duration of curing, storage and testing procedures. Therefore, all specimens (except the tensile relaxation specimens) were cured, kept and tested under strictly controlled conditions, with a temperature of approx. 25 ^{o}C and a relative humidity of approx. 50%.

The tensile relaxation specimens, which were tested outside the controlled environment for 48 hours, were coated in a wax layer to prevent moisture loss during this time.

3.3.5 Summary

A total of fifteen different repair concrete mixes were tested in this investigation to thoroughly examine the influence of coarse aggregate volume and size on the performance of bonded concrete overlays. Due to the extensive nature of the testing program, it was determined that the influence of coarse aggregate size would only be tested using one of the laboratory mixes. The w:c = 0.6 laboratory mix was selected as it was representative of a commonly used repair mix design, with a mid-range w:c ratio. A summary of the mixes tested is shown in Figure 3.4 below:

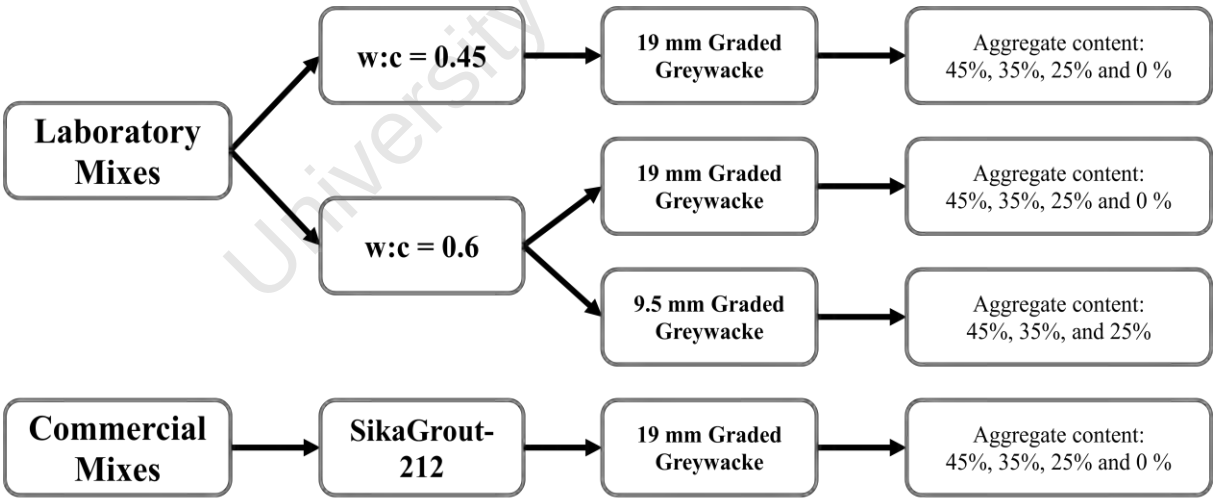

Figure 3.4: Summary of concrete repair mixes tested in this investigation

3.4 Test methods for repair concrete properties

As detailed above, Part 1 of the experimental programme consisted of testing specific concrete properties that were relevant to the performance of bonded concrete overlays.

These tests were conducted in accordance with specific codes and practices that have been reviewed in Chapter 2. However, due to limitations of available equipment and testing devices, some of the test methods used in this investigation were modified and adapted to utilize available resources.

3.4.1 Tensile strength

Tensile strength was tested using notched dog bone specimens with dimensions shown in Figure 3.5. The notches on two opposite sides of the centre of the specimen were created by a protrusions on the respective sides of the dog bone mould and were cast into the specimen to ensure that failure would occur at the same location for all specimens tested.

Cementitious materials are relatively notch sensitive with regard to failure, particularly in tension. Cutting the notches after casting would result in a jagged square notch shape that would contribute to increased stress concentrations around the notch during loading. Cut notches may also pass through larger aggregate inclusions in the material resulting in an increase in notch sensitivity. The influence of notch sensitivity was therefore minimized by casting notches in the specimen and ensuring that the width and depth of the notches were small (1 mm width by 2 mm depth) compared to the specimen dimensions as shown in Figure 3.5. Furthermore, as all tensile specimens were notched, the notch sensitivity would not affect the comparative value of the tensile test results.

The specimens were tested in the Zwick Roell Z020 Testing Machine. Two specimens were tested to failure at ages 7, 10 and 28 days with the average of these two specimens being used.

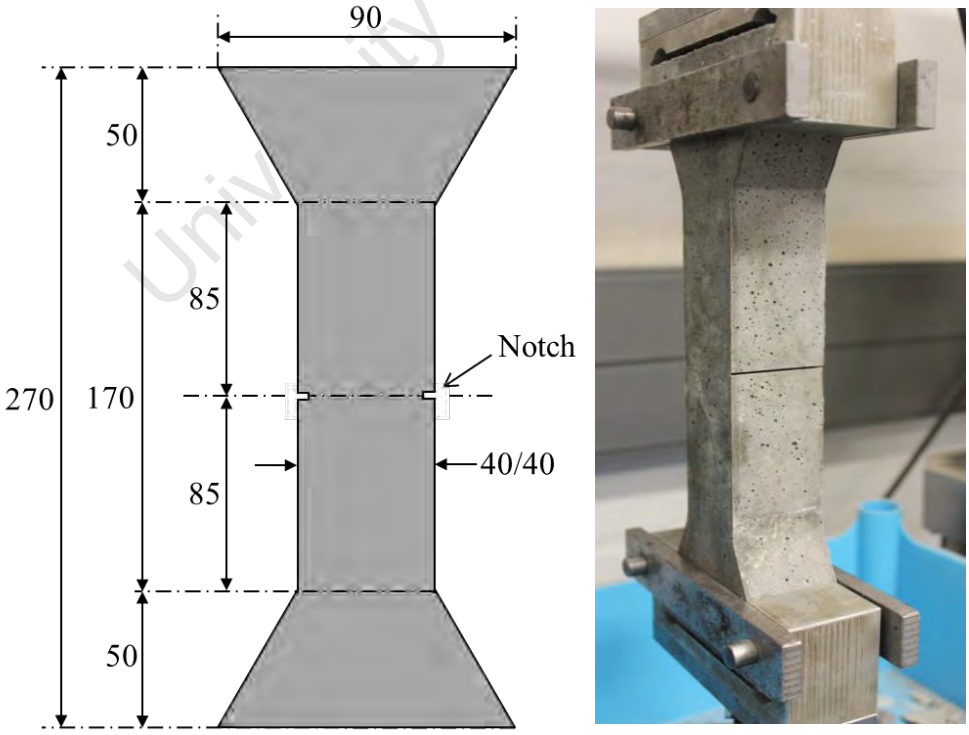

Figure 3.5: Notched dog bone specimen (dimensions in millimetres)

The testing procedure was conducted as follows:

- The specimen was removed from the curing environment or storage in a controlled environment and wiped down. It was ensured that loose material was removed from the specimen as this could have caused unnecessary eccentricity of loading forces when the specimen was placed in the gripping jaws.
- The specimen was then placed into the testing machine and a load was applied by the upper crosshead which moved at a rate of 0.2 mm per minute (approx. 1.2 microstrain per minute) until specimen failure.
- The uniaxial tensile strength was then determined.

3.4.2 Tensile relaxation

Dog bone specimens with the same dimensions as specified for the tensile strength (Figure 3.5) tests were also used to test tensile relaxation. However, the relaxation specimens were not notched as they would not be tested to failure.

Relaxation tests were carried out using the Zwick Roell Z020 Test Machine and the Zwick Roel Z100 Test Machine for a period of 48 hours to determine an 'ultimate' relaxation value.

Two specimens were tested simultaneously in each of the two testing machines for each relaxation test. These tests were conducted at 7 and 28 days. The determination of an 'ultimate' relaxation value allowed all other relaxation values to then be expressed as a percentage of this 'ultimate' value. This 'ultimate' relaxation value was used in the analysis of the results and applied to the prediction model specified in Chapter 5.

The testing procedure was conducted as follows:

- The specimens were removed from the curing environment or storage in a controlled environment and wiped down. The same preparation procedure as discussed for tensile strength above was followed and it was ensured that loose material was removed from the specimen as this could have caused unnecessary eccentricity of loading forces when the specimen was placed in the gripping jaws.
- As the specimens were tested for an extended period of time in the open laboratory environment, they were coated in paraffin wax to ensure no moisture loss would occur during the test.
- The test specimens were then loaded to a stress level that is equivalent to 80% of their ultimate tensile stress at that age. This stress level of 80% of ultimate was selected based on previous work done by Beushausen *et al.* (2012) and Chilwesa (2012). The resulting strain induced by this stress was kept constant and the stress decay was recorded by the test machine.
- After 48 hours the tests were automatically stopped and the final decayed stress value was recorded and compared with the initial stress to determine an 'ultimate' relaxation value.

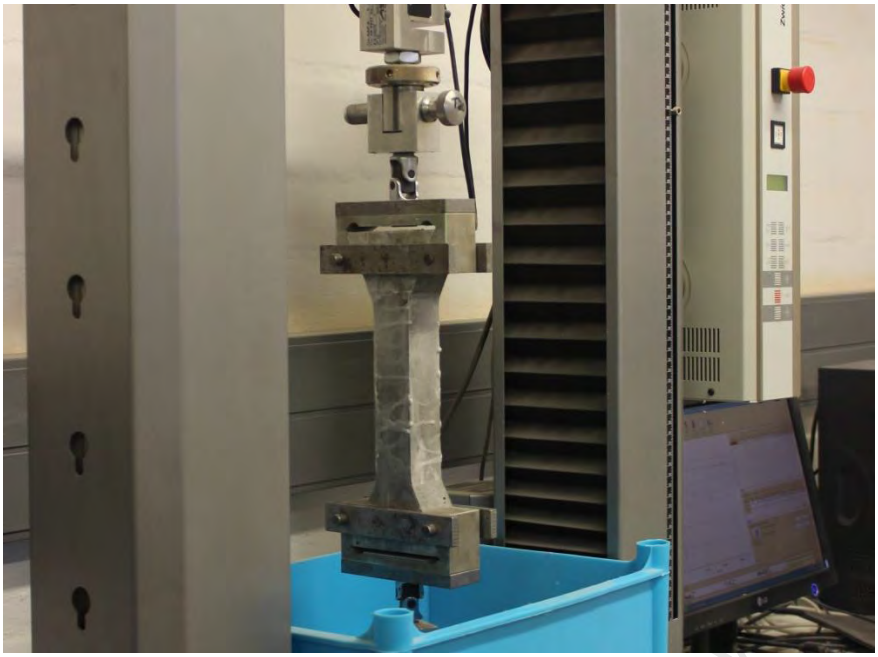

Figure 3.6: Wax coated relaxation specimen being tested in the Zwick Roell Z020 Testing Machine

3.4.3 Elastic modulus

Tests for elastic modulus were carried out using 80 x 150 mm cylindrical specimens. As it was not practically possible to measure the elastic modulus in tension, it was determined that elastic modulus in compression would be tested for this investigation.

It is the opinion of many researchers that the elastic modulus of concrete is very similar in tension and compression, and the use of compressive elastic modulus has been shown to produce accurate results by Chilwesa's (2012).

The tests were conducted using a method that was developed and adapted to make use of the Zwick Roel Z100 Test Machine. The modulus of elasticity was calculated by determining the gradient of the curve in the linear portion of the stress strain curve, from 5% to 20% of ultimate compressive strength at that age. Strain measurements during loading were determined using Demec targets and measured using the Demec strain gauge. Elastic modulus was tested on three specimens at 7 and 28 days.

The testing procedure was conducted as follows:

- The specimens were removed from the curing environment or storage in a controlled environment and wiped down.
- The ends of each specimen were ground with a grinder to ensure that they were smooth and square.
- Brass Demec targets were attached to the specimens using epoxy so that strain readings could be recorded using the Demec strain gauge. As specimens can compress unevenly, pairs of targets, placed 100 mm apart, were placed evenly on three sides of the cylinder to allow circumferential readings to be taken (Figure 3.7).

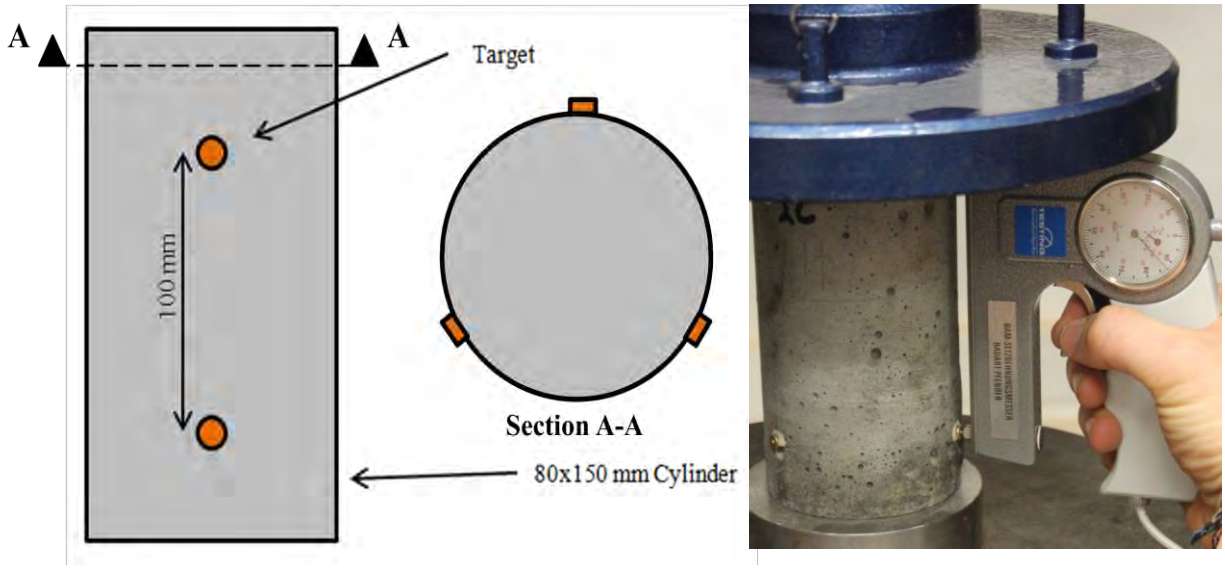

Figure 3.7: Demec target layout on elastic modulus specimens and strain readings being measured using the Demec strain gauge

- The specimen was positioned on a level platen and a swivel head adaptor was used on the top platen of the Zwick Roel Z100 Test Machine to ensure that loading was applied evenly on the specimen.
- The specimen was then loaded to 5% ultimate tensile strength and initial measurements were taken using the Demec strain gauge.
- The specimen was then loaded to 20% ultimate compressive strength and the change in length between the targets was recorded. This process was repeated for three specimens.
- This information was then used to calculate strain values for the different compressive loads which were used to plot a stress/strain curve for the specimen and calculate the elastic modulus by determining the gradient of the curve.
- Specimens were not tested to failure and therefore were reused for future tests.

3.4.4 Free drying shrinkage

Free drying shrinkage strain was tested using 100 x 100 x 200 mm prism specimens (Figure 3.8). Although the prism specimens differed in size and dimension when compared to the ring tests used to measure restrained shrinkage, the prisms had a drying area/volume ratio of 0.045 which was similar to the 0.048 drying area/volume ratio of the ring specimens. It was therefore deduced that drying shrinkage property measurements from the prism specimens were adequately comparable to the direct ring test outputs, and could effectively be used as inputs for the material property analytical model.

Two pairs of Demec targets were attached to the prism specimens on opposite sides and a Demec strain gauge was used to measure shrinkage strain. Three prism specimens were tested for each mix design for a period of 56 days.

Figure 3.8: 100 x 100 x 200 mm prism specimen with Demec targets

The testing procedure was conducted as follows:

- After curing the pairs of Demec targets were attached to the prism specimens, with 100 mm spacing.
- The specimens were kept under strictly controlled conditions, with a temperature of approx. 25 ºC and a relative humidity of approx. 50%. All sides of the specimens were left exposed.
- Strain readings were recorded as often as possible using the Demec strain gauge for 56 days.

3.4.5 Compressive strength

Compressive strength tests were conducted to aid in characterizing the material and monitoring the progression in strength development, as well as to provide the ultimate strength inputs for the elastic modulus testing. Tests were conducted according to the specifications detailed in SANS 5863:2006. Testing was conducted using the Amsler Compression Testing Machine at 7 and 28 days. Three cubes were tested to failure for at each age and the average of the three specimens was used.

3.5 Direct test methods

Part 2 of the experimental program involved the direct testing of concrete repair mixes under conditions of restrained shrinkage. This provided direct results with regard to time to first crack and crack intensity that could then be compared and contrasted with concrete property test results from the previous part of the experimental program.

The direct tests also provided reference data that was used to judge the accuracy of analytical model outputs discussed in Chapter 5.

3.5.1 Ring test

Ring tests were conducted to measure the restrained shrinkage of the concrete repair mixes. The ring test is the most common test method that is used for testing restrained shrinkage of repair mortars and concretes. The ring test method used for this investigation was based on the method described in the ASTM C 1581-04 (2004) standard.

The ring setup for this experiment used a steel ring with a wall thickness of approx. 13 mm, an outer diameter of 326 mm and a height of 155 mm. These dimensions were consistent with those given in the ASTM C 1581-04 (2004) standard. The ring was mounted on a plywood base that had been treated with a non-absorptive substance to ensure that no moisture was lost through the base. The outer ring mould was made with PVC and has a 370 mm inside diameter, creating ring specimens that are 22 mm thick (Figure 3.9).

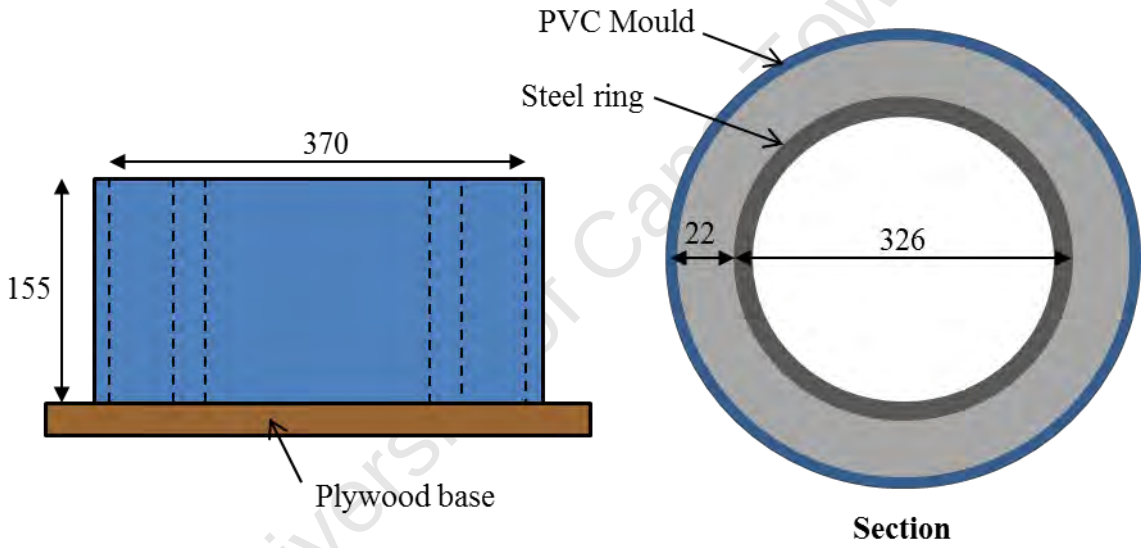

Figure 3.9: Ring test apparatus (dimensions in mm)

The testing procedure was conducted as follows:

- It was ensured that the outer surface of the steel ring and inner surface of the PVC mould ring were coated with oil to ensure that the outer ring can easily be removed after casting.
- The ring mould was filled in two equal layers, with each layer being compacted using a vibrating compactor.
- The specimen was then left to set in a controlled environment for 24 hours.
- After 24 hours the outer mould was removed (Figure 3.10) and the sample was moist cured for 7 days.

Figure 3.10: Ring specimen before and after demoulding

- After curing, the top surface of the specimen was coated in a paraffin wax layer to ensure that moisture loss was limited to the outer circumferential surface only.
- The specimen was then placed in a controlled environment and monitored twice daily.

Two ring specimens were cast for each mix to ensure that an effective average could be determined.

3.5.1.1 Time to first crack

The age at cracking was determined by measuring the time taken for the first crack to initiate on the ring specimens. This was done through careful observations of the specimens that were conducted twice daily. A magnifying glass and bright light was used to aid in identifying these cracks.

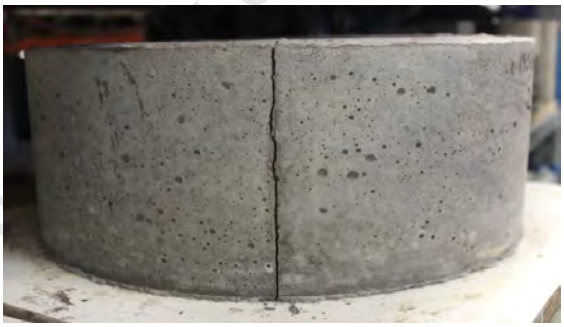

Figure 3.11: Cracked ring specimen

3.5.1.2 Crack intensity

Crack intensity was determined by calculating the total cracked area of the specimen two weeks after the first initiation of cracking. This was calculated by multiplying the average width of the cracks by the total length of the cracks. Average width was determined by measuring crack widths at five positions evenly spaced along the length of the crack. This was done using a crack card which was positioned over the crack to determine the width (Figure 3.12).

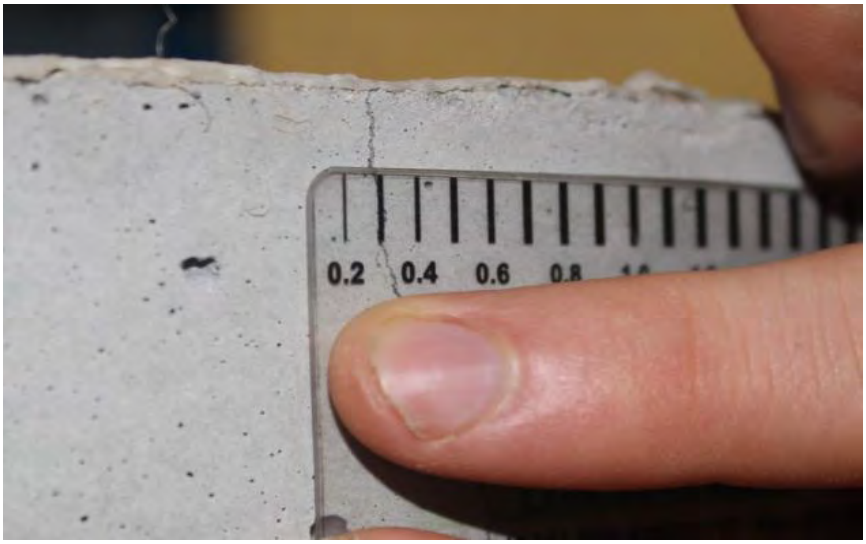

Figure 3.12: Using a crack card to measure crack width

3.6 Conclusion

The experimental program described in this Chapter provided the investigation with extensive experimental data that allowed the influence of aggregate volume content and size on the performance of bonded concrete overlay repair concrete to be comprehensively analysed and discussed, as well as providing inputs and comparative values for analytical modelling. This will now be covered in detail in the next Chapters.

Chapter 4: Experimental results

4.1 Introduction

The following Chapter details and discusses results from the experimental program outlined in Chapter 3. This will allow for the effective analysis of the influence of coarse aggregate volume content and size on the performance of bonded concrete overlays. These results are then compared with outputs from analytical modelling discussed in Chapter 5 and the formulation of final conclusions about this research are made in Chapter 6.

4.2 Repair concrete properties

4.2.1 Tensile strength

Tensile strength is the key concrete property that directly influences the failure of bonded concrete overlays as cracking will occur when the stresses induced by restrained deformation exceed this tensile strength. The influence of coarse aggregate on concrete tensile strength can be directly linked to the different phases that form its composition. Alexander & Mindess (2005) explain how concrete compressive and tensile strength is dependent on the strength of the binder phase, aggregate phase and the interfacial bond between the binder and the aggregate particles.

The importance of coarse aggregate shape with respect to tensile strength is also highlighted by Alexander & Mindess (2005), where angular particles are considered to improve concrete strength, and in particular tensile strength, over rounded particles. The influence of aggregate volume and size was tested with a coarse Greywacke aggregate using notched dog bone specimens tested to failure in the Zwick Roell Z020 Testing Machine, as detailed in 3.4.1.

Figure 4.1: Failed notched dog bone specimen

4.2.1.1 Effect of coarse aggregate content

It was noted that the results of the tensile testing component of this investigation were highly variable in nature and had a large scatter. This variability is expected and inherent to this form of testing. However, this variability was observed to increase as the aggregate volume content was increased. As tensile strength depends mostly on tensile paste strength and on the strength of the ITZ (interfacial transition zone), it can be deduced that the variable nature and increased presence of ITZ, associated with an increase in aggregate content, resulted in the wide variability of results. The magnitude of this variability was observed to be largest for the commercial SikaGrout-212 mixes.

The influence of coarse aggregate content on tensile strength at 7 and 28 days for the laboratory and commercial mixes are shown in Figures 4.2, 4.3 and 4.4 (Note: error bars refer to standard deviation from the mean). As the same graded Greywacke coarse aggregate was used for all mixes, aggregate properties that have been shown by Alexander & Mindess (2005) to directly influence tensile strength, such as surface texture, shape, stiffness, grading, strength and toughness, can be assumed to be constant. However, varying the content of coarse aggregate used and therefore varying the impact of these aggregate properties is shown to influence tensile strength.

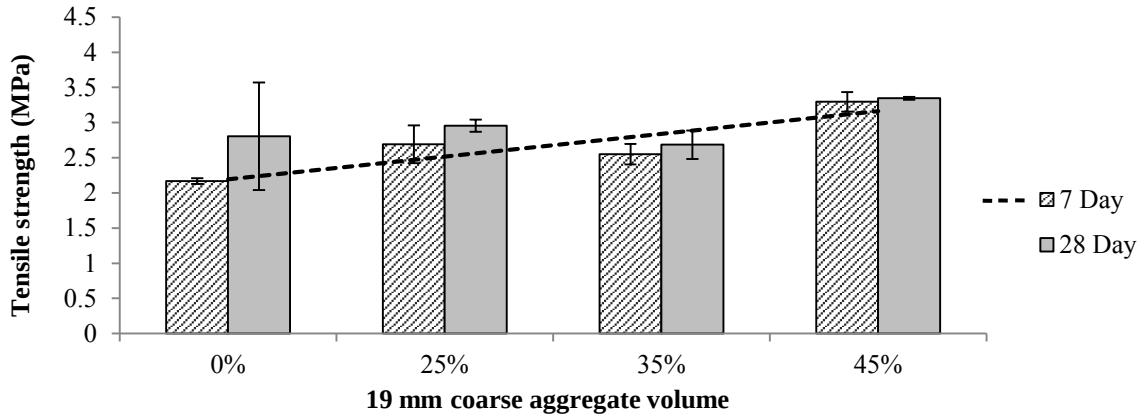

Figure 4.2: Tensile strength - Laboratory mix (w:c = 0.6)

The only noticeable trend that was observed with regard to the influence of aggregate volume on tensile strength was for the 7 day w:c = 0.6 laboratory mix results shown by the linear trend line in Figure 4.2. At 7 days, it can be seen that the tensile strength tends to increase as the coarse aggregate volume content is increased, with the 45% aggregate content having a tensile strength that is roughly 35% higher than the 0% control mix. However, it was observed that this same trend is not as apparent for the 28 day tensile strengths of the w:c = 0.6 mix.

This can be explained by the fact that at younger ages (7 days) the tensile strength of the cement paste is lower and therefore the influence of the changing tensile strength of the ITZ and aggregate itself has a notable effect on the overall tensile strength of the concrete. At later ages (28 days), the tensile strength of the paste has developed to such a degree that the varying influence of the ITZ and aggregate tensile strength has a much smaller effect on the overall tensile strength of the concrete.

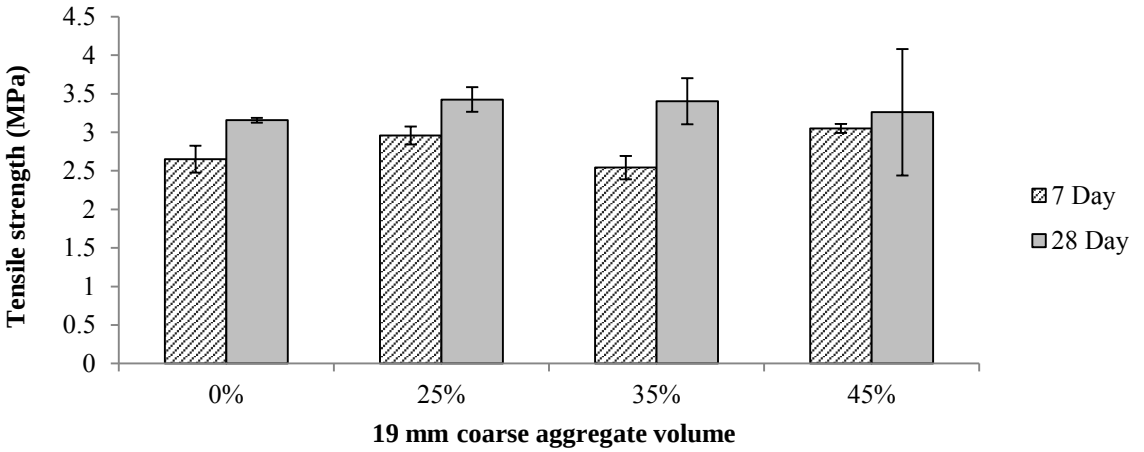

Figure 4.3: Tensile strength - Laboratory mix (w:c = 0.45)

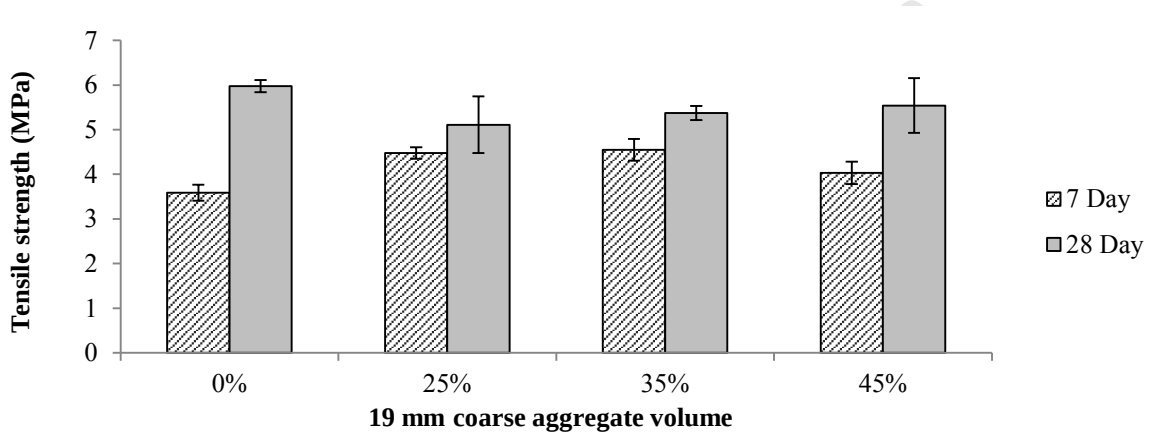

Figure 4.4: Tensile strength - Commercial mix (SikaGrout – 212)

The influence of aggregate volume content on the tensile strength of the w:c = 0.45 mixes and the SikaGrout-212 mixes is shown to be very minimal (Figure 4.3 and 4.4). Results observed for the 7 day tensile strength values for these mixes show a very slight increase in tensile strength as aggregate volume is increased. A similar result is also observed for the 28 day tensile strength of the w:c = 0.45 mixes . There is also no noticeable trend evident for the 28 day tensile strength results of the SikaGrout-212 mixes.

This also ties in with the explanation presented previously, which explains how an increase in the tensile strength of the cement paste will reduce the influence of aggregate volume content on overall concrete tensile strength. It can therefore be deduced that the more rapid increase in cement paste tensile strength development associated with both the w:c = 0.45 and SikaGrout-212 mixes results in the limited impact of aggregate volume content on overall concrete tensile strength at younger ages (7 days).

4.2.1.2 Effect of coarse aggregate size

As detailed in 3.4.1, the influence of aggregate size was tested by using two graded Greywacke coarse aggregates with a maximum size of 19 mm and 9.5 mm. These were tested using laboratory mixes with a water:cement ratio of 0.6.

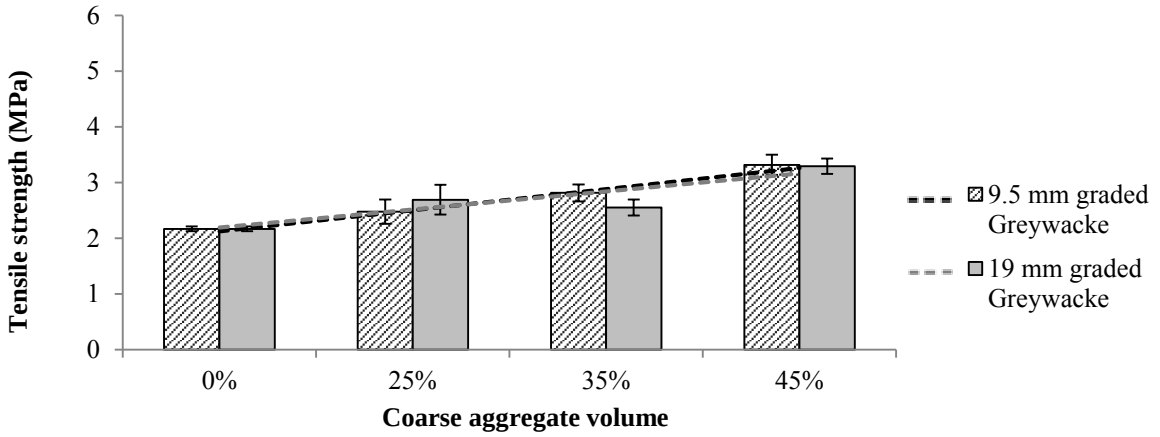

Figure 4.5: 7 day tensile strength – Laboratory mix (w:c = 0.6)

The linear trends observed in Figure 4.5 which show the 7 day tensile strengths of w:c = 0.6 mixes made with varying contents of 9.5 mm and 19 mm graded coarse aggregate indicate that there is no notable influence of aggregate size on the tensile strength of concrete at this age. This trend is evident for all aggregate volume contents and it is observed that tensile strength increases as the volume content of aggregate increases at the same rate for both aggregate sizes.

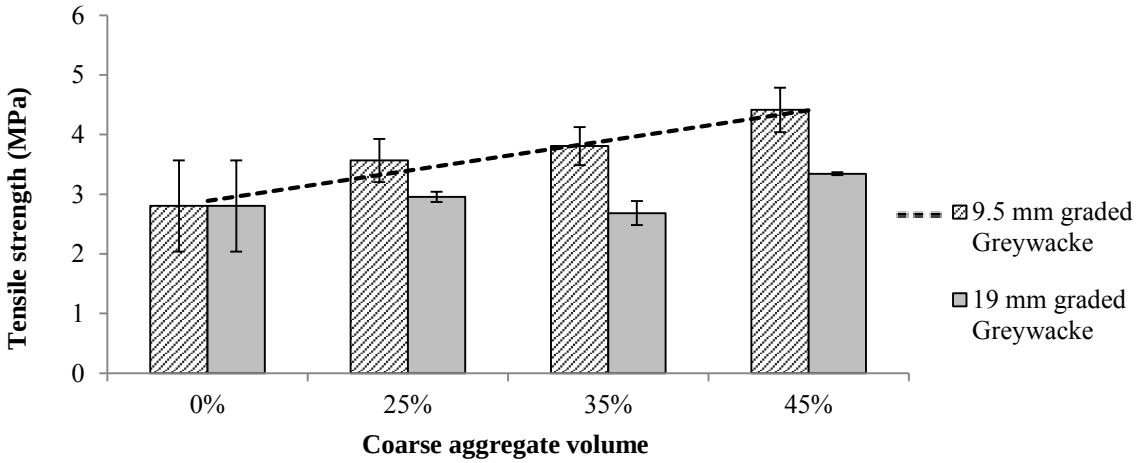

Figure 4.6: 28 day tensile strength – Laboratory mix (w:c = 0.6)

In stark contrast to the 7 day tensile strength results, the linear trend observed in Figure 4.6 which show the 28 day tensile strengths of w:c = 0.6 mixes made with varying contents of 9.5 mm and 19 mm graded coarse aggregate indicate that there is a notable influence of aggregate size on the concrete tensile strength at an older age.

While the influence of varying 19 mm aggregate contents is observed to become far less pronounced for reasons discussed in 4.2.1.1, the influence of varying 9.5 mm aggregate contents is still observed to have a substantial effect on the tensile strength, with the 45% content (9.5 mm) mix having a tensile strength 40% higher than the 0% control mix. Furthermore, the magnitudes of the 28 day tensile strength of the 9.5 mm mixes are shown to be higher (approx. 30%) than the 19 mm mixes for all aggregate volume contents.

This is not expected as the increase in the presence of the weaker ITZ associated with the smaller coarse aggregate would be expected to result in a lower tensile strength for the mixes with the smaller coarse aggregate. The results also do not comply with the concept of strain softening discussed by Chiaia *et al.* (1998) and Wittmann (2002), who propose a direct relationship between required fracture energy and coarse aggregate particle size. Based on this concept, it would be expected that the increased strain softening associated with the larger 19 mm coarse aggregate should result in a delay in tensile cracking failure, which is not observed in the results.

Zhang *et al.* (2005) also found that smaller coarse aggregate size leads to an increase in tensile strength for normal strength concrete (approx. 40 MPa). It is suggested that this can be attributed to an increase in the number of particles that are able to effectively bridge the propagation of cracks, which increases as aggregate particle size decreases. However, limited research has been done to corroborate this theory.

4.2.1.3 Effect of mix type

As previously mentioned, the scatter of results associated with tensile strength testing produces highly variable results, making a meaningful comparison of the effect of mix types challenging. However, there are a number of trends that have been identified in the results shown in Figure 4.7 and 4.8.

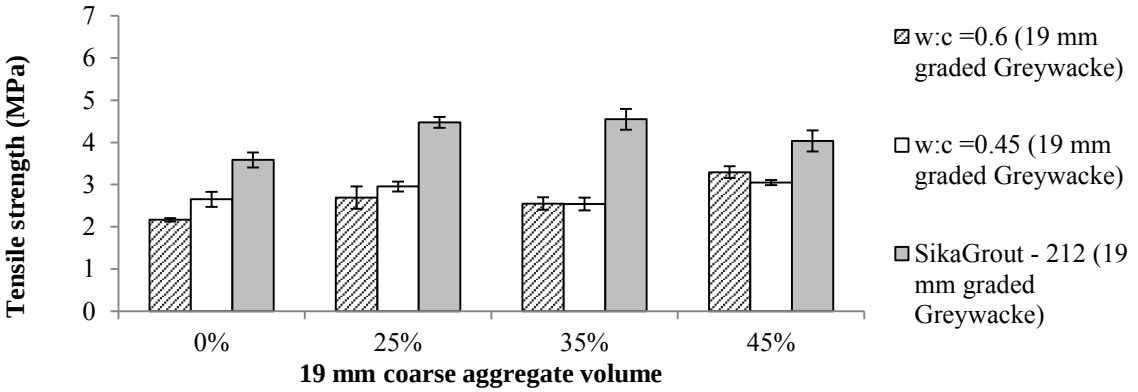

Figure 4.7: 7 day tensile strength

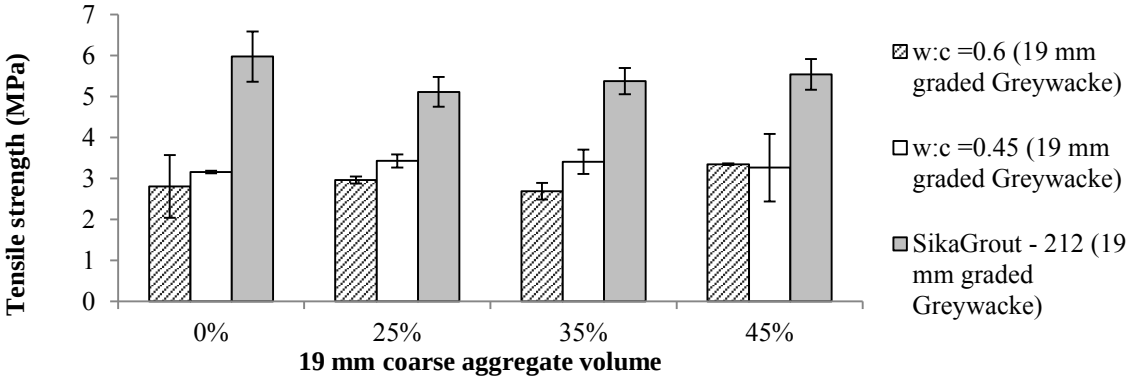

Figure 4.8: 28 day tensile strength

The control laboratory mixes (0% aggregate content) indicate that the lower water cement ratio of the w:c = 0.45 mix produced a concrete with a tensile strength that was slightly higher than the w:c = 0.6 mix. However, at 7 days, this trend was only observed for the control laboratory mixes and the 25% aggregate content mixes (Figure 4.7). This trend was more evident throughout at 28 days where it was observed that the w:c = 0.45 mixes produced a concrete with a tensile strength that was generally higher than the w:c = 0.6 mixes (Figure 4.8).

It is noted that the commercial SikaGrout-212 mixes have a substantially higher tensile strength at both 7 and 28 days. This difference is observed to be relatively consistent in magnitude for all aggregate volume contents at both ages.

4.2.2 Tensile relaxation

Tensile relaxation has been shown to have a key influence on the stress development in concrete under restrained deformation, with increased levels of relaxation being shown to notably reduce tensile stresses in bonded overlay repairs and thus improve performance.

Although there are certain links between tensile creep and tensile relaxation, Beushausen *et al.* (2012) warns against the use of predictions based on creep as they have been shown to have a significant degree of inaccuracy. Therefore, as detailed in 3.4.2, the influence of aggregate volume and size on tensile relaxation was tested directly with a coarse Greywacke aggregate using dog bone specimens in the Zwick Roell Z020 Test Machine and the Zwick Roel Z100 Test Machine for a period of 48 hours to determine an 'ultimate' relaxation value. Tests on laboratory and commercial mixes with varying aggregate sizes and volume contents were tested at 7 and 28 days. It was noted that the variability associated with this form of tensile testing meant that some samples failed during testing.

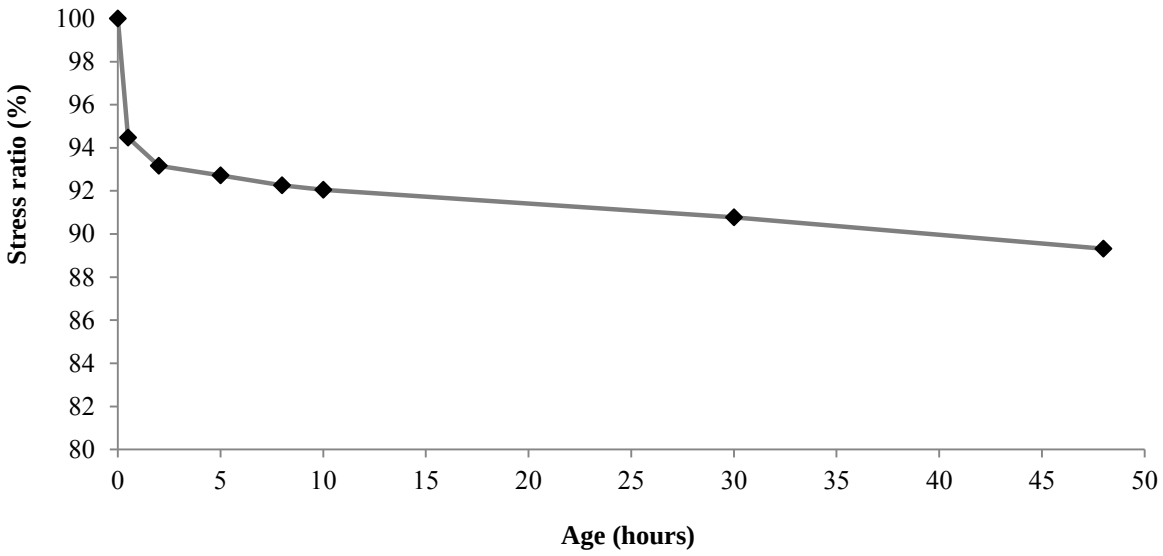

Figure 4.9: Typical 48 hour relaxation curve (7 day old w:c = 0.45 laboratory mix with 45% coarse aggregate)

A typical 48 hour relaxation curve is shown in Figure 4.9, and a very similar trend was observed for all relaxation tests on all mixes.

It was observed that directly after (approx. 1 hour) initial stressing the rate of stress decay was notably higher, with an almost vertical gradient, after which it then tended to level off substantially with a very low rate of stress decay for the remainder of the test. The final 48 hour 'ultimate' relaxation percentage was determined based on the magnitude of stress decay during the 48 hour test, shown as a percentage of the initial stress at loading.

4.2.2.1 Effect of coarse aggregate content

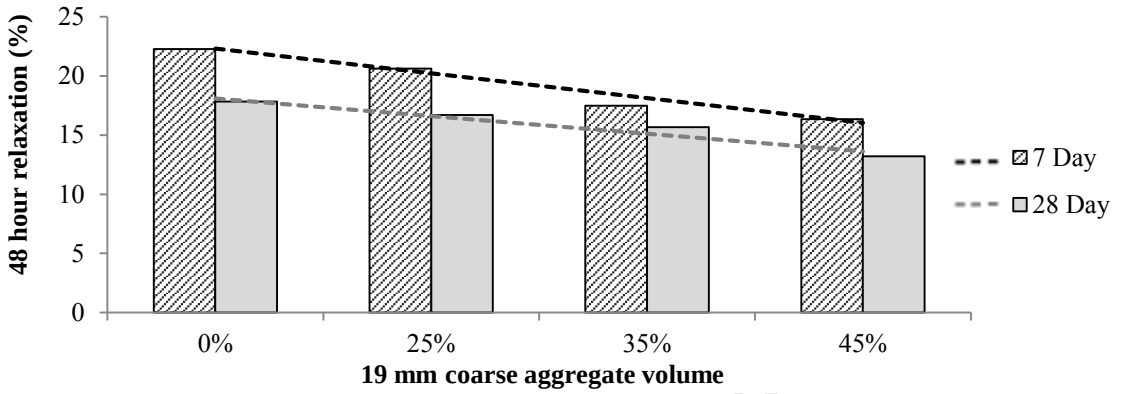

Figure 4.10: Tensile relaxation - Laboratory mix (w:c = 0.6)

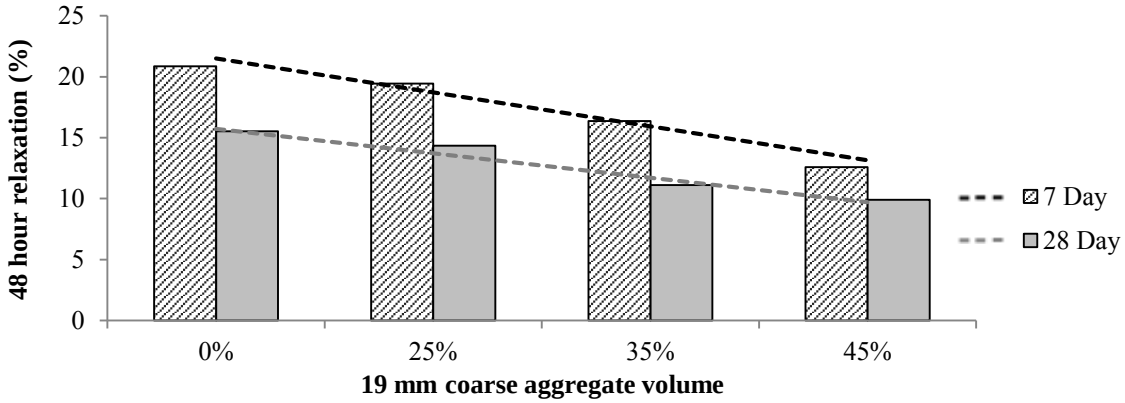

Figure 4.11: Tensile relaxation - Laboratory mix (w:c = 0.45)

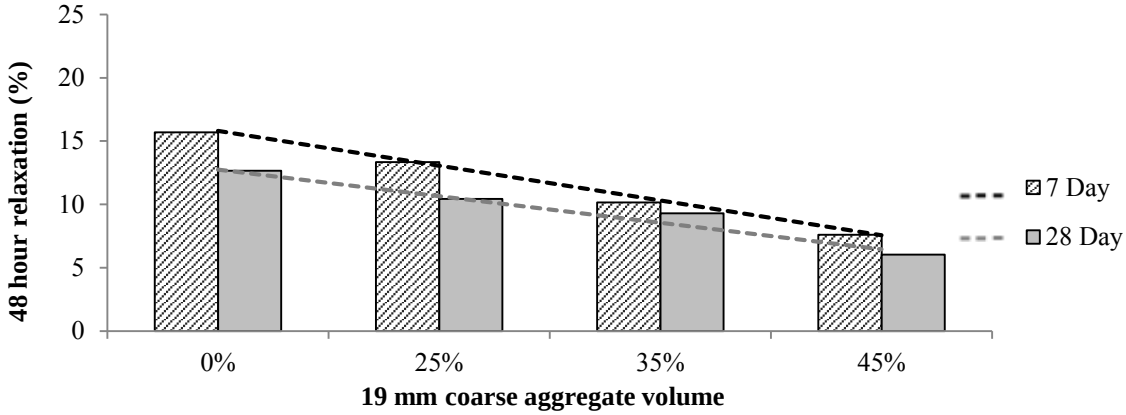

Figure 4.12: Tensile relaxation - Commercial mix (SikaGrout – 212)

The influence of coarse aggregate volume content on tensile relaxation of the laboratory and commercial mixes is shown in Figure 4.10, 4.11 and 4.12. There are two prominent and obvious trends, which have been illustrated using linear trend lines, with regard to the influence of coarse aggregate volume and the age at testing.

Aggregate volume content was shown to be inversely proportional to tensile relaxation, with the magnitude of relaxation reducing as the volume content of aggregate was increased. This trend was evident for the w:c = 0.6 , w:c = 0.45 and the SikaGrout-212 mixes, and the influence of coarse aggregate was evident at both young and older ages (7 and 28 days). This trend can be explained by the idea proposed by Alexander & Beushausen (2009) that relaxation is a function of the cement paste and therefore, an increase in coarse aggregate volume will result in a greater dilution of this cement paste. This effect was enhanced by the fact that a graded coarse aggregate was used, improving the ability of the coarse aggregate to dilute the paste even further. In addition to this, the presence of a greater coarse aggregate volume will provide better restraint to the matrix and therefore reduce the magnitude of relaxation in the cement paste.

Secondly, it was observed that there is a general reduction in the magnitude of relaxation between 7 and 28 days for all aggregate volumes. This trend can be attributed to the time dependant strength development of the cement paste which is therefore less susceptible to relaxation at older ages (28 days).

4.2.2.2 Effect of coarse aggregate size

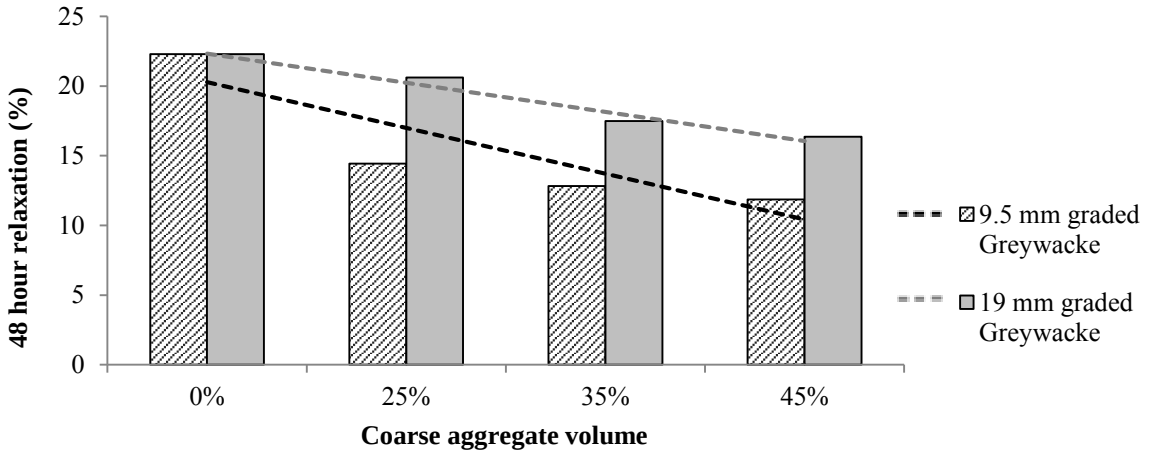

Figure 4.13: 7 day tensile relaxation – Laboratory mix (w:c = 0.6)

The influence of coarse aggregate size on tensile relaxation at 7 days is illustrated in Figure 4.13. There is an obvious trend that was observed in the results which shows that the smaller 9.5 mm coarse aggregate consistently resulted in a noticeably lower level of relaxation for all aggregate volumes when compared with the larger 19 mm coarse aggregate.

As previously mentioned, the functions of coarse aggregate that relate to tensile relaxation are traditionally viewed to be those of dilution and restraint. According to the literature (Alexander & Mindess, 2005 and Alexander & Beushausen, 2009), the ability of coarse aggregate to provide restraint is improved with an increase in aggregate size.

Furthermore, the increase in the presence of the weaker ITZ that is associated with the use of smaller coarse aggregate is also expected to result in higher relaxation levels for concretes with smaller coarse aggregate sizes.

Therefore, the results observed in Figure 4.13 tend to contradict these ideas, with the larger aggregate mixes being shown to have a greater level of relaxation. However, it is possible that the reason for these findings can be explained by examining the concepts relating to the mechanisms associated with the cracking of concrete with the presence of coarse aggregate on a 'local' scale within the paste/aggregate matrix.

Studies by Chiaia *et al.* (1998), Wittmann (2002) and Hillerborg (1985) have indicated a direct relationship between cracking fracture energy and coarse aggregate size. This is related to the concept of strain softening where energy is absorbed by microcracking occurring along the matrix/aggregate interface before actual macrocracking failure. As the level and degree of microcracking is shown to increase with aggregate size, it is therefore possible that the higher tensile relaxation of the mixes containing the larger 19 mm coarse aggregate can be explained by the increase in strain softening associated with the larger coarse aggregate particles.

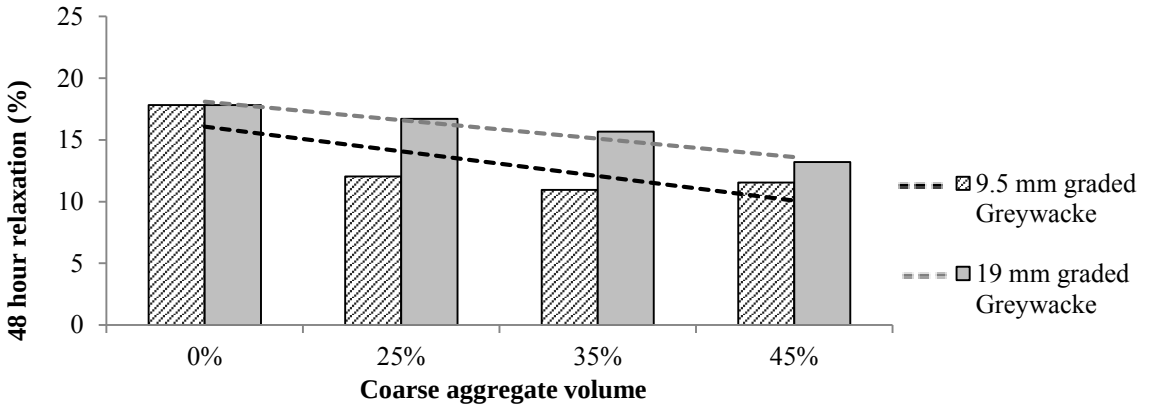

Figure 4.14: 28 day tensile relaxation – Laboratory mix (w:c = 0.6)

The same trend was observed for the 28 day relaxation tests shown in Figure 4.14.

4.2.2.3 Effect of mix type

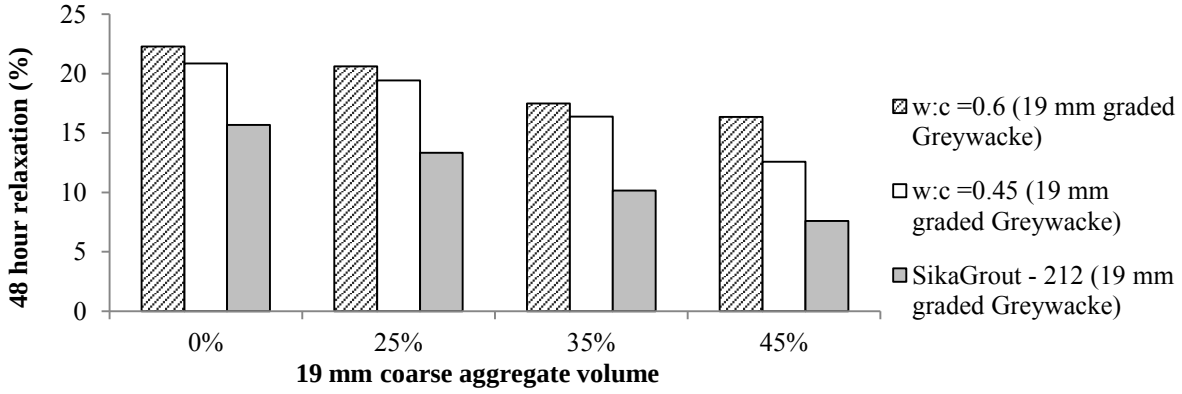

Figure 4.15: 7 day tensile relaxation

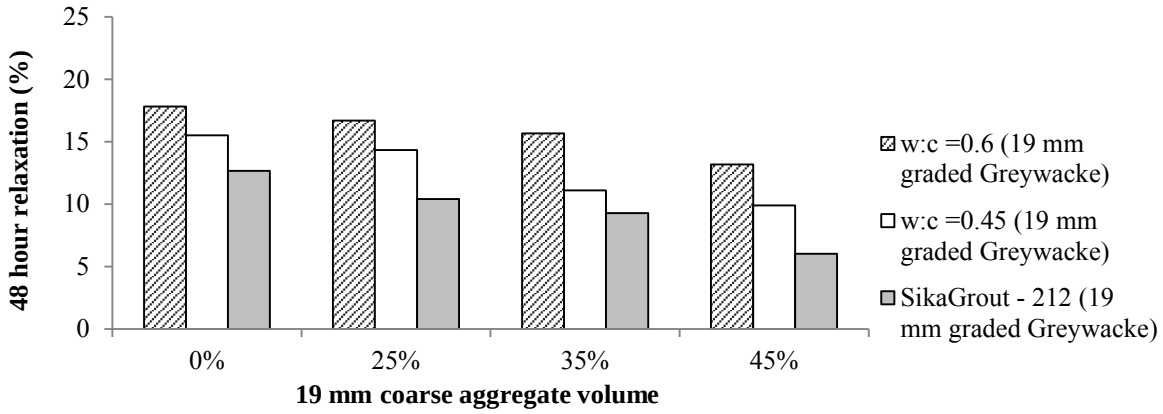

Figure 4.16: 28 day tensile relaxation

From the 7 and 28 day tensile relaxation comparisons shown in Figure 4.15 and 4.16 respectively, it was noted that mix type had a direct effect on the magnitude of tensile relaxation. The w:c = 0.6 mixes where shown to have the highest relaxation levels for all aggregate contents at both young and older ages. These were followed by the w:c = 0.45 mixes and finally the SikaGrout-212 mixes which showed the lowest levels of relaxation. This is supported by the theory proposed by Alexander & Beushausen (2009), which states that tensile relaxation is dependent on the cement paste and is therefore shown to be inversely proportional to paste strength.

4.2.3 Compressive strength

Compressive strength tests were conducted primarily to characterize the different mixes that were tested. The tests also served to provide ultimate strength inputs for the elastic modulus testing. However, although compressive strength is far less relevant to the mechanisms associated with the restrained deformation of bonded concrete overlays than tensile strength, the influence of coarse aggregate volume content and size on compressive strength will be discussed briefly in this section. Compressive strength tests were conducted as specified in 3.4.5 and were tested at 7 and 28 days.

4.2.3.1 Effect of coarse aggregate content

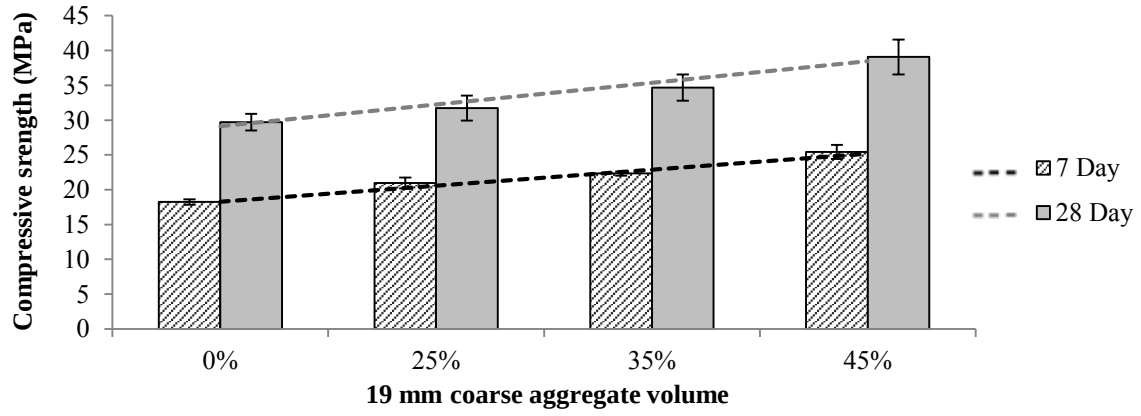

Figure 4.17: Compressive strength - Laboratory mix (w:c = 0.6)

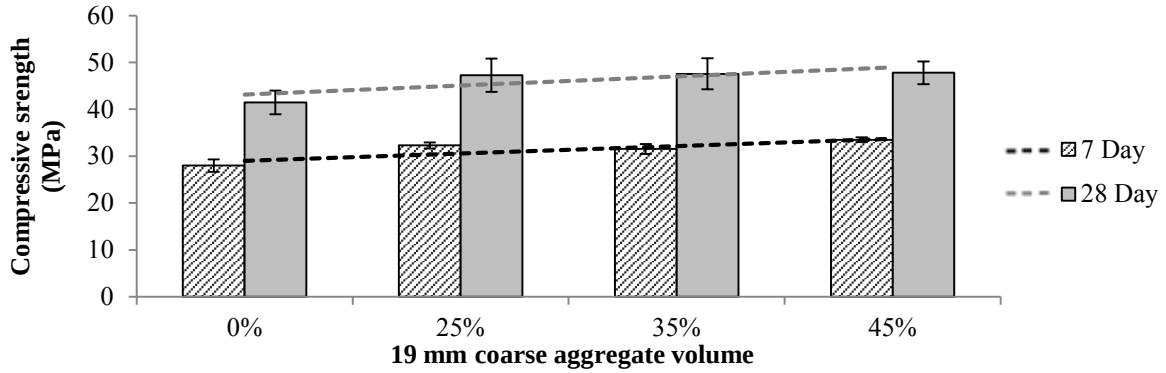

Figure 4.18: Compressive strength - Laboratory mix (w:c = 0.45)

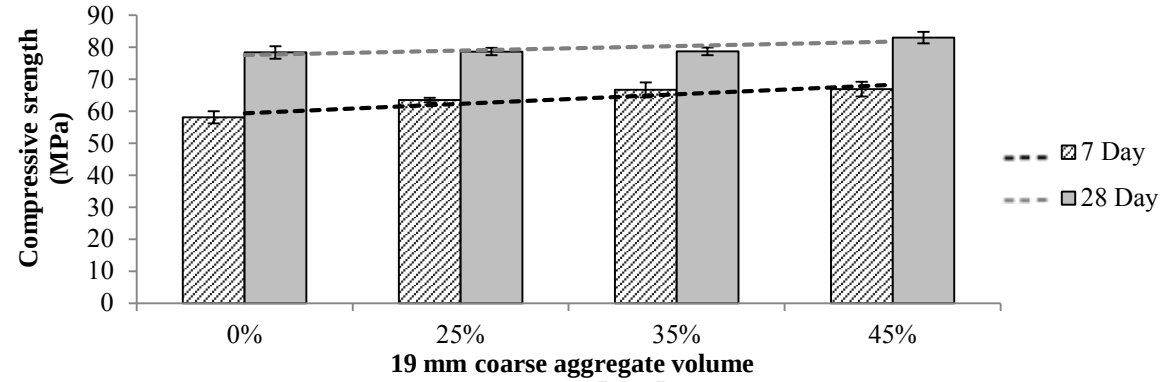

Figure 4.19: Compressive strength - Commercial mix (SikaGrout – 212)

From the compressive strength results shown in Figure 4.17, 4.18 and 4.19 it is evident that aggregate volume content had a consistent, but minor effect on compressive strength at younger ages (7 days), with compressive strength magnitude increasing slightly as aggregate volume was increase for all mixes.

However, at older ages (28 days) this same, directly proportional, trend is only evident for the w:c = 0.6 mixes. Although the w:c = 0.45 control mix (0% aggregate) was shown to have a lower compressive strength than the mixes containing aggregate, the 25%, 35% and 45% w:c = 0.45 mixes all had an almost identical 28 day compressive strength. All of the SikaGrout-212 mixes were shown to have a very similar 28 day compressive strength, with no obvious influence of aggregate content.

These trends can be explained by the time development of the strength of the cement paste and the ITZ. At 7 days, the development of the paste and aggregate-paste interface strength is limited and therefore the influence of aggregate volume is more apparent. By nature, the w:c = 0.6 paste and ITZ has a lower strength development and magnitude when compared to the w:c = 0.45 and the SikaGrout-212 mixes. This is why the influence of aggregate content is still evident in the 28 day compressive strengths for the w:c = 0.6 mixes. The development of paste and ITZ strength in the w:c = 0.45 and SikaGrout-212 mixes has developed sufficiently at 28 days, that there is no longer a noticeable influence of aggregate volume on compressive strength.

4.2.3.2 Effect of coarse aggregate size

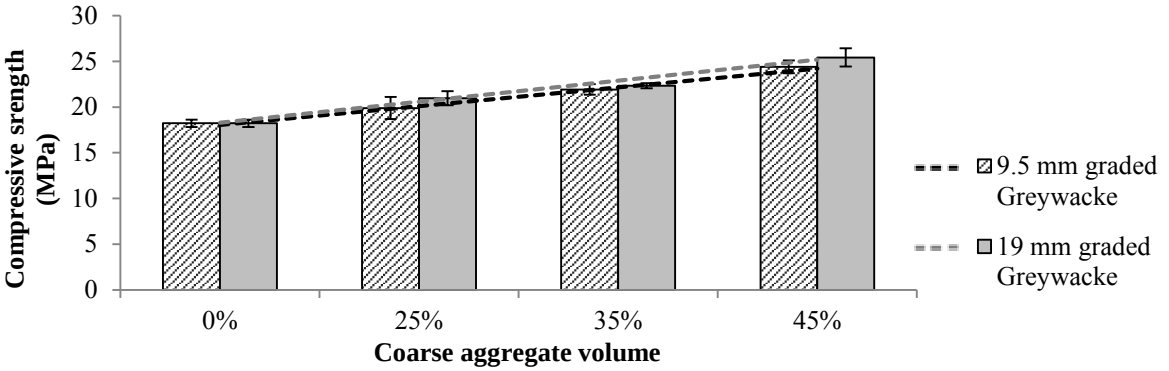

Figure 4.20: 7 day compressive strength - Laboratory mix (w:c = 0.6)

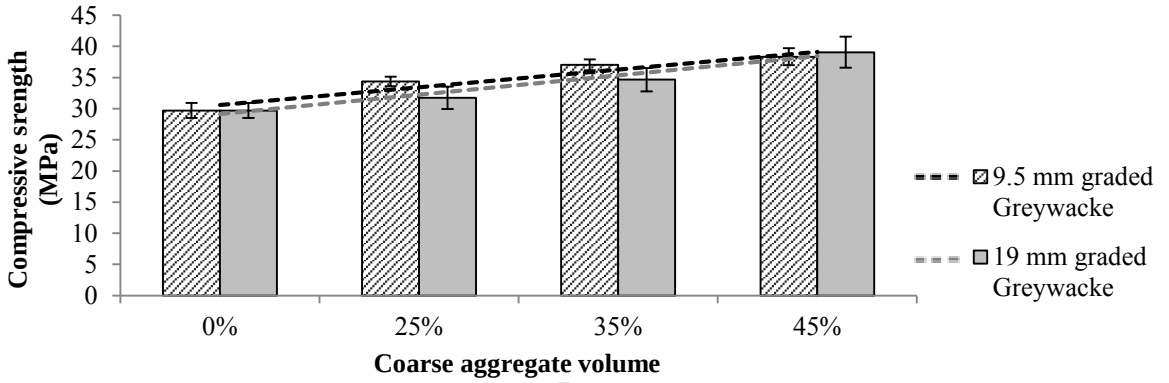

Figure 4.21: 28 day compressive strength - Laboratory mix (w:c = 0.6)

The influence of coarse aggregate size on the 7 and 28 day compressive strength of w:c = 0.6 mixes is shown in Figure 4.20 and 4.21. It is evident that there was little or no effect of aggregate size on the compressive strength for all aggregate volume contents at both young (7 day) and older (28 day) ages.

4.2.3.3 Effect of mix type

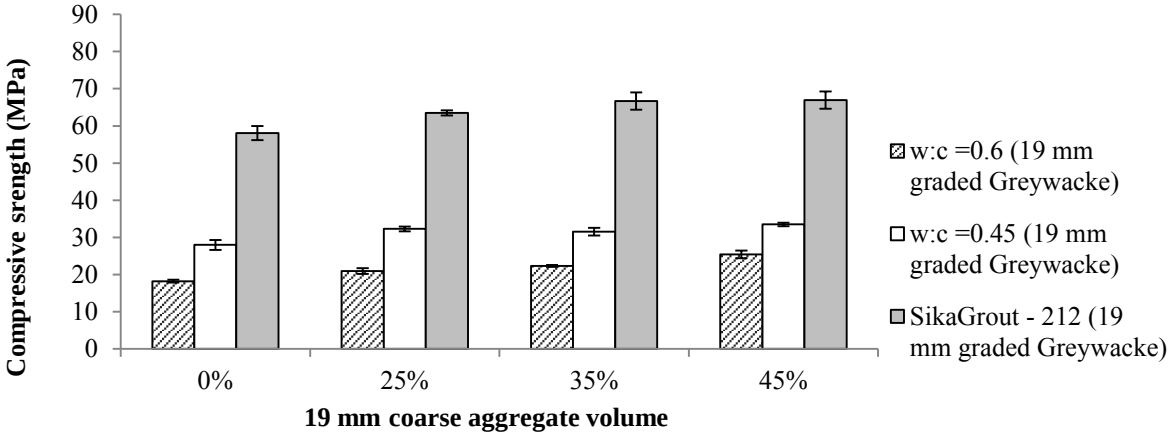

Figure 4.22: 7 day compressive strength

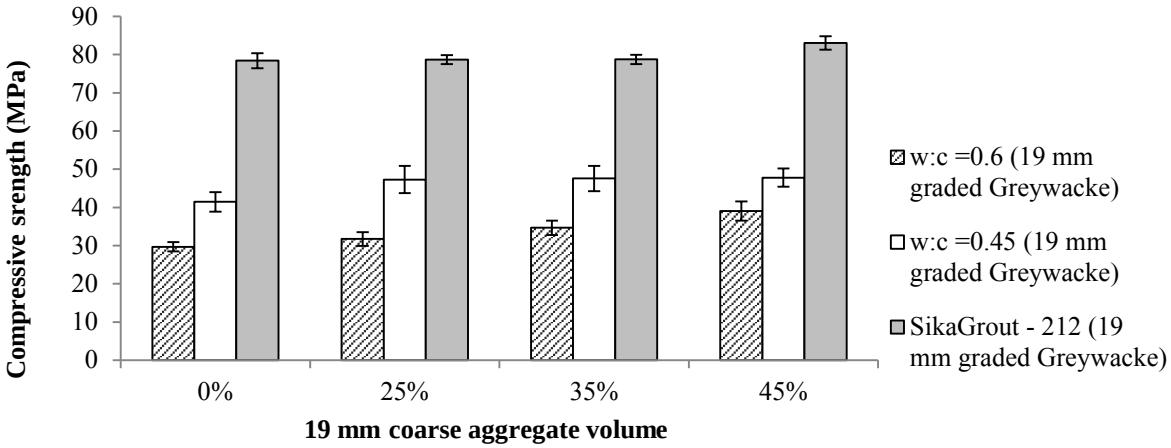

Figure 4.23: 28 day compressive strength

The trends observed with regard to the influence of mix type on compressive strength shown in Figure 4.22 and 4.23 are consistent at both 7 and 28 days. The compressive strength of the w:c = 0.6 and w:c = 0.45 laboratory mixes adhere to the accepted concept that compressive strength increases as the water:cement ratio is reduced. This was evident at both 7 and 28 days for these laboratory mixes.

The SikaGrout-212 mixes show an exceptionally high early age (7 day) compressive strength of roughly 60 MPa and older age (28 day) compressive strength of roughly 80 MPa for all mixes. This indicates that this commercial repair material has exceptional compressive strength development and magnitude qualities that far surpass those of the conventional laboratory mixes tested.

4.2.4 Elastic modulus

The elastic properties of repair concrete have been shown to have a key influence on the restrained deformation of bonded concrete overlays and directly affect the load-sharing capacity of the repair concrete. Gilbert (1988) explains how the tensile elastic modulus has been shown to have a direct influence on the elastic tensile stress that results from restrained deformation.

The influence of coarse aggregate on the elastic modulus of concrete is based on the idea, proposed by Alexander & Mindess (2005) and Alexander & Beushausen (2009) that concrete stiffness is directly proportional to the stiffness of the individual phases that form its composition, namely, aggregate stiffness, ITZ stiffness and paste stiffness. As the same coarse Greywacke aggregate type was used, the results of this investigation reveal the influence of varying aggregate volume content and size.

As detailed in 3.4.3, compressive elastic modulus tests were conducted using an adapted method that made use of the Zwick Roel Z100 Test Machine and the Demec strain gauge (Figure 4.24). The loading for these tests was determined based on compressive strength tests conducted on cube specimens. It is the opinion of many researchers that the elastic modulus of concrete is very similar in tension and compression, and the use of compressive elastic modulus to analyse repair materials has been used by Chilwesa's (2012).

Figure 4.24: Elastic modulus testing in the Zwick Roel Z100 Test Machine using the Demec strain gauge

4.2.4.1 Effect of coarse aggregate content

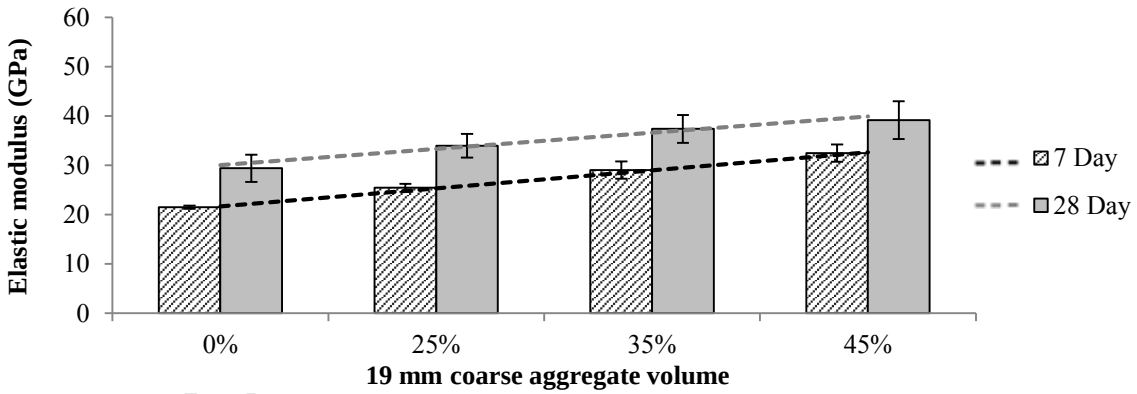

Figure 4.25: Elastic modulus - Laboratory mix (w:c = 0.6)

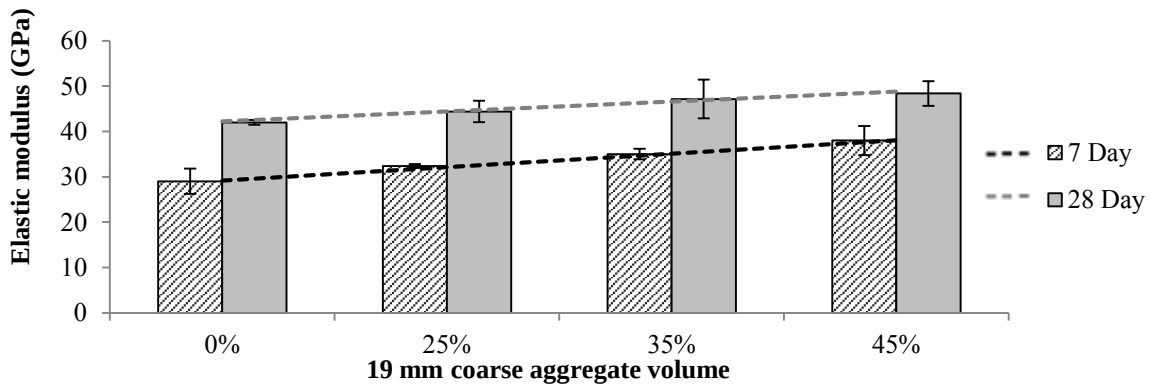

Figure 4.26: Elastic modulus - Laboratory mix (w:c = 0.45)

The influence of coarse aggregate volume content on the elastic properties of the laboratory repair concrete mixes is shown in Figure 4.25 and 4.26. The trends that were observed in both Figures are consistent with the theory proposed by Alexander & Mindess (2005) and Alexander & Beushausen (2009) and showed that as the volume concentration of the coarse aggregate was increased, so the volume concentration of the stiffer phase was increased, and therefore the overall elastic properties of the concrete was observed to increase. As the paste stiffness and aggregate type was constant it can be assumed that the ITZ stiffness was also relatively constant, and therefore this increase can be directly attributed to an increased volume of the stiffer aggregate phase.

The trends observed with regard to the development of elastic properties from younger (7 day) to older (28 day) ages were also expected for the laboratory mixes. The w:c = 0.6 showed an approx. 25% increase from 7 to 28 days for all aggregate contents while the w:c = 0.45 showed an approx. 30% increase from 7 to 28 days for all aggregate contents. It can therefore be seen that the influence of coarse aggregate volume on the elastic modulus of the concrete was the same at young (7 day) and older (28 day) ages.

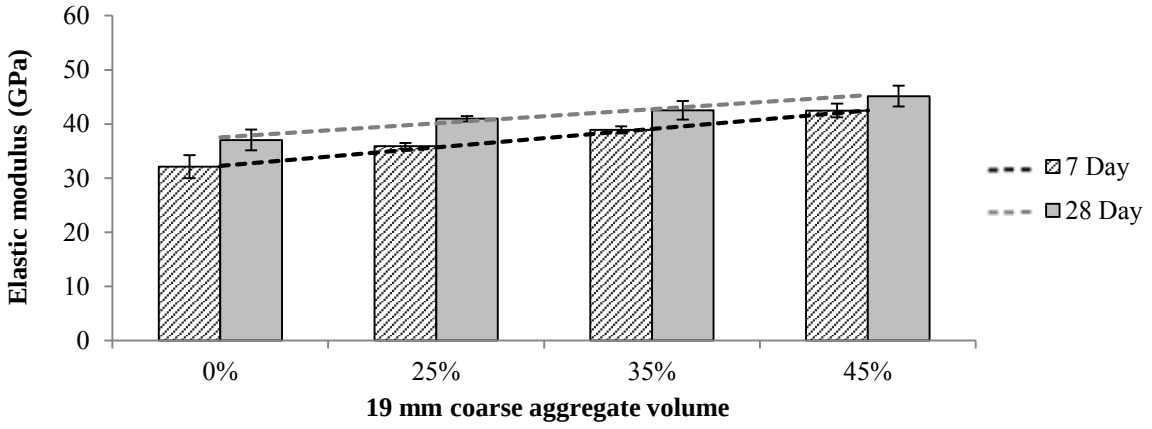

Figure 4.27: Elastic modulus - Commercial mix (SikaGrout – 212)

The influence of aggregate volume on the commercial mixes is shown in Figure 4.27 and it was evident that aggregate volume had a similar influence on the elastic properties of these mixes.

It is noted that that there was only an approx. 15% increase from 7 to 28 days for all aggregate contents. This may indicate a more rapid initial development of elastic properties during the first 7 days, which would account for the reduced increase observed between 7 and 28 days. However, it can be seen that the influence of coarse aggregate volume was still the same at young (7 day) and older (28 day) ages.

4.2.4.2 Effect of coarse aggregate size

The influence of aggregate size on the 7 and 28 day elastic modulus of the w:c = 0.6 mixes are shown in Figure 4.28 and 4.29 respectively.

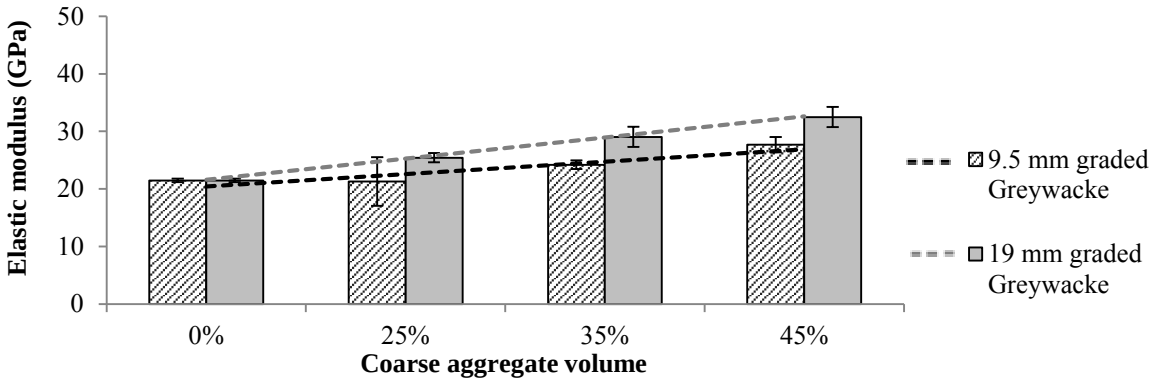

Figure 4.28: 7 day elastic modulus – Laboratory mix (w:c = 0.6)

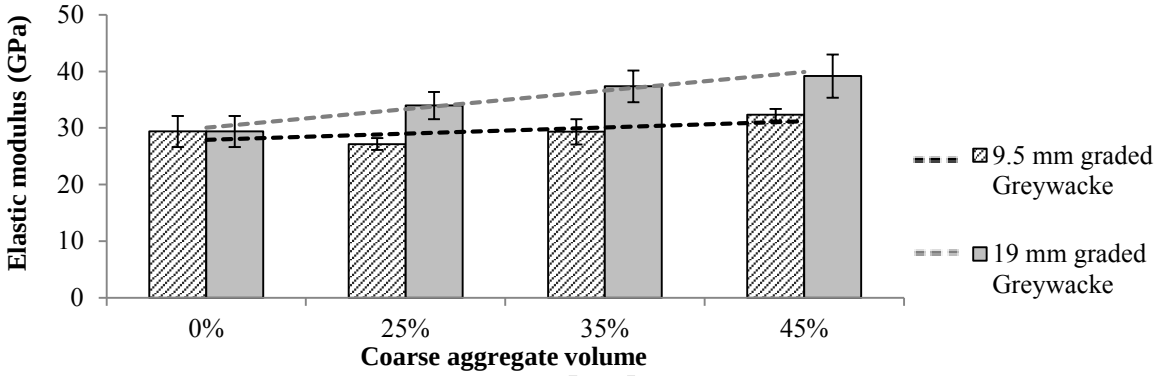

Figure 4.29: 28 day elastic modulus – Laboratory mix (w:c = 0.6)

From the Figures it can be seen that there is a definite trend that is noticeable in both the 7 and 28 day elastic modulus results. The influence of the smaller sized, 9.5 mm, graded aggregate was shown to be considerably less apparent for all aggregate volume contents. This is expected and can be explained by the concept that the presence of a larger coarse aggregate provides much better restraint to the concrete matrix. Although the volumes of the stiffer aggregate phase were constant for both aggregate sizes, the superior level of restraint associated with the larger, 19 mm, grade aggregate resulted in the noticeable influence of coarse aggregate that was observed for all volume contents at both 7 and 28 days.

4.2.4.3 Effect of mix type

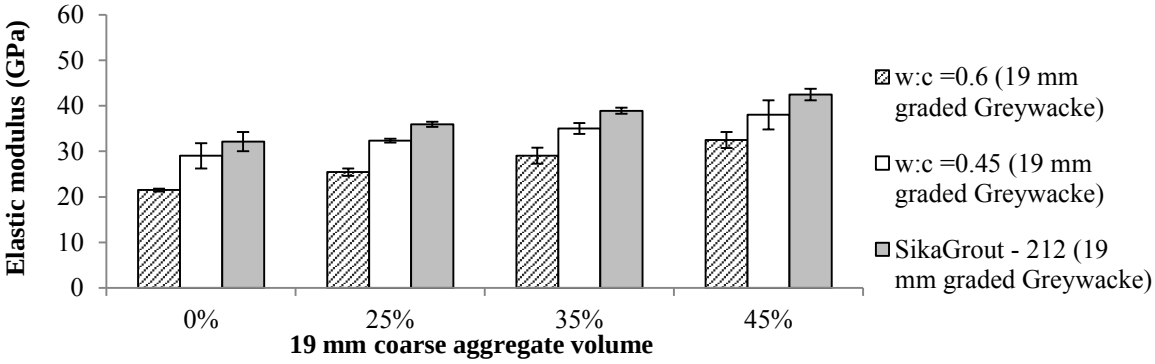

Figure 4.30: 7 Day elastic modulus

The influence of mix type on the 7 day elastic modulus of the laboratory and commercial mixes is shown in Figure 4.30. As expected, the trend observed in the 7 day results was similar in nature to that of the compressive strength at this age, discussed in 4.2.3. The w:c = 0.6 mixes had the lowest elastic modulus for all aggregate contents followed by the w:c = 0.6 mixes and finally the SikaGrout-212 mixes which had the highest 7 day elastic properties.

However, it was noted that the elastic properties of the commercial SikaGrout-212 mixes were only slightly higher (approx. 4 GPa) than the w:c = 0.45 mixes, despite the fact that the compressive strength of the SikaGrout-212 mixes being shown to be almost double the compressive strength of the w:c = 0.45 mixes (approx. 30 MPa higher). This indicates that there is not a proportional relationship between compressive strength and elastic modulus for the SikaGrout-212 commercial repair concrete. These findings are supported by work done by Alexander & Mindess (2005), who showed that actual concrete strength has a relatively minor contribution to the concrete elastic modulus.

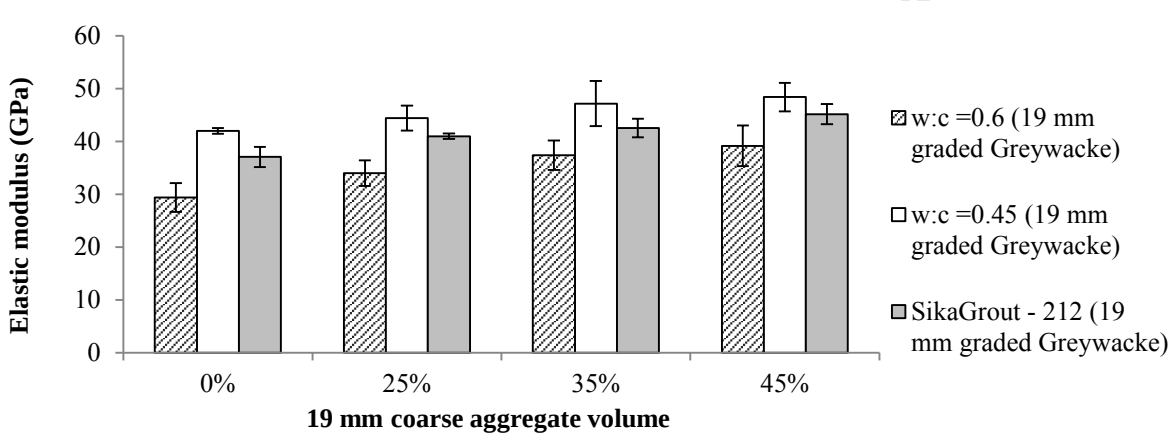

Figure 4.31: 28 Day elastic modulus

The 28 day elastic modulus results shown in Figure 4.31 indicate that the development of elastic stiffness of the laboratory mixes is much greater than the commercial mixes between 7 and 28 days. The stiffness of the laboratory mixes were shown to increase by approx. 30% for all aggregate volumes while the commercial mixes only increased by approx. 15%. As a result of this, the w:c = 0.45 mixes are shown to have a higher elastic modulus than the SikaGrout-212 for all aggregate volume contents.

The SikaGrout-212 has been shown to have high early age compressive strength characteristics and therefore it is possible that the majority of development of elastic stiffness occurred during the first 7 days. This would account for the lower rate of development observed between 7 and 28 days. The 28 day elastic modulus results for the commercial mixes further reiterate the idea that concrete strength has a minor contribution to the concrete elastic modulus.

4.2.5 Free drying shrinkage

The direct influence of drying shrinkage on the performance of bonded concrete overlays has been emphasised and discussed extensively in the literature in Chapter 2.

Although the type of drying shrinkage that relates directly to the performance of these overlays is restrained drying shrinkage, work done by Beushausen (2005) was able to establish a numerical link between free drying shrinkage and restrained drying shrinkage. Restrained drying shrinkage was shown to be roughly 60% the value of free drying shrinkage for the same concrete type.

Therefore the influence of coarse aggregate volume content and size was tested for free shrinkage, as detailed in 3.4.4. Tests were conducted on 100 x 100 x 200 mm prism specimens with Demec targets and strain readings were recorded with the Demec strain gauge. Tests were conducted for 56 days after curing.

The influence of autogeneous shrinkage has been shown to occur directly after casting. As the shrinkage specimens were cured for 7 days before drying shrinkage was tested it can be assumed that almost all of the autogeneous shrinkage has already occurred by this stage and will therefore not influence the drying shrinkage results.

Figure 4.32: 100 x 100 x 200 mm prism specimens with Demec targets

4.2.5.1 Effect of coarse aggregate content

Alexander & Mindess (2005) and Alexander & Beushausen (2009) explain how coarse aggregates have been shown to have two key effects on paste shrinkage, namely dilution and restraint.

It is therefore expected that an increase in coarse aggregate volume will reduce the amount of shrinking paste in the mixture, as well as provide increased restraint to the concrete matrix, and therefore reduce the magnitude of drying shrinkage. The influence of coarse aggregate volume content for the laboratory and commercial mixes is shown in Figure 4.33, 4.34 and 4.35 respectively.

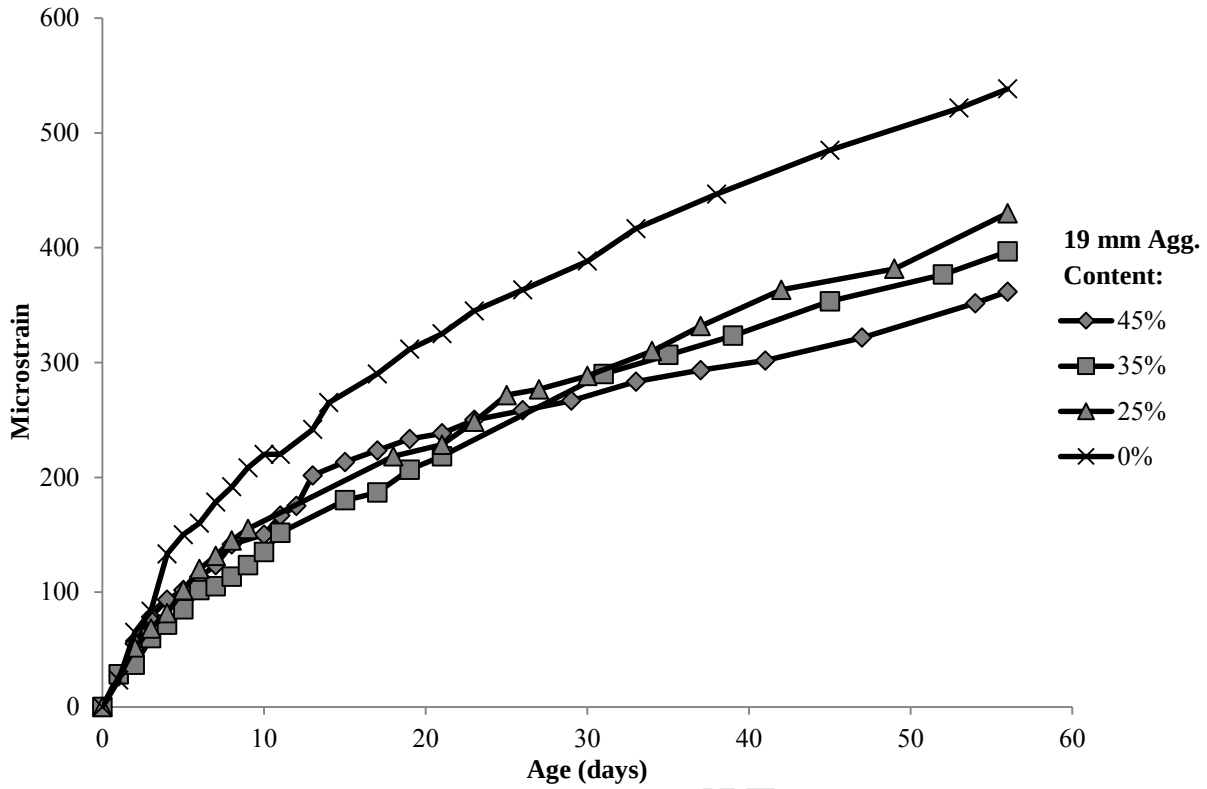

Figure 4.33: Free drying shrinkage - Laboratory mix (w:c = 0.6)

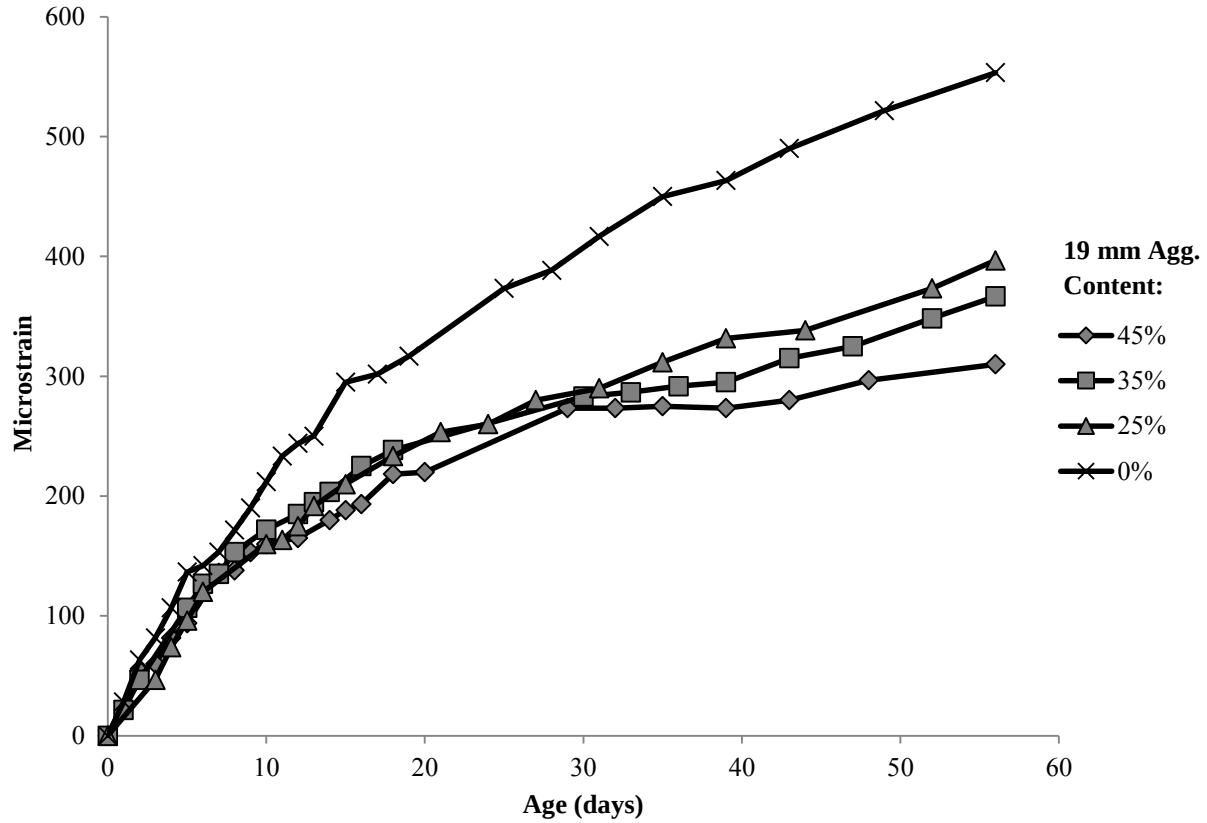

Figure 4.34: Free drying shrinkage - Laboratory mix (w:c = 0.45)

It is evident in the trends observed in the results in Figure 4.33 and 4.34 that there is indeed a direct linear influence of coarse aggregate volume on free drying shrinkage. This direct relationship is illustrated by the linear trend lines in Figure 4.35.

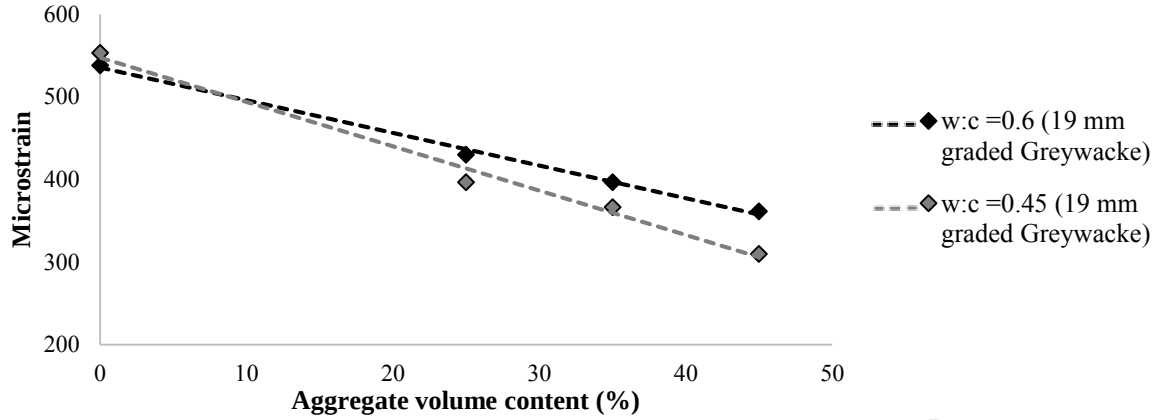

Figure 4.35: 56 day free drying shrinkage/aggregate volume content relationship - Laboratory mixes

For the laboratory mixes, it was shown that there was a distinctive trend with regard to coarse aggregate content, with the level of drying shrinkage increasing as coarse aggregate content was decreased. This trend was noted to be far more apparent at older ages (>30 days). At younger ages, there was far less distinction between the different aggregate contents, however, the control mixes were shown to be higher even at younger ages. It can therefore be deduced that the influence of coarse aggregate volume on the laboratory mixes is less at younger ages (<20 days) and only becomes more clear later on.

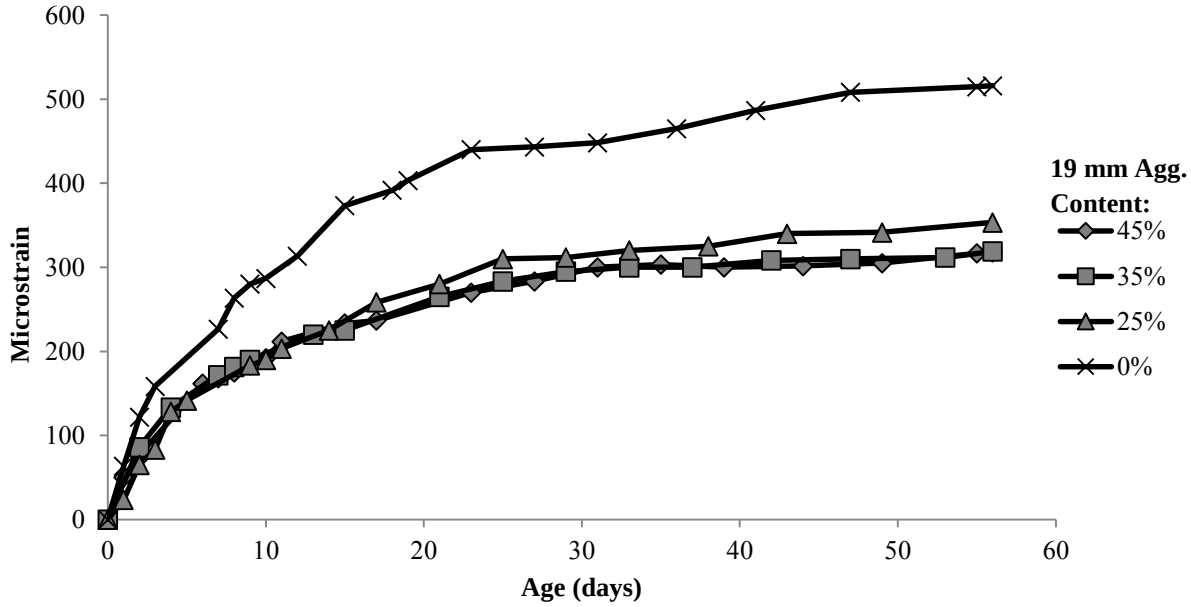

Figure 4.36: Free drying shrinkage - Commercial mix (SikaGrout-212)

A similar trend with regard to the control mix (0% aggregate content) was observed for the commercial mix in Figure 4.36. It was also noted that the commercial control mix had a higher level of drying shrinkage at both young and older ages when compared to the laboratory control mixes.

The influence of varied aggregate contents was far less apparent for the commercial mixes with the 45% and 35% SikaGrout-212 mixes having almost an identical development and magnitude of shrinkage, and the 25% SikaGrout-212 mix being shown to have only a slightly higher level of shrinkage. It was therefore shown that the effect of the inclusion of a coarse aggregate did have a profound effect on reducing the drying shrinkage of the commercial mixes, but the influence of varied coarse aggregate contents had a limited effect.

4.2.5.2 Effect of coarse aggregate size

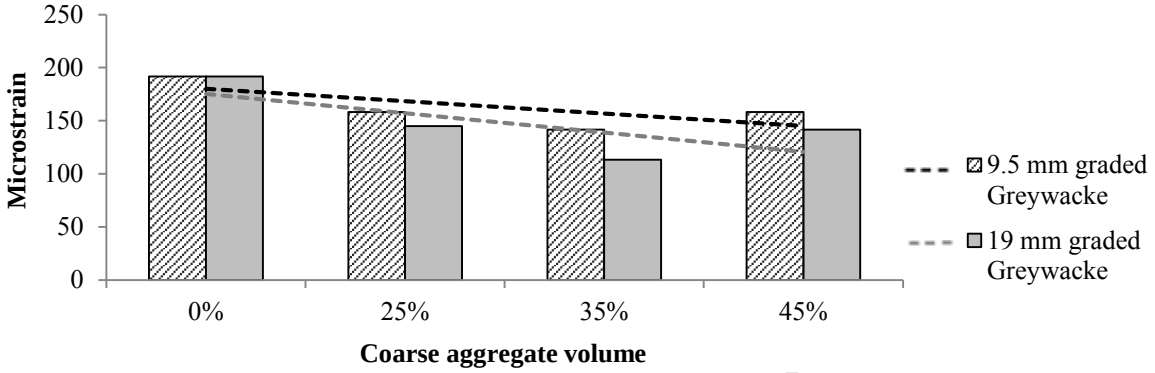

Figure 4.37: 7 day free drying shrinkage

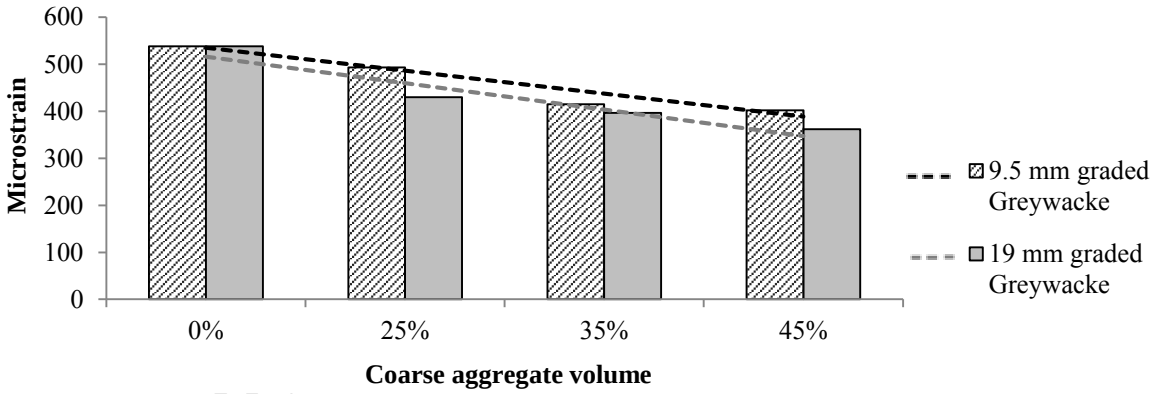

Figure 4.38: 56 day free drying shrinkage

Figure 4.37 and 4.38 show the influence of coarse aggregate size on free drying shrinkage at early ages (7 days drying) and older ages (56 days drying). From the liner trend lines, it is apparent that there was a direct influence of coarse aggregate size on drying shrinkage, with the smaller 9.5 mm coarse aggregate mixes being shown to have a greater magnitude of drying shrinkage at both younger and older ages than the larger 19 mm aggregate mixes. This is supported by Alexander & Mindess (2005) and Alexander & Beushausen (2009) who explain how larger sized aggregate particles provide better restraint for the shrinking cement paste and therefore reduce the magnitude of drying shrinkage of the concrete.

As aggregate volume contents were constant for both aggregate sizes, the diluting function of the coarse aggregate was the same for both mix types, and therefore the reduced shrinkage can be attributed to the better restraint of the larger 19 mm aggregate particles in the concrete matrix.

Furthermore, the trends observed in Figure 4.37 and 4.38 can also be explained by the increase in the presence of the weaker ITZ associated with the smaller coarse aggregate particles, which results in the concrete matrix being more susceptible to volume changes associated with drying shrinkage.

4.2.5.3 Effect of mix type

In order to illustrate and compare the influence of mix type on shrinkage results, it was necessary to plot separate graphs for the two laboratory mixes and the commercial mix. A graph was therefore plotted for the mixes with a 0% coarse aggregate content and another graph for mixes with a 45% coarse aggregate content to allow for an effective comparison. See Figure 4.39 and 4.40.

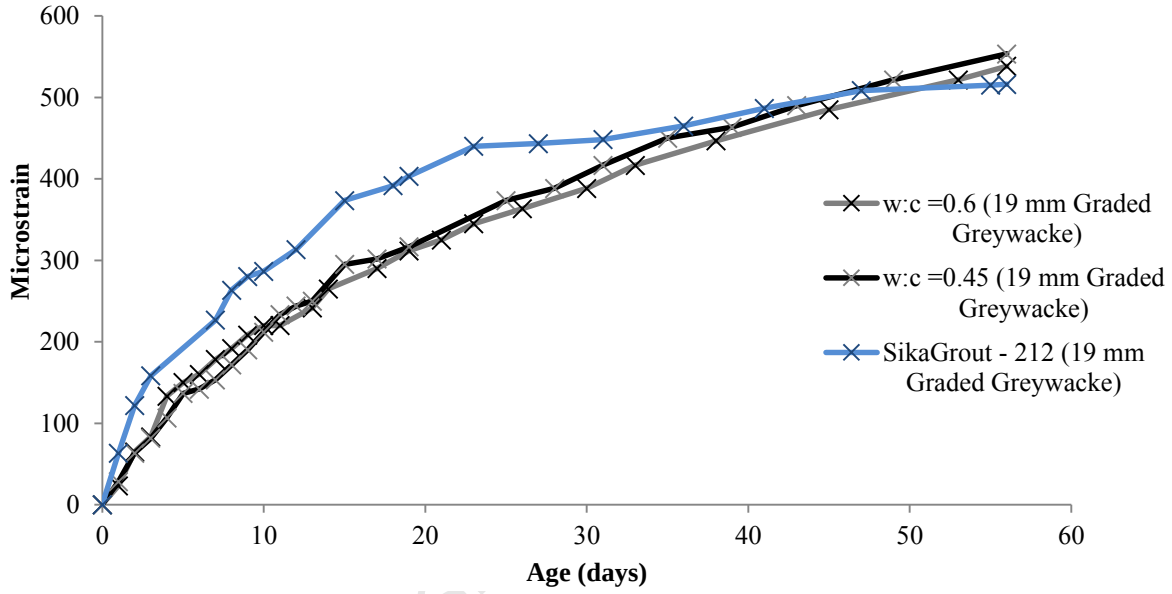

Figure 4.39: Free drying shrinkage (0% aggregate content)

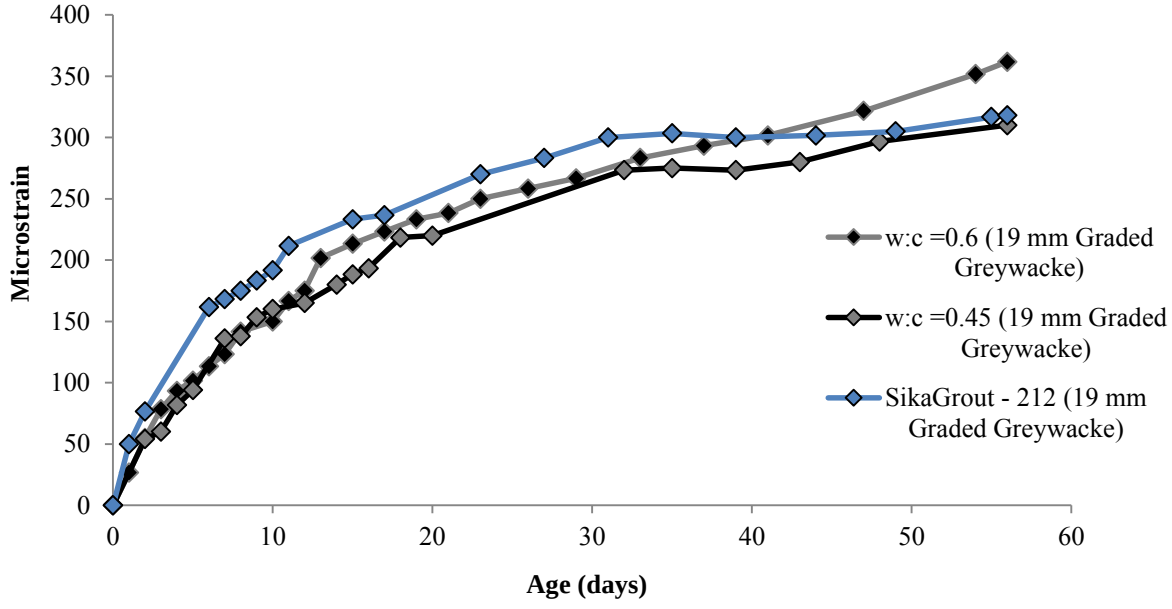

Figure 4.40: Free drying shrinkage (45% aggregate content)

There is an obvious trend with regard to the influence of mix type on free drying shrinkage. This same trend is noted to be consistent when no coarse aggregate is present (Figure 4.39) and when 45 % coarse aggregate is present (Figure 4.40).

The commercial SikaGrout-212 mix is observed to have a comparatively rapid rate of shrinkage at early ages, which then tends to level out substantially after approx. 25 days. No major increase in shrinkage was observed for the period after 25 days, with or without the presence of a coarse aggregate.

The influence of mix type on the laboratory mixes is relatively small, particularly when no coarse aggregate is included (Figure 4.39). During the first 10 days, there is no noticeable difference between the shrinkage of the two laboratory mix types, with 0% and 45% coarse aggregate.

However, after 10 days, the w:c = 0.45 mix is shown to have a slightly higher level of drying shrinkage than the w:c = 0.6 with no coarse aggregate. This trend was expected, as the w:c = 0.45 mix is expected to have a higher level of drying shrinkage due to a higher cement paste content as a result of an increased cement content when compared to the w:c = 0.6 mix. In contrast, the trend observed with the laboratory mixes with 45% aggregate, where the w:c = 0.6 is shown to have a higher level of shrinkage than the w:c = 0.45, is not expected.

No explanation can be offered for the contradiction in these findings, but it must be stressed that the method used for testing free drying shrinkage was highly variable in nature and can produce a wide scatter of data.

It is also noted that laboratory mixes, with and without a coarse aggregate, had a more gradual rate of shrinkage, but did not tend to level of as rapidly as the SikaGrou-212 mixes. After a more rapid initial shrinkage rate, both the 0% and 45% laboratory mixes continued to shrink at a relatively constant rate for the duration of the testing, without levelling off significantly.

4.3 Direct test results

The direct testing component of the investigation used the restrained shrinkage, ring test, technique to directly measure the influence of coarse aggregate volume content and size on the time to first crack and crack intensity of laboratory and commercial repair concretes. These outputs were then compared with the outputs from the concrete property tests and the analytical modelling phase, discussed in Chapter 5.

4.3.1 Time to first crack

The direct testing of time to first crack of repair concretes exposed to restrained shrinkage was conducted using ring tests and followed the procedures set out in the ASTM C 1581-04 (2004) standard, detailed in 3.5.1. Two rings were cast for each of the mixes and were monitored for signs of failure (cracking) twice daily, seven days a week.

The time to first crack results were a key component for the investigation, as they provided a direct indication of the influence of aggregate volume content and size on the crack resistance of the different concrete repair mixes. Furthermore, the time to first crack results were fundamentally important in judging the influence of individual concrete properties, as well as the accuracy of analytical predictions based on these specific concrete properties. This discussion of results is shown in Chapter 6.

Figure 4.41: Cracked ring test specimens

4.3.1.1 Effect of coarse aggregate content

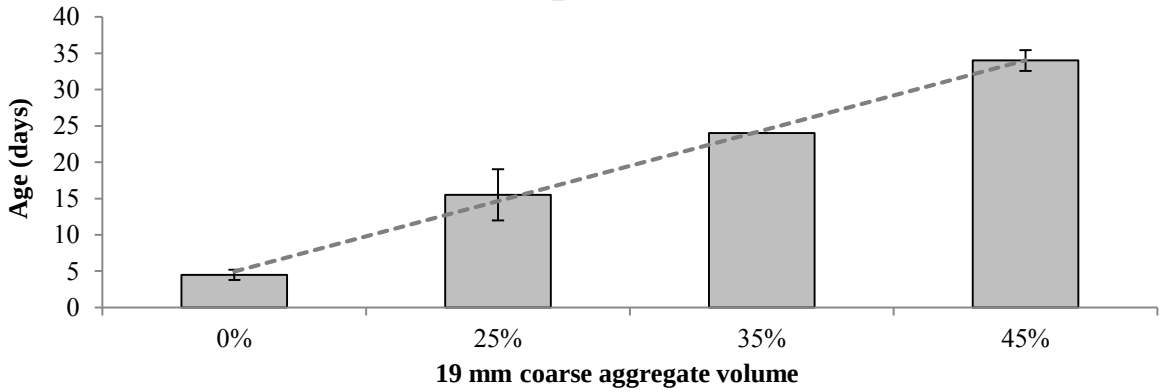

Figure 4.42: Time to first crack - Laboratory mix (w:c = 0.6)

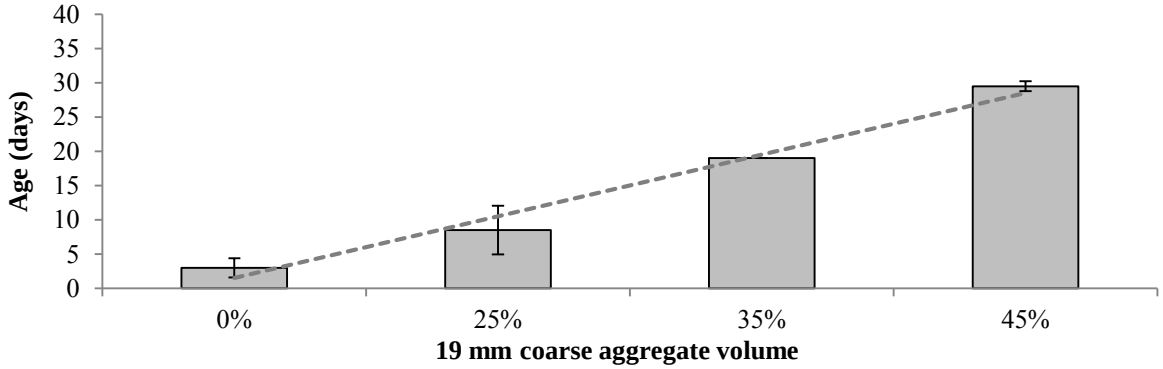

Figure 4.43: Time to first crack - Laboratory mix (w:c = 0.45)

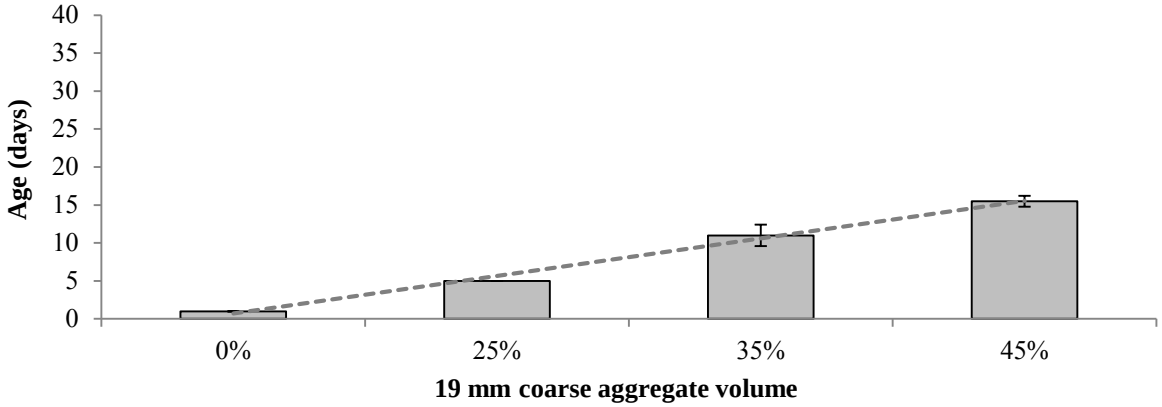

Figure 4.44: Time to first crack - Commercial mix (SikaGrout-212)

There is a remarkable consistency in the trends observed in the results of the influence of aggregate content on the time to first cracking shown in Figure 4.42, 4.43 and 4.44. This level of consistency is not often associated with this form of testing, as cracking tends to be a highly variable phenomenon.

The results showed that there was a direct relationship between coarse aggregate volume content and the time to first cracking. This trend was shown to be consistent for both the laboratory mixes and the commercial mixes.

The impact of coarse aggregate content was shown to be greatest for the w:c = 0.6 mixes, with the 45% aggregate content mix failing 30 days after the 0% aggregate content mix. This was followed by the w:c = 0.45 mixes, with the 45% aggregate content mix failing 26 days after the 0% aggregate content mix. Finally, the lowest impact of aggregate volume was observed for the SikaGrout-212 mixes, with the 45% aggregate content mix failing only 14 days after the 0% aggregate content mix.

4.3.1.2 Effect of coarse aggregate size

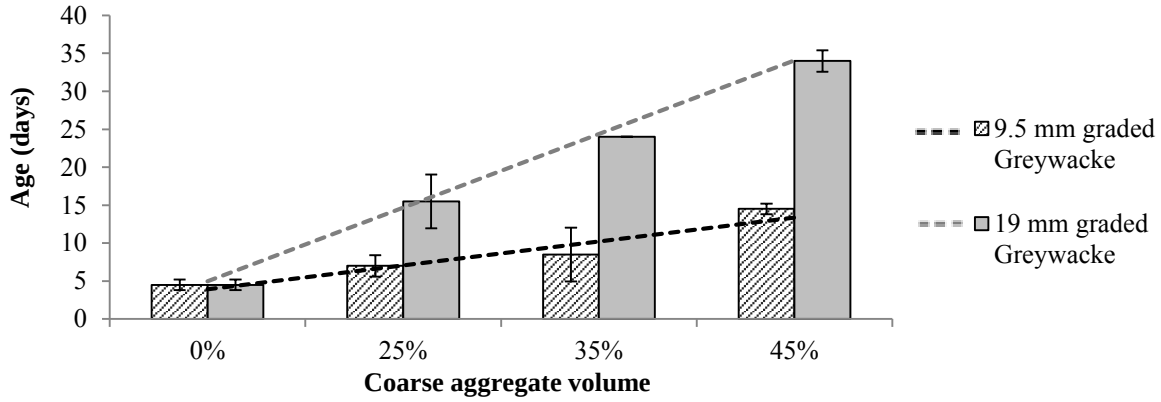

Figure 4.45: Time to first crack - Laboratory mix (w:c = 0.6)

There is a very clear influence of coarse aggregate size on the time to first cracking of restrained repair concrete, illustrated in Figure 4.45. It was shown that the smaller, 9.5 mm, coarse aggregate mixes failed at noticeably younger ages when compared to mixes made with identical volumes of the larger, 19 mm, coarse aggregate.

This difference tended to increase as the aggregate content increased, with the 9.5 mm mix failing 8 days before the 19 mm mix with 25% aggregate volume, the 9.5 mm mix failing 15 days before the 19 mm mix with 35% aggregate volume and the 9.5 mm mix failing 19 days before the 19 mm mix with 45% aggregate volume.

This suggests that the influence of coarse aggregate size became far more pronounced as the volume content of the aggregate was increased. A combination of high coarse aggregate content and larger coarse aggregate size was therefore shown to be the most effective.

4.3.1.3 Effect of mix type

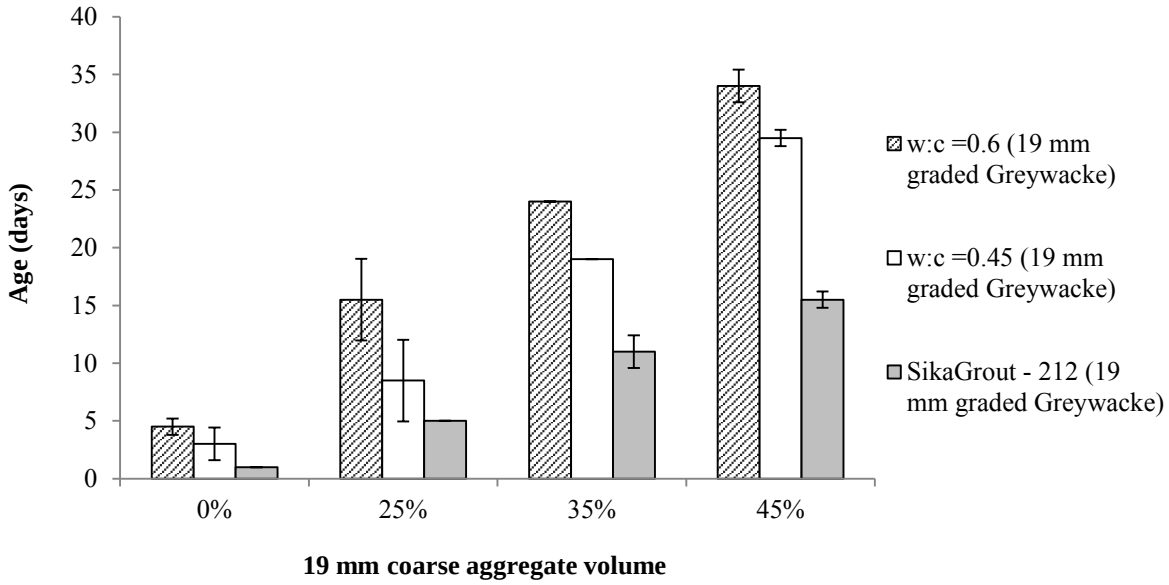

Figure 4.46: Time to first crack

The influence of repair mix type on the time to first crack is shown in Figure 4.46. It was shown that the w:c = 0.6 mixes had by far the best performance for all aggregate volume contents. The performance of the w:c = 0.45 mixes were shown to be substantially lower than the w:c = 0.6 mixes.

The SikaGrout-212 mixes were shown to have an exceptionally lower level of performance when compared to the laboratory mixes, for all coarse aggregate contents. Again, this was not expected, as the SikaGrout-212 had been shown to have very high strength levels in both tension and compression.

4.3.2 Crack intensity

Crack intensity was tested in order to further directly examine the influence of coarse aggregate volume and size on the performance of repair concretes subjected to restrained deformation. This crack intensity information could then be correlated with the time to first crack results and provide further insight into the trends observed in the previous section. Crack intensity was determined by estimating the total crack area of the cracked ring test specimens, two weeks after initial failure was observed. See Section 3.5.1.2.

4.3.2.1 Effect of coarse aggregate content

The effect of varying coarse aggregate content on the crack intensity of the laboratory and commercial mixes is shown in Figure 4.47, 4.48 and 4.49 respectively.

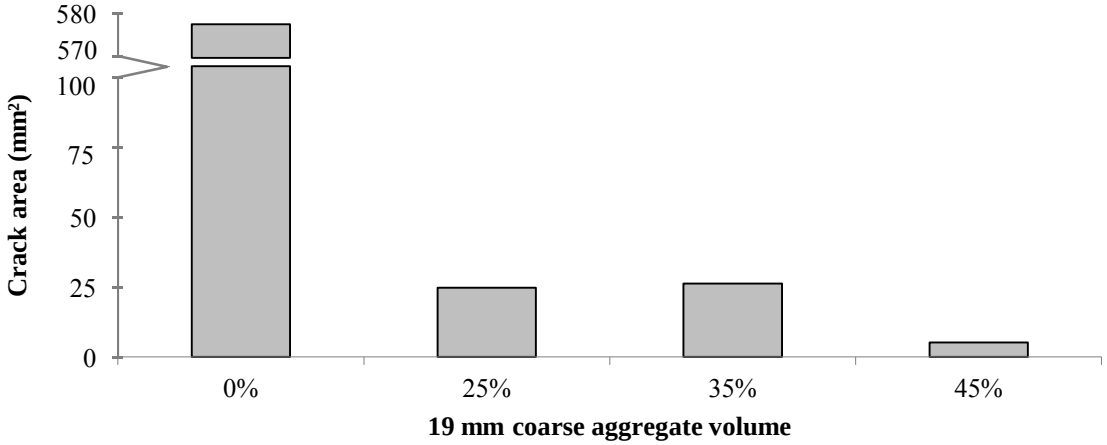

Figure 4.47: Crack intensity - Laboratory mix (w:c = 0.6)

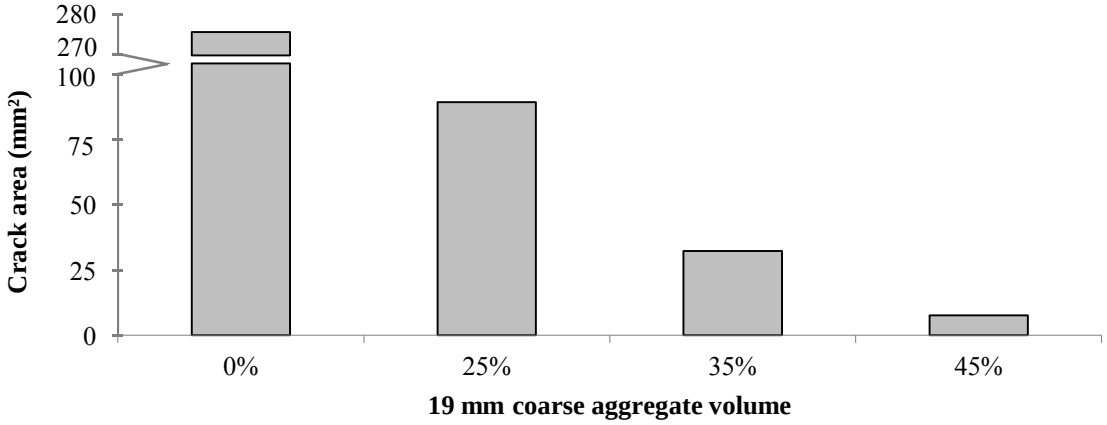

Figure 4.48: Crack intensity - Laboratory mix (w:c = 0.45)

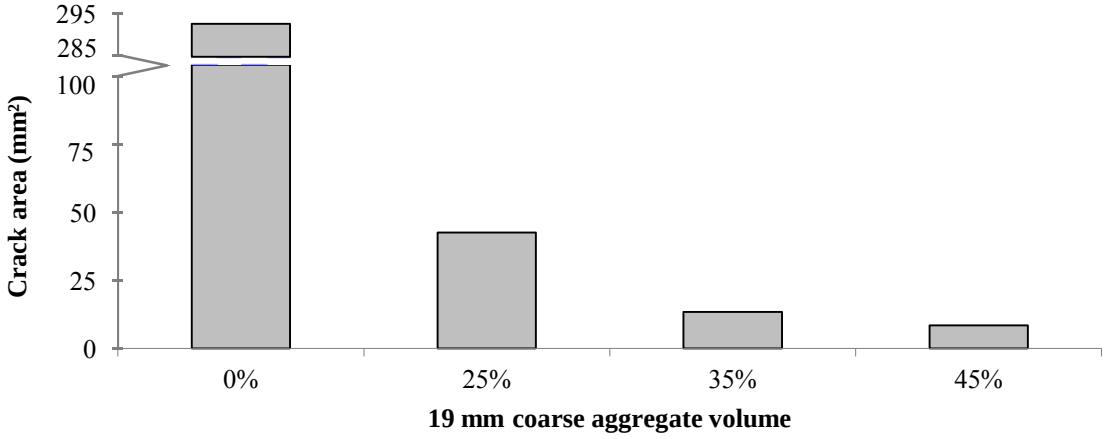

Figure 4.49: Crack intensity - Commercial mix (SikaGrout-212)

From the results, it was evident that the crack intensity of the control (0% aggregate content) mixes for both the laboratory mixes and the commercial mix were substantially higher than the crack intensity observed for the mixes that included a coarse aggregate.

It was noted that there was a definite linear trend with regard to the influence of aggregate volume content on crack intensity, with the crack intensity being shown to decrease as the coarse aggregate content increases. This general trend was observed for all mixes, but was shown to be more pronounced for the higher strength w:c = 0.45 and SikaGrout-212 mixes. It can therefore be deduced that an increase in coarse aggregate volume will result in a longer time to first crack and lower crack intensity.

4.3.2.2 Effect of coarse aggregate size

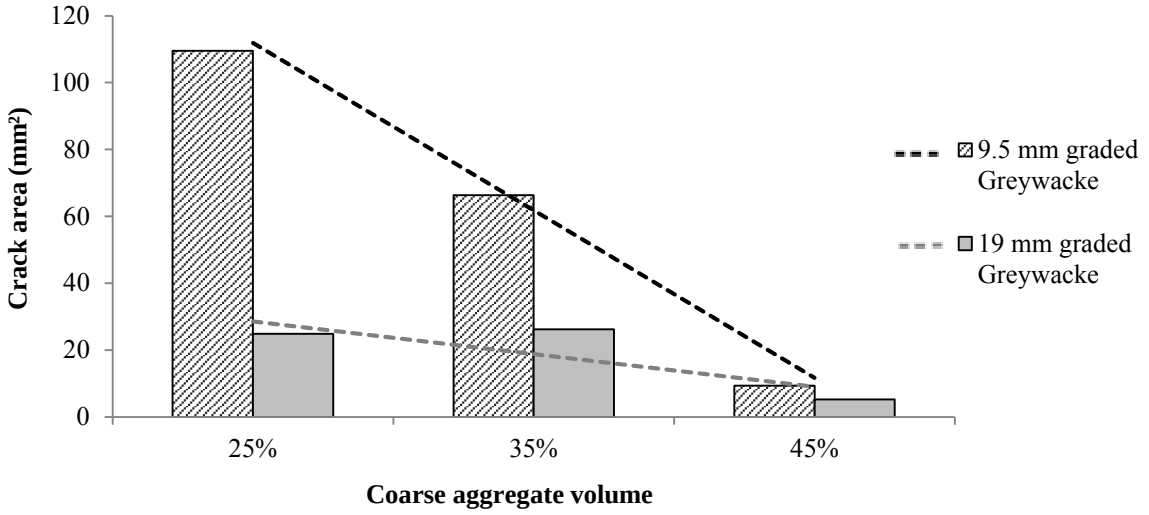

Figure 4.50: Crack intensity - Laboratory mix (w:c = 0.6)

The effect of coarse aggregate size on crack intensity is shown in Figure 4.50, and it was evident that the size of coarse aggregate used had a profound influence on the intensity of cracking. The crack intensity of mixes that used the larger, 19 mm, aggregate showed substantially lower levels of crack intensity when compared to the mixes with identical volume contents of the smaller, 9.5 mm, aggregate.

However, it was noted that the influence of aggregate size on crack intensity decreased as the volume content of coarse aggregate was increased. With a volume content of 25%, the 9.5 mm mix was shown to have a crack intensity of approx. 85 mm^2 higher than the 19 mm mix, but with a volume content of 45%, the 9.5 mm mix was shown to only have a crack intensity of approx. 5 mm^2 higher than the 19 mm mix.

4.3.2.3 Effect of mix type

Due to the very high crack intensity readings for the 0% control mixes, they have been shown separately in Figure 4.51.

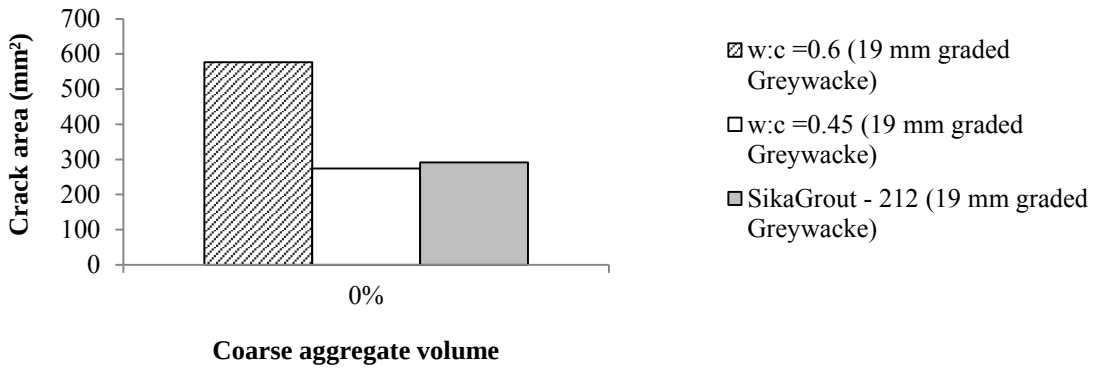

Figure 4.51: Crack intensity (0% coarse aggregate volume)

In Figure 4.51, the crack intensity of the w:c = 0.6 control mix was shown to be more than double the crack intensity of the w:c = 0.45 and SikaGrout-212 mixes, which were shown to be relatively similar. This was not expected, as the w:c = 0.6 mix was shown to have the best performance and the highest time to first crack. Therefore, it is possible that this unusually high reading could have been an outlier that can be associated with this form of testing.

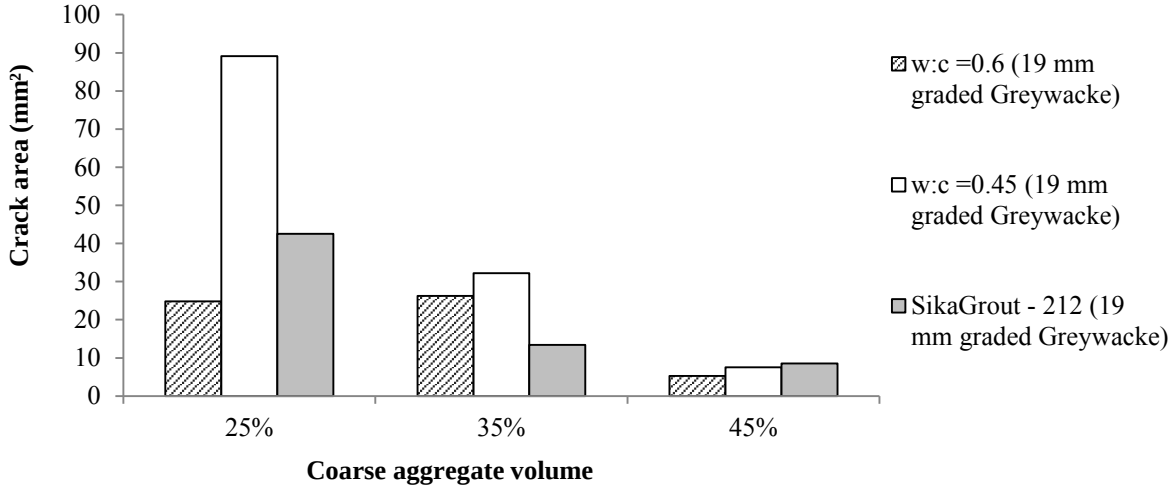

Figure 4.52: Crack intensity

The comparison of the mixes with the presence of a coarse aggregate shown in Figure 4.52 also provide very scattered results, with no particular trends evident. This is again indicative of the variable nature of concrete crack testing. No specific findings can therefore be given for the influence of repair mix type on crack intensity.

4.4 Summary and conclusion

Results have been presented and discussed that pertain to the influence of coarse aggregate volume content and size on the key concrete properties that have been shown to directly influence the performance of bonded concrete overlays. The influence of the repair material mix type on these specific material properties has also been examined and presented. These findings are summarised in Table 4.1.

Table 4.1: Summary of material property experimental findings

Property	Influence of coarse aggregate volume content	Influence of coarse aggregate size	Influence of mix type
Tensile strength	– The directly proportional impact of an increase in coarse aggregate volume content was only shown to be significant for the w:c = 0.6 laboratory mixes at younger ages. – In general, it was shown that coarse aggregate volume content did not have a substantial impact on tensile strength.	– The impact of coarse aggregate size on tensile strength was observed to be negligible at younger ages (7 days). – At older ages (28 days) mixes with the smaller 9.5 mm aggregate were shown to have a higher tensile strength when compared to mixes made with the larger 19 mm coarse aggregate.	– It was shown that in general, the w:c = 0.45 mixes produced concrete with a tensile strength that was slightly higher than the w:c = 0.6 mixes at all ages. – The SikaGrout-212 mixes were shown to have a higher tensile strength when compared to the laboratory mixes.
Tensile relaxation	– Tensile relaxation was shown to decrease as coarse aggregate volume increased at all ages.	– The magnitude of tensile relaxation of mixes with smaller coarse aggregate was observed to be less than mixes containing larger coarse aggregate for all aggregate volume contents at all ages.	– The w:c = 0.6 mixes were shown to have the highest relaxation levels, while the SikaGrout-212 mixes showed the lowest level of relaxation at all ages.
Elastic modulus	- A direct relationship between coarse aggregate volume content and elastic stiffness was observed at all ages.	– An increase in coarse aggregate size was observed to increase elastic stiffness for all aggregate volume contents and at all ages.	– At younger ages (7 days) the w:c=0.6 mixes had the lowest elastic modulus and the SikaGrout-212 mixes had the highest. – At older ages (28 days) the w:c = 0.45 mixes were shown to have an elastic modulus greater than the SikaGrout-212 mixes.
Free drying shrinkage	– The total magnitude of drying shrinkage was shown to decrease as coarse aggregate volume content was increased	– Drying shrinkage was shown to be greater for mixes containing smaller coarse aggregate at all ages.	– The w:c = 0.45 mixes were shown to have a slightly higher level of shrinkage compared to the w:c = 0.6 mixes during the first 10 days. – At ages greater than 10 days, the w:c = 0.6 mixes were shown to have a higher level of shrinkage compared to the w:c = 0.45 mixes. – The SikaGrout-212 mixes showed a very rapid initial rate of shrinkage when compared to the laboratory mixes.

The results of direct restrained shrinkage testing of the time to first crack and crack intensity of these different repair mixes, with varying aggregate contents and sizes, have also been presented and are summarised in Table 4.2.

Table 4.2: Summary of direct test experimental findings

Property	Influence of coarse aggregate volume content	Influence of coarse aggregate size	Influence of mix type
Time to first cracking	– The results indicate a direct relationship between the time to first cracking and coarse aggregate volume content, and this was observed for the commercial and laboratory mixes.	– Mixes containing the smaller 9.5 mm coarse aggregate were shown to fail at noticeably younger ages than equivalent mixes containing the larger 19 mm coarse aggregate.	– The longest time to first cracking was observed for the w:c = 0.6 mixes. – The SikaGrout-212 mixes were shown to have the poorest performance, with failure occurring well before the equivalent laboratory mixes.
Crack intensity	– The influence of coarse aggregate volume content on crack intensity was shown to be significant, with the crack intensity of the control (0% aggregate content) mixes being shown to be substantially higher than the mixes containing coarse aggregate.	– The crack intensity of the mixes containing the smaller 9.5 mm coarse aggregate were substantially higher than the mixes containing the larger 19 mm coarse aggregate.	– No particular trends were identified with regard to the influence of mix type on crack intensity

A critical comparison and discussion of these results and the links between the repair concrete properties and the direct test results is presented in Chapter 6. In addition to this, analytical modelling based on these concrete property results is done in Chapter 5 and these analytical predictions are then compared and contrasted with the direct test results.

Chapter 5: Analytical modelling and analysis

5.1 Introduction

The analytical modelling method that was used in this investigation to predict the age at cracking of bonded concrete overlays is based on the material property analytical approach that was discussed in Chapter 2. In this Chapter, the key components of this modelling technique will be presented along with the fundamental assumptions that are made. Prediction outputs will then be presented for the varying mixes and will be evaluated against the direct test results from the ring tests. Conclusions can then be drawn with regard to the accuracy and effectiveness of this prediction method for determining the age at first cracking of bonded concrete overlays.

5.2 Analytical modelling method

The analytical modelling method that is used in this investigation is based on the concept of using the time development of specific repair material properties to estimate the time of first cracking of the material. This revolves around the idea that the induced stress caused by restrained deformation of the overlay material can be determined based on its elastic, restrained shrinkage and relaxation properties. This predicted stress can then be compared with the intrinsic tensile strength of the material, with cracking occurring when the induced stress exceeds this intrinsic tensile strength. The influence of tensile relaxation and the resulting 'stress relief' is considered and shown to increase the time taken for the elastic stress to exceed the material tensile strength. This is illustrated in Figure 5.1.

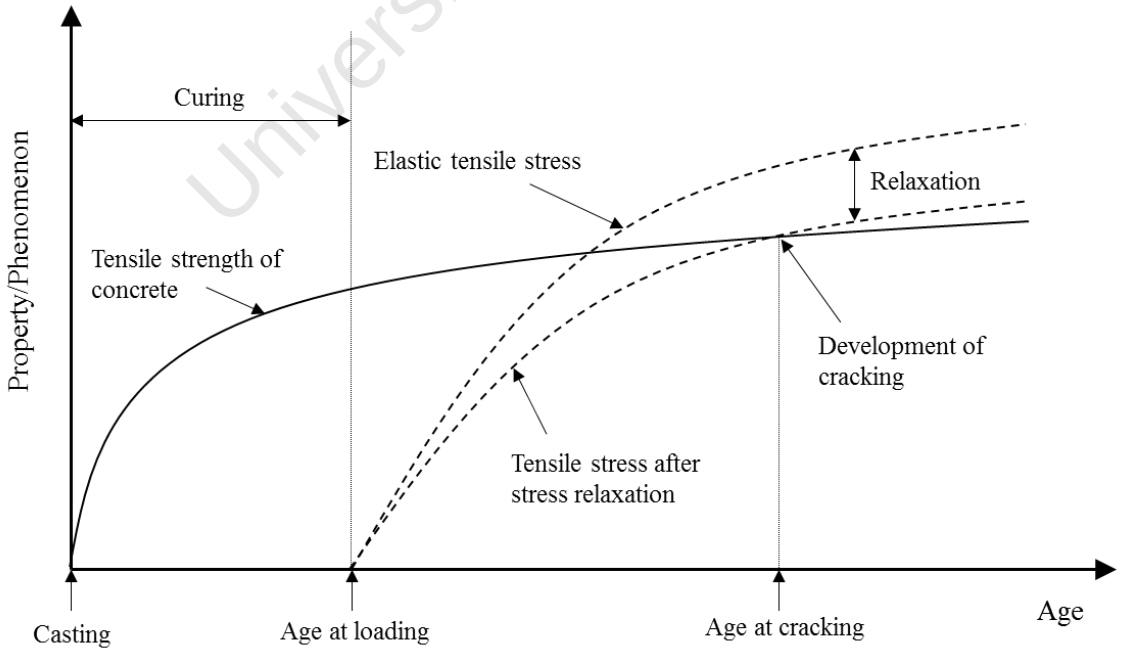

Figure 5.1: Prediction of the age at cracking of repair overlay based on material properties (adapted from Chilwesa, 2012)

This modelling concept is based on work done by Gilbert (1988) and has been successfully used by Chilwesa (2012) to predict the time to cracking failure of different repair mortars with an acceptable degree of accuracy.

Chilwesa (2012) explains that estimating the time development of the elastic stress was achieved by dividing the total time into a number of separate time intervals and using the change in shrinkage strain for each separate time interval to determine the resulting stress increment. This relies on the principle of superposition which is outlined by Gilbert (1988) and Ghali *et al*. (2006), which states that the strain increment applied at any time (t_i) will not be affected by another strain applied before or after this time. This concept is illustrated in Figure 5.1.

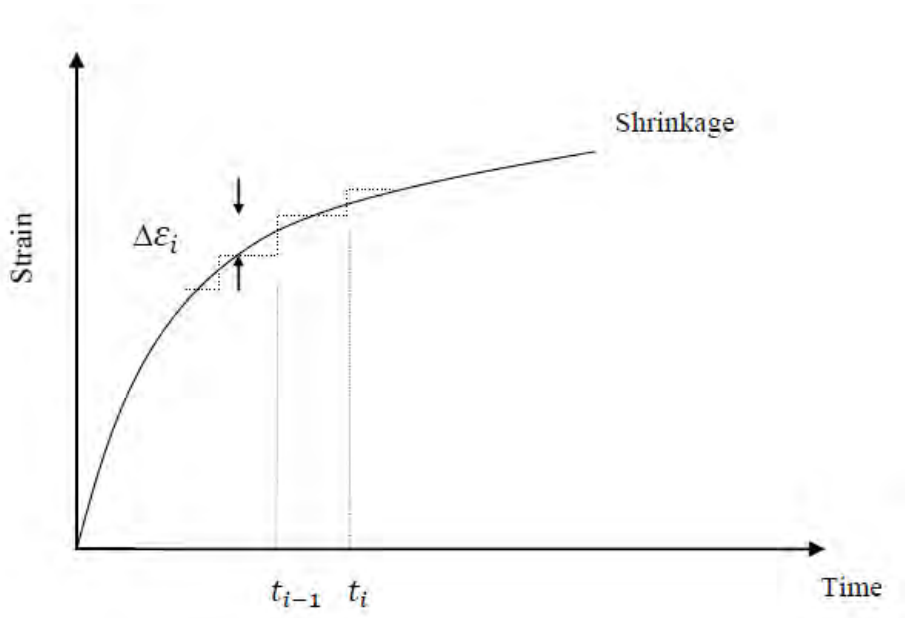

Figure 5.2: Strain increments based on the theory of super position (Chilwesa, 2012)

Based on this, Gilbert (1988) proposes the following expression for the elastic stress (σ_i) at any time (t_i):

$$\sigma_i = \sigma_{i-1} + \Delta\varepsilon_i . E_i \qquad (5.1)$$

Where:

σ_i = Remaining stress at time t_i
σ_{i-1} = Remaining stress at time t_{i-1}
$\Delta\varepsilon_i$ = Change in shrinkage in the interval $t_{i-1} - t_i$
E_i = Mean elastic modulus in the interval $t_{i-1} - t_i$

Strain increments ($\Delta\varepsilon_i$) are assumed to be applied in the middle of the time intervals, with the mean elastic modulus (E_i) also being taken at the middle of the interval. Gilbert (1988) goes on to propose that the 'stress relief' caused by tensile relaxation can be accounted for with the inclusion of a relaxation factor (ψ_i).

The following equation is therefore proposed for the remaining stress ($\ddot{\sigma}_i$) at any time (t_i):

$$\ddot{\sigma}_i = \ddot{\sigma}_{i-1} + \Delta\varepsilon_i . E_i . \psi_i \quad (5.2)$$

Where:

$\ddot{\sigma}_i$ = Remaining stress at time t_i
$\ddot{\sigma}_{i-1}$ = Remaining stress at time t_{i-1}
$\Delta\varepsilon_i$ = Change in shrinkage in the interval $t_{i-1} - t_i$
E_i = Mean elastic modulus in the interval $t_{i-1} - t_i$
ψ_i = Factor accounting for the magnitude of mean relaxation in the interval $t_{i-1} - t_i$

The relaxation factor (ψ_i) is also calculated for the middle of the time interval, as assumed for the mean elastic modulus (E_i). This calculated remaining stress functions can then be plotted with the tensile strength curve for the material to determine time of first overlay cracking.

5.3 Assumptions

Due to the highly complex interaction of factors that influence overlay cracking and the mechanisms involved a number of fundamental assumptions had to be made. Chilwesa (2012) explains that these assumptions were necessary to ensure that the prediction model remained simple and user friendly.

5.3.1 No shrinkage during curing

The first key assumption that was made was that no shrinkage occurred during the curing period.

As discussed in detail in Chapter 2, there are a number of different types of shrinkage that occur in concrete. Effective curing has been shown to mitigate and delay many of these different forms of shrinkage by preventing moisture loss from the concrete into the environment. However, autogeneous shrinkage, which is defined by Alexander & Beushausen (2009) as the reduction of volume due to the internal consumption of water during the hydration process, is independent of the environmental conditions and will therefore occur during the curing process.

However, Alexander & Beushausen (2009) go on to explain that it is generally accepted that autogeneous shrinkage for mixes with a w:c that exceeds 0.4 can be considered negligible, making this assumption by Chilwesa (2012) applicable to the modelling of overlay repair materials.

Chilwesa (2012) does make a recommendation that a more sophisticated modelling system should consider the influence of autogeneous shrinkage to achieve a greater level of accuracy with regard to predictions.

5.3.2 Instantaneous tensile relaxation

Tensile relaxation has been extensively studied (Kordina *et al.*, 2000, Morimoto & Koyanagi, 1995, Beushausen & Alexander, 2005 and Gutsch & Rostasy, 1995), and it is the general consensus amoung researchers that significant amounts of tensile relaxation take place very soon after loading.

Chilwesa (2012) therefore suggests that in order to facilitate analytical modelling of overlay stresses it is appropriate to account for relaxation as occurring instantaneously after loading (see Figure 5.3). This assumption is supported by work done by Masuku (2009). For the purpose of this investigation, a 48 hour relaxation value is taken as the ultimate.

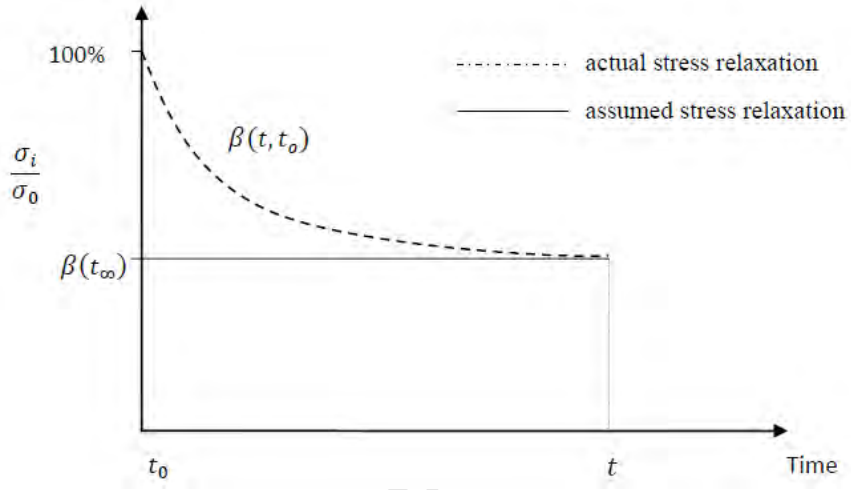

Figure 5.3: Simplified instantaneous ultimate relaxation used for analytical modelling (Chilwesa, 2012)

5.3.3 Relationship between free and restrained shrinkage

In a previous study by Beushausen (2005), it was shown that the restrained shrinkage due to the differential volume changes of overlay and substrate was 60% of the overlay free shrinkage. The following conversion equation was therefore applied to the change in free shrinkage strain ($\Delta\varepsilon_{FSSi}$) to determine the change in restrained shrinkage strain ($\Delta\varepsilon_i$):

$$\Delta\varepsilon_i = 0{,}6.\,\Delta\varepsilon_{FSSi} \qquad (5.3)$$

Where:

$\Delta\varepsilon_i$ = Change in restrained shrinkage in the interval $t_{i-1} - t_i$
$\Delta\varepsilon_{FSSi}$ = Change in free shrinkage in the interval $t_{i-1} - t_i$

5.4 Experimental inputs

The experimental component of the investigation provided the inputs required for the analytical modelling. Although free shrinkage was tested daily, elastic modulus and tensile relaxation was only tested at 7 and 28 days. Tensile strength was tested at 7, 10 and 28 days. The use of regression functions was therefore required to interpolate values for the periods when no test results were available.

Chilwesa (2012) conducted an extensive literature survey and found that a number of different regression functions have been developed to modal the trends of concrete material properties. Chilwesa (2012) concluded that logarithmic regression functions showed the best fit with the experimental data, and were therefore deemed suitable for the modelling component of this investigation. The following regression functions were therefore used:

Inputs:

$E_i(t_i)$ = Mean elastic modulus in the interval $t_{i-1} - t_i$
$F_{Yi}(t_i)$ = Tensile strength at time t_i
$\beta_i(t_i)$ = Mean relaxation in the interval $t_{i-1} - t_i$
$\psi_i(t_i)$ = Relaxation factor in the interval $t_{i-1} - t_i$
$A, B, C, D, N \text{ and } M$ = Constants depending on regression analysis

$$E_i(t_i) = A.\ln(t_i) + B \tag{5.4}$$

$$F_{Yi}(t_i) = C.\ln(t_i) + D \tag{5.5}$$

$$\beta_i(t_i) = N.\ln(t_i) + M \tag{5.6}$$

$$\psi_i(t_i) = (100 - \beta_i(t_i)).\frac{1}{100} \tag{5.7}$$

Examples of these regression curves are shown in Figure 5.4, 5.5 and 5.6. All of the regression curves are presented in Appendix B.

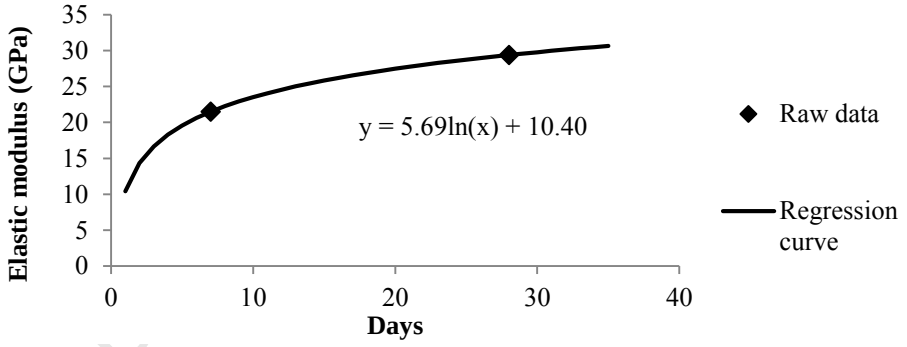

Figure 5.4: Typical elastic modulus regression curve

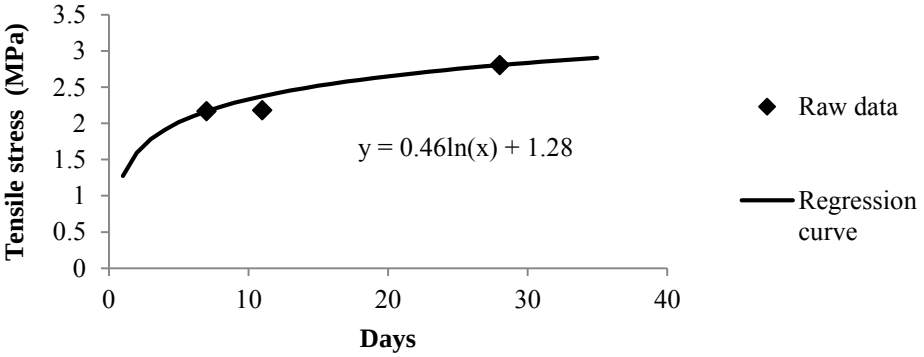

Figure 5.5: Typical tensile strength regression curve

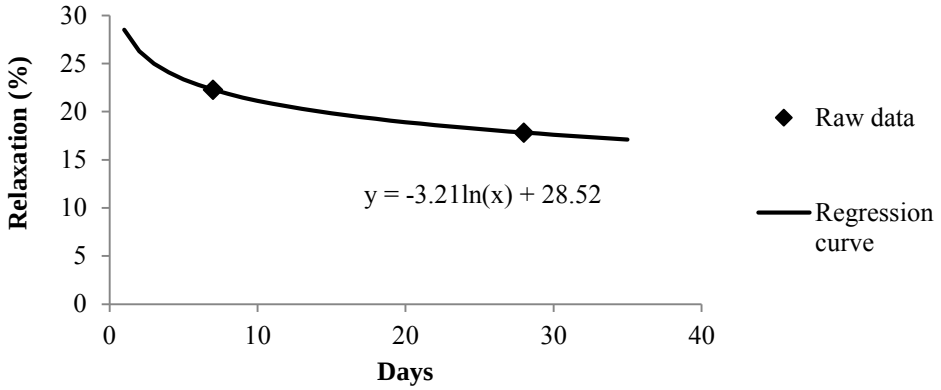

Figure 5.6: Typical tensile relaxation regression curve

5.5 Analytical model outputs

The repair material property analytical model that has been discussed is applied to the different mixes that were tested in the investigation and used to generate predicted times to first cracking. As specimens were cured for 7 days, the predicted elastic and remaining elastic stresses generated by the models start directly after curing. This is because a shrinkage strain of 0 is assumed during the curing phase.

5.5.1 Laboratory mix (w:c =0.45)

0% coarse aggregate volume

The input data used to model the time to first cracking of the w:c =0.45 laboratory mix with 0% coarse aggregate volume content is shown in Table 5.1.

Table 5.1: Material property inputs for w:c = 0.45 laboratory mix (0% coarse aggregate content)

Period (days)	Change in restrained shrinkage strain	Mean elastic modulus (GPa)	Tensile strength (MPa)	Relaxation function	Elastic stress (MPa)	Remaining stress (MPa)
Curing (0 to 7)	0	27.6	2.6	0.79	0	0
7 to 8	17.0	29.0	2.7	0.79	0.5	0.4
8 to 9	21.0	30.3	2.7	0.80	1.1	0.9
9 to 10	11.0	31.4	2.7	0.80	1.5	1.2
10 to 11	15.0	32.4	2.8	0.81	2.0	1.6
11 to 12	14.0	33.3	2.8	0.81	2.4	2.0
12 to 13	7.2	34.1	2.8	0.81	2.7	2.2
13 to 14	6.8	34.8	2.9	0.82	2.9	2.4
14 to 15	11.0	35.5	2.9	0.82	3.3	2.7
15 to 16	11.0	36.2	2.9	0.82	3.7	3.0
16 to 17	13.2	36.8	3.0	0.82	4.2	3.4
17 to 18	12.8	37.3	3.0	0.83	4.7	3.8
18 to 19	6.4	37.9	3.0	0.83	4.9	4.1
19 to 20	3.6	38.4	3.0	0.83	5.0	4.2

This data in Table 5.1 is plotted to determine time to first cracking. See Figure 5.7.

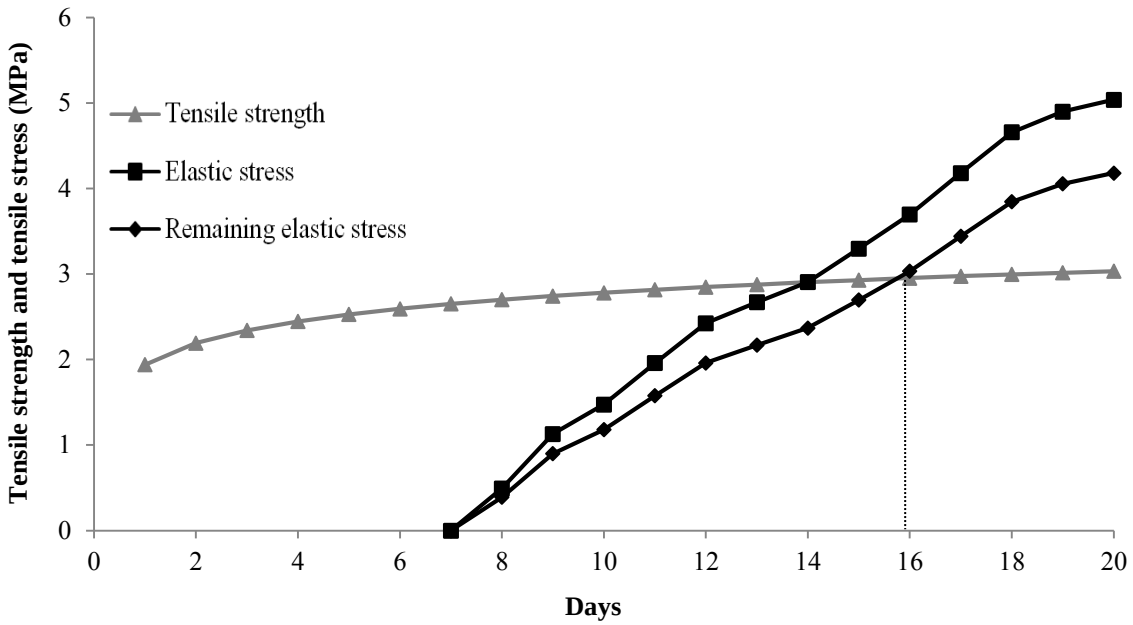

Figure 5.7: Overlay tensile strength and stress development for w:c = 0.45 laboratory mix (0% coarse aggregate content)

The material inputs for the remaining w:c = 0.45 laboratory mixes are given in Appendix B and have been plotted in Figure 5.8, 5.9 and 5.10 respectively.

25% coarse aggregate volume (19 mm)

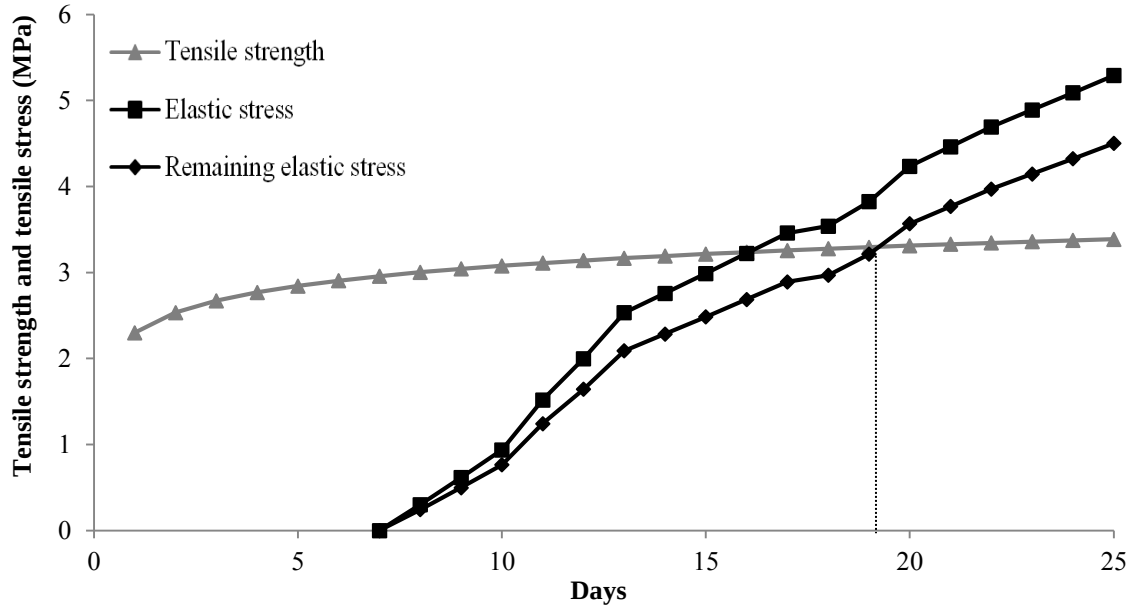

Figure 5.8: Overlay tensile strength and stress development for w:c = 0.45 laboratory mix (25% 19 mm coarse aggregate content)

35% coarse aggregate volume (19 mm)

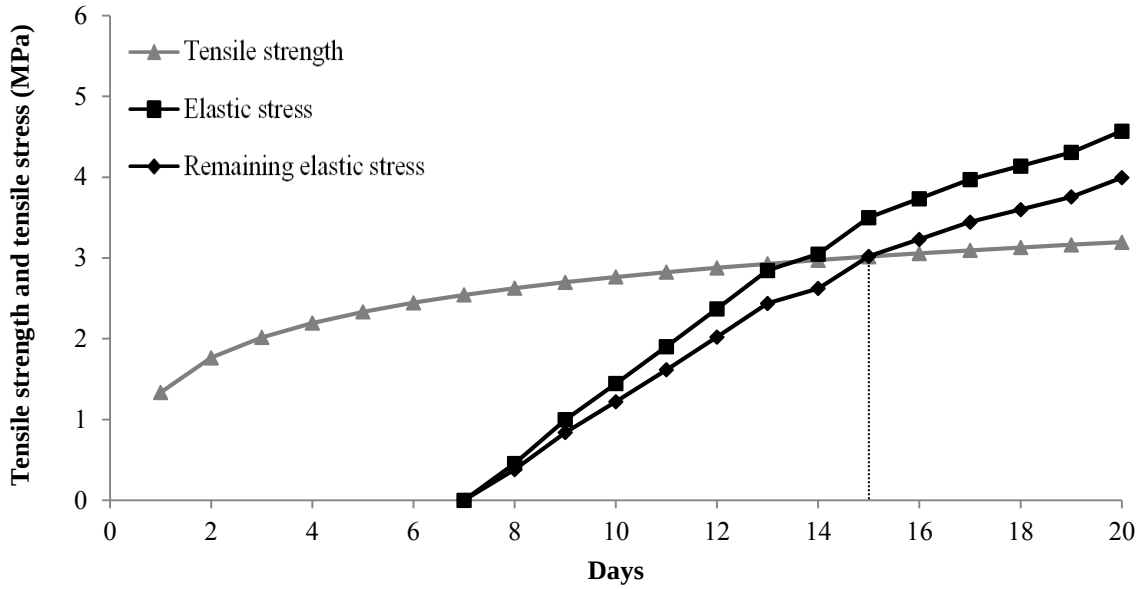

Figure 5.9: Overlay tensile strength and stress development for w:c = 0.45 laboratory mix (35% 19 mm coarse aggregate content)

45% coarse aggregate volume (19 mm)

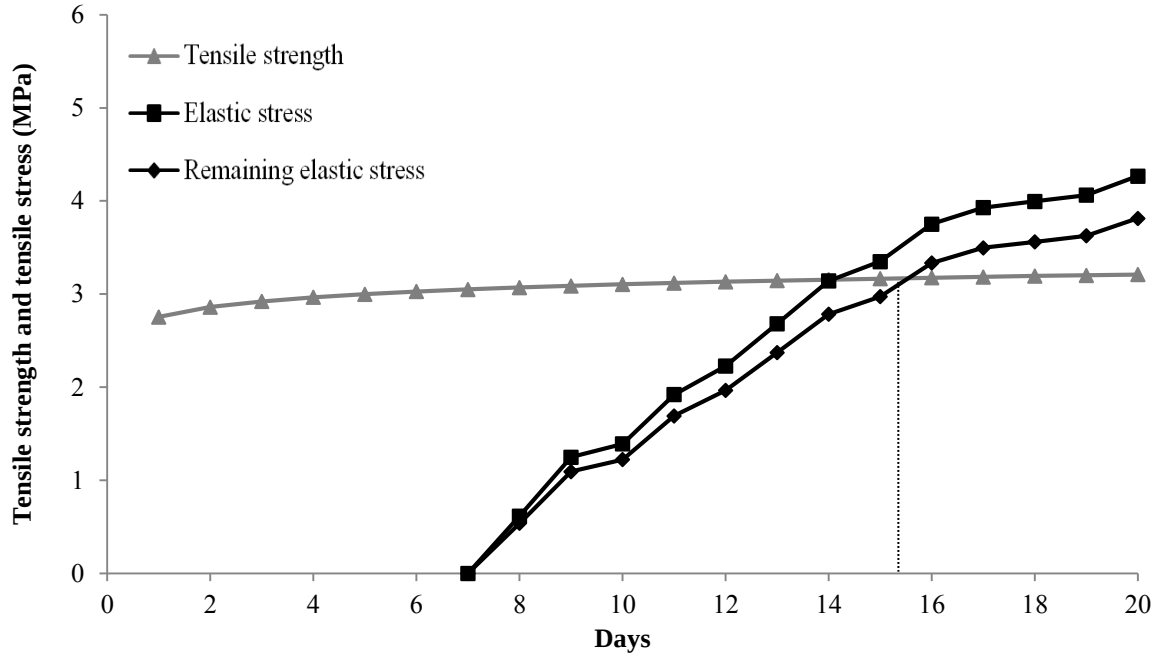

Figure 5.10: Overlay tensile strength and stress development for w:c = 0.45 laboratory mix (45% 19 mm coarse aggregate content)

From the analysis results (Figure 5.7, 5.8, 5.9 and 5.10) it is predicted that it will take 16 days for the w:c = 0.45 0% aggregate content mix to fail. This is followed by the 25 % 19 mm aggregate content mix which is predicted to fail at 19 days after casting. The 35% and 45% 19 mm aggregate mixes are both predicted to fail at 15 days after casting.

5.5.2 Laboratory mix (w:c =0.6)

The material inputs for the w:c = 0.6 laboratory mixes containing 19 mm coarse aggregate are given in Appendix B and have been plotted in Figure 5.11, 5.12, 5.13 and 5.14 respectively.

0% coarse aggregate volume

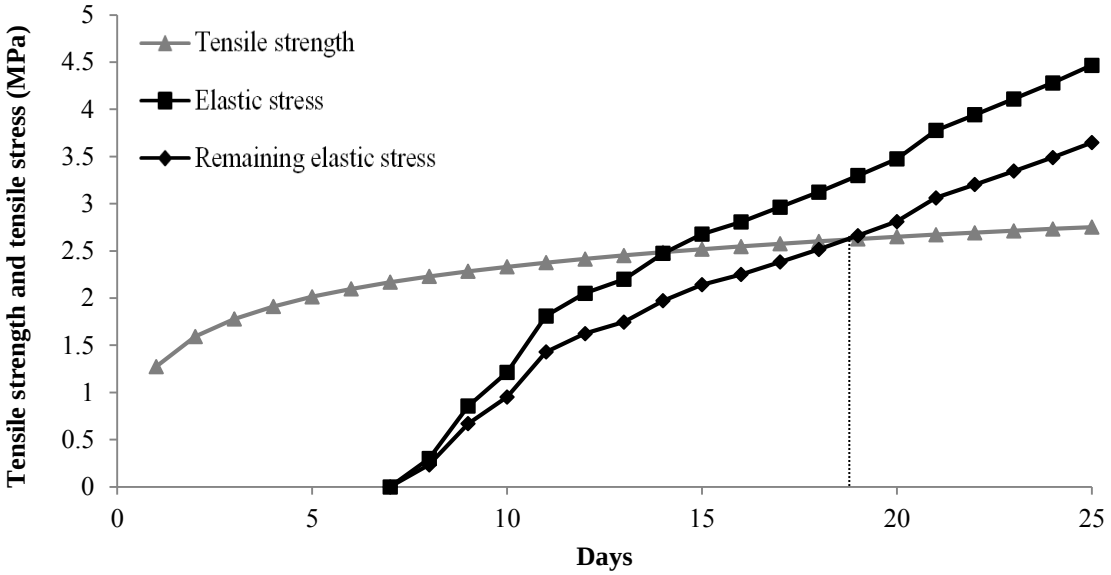

Figure 5.11: Overlay tensile strength and stress development for w:c = 0.6 laboratory mix (0% coarse aggregate content)

25% coarse aggregate volume (19 mm)

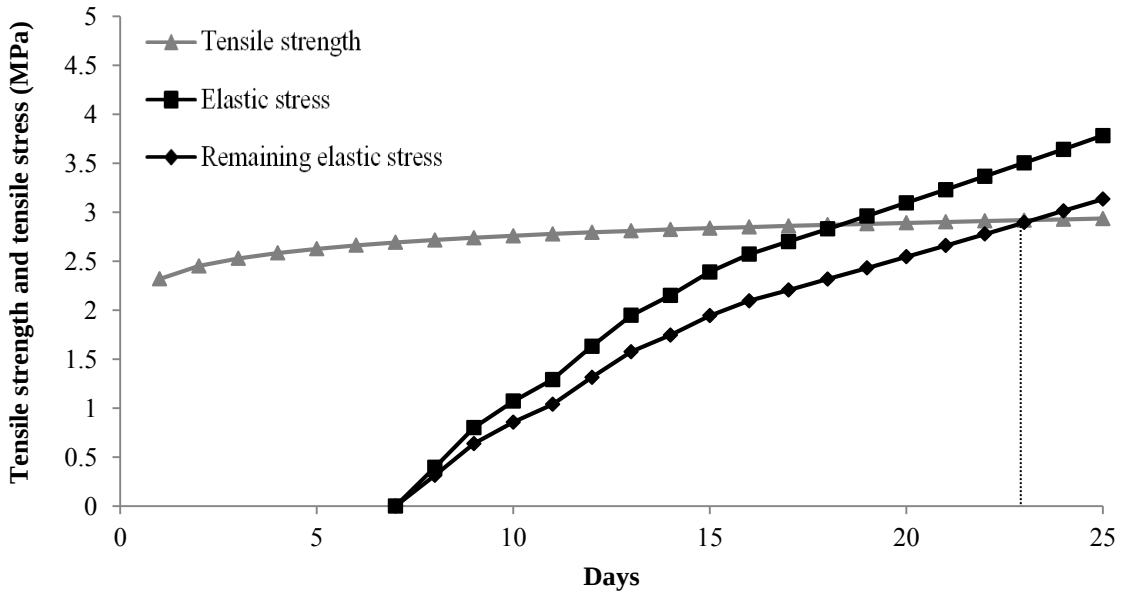

Figure 5.12: Overlay tensile strength and stress development for w:c = 0.6 laboratory mix (25% 19 mm coarse aggregate content)

35% coarse aggregate volume (19 mm)

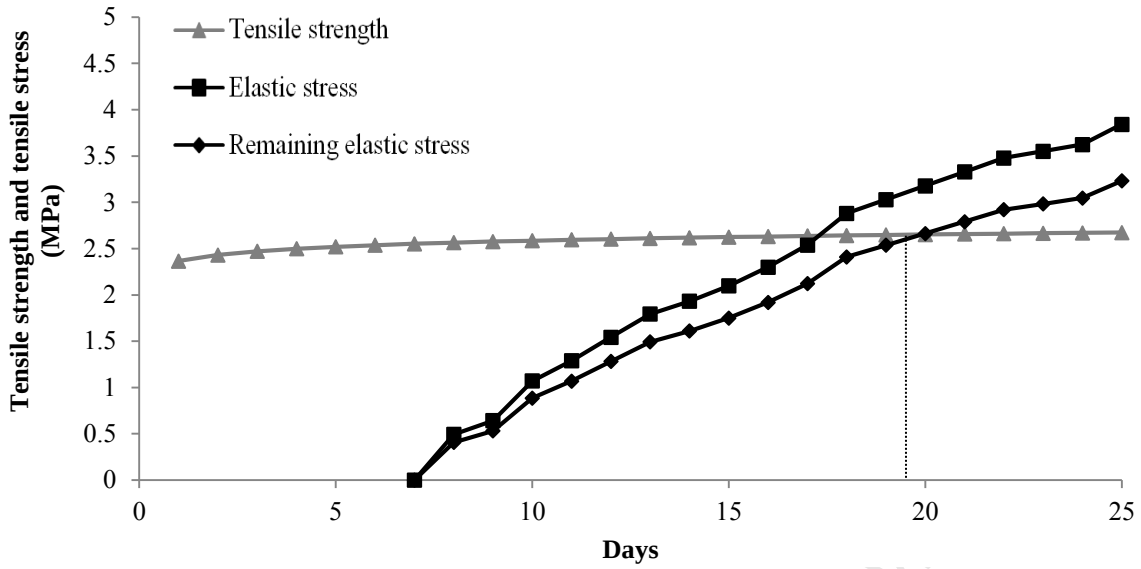

Figure 5.13: Overlay tensile strength and stress development for w:c = 0.6 laboratory mix (35% 19 mm coarse aggregate content)

45% coarse aggregate volume (19 mm)

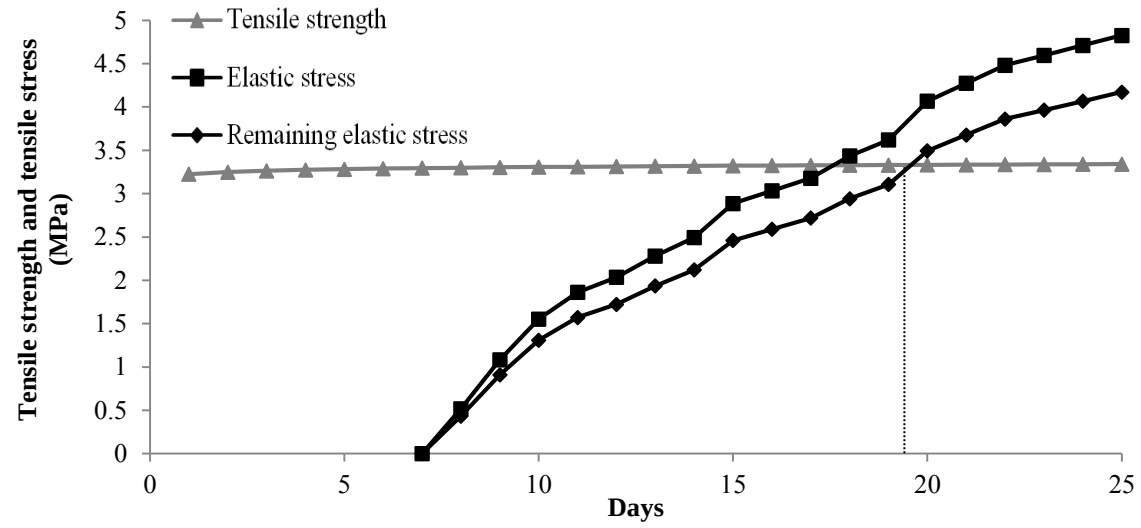

Figure 5.14: Overlay tensile strength and stress development for w:c = 0.6 laboratory mix (45% 19 mm coarse aggregate content)

The results (Figure 5.11, 5.12, 5.13 and 5.14) show that it is predicted that it will take 18 days for the w:c = 0.6 0% aggregate content mix to fail. This is followed by the 25 % 19 mm aggregate content mix which is predicted to fail at 23 days after casting. However, the 35% and 45% 19 mm aggregate mixes are both predicted to fail at 19 days after casting.

A similar trend is observed in the predicted results for the w:c = 0.6 mixes with 19 mm aggregate that was observed for the w:c = 0.45 mixes with 19 mm aggregate.

The material inputs for the w:c = 0.6 laboratory mixes containing the smaller 9.5 mm coarse aggregate are given in Appendix B and have been plotted in Figure 5.15, 5.16 and 5.17 respectively.

25% coarse aggregate volume (9.5 mm)

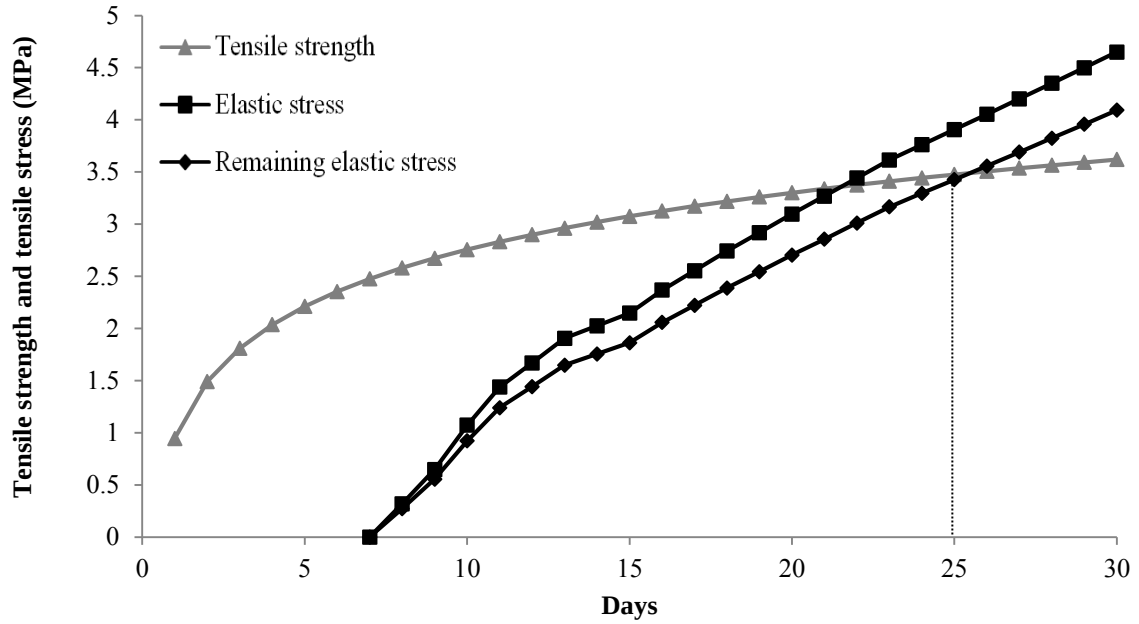

Figure 5.15: Overlay tensile strength and stress development for w:c = 0.6 laboratory mix (25% 9.5 mm coarse aggregate content)

35% coarse aggregate volume (9.5 mm)

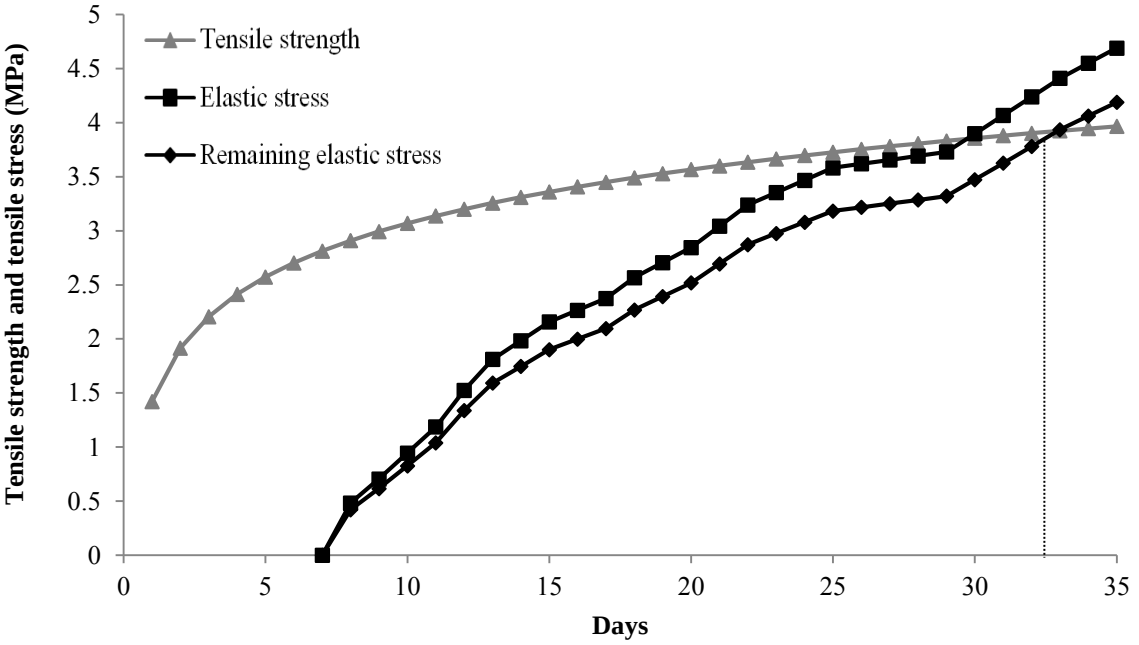

Figure 5.16: Overlay tensile strength and stress development for w:c = 0.6 laboratory mix (35% 9.5 mm coarse aggregate content)

45% coarse aggregate volume (9.5 mm)

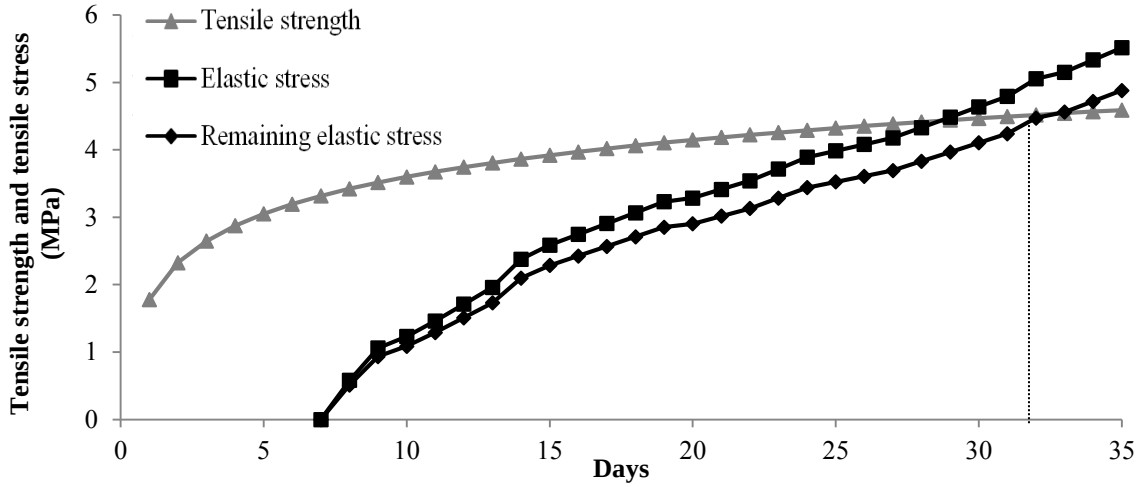

Figure 5.17: Overlay tensile strength and stress development for w:c = 0.6 laboratory mix (45% 9.5 mm coarse aggregate content)

From the analysis results (Figure 5.15, 5.16 and 5.17) it is predicted that it will take 25 days for the w:c = 0.6 25% 9.5 mm aggregate content mix to fail. This is followed by the 35 % 9.5 mm aggregate content mix which is predicted to fail at 32 days, with the 45 % 9.5 mm aggregate content mix being predicted to fail just over 31 days after casting. The trend observed for the predicted results of the mixes containing the smaller 9.5 mm aggregate differs substantially from the trends observed for both laboratory mixes with the larger 19 mm coarse aggregate.

5.5.3 Commercial mix (SikaGrout-212)

The material inputs for the commercial SikaGrout-212 mixes with 19 mm aggregate are given in Appendix B and have been plotted in Figure 5.18, 5.19, 5.20 and 5.21 respectively.

0% coarse aggregate volume

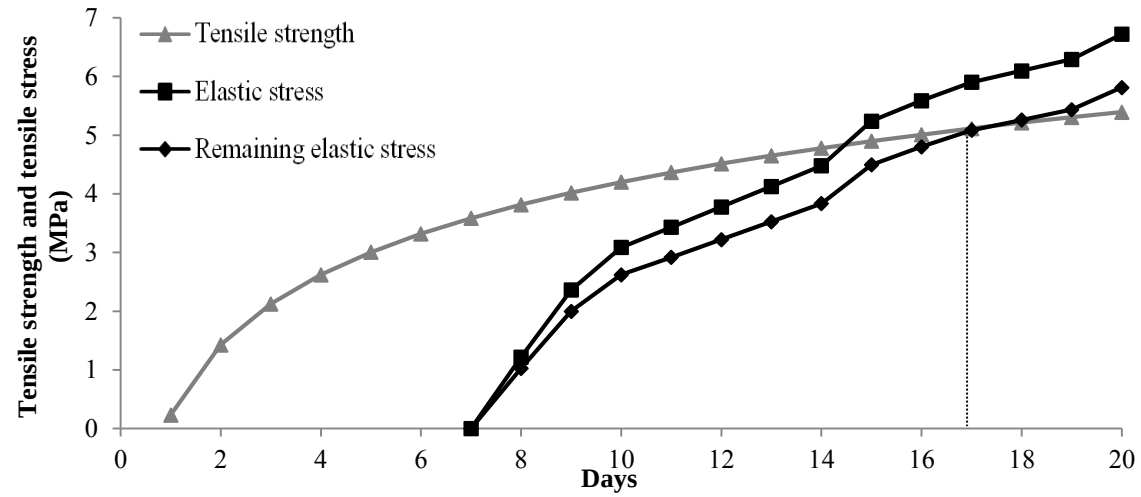

Figure 5.18: Overlay tensile strength and stress development for SikaGrout-212 commercial mix (0% coarse aggregate content)

25% coarse aggregate volume (19 mm)

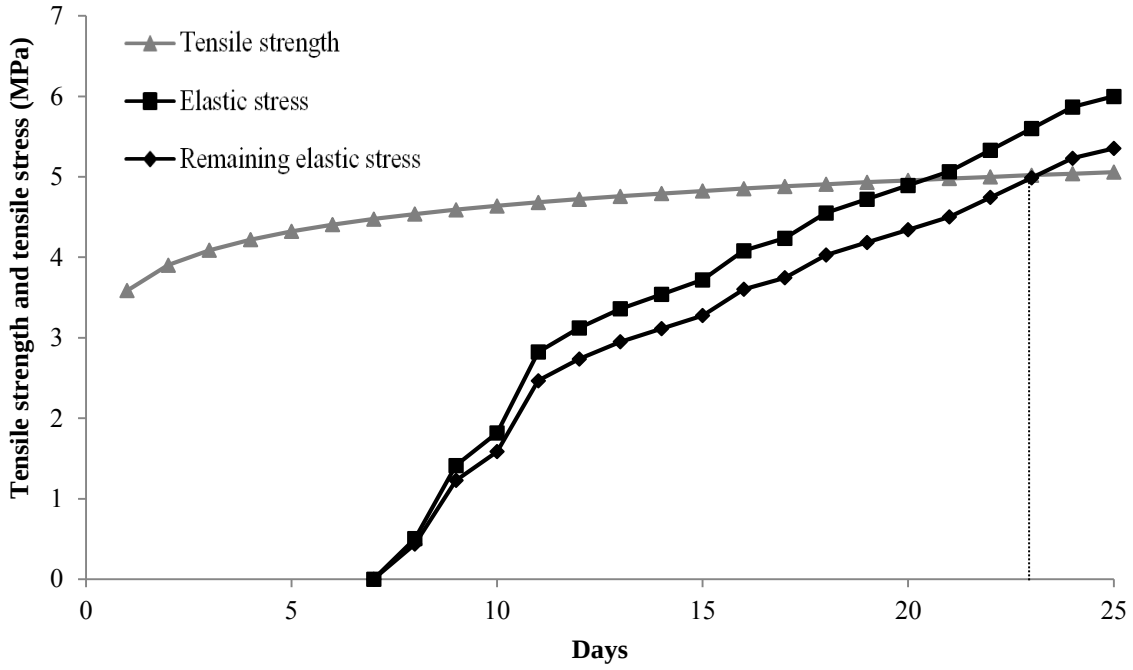

Figure 5.19: Overlay tensile strength and stress development for SikaGrout-212 commercial mix (25% 19 mm coarse aggregate content)

35% coarse aggregate volume (19 mm)

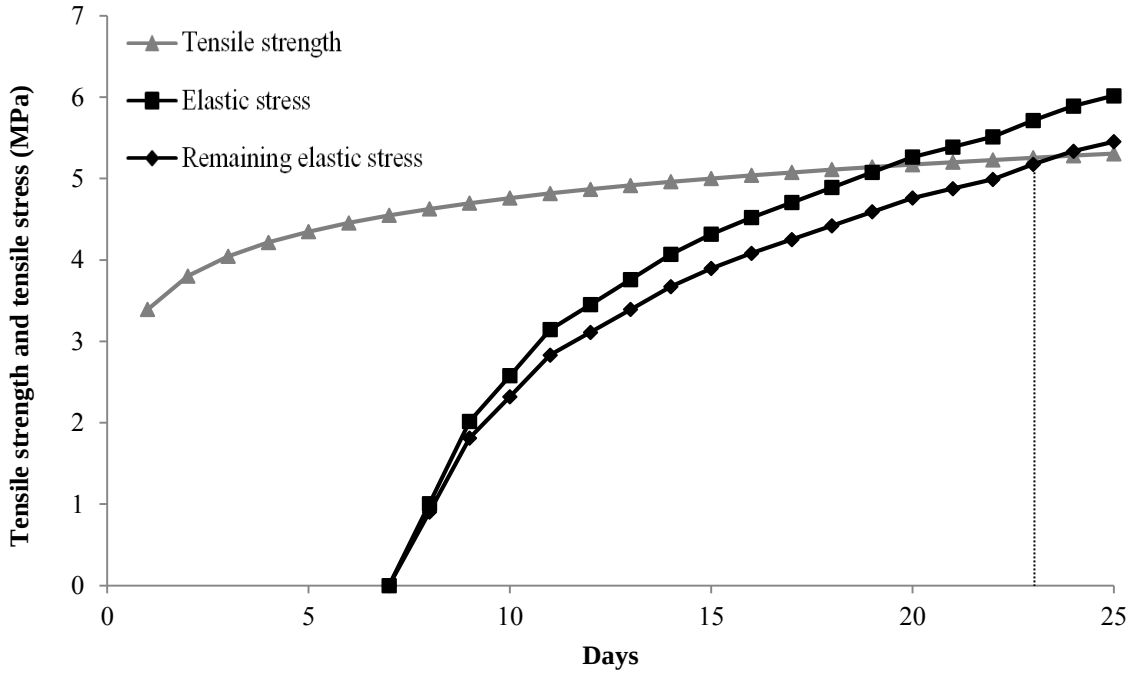

Figure 5.20: Overlay tensile strength and stress development for SikaGrout-212 commercial mix (35% 19 mm coarse aggregate content)

45% coarse aggregate volume (19 mm)

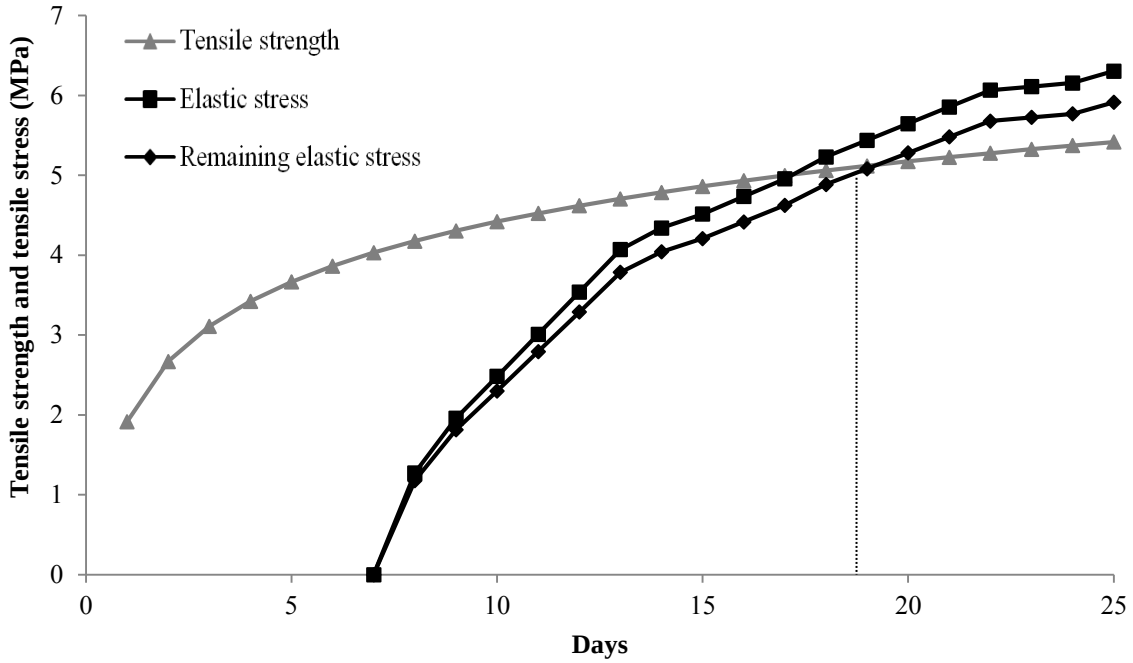

Figure 5.21: Overlay tensile strength and stress development for SikaGrout-212 commercial mix (45% 19 mm coarse aggregate content)

As the results (Figure 5.18, 5.19, 5.20 and 5.21) indicate, it is predicted that it will 17 days for the SikaGrout-212 19 mm aggregate content mix to fail. This is followed by the 25 % 19 mm aggregate content mix which is predicted to fail at just under 23 days, with the 35 % 19 mm aggregate content mix being predicted to also fail just over 23 days after casting. The 45% 19 mm mix is predicted to fail at only 18 days after casting.

The prediction outputs for the commercial mixes are similar in nature to the predicted outputs for the laboratory mixes with the same 19 mm coarse aggregate.

5.6 Evaluation of model outputs

The predicted time to first cracking outputs can be compared to the direct test results to analyse and evaluate their accuracy.

Direct testing in this investigation was done in the form of ring tests. Chilwesa (2012) found that the time to first cracking measured using the ring tests did not correspond with the predicted age at cracking generated by the analytical model. However, the ring test was shown to give the correct order of cracking when comparing different repair mortars.

Chilwesa (2012) also conducted direct tests using actual bonded concrete overlays that were closely monitored to record the time to first cracking. It was found that the age at cracking of the bonded concrete overlays was successfully predicted based on the material properties prediction model.

After careful examination of the results obtained by Chilwesa (2012) it was noted that, on average, the time to first crack measurements for the overlays were 65 ± 30 % higher than the measurements for the ring tests. Although this was a very rough correlation, it can be used to estimate possible time to first cracking of overlays ($t_{first\ crack,overlay}$) based on measured information about time to first cracking of the ring tests ($t_{first\ crack,ring}$).

$$t_{first\ crack,overlay} = 1{,}65.\, t_{first\ crack,ring} \tag{5.8}$$

Table 5.2 presents the comparison of results generated from the ring test, predicted overlay results and the analytical model outputs for the laboratory mixes with varying 19 mm aggregate contents.

Table 5.2: Comparison of analytical modelling and experimental results for w:c = 0.45 laboratory mixes with varying 19 mm coarse aggregate volumes (age at cracking, days)

Test type	w:c = 0.45 (19 mm coarse aggregate)				w:c = 0.6 (19 mm coarse aggregate)			
	0%	**25%**	**35%**	**45%**	**0%**	**25%**	**35%**	**45%**
Ring test	9	15	25	36	11	22	30	40
Predicted bonded overlay results	15	25	41	59	18	36	49	66
Analytical model output	16	19	15	15	18	23	19	19
Average	16				20			
Standard deviation	1.9				2.2			

This comparison is shown graphically in Figure 5.22 and 5.23

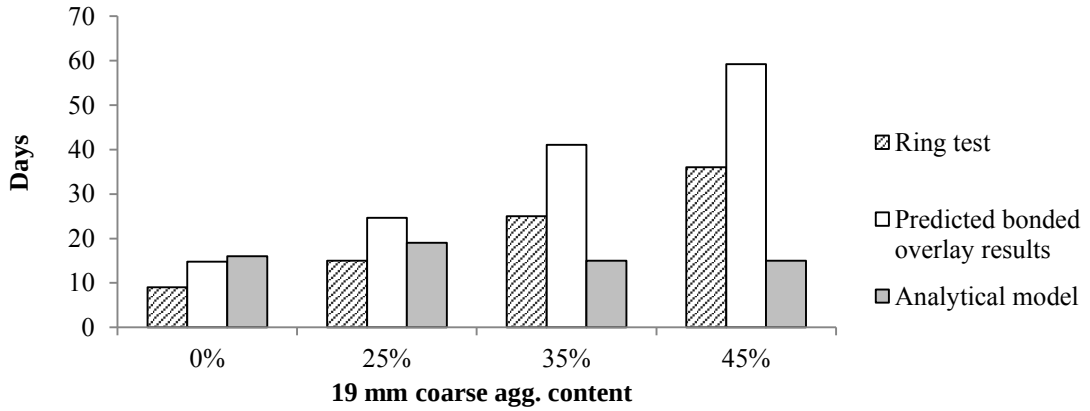

Figure 5.22: Comparison of analytical modelling and experimental results for w:c = 0.45 laboratory mixes with varying 19 mm coarse aggregate volumes

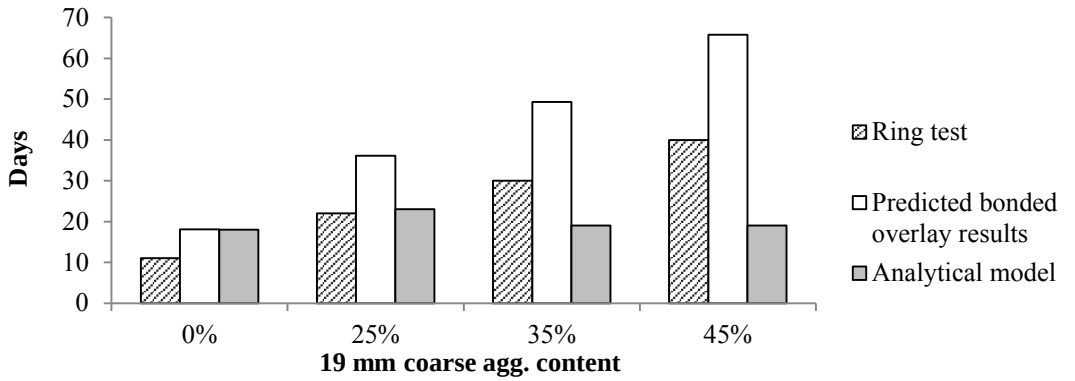

Figure 5.23: Comparison of analytical modelling and experimental results for w:c = 0.6 laboratory mixes with varying 19 mm coarse aggregate volumes

From the comparison of the results for the w:c = 0.45 and w:c = 0.6 laboratory mixes with varying 19 mm coarse aggregate volumes shown in Table 5.2 and illustrated in Figure 5.22 and 5.23 respectively, it is obvious to note that the analytical model fails to correlate with the trends observed in both the ring and bonded overlay tests.

It is initially observed that the analytical output for the 0% content mixes does correspond with the bonded overlay results. However, it appears that the analytical model fails to account at all for the influence of an increase in coarse aggregate volume content for both laboratory mix types. This can be illustrated by observing the standard deviation of the predicted model outputs for all of the aggregate volume contents modelled, which is shown to be only 1.9 days for the w:c = 0.45 mixes and 2.2 days for the w:c = 0.6 mixes. This suggests that there is no difference in the model outputs, irrespective of aggregate content.

It is noted that the average of the analytical model outputs of 16 days for the w:c = 0.45 mixes and 20 days for the w:c = 0.6 mixes correlates almost exactly with the bonded overlay result for the 0% content mixes. This further illustrates the inability of the model to effectively account for the influence of coarse aggregate on the resistance to cracking of repair material.

Table 5.3 presents the comparison of results generated from the ring test, predicted overlay results and the analytical model outputs for the SikaGrout-212 commercial mixes with varying 19 mm aggregate contents.

Table 5.3: Comparison of analytical modelling and experimental results for SikaGrout-212 commercial mixes with varying 19 mm coarse aggregate volumes (age at cracking, days)

Test type	SikaGrout-212 (19 mm coarse aggregate)			
	0%	**25%**	**35%**	**45%**
Ring test	8	11	17	22
Predicted bonded overlay results	13	18	28	36
Analytical model output	17	23	23	18
Average			20	
Standard deviation			3.3	

This comparison is shown graphically in Figure 5.24

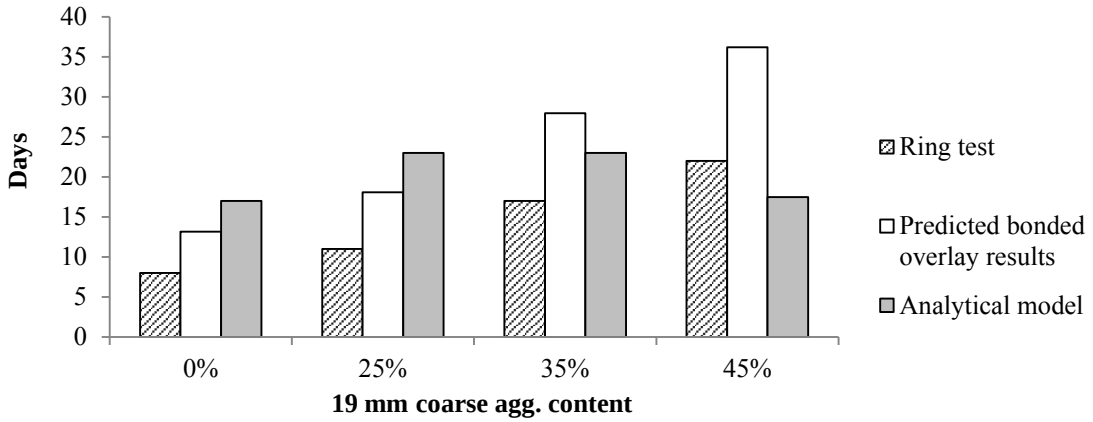

Figure 5.24: Comparison of analytical modelling and experimental results for SikaGrout-212 commercial mixes with varying 19 mm coarse aggregate volumes

The results observed in Table 5.3 and Figure 5.24 have a similar trend to what has been observed for the laboratory mixes.

The analytical model outputs for all of the commercial mixes with varying coarse aggregate contents are relatively similar, with a standard deviation of 3.3 days. The average of these model outputs is 20 days and is observed to only be slightly higher than the bonded overlay result for the 0% content mix. It can therefore be determined that the analytical model is also unable to account for the influence of the inclusion of coarse aggregate in the commercial repair mixes, in the same way that has been shown for the laboratory mixes.

It is possible that the inability of the material property analytical model to accurately account for the influence of varying coarse aggregate volume contents observed for the laboratory and commercial mixes can be traced back to the concept of strain softening and fracture energy discussed by Chiaia *et al.* (1998) and Wittmann (2002).

The process of strain softening involves the formation and nucleation of microcracks at stress concentration zones and microdefects in the interfacial zone between the aggregate and the cement matrix. This is followed by macrocracking which is characterised by the growth and expansion of the microcracks through the matrix. Complete cracking failure is only observed when macrocracking becomes continuous through the matrix.

The concept of fracture energy must also be considered. Fracture energy is defined by Wittmann (2002) as the specific energy required for cracking to occur in concrete. Studies by Hillerborg (1985) and Wittmann (2002) have shown that there is a direct relationship between aggregate size and the specific energy required for cracking to occur. This is attributed to the increase in distance of crack propagation around the aggregate inclusions. An increase in coarse aggregate volume content will have the same effect on fracture energy and increase the distance of crack propagation and energy required for cracking to occur.

These failure mechanisms associated with overlay cracking failure relate specifically to phenomenon caused by 'local' strains within the cement paste/aggregate matrix around the area of cracking.

It is therefore believed that the material property analytical model, which is based on separately tested, time dependant material properties, does not account for the delay in time to cracking that is caused by strain softening and increased required fracture energy around the aggregate inclusions.

This can be explained by the fact that the separate material properties used in the model are examined on a 'global' scale, where the influence of coarse aggregate on the properties of whole concrete specimens is measured, rather than on a 'local' scale where the specific influence of coarse aggregate inclusions on mechanisms such as strain softening and fracture energy should be considered.

This is particularly relevant to properties such as tensile strength, tensile relaxation and drying shrinkage, where the influence of strain softening and fracture energy associated with the inclusion of coarse aggregate is believed to be substantial. However, these 'local' factors are not considered in the 'global' property tests that are used to determine the property inputs for the analytical model.

This inability to account for 'local' failure mechanisms associated with the failure of concrete with coarse aggregate inclusions would explain why the prediction model outputs appear to not account at all for the influence of the inclusion of increasing coarse aggregate volume contents, and therefore do not reflect what is observed in the direct test results.

Furthermore, it is noted that all of the predicted model results, irrespective of coarse aggregate content, are similar for each laboratory mix. This can be explained by examining the influence of an increase in coarse aggregate volume on the 'globally' determined individual material properties that are used in the model. A decrease in drying shrinkage is noted as coarse aggregate volume increases. However, this is offset by an increase in material stiffness and a decrease in tensile relaxation that is also associated with an increase in coarse aggregate content. It can therefore be deduced that the inverse nature of these 'globally' determined properties with regard to aggregate content, combined with the inability to account for the effect of 'local' cracking mechanisms, result in prediction outputs that are relatively similar, irrespective of aggregate content.

Another factor that can be considered is the implication of the specimen type and size used to determine the shrinkage property inputs for the analytical model. Although the drying area/volume ratio for the prism specimens and the ring specimens are similar, it is possible that differences in the size and shape of the different specimens could result in a degree of variability between the property drying shrinkage measurements and the direct restrained shrinkage observed for the ring specimens, which could also contribute to the inaccuracies observed in the analytical predictions.

Table 5.4 presents the comparison of results generated from the ring test, predicted overlay results and the analytical model outputs for the w:c = 0.6 laboratory mixes with varying 9.5 mm aggregate contents.

Table 5.4: Comparison of analytical modelling and experimental results for w:c = 0.6 laboratory mixes with varying 9.5 mm coarse aggregate volumes (age at cracking, days)

Test type	w:c = 0.6 (9.5 mm coarse aggregate)			
	0%	**25%**	**35%**	**45%**
Ring test	11	13	15	21
Predicted bonded overlay results	18	21	25	35
Analytical model output	18	25	32	31
Average			27	
Standard deviation			6.5	

This comparison is shown graphically in Figure 5.25

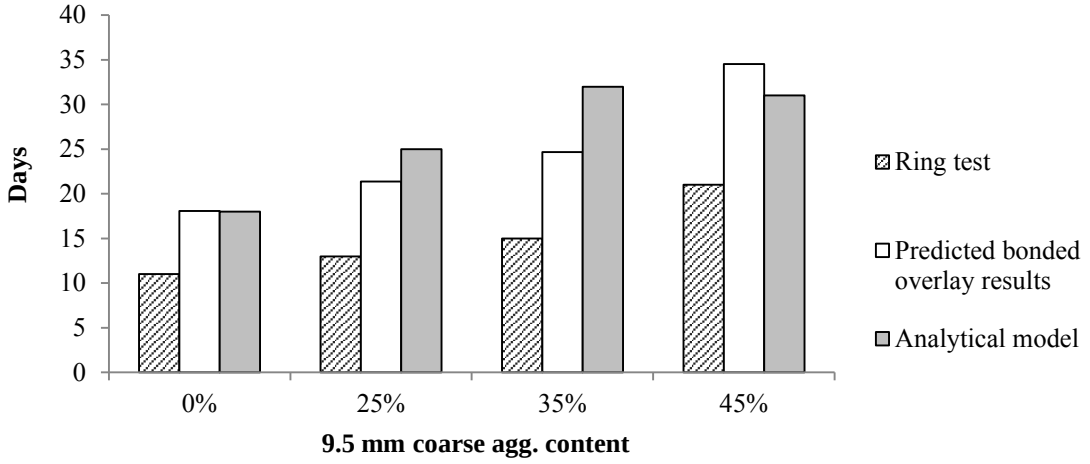

Figure 5.25: Comparison of analytical modelling and experimental results for w:c = 0.6 laboratory mixes with varying 9.5 mm coarse aggregate volumes

A slightly better correlation is observed for the analytical predicted outputs with the smaller 9.5 mm coarse aggregate, when compared to the overlay results (Table 5.4 and Figure 5.25). A substantially higher standard deviation is also noted for the model outputs.

These findings can also be related to the concept of strain softening and fracture energy discussed previously. Strain softening and the length of crack propagation have been shown to be directly influenced by aggregate particle size, as this will affect the degree and frequency of stress concentrations and the length that cracks will propagate along. The fracture energy required for cracking has also been shown to be dependent on the length of crack propagation and therefore proportional to particle size. The reduced strain softening and fracture energy associated with the smaller aggregate results in less inaccurate 'globally' determined material properties, which in turn result in analytical model outputs being shown to be slightly more accurate and account to some degree for the influences of the smaller 9.5 mm coarse aggregate content. This is observed to be specifically evident at lower volume contents.

Although there is a more obvious correlation between the analytical model outputs and the measured results for the smaller 9.5 mm aggregate mixes, it is hard to say what degree of this accuracy can be attributed to the effective modelling of the influence of coarse aggregate volume content and what can be attributed to experimental discrepancy which is associated with this form of testing.

5.7 Conclusion

It can be concluded that the material property analytical model, which was used successfully by Chilwesa (2012) to predict the time to first cracking of different concrete repair mortars, is ineffective in accounting for the influence of changes in coarse aggregate volume content.

This can be attributed to the fact that there are certain 'localised' aspects that are associated with the mechanics of concrete cracking failure, such as strain softening and required fracture energy, which are not accounted for by the individual material properties that are tested on a 'global' scale and form the inputs for the analytical model.

The use of the material property analytical prediction model is therefore not recommended for modelling and assessing the cracking of overlay repair materials that include a coarse aggregate.

Chapter 6: Discussion, conclusions and recommendations

6.1 Introduction

The results of the experimental component of this investigation into the influence of coarse aggregate volume content and size on the performance of bonded concrete overlays have been presented in Chapter 4. Furthermore, the outputs from analytical models have been presented in Chapter 5. The following chapter now serves to comprehensively compare and contrast these experimental and analytical results in a detailed discussion, which will allow key findings and conclusions for this investigation to be drawn. Recommendations about further areas of interest and possible follow-up investigations will also be provided in this chapter.

6.2 Discussion

6.2.1 Experimental findings

The experimental testing component of this investigation revolves around the concept of comparing repair concrete property test results with direct restrained shrinkage test results. This allows for the effective identification of the influence of coarse aggregate volume and sizes on specific concrete properties and in turn, the influence of these properties on the performance of bonded concrete overlays.

6.2.1.1 Influence of aggregate volume content

The results of the direct restrained shrinkage testing shown in 4.3.1.1 indicated that there was a direct relationship between coarse aggregate volume content and the time to first cracking. This impact was shown to be greatest for the w:c = 0.6 laboratory mixes, followed by the w:c = 0.45 laboratory mixes and finally the SikaGrout-212 commercial mixes. Furthermore, a corresponding trend was noted for crack intensity in 4.3.2.1, where it was shown that the crack area decreased as the coarse aggregate volume content was increased.

The impact of coarse aggregate volume content on tensile strength was shown to only be relatively noticeable for the w:c = 0.6 laboratory mixes at younger ages. This increased impact may partially contribute to the more noticeable influence of coarse aggregate volume content on the w:c = 0.6 mixes in the direct testing results. However, in general, it can be deduced that the influence of coarse aggregate volume content on tensile strength did not have a substantial influence on restrained shrinkage cracking.

The influence of coarse aggregate volume content on tensile relaxation was shown to be inversely proportional to coarse aggregate volume. This was interesting to note, as a decrease in relaxation has been shown in the literature to have a profoundly negative effect on the performance of repair concrete.

The influence of coarse aggregate volume content on the concrete elastic properties was shown to be directly proportional. Again this was interesting to note as it was shown in the literature that a higher elastic stiffness will have a negative effect on the resistance to cracking, and therefore an increase in aggregate content was shown to have an unfavourable impact on performance.

The influence of aggregate volume content on free drying shrinkage was shown to be indirectly proportional, with an increase in aggregate content producing lower shrinkage levels. This reduced level of free drying shrinkage associated with the improved dilution and restraint resulting from an increase in coarse aggregate content has been shown to greatly improve the performance of concrete exposed to restrained deformation, as observed in the direct test results.

Therefore, in contrast to the free drying shrinkage results, the influence of an increase in coarse aggregate volume was shown to produce less favourable relaxation and elastic properties with regard to the resistance of the material to restrained deformation. However, the trends observed in the direct test results suggest that this negative influence of an increased aggregate content on tensile relaxation and elastic modulus was possibly offset by the positive effects that it has on free drying shrinkage, thus resulting in the increase in aggregate volume content having a positive effect on restrained shrinkage performance.

This is summarized in Table 6.1.

Table 6.1: Summary of material property/aggregate content relationship and influence on crack resistance

Concrete property	Property/Aggregate content relationship	Influence of an increase in aggregate content on crack resistance
Tensile strength	Negligible (direct relationship observed for w:c = 0.6 laboratory mix at young ages only)	Negligible
Tensile relaxation	Inversely proportional	Negative
Elastic modulus	Directly proportional	Negative
Free drying shrinkage	Inversely proportional	Positive

However, this is a highly simplistic explanation. It has been noted that the influence of coarse aggregate volume content on the individual material properties that contribute to overlay performance have been tested and evaluated on a ‘global’ scale, relating to the effect of coarse aggregate on the material properties of whole specimens. However, ‘localised’ mechanisms associated with the cracking failure of concrete with the presence of coarse aggregate particles have been suggested to have a profound effect on cracking failure. These mechanisms are not considered in a ‘global’ sense, but relate to ‘local’ phenomenon within the cement paste/aggregate matrix around the area of cracking. It must therefore be noted that factors not associated with the material properties may have also had an impact on the trends observed in the direct test results.

Studies have shown that an increase in coarse aggregate volume content can greatly increase the magnitude of strain softening and the length of crack propagation around the aggregate inclusions. This increase in fracture energy dissipation and the length of cracks results in an increase in fracture energy required for cracking leading to substantial delays in time to crack initiation.

Furthermore, the substantial difference in crack intensity of the control mixes (0% course aggregate) and the mixes containing coarse aggregate can also possibly be explained by the influence of fracture energy dissipation due to strain softening. The increase in fracture energy required for cracking to occur, due to the increase in microcracking along the aggregate/matrix interface, and the increase in crack propagation length results in very little residual energy remaining at final cracking failure. This therefore results in the substantially reduced crack areas that were observed in the direct test results of the mixes containing coarse aggregate.

As these failure mechanisms are associated with the actual cracking process, it is possible that the scope of their influence cannot be determined based on the 'global' analysis of separate repair material properties, but is only observed in the direct test results.

6.2.1.2 Influence of aggregate size

The results from the direct restrained shrinkage tests shown in 4.3.1.2 suggest that there was a clear influence of coarse aggregate size on the time to first cracking, with the mixes made using the 19 mm coarse aggregate being shown to outperform the mixes made with 9.5 mm graded aggregate. Furthermore, it was shown in 4.3.2.2 that the influence of coarse aggregate size on crack intensity was also very profound with the crack intensity of mixes that used the larger aggregate having lower levels.

The impact of coarse aggregate size on tensile strength was shown to only be relevant at older ages (28 days), where the smaller 9.5 mm aggregate mixes were shown to have a substantially higher tensile strength. No noticeable impact was observed for the influence of aggregate size at younger ages. It was this lack of influence of aggregate size at younger ages that may explain why the results of the direct testing tend to contradict the tensile strength findings. As the direct test specimens tended to fail at much younger ages (<28 days), the benefits of the increase in tensile strength associated with the smaller aggregate size had not developed sufficiently to have a telling impact on the direct test results.

The results of the effect of coarse aggregate size on tensile relaxation indicate that the smaller, 9.5 mm, aggregate had lower levels of relaxation when compared to the larger, 19 mm aggregate mixes. As a lower level of relaxation has been shown to negatively influence the performance of concrete under restrained deformation, these findings tend to correlate with the direct test results with the smaller aggregate being shown to produce less favourable results.

The influence of coarse aggregate size on the elastic modulus of the mixes was consistent at all ages, with the larger aggregate particles providing higher restraint to the matrix and therefore producing concrete with a higher elastic modulus.

This trend was not reflected in the results of the direct testing, as the lower elastic modulus associated with the smaller aggregate would be expected to improve the crack resistance of smaller aggregate concrete over larger aggregate concrete.

The free drying shrinkage results do tend to support the direct testing results, with the smaller coarse aggregate mixes being shown to have higher levels of shrinkage at both younger and older ages. This increased level of drying shrinkage would account for the poorer performance of the smaller sized aggregate mixes in the direct test results.

It is possible that the reduced levels of relaxation and increased magnitude of drying shrinkage associated with the inclusion of a smaller coarse aggregate offset the benefits gained from the reduced elastic stiffness of the smaller aggregate and resulted in the trend that is observed in the direct test results.

This is summarized in Table 6.2.

Table 6.2: Summary of material property/aggregate size relationship and influence on crack resistance

Concrete property	Property/Aggregate size relationship	Influence of an increase in aggregate size on crack resistance
Tensile strength	Negligible at younger ages (7 days), but an indirect relationship is observed at older ages (28 days)	Negligible
Tensile relaxation	Directly proportional	Positive
Elastic modulus	Directly proportional	Negative
Free drying shrinkage	Inversely proportional	Positive

However, concepts relating to the 'localised' mechanisms of cracking and crack fracture energy, which are not considered by the 'global' scale material property tests, must also be considered. The influence of coarse aggregate size on strain softening has been shown to be directly proportional, with the magnitude of energy dissipated by microcracking around aggregate particles increasing as aggregate size increases. The increase in length of crack propagation paths associated with an increase in coarse aggregate size has also been shown to increase fracture energy required for cracking.

This influence of coarse aggregate size on fracture energy can be numerically analysed based on the linear relationship presented by Wittmann (2002) in Figure 2.4. It is shown that specific fracture energy (G_f) required for cracking of concrete with 19 mm coarse aggregate is approx. 45 N/m higher than the fracture energy required for cracking failure of concrete with 9.5 mm coarse aggregate.

Furthermore, the increase in crack intensity associated with the smaller coarse aggregate size can also be attributed to this direct relationship between fracture energy dissipation (strain softening) and coarse aggregate particle size. As more energy is dissipated by increased microcracking and crack lengths associated with the larger aggregate particles, there is less residual fracture energy at the time of final cracking. This results in the lower crack areas observed for the larger coarse aggregate mixes.

It is therefore more likely that the combined influence of an increase in required fracture energy and strain softening, the reduced drying shrinkage and the increase in tensile relaxation associated with the inclusion of a larger coarse aggregate can explain the trend observed in the direct test results.

6.2.1.3 Influence of mix type

Although the influence of concrete mix type does not pertain directly to understanding the influence of coarse aggregate volume content and size on the performance of concrete subjected to restrained deformation, it is important to discuss these trends to more comprehensively understand how to achieve optimum performance from overlay repair concretes.

The direct test results shown in 4.3.1.3 indicated that the w:c = 0.6 laboratory mixes had by far the best performance for all aggregate contents. This was followed by the w:c = 0.45 laboratory mixes and finally the SikaGrout-212 commercial mixes which showed the poorest performance. These findings contradicted the generally accepted idea that 'stronger' repair concretes produced better results. No definitive trends were observed in 4.3.2.3 with regard to the influence of mix type on crack intensity. However, this can be partially attributed to the variable nature of this form of testing.

The tensile strength results were shown to reflect existing views, with the 'stronger' SikaGrout-212 mixes being shown to have a tensile strength much higher than the laboratory mixes. As expected, the w:c = 0.45 mixes outperformed the w:c = 0.6 mixes with regard to tensile strength. However, these findings contradicted the direct testing results and indicated that superior tensile strength qualities did not ensure superior crack resistance.

This apparent contradiction can be explained by examining the other key concrete properties. It can be seen that the poor performance of the SikaGrout-212 mixes can be attributed to a noticeably lower level of tensile relaxation, an increased elastic modulus and a very rapid increase in early age free drying shrinkage.

In contrast, the higher levels of tensile relaxation, lower elastic modulus and lower free drying shrinkage of the w:c = 0.6 mixes were shown to significantly offset the lower tensile strength properties and resulted in the superior performance observed in the direct test results.

6.2.2 Analytical modelling predictions

Analytical modelling was conducted based on the material property analytical model that has been used successfully by Chilwesa (2012) to predict the time to first cracking of different concrete mortars. Model outputs were determined based on specific material properties which were determined in the experimental component of the investigation, namely: tensile strength, tensile relaxation, elastic modulus and free drying shrinkage. The outputs of the analytical model were then compared with the direct test results for the various mixes, allowing for the accuracy of the model to be evaluated.

The direct test results that were used for this comparison were based on the ring tests conducted in this investigation.

Chilwesa (2012) found that the ring tests did not correlate specifically with the time to first crack predictions of the analytical model, but did predict the correct order of cracking for the different mixes. Chilwesa (2012) observed a better correlation for direct tests done using bonded overlays. A conversion equation was therefore used in this investigation to generate predicted overlay results based on the measured results of the ring tests. This allowed for a more extensive comparison and evaluation of the prediction model.

It was found that the material property analytical prediction model did not account for the effect of the inclusion of varying volume contents of coarse aggregate on the time to first cracking. The model outputs were found to correlate very accurately with the direct overlay test results for the 0% content mixes, but failed to effectively model the increase in time to first cracking associated with the inclusion of varying contents of coarse aggregate.

As discussed in detail in Chapter 5, it is proposed that this inaccuracy of the model can be attributed to the fact that 'globally' determined individual material properties, when measured separately and then combined in the model, do not account for the influence of 'local' crack mechanisms, such as strain softening and fracture energy, that are associated with the cracking failure of materials with coarse aggregate inclusions. These crack mechanisms have been shown to substantially prolong the time to first cracking of materials that contain coarse aggregate inclusions, which can also explain the trends observed in the direct ring test results.

These findings from the analysis of the material property analytical model are important to note because they highlight an important point with regard to the influence of coarse aggregate on the crack resistance of repair materials. Although the material properties of repair materials can provide an indication of their performance and resistance to cracking failure, the specific crack mechanisms associated with the cracking of the repair material with coarse aggregate inclusions will also have a substantial effect on their performance and therefore must be considered.

6.3 Final conclusions

The following final conclusions can be drawn from the experimental component of the investigation:

1. An increase in coarse aggregate volume content has been shown to have a negligible influence on tensile strength, decrease tensile relaxation properties, increase elastic stiffness and reduce free drying shrinkage.

2. In general, the influence of an increase in coarse aggregate content on bonded concrete overlay performance has been shown to prolong the time to first cracking and reduce the crack intensity.

3. An increase in coarse aggregate size has been shown to have negligible effect on tensile strength at younger ages, increase tensile relaxation, increase elastic stiffness and reduce free drying shrinkage.

4. In general, the influence of an increase in coarse aggregate size on bonded concrete overlay performance has been shown to prolong the time to first cracking and reduce the crack intensity.

5. The w:c = 0.6 laboratory mixes showed superior performance with regard to resistance against cracking when compared to the w:c = 0.45 laboratory mixes, while the SikaGrout-212 commercial mix had the lowest performance with regard to crack resistance. It can therefore be noted that an increase in strength results in an increase in cracking.

The following final conclusions can be drawn based on the analytical modelling component of the investigation:

6. It can be concluded that the material property analytical model, which was used successfully by Chilwesa (2012) to predict the time to first cracking of different concrete repair mortars, is ineffective in accounting for the influence of changes in coarse aggregate volume content on the predicted time to first cracking of repair materials.

7. The use of the material property analytical prediction model is therefore not recommended for modelling and assessing the cracking of overlay repair materials that include coarse aggregates.

6.4 Recommendations

This study has shown that significant work is required on investigating the influence of coarse aggregate on bonded concrete overlay performance.

The experimental component of this investigation was limited to examining the influence of coarse aggregate volume content and size. Further work is therefore required to investigate the influence of other aggregate properties such as type, shape and grading. A greater range of varying coarse aggregate sizes should also be tested.

The investigation has also identified a key area that requires significantly more work. It has been shown that the cracking failure of materials containing coarse aggregate is not only dependant on the individual material properties, but also on the cracking mechanisms associated with this failure. An in-depth study is therefore required to gain a better understanding of the cracking mechanisms involved with the failure of materials that contain coarse aggregate inclusions, and the influence that these mechanisms have on delaying the time to first cracking.

The following investigative techniques are suggested:

- The study of cracking mechanisms and fracture mechanics using detailed measurements and analysis performed using microscopy. This will help to gain a better understanding of the microcracking mechanisms involved with strain softening and the influence of crack propagation length on fracture energy and ultimately, the delay in time to first cracking.

- Another method that can be used is to develop a Finite Element (FE) model of the cement and aggregate matrix that will model crack energies and allow fracture paths around the coarse aggregate inclusions to be predicted and analysed.

If sufficient analysis and understanding of the cracking mechanisms is achieved, an amended version of the material parameter prediction model can be proposed that effectively incorporates the influence of coarse aggregate on the time to first cracking of repair materials.

References

ACI 209R-92. 1997. Prediction of creep, shrinkage and temperature effects in concrete structures, Farmington Hills, Michigan: American Concrete Institute, 1-12.

ACI 325.13-R06. 2006. Concrete overlays for pavement rehabilitation. Committee 325 Pavements, American Concrete Institute, Detroit.

ACPA. 1990. Guidelines for bonded concrete overlays. *Technical Bulletin TB-007P*, American Concrete Pavement Association, Arlington Heights.

Alexander, M. & Beushausen, H. 2009. Deformation and volume change of hardened concrete. *Fulton's concrete technology.* 9th ed. South Africa: Cement & Concrete Institute. Ch. 8: 111-144.

Alexander, M. G. & Davis, D. E. 1991. Aggregates in concrete – a new assessment of their role. *Concrete Beton*. 59: 10-20.

Alexander, M. G. & Mindess, S. 2005. *Aggregates in Concrete*. Taylor & Frances. Abingdon, Oxon.

Alexander, M.G, Mindess, S, Diamond, L. 1995. Properties of paste-rock interfaces and their influences on composite behaviour. University of British Columbia, Canada. 497 – 506.

Almusallam, A., Maslehuddin, M., Abdul-Waris, M. & Khan, M. 1998. Effect of mix proportions on plastic shrinkage cracking of concrete in hot environments. *Construction and Building Materials*. *12*(6-7):353-358.

Alonso, M.T. 1997. Zur Rissicherheit zementgebundener dehnungsbehinderter Schichten unter Berücksichtigung von Dauereinflüssen (On the crack resistance of cement-based restrained members with consideration of long-term influences). PhD thesis, Universitat Hamburg-Harburg, Shaker Verlag, Aachen, Germany.

Asad, M., Baluchi, M.H. & Al-Ghadib, A.H. 1997. Drying shrinkage stresses in concrete patch repair systems. *Magazine of concrete research*. 49:283-293.

Atis C. D., Kilic A. & Sevim U. K. 2003. Strength and shrinkage properties of mortar containing a nonstandard high calcium fly ash. *Cement and Concrete Research*. 34(1):99–102.

Atis, C. D. 2003. High-Volume Fly Ash Concrete with High Strength and Low Drying Shrinkage. *Journal of Materials in Civil Engineering*. *15*(2), 153–156.

Baalbaki, W., Aitcin, P. C. & Ballivy, G. 1992. On predicting modulus of elasticity in high-strength concrete. *ACI Materials Journal*. 89(5):517-520.

Banthia, N. & Gupta, R. 2006. Repairing with fiber reinforced concrete repairs. *ACI Concrete International*. 28(11):36-40.

Banthia, N. & Gupta, R. 2008. Plastic shrinkage cracking in cementitious repairs and overlays. *Materials and Structures*. 42(5), 567-579.

Baroghel-Bouny, V. & Godin, J. 2001. Experimental study on drying shrinkage of ordinary and high-performance cementitious materials. *Concrete Science and Engineering*. 3(9): 13-22.

Barr, B., Hoseinian, S.B. & Beygi, M.A. 2003. Shrinkage of concrete stored in natural environments. *Cement and Concrete Composites*. 25(1):19-29.

Bazant, P. 1995. Creep and shrinkage prediction model for analysis and design of concrete structures—Model B3. *Mat. Struct*. 28:357– 365.

Bernard, O. 2000. Comportementà long termedes elements de structure formés de bétons d'âges différents. PhD Thesis, Swiss Federal Institute of Technology No 2283, Lausanne, Switzerland.

Beushausen H. & Alexander M. 2005. Crack development in bonded concrete overlays subjected to differential shrinkage: a parameter study. *Proceedings of the international conference on concrete repair, rehabilitation and retrofitting*, South Africa. 1053–1058.

Beushausen, H. & Alexander, M. 2009. Concrete repair. *Fulton's concrete technology.* 9th ed. South Africa: Cement & Concrete Institute. Ch. 27: 393-409.

Beushausen, H. & Alexander, M. G. 2006a. Localised strain and stress in bonded concrete overlays subjected to differential shrinkage. *Materials and Structures*. 40(2), 189-199.

Beushausen, H. & Alexander, M. G. 2006b. Failure mechanisms and tensile relaxation of bonded concrete overlays subjected to differential shrinkage. *Cement and Concrete Research*. 36:1908–1914.

Beushausen, H. 2005. Performance of bonded concrete overlays subjected to differential shrinkage. University of Cape Town, South Africa.

Beushausen, H. 2010. The influence of concrete substrate preparation on overlay bond strength. *Magazine of Concrete Research.* 62(11): 845–852.

Beushausen, H., Masuku, C. & Moyo, P. 2012. Relaxation characteristics of cement mortar subjected to tensile strain. *Materials and Structures*. 45(8): 1181-1188.

Birkeland, H.W. 1960. Differential shrinkage in composite beams. *Journal of the American Concrete Institute*. 1123–1136.

Bissonnette, B., Courard, L., Beushausen, H., Fowler, D., Trevino, A. & Vaysburd. 2013. Recommendations for the repair, the lining or strengthening of concrete slabs or pavements with bonded cement-based material overlays. *Materials and Structures*. 46:481-494.

Bissonnette, B., Pierre, P. & Pigeon, M. 1999. Influence of key parameters on drying shrinkage of cementitious materials. *Cement and Concrete Research*. 29:1655-1662.

Bloom, R. & Bentur, A. 1995. Free and restrained shrinkage of normal and high strength concrete. *ACI Material Journal*. 92(2): 211–217.

BS 8110-2:1985, Structural use of concrete. Part 2: Code of practice for special circumstances, London: British Standards Institution, 1985.

BS EN 1992: Eurocode 2: Design of concrete structures. Part 1: General rules and rules for buildings, Brussels: European Committee for Standardization.

Carlswärd, J. 2006. Shrinkage cracking of fiber reinforced self-compacting concrete overlays- Test methods and theoretical modeling. PhD Thesis, University of Lulea University of Technology, Sweden.

CEB 1993. CEB-FIP Model Code 1990, *Bulletin d'Information 213/214*, Lausanne, Switzerland. 437.

Chiaia, B., van Mier, J. G. M. & Vervuurt. 1998. Crack growth mechanisms in four different concretes: Microscopic observations and fractal analysis. *Cement and Concrete Research*. 28(1): 103–114.

Chilwesa, M. 2012. Assessing the age at cracking of concrete repair mortars/overlays subjected to restrained drying shrinkage. Masters Thesis, University of Cape Town, South Africa.

Counto, U. J. 1964. The effect of the elastic modulus of the aggregate on the elastic modulus, creep and creep recovery of concrete. *Mag of Concrete Res*. 16(48):129-138.

Dantu, P. 1957. A contribution to the mechanical and geometrical study of non-cohesive masses. *Proceedings of the 4th International Conference on Soil Mechanics and Foundation Engineering*. 1:144–157.

Denarié, E., & Silfwerbrand, J. 2004. Structural behaviour of bonded concrete overlays. Proceedings, International RILEM Workshop on 'Bonded Concrete Overlays, June 7–8, 2004, Stockholm, Sweden. 37–45.

Emberson, N. & Mays, G. 1990. Significance of property mismatch in the patch repair of structural concrete, Part 1: Properties of repair system. *Mag Concr Res.* 42 (152):147–60.

Emmons P.H. & Vaysburd A.M. 1993. Compatibility considerations for durable concrete repairs. *Transp Res Rec.* 1382:13–19.

Evans, R.H. & Chung, H.W. 1967. Shrinkage and deflection of composite prestressed concrete beams. *Concrete*. 157–166.

Feldman, R.F. & Sereda, P.J. 1968. A model for hydrated Portland cement paste as deduced from sorption-length change and mechanical properties. *Matériaux et construct*. 1:509-520.

Folliard, K. & Berke, S. 1997. Properties of high-performance concrete containing shrinkage reducing admixtures. *Cement and Concrete Research.* 27(9):1357-1364.

Gesoglu, M., Ozturan, T. & Guneyisi, E. 2006. Effects of cold-bonded fly ash aggregate properties on the shrinkage cracking of lightweight concretes. *Cement & Concrete Composites*, *28*, 598-605.

Ghali, A., Favre, R. & Eldbadry, M. 2006. *Concrete Structures: Stresses and deformations.* Third edition e-copy ed. London: Taylor & Francis e-library.

Giaccio, G. & Zerbino, R. 1998. Failure mechanism of concrete: Combined effects of coarse aggregates and strength level. *Advanced Cement Based Materials*. (7)41–48.

Gilbert, R.I. 1988. *Time Effects in Concrete Structures*. Netherlands: ELSEVIER.

Goodman, H.J. 1991. An investigation into SABS Method 1085: Initial drying shrinkage and wetting expansion of concrete, Project Report. Advanced Concrete Technology Course, Halfway House: Portland Cement Institute.

Granju, J.L., Sabathier, V., Turatsinze, A. & Toumi, A. 2004. Interface between an old concrete and a bonded overlay: Debonding mechanism. *Interface Science*. 12(4):381 388.

Grieve, G. 2009. Aggregates for concrete. *Fulton's concrete technology.* 9th ed. South Africa: Cement & Concrete Institute. Ch. 7: 97-106.

Grzybowski, M. & Shah, S.P. 1990. Shrinkage Cracking of Fiber Reinforced Concrete. *ACI materials journal.* 87(2):138.

Gutsch A. & Rostásy S.1995. Young concrete under high tensile stresses - creep relaxation and cracking. Proceedings: *RILEM symposium on thermal cracking in concrete at early ages*. Chapman & Hall, London, 111–116.

Gutsch A.W. 2002. Properties of early age concrete experiments and modeling. *Mater. Struct.,* 35:76–79.

Haardt, P. 1991. Zementgebundene und kunststoffvergütete Beschichtungen auf Beton (cement-based and polymermodified overlays for concrete). *Massivbau Baustofftechnologie Karlsruhe*, Heft 13, TH Karlsruhe, Germany.

Haller, P. 1940. Shrinkage and creep of mortar and concrete. Zurich: EMPA, (Diskussionbericht No. 124).

Hassan, K.E., Robery, P.C. & Al-Alawi, L. 2000. Effect of hot-dry curing environment on the intrinsic properties of repair materials. *Cement & Concrete Composites*. 22: 453-458.

Hillerborg, A. 1985. Results of three comparative test series for determining the fracture energy GF of concrete. *Mater. Struct.* 18: 407–413.

Holt, E. & Leivo, M. 2004. Cracking risks associated with early age shrinkage. *Cement &Concrete Composites*. (26)5:521-530.

Júlio, E. N. B. S., Branco, F. a. B., Silva, V. D. & Lourenço, J. F. 2006. Influence of added concrete compressive strength on adhesion to an existing concrete substrate. *Building and Environment*. *41*(12), 1934-1939.

Kaplan, M.F. 1959. Ultrasonic pulse velocity, dynamic modulus of elasticity, Poisson's ratio, and the strength of concrete made with thirteen different coarse aggregates. *RILEM Bulletin*. No. 1.

Klopfer, H. 1987. Spannungen und Verformungen von Industrie-Estrichen (Stresses and deformations of industrial screeds). *Technische Akademie Esslingen*, International Colloquium: Industry Floors, Germany.

Kordina K., Schubert L. & Troitzsch U. 2000. *Creep of concrete subjected to tensile stress*. Deutscher Ausschuss fur Stahlbeton, Heft 498, Beuth Verlag, Berlin, Germany.

Kovler, K. & Bentur, A. 2009. Cracking sensitivity of Normal- and High-Strength Concretes. *ACI Materials Journal*. 106(6): 537-542.

Lee, S., Song, Y. & Han, S. 2004. Biaxial behavior of plain concrete of nuclear containment building. *Nuclear Engineering and Design.* 227:143–153.

Loedolff, G.F. & Chambers, S.L. 1994. Die indirekte treksterkte of splyttoets van beton gemaak met 19mm gebreekte klip van Malmesbury shale. *Concrete Beton*. 17:13.

Mangat, P. & O'Flaherty, F. 2000. Influence of elastic modulus on stress redistribution and cracking in repair patches. *Cement and Concrete Research*. 30(1), 125-136.

Masuku, C. 2009. Tensile relaxation of bonded concrete overlays. Masters Thesis. University of Cape Town.

Mehta, K.P. & Monteiro, P.J.M. 2006. Micro-structure of Concrete. *In Concrete: Microstructure, Properties, and Materials.* Third ed. United States of America: McGraw-Hill Companies. 21.

Mindess, S. &Young, J.F. 1981. *Concrete*, New Jersey: Prentice-Hall.

Mindess, S., Young, J.F. & Darwin, D. 2003. *Concrete.* Second ed. Upper Saddle River, NJ07458: Prentice Hall, Pearson Education Inc.

Mokarem, D. W., Weyers, R. E., & Lane, D. S. 2005. Development of a Shrinkage Performance Specifications and Prediction Model Analysis for Supplemental Cementitious Material Concrete Mixtures. *Cem. Conc. Res*. 35:918– 925.

Morimoto H. & Koyanagi W. 1995. Estimation of stress relaxation in concrete at early ages. Proceedings*: RILEM symposium on thermal cracking in concrete at early ages*. Chapman & Hall, London. 95–102.

Naderi, M. & Ghodousian, O. 2012. Adhesion of Self-Compacting Overlays Applied to Different Concrete Substrates and Its Prediction by Fuzzy Logic. *Journal of Adhesion*. 88 (10): 848-865.

Naik, T. R., Ramme, B. W. & Tews, J. H. 1995. Pavement construction with high-volume class C and class F fly-ash concrete. *ACI Material Journal*. 92(2):200–210.

Neville, A.M. 1996. *Properties of Concrete*. England: Pearson Education Limited-Prentice Hall.

Ozturan, T. & Cecen, C. 1997. Effect of aggregate type on mechanical properties of concretes with different strengths. *Cement and Concrete Research*. 27(2), 165-170.

Perrie, B. 2009. Strength of hardened concrete. Fulton's concrete technology. 9th ed. South Africa: Cement & Concrete Institute. Ch. 7: 97-106.

Pigeon, M. & Bissonnette, B. 1999. Tensile Creep and Cracking Potential. *Concrete international.* 31-35.

Powers, T.C. 1968. The thermodynamics of volume change and creep. *Materiaux et constructions*. 1(6):487-507.

Powers, T.C. 1971. Fundamental aspects of concrete shrinkage, Rev. *Materiaux et Constructions*. 545:79-85.

Rahman, M.K., Baluch, M.H. & Al-Gadhib, A.H. 2000. Simulation of shrinkage distress and creep relief in concrete repair. *Composites*. Part B (31):541-553.

RILEM Draft Recommendation: 107-GCS: Guidelines for the formulation of creep and shrinkage prediction models: Creep and shrinkage prediction model for analysis and design of concrete structures – Model B3, Materials and Structures 1995, 28(180:357 365; errata 1996, 29(186):126.

Rongbing, B. & Jian, S. 2005. Synthesis and evaluation of shrinkage-reducing admixtures for cementitious materials. *Cement and Concrete Research*. 35(3): 445-448.

SANS 10100-1:2000, Code of practice for the structural use of concrete, Pretoria: South African Bureau of Standards, 2000.

Shin, A. & Lange, D.A. 2012. Effects of overlay thickness on surface cracking and debonding in bonded concrete overlays. *Can. J. Civ. Eng*. 39: 304–312.

Sika. 2012. SikaGrout-212 Product Data Sheet.

Topcu, I. B. & Elgun, V. B. 2003. Influence of concrete properties on bleeding and evaporation. *Cement and Concrete Research*. 34, 275–281.

Troxell, G.E., Raphael, J.M. & Davis, R.E. 1958. Long-time creep and shrinkage tests of plain and reinforced concrete. *Proceedings American Society for Testing and Materials.* 58:1101-1120.

Verbeck, G.J. 1958. Carbonation of hydrated Portland cement. *Research Department Bulletin, Portland Cement Association.*17-36.

Weiss, J., Yang, W. & Shah, S.P. 1998. Shrinkage cracking of restrained concrete slabs. *Journal of Engineering Mechanics*. 124(7):765-774.

Westman, G. 1999. Concrete Creep and Thermal Stresses – New Creep Models and Their Effects on Stress Development. PhD Thesis, Department of Civil and Mining Engineering, Division of Structural Engineering, Luleå University of Technology, Luleå, Sweden.

Wittmann, F. H. 2002. Crack formation and fracture energy of normal and high strength concrete. *Sadhana.* 27(4): 413–423.

Yuan, Y. & Marsszeky, M. 1994. Restrained shrinkage in repaired reinforced concrete elements. *Materials and Structures*. 27:375–382.

Yuan, Y., Li, G. & Cai, Y.2002. Modeling for prediction of restrained shrinkage effect in concrete repair. *Cement & Concrete Research*. 33: 347-352.

Zheng, J., Li, C. and Zhou, X. 2006. An analytical method for prediction of the elastic modulus of concrete. *Magazine of Concrete Research*. 58(10):665–673.

Zhang, J., Liu, Q. & Wang, L. 2005. Effect of coarse aggregate size on relationships between stress and crack opening in normal and high strength concretes. *Journal of Material Science and Technology*. 21(5), 691-700.

Zhou, F.P., Balendran, R.V. & Jeary, A.P. 1998. Size effect on flexural, splitting tensile and torsional strengths of high-strength concrete. *Cement and Concrete Research*. 28(12):1725-1736.

Appendix A: Laboratory results

Compressive strength

w:c = 0.45 Laboratory Mix (19 mm Coarse Aggregate) (MPa)								
	0%				25%			
	Sp. 1	Sp. 2	Sp. 3	Average	Sp. 1	Sp. 2	Sp. 3	Average
7 Day	27.00	29.50	27.50	**28.00**	33.00	31.70	32.20	**32.30**
28 Day	41.50	44.00	38.90	**41.47**	50.70	47.50	43.60	**47.27**
	35%				45%			
	Sp. 1	Sp. 2	Sp. 3	Average	Sp. 1	Sp. 2	Sp. 3	Average
7 Day	32.60	31.50	30.50	**31.53**	33.50	33.00	34.00	**33.50**
28 Day	51.10	47.00	44.60	**47.57**	50.40	45.60	47.40	**47.80**

w:c = 0.6 Laboratory Mix (19 mm Coarse Aggregate) (MPa)								
	0%				25%			
	Sp. 1	Sp. 2	Sp. 3	Average	Sp. 1	Sp. 2	Sp. 3	Average
7 Day	18.00	18.70	18.00	**18.23**	20.90	22.00	20.00	**20.97**
28 Day	28.60	31.00	29.50	**29.70**	33.80	30.80	30.60	**31.73**
	35%				45%			
	Sp. 1	Sp. 2	Sp. 3	Average	Sp. 1	Sp. 2	Sp. 3	Average
7 Day	22.50	22.50	22.00	**22.33**	26.40	25.50	24.40	**25.43**
28 Day	35.70	32.50	35.80	**34.67**	41.50	39.20	36.50	**39.07**

w:c = 0.6 Laboratory Mix (9.5 mm Coarse Aggregate) (MPa)								
	0%				25%			
	Sp. 1	Sp. 2	Sp. 3	Average	Sp. 1	Sp. 2	Sp. 3	Average
7 Day	18.00	18.70	18.00	**18.23**	21.30	19.10	19.30	**19.90**
28 Day	28.60	31.00	29.50	**29.70**	35.00	33.50	34.60	**34.37**
	35%				45%			
	Sp. 1	Sp. 2	Sp. 3	Average	Sp. 1	Sp. 2	Sp. 3	Average
7 Day	21.30	22.40	22.10	**21.93**	24.00	25.20	24.00	**24.40**
28 Day	37.20	36.10	37.80	**37.03**	37.10	38.10	39.80	**38.33**

SikaGrout-212 Commercial Mix (19 mm Coarse Aggregate) (MPa)								
	0%				25%			
	Sp. 1	Sp. 2	Sp. 3	Average	Sp. 1	Sp. 2	Sp. 3	Average
7 Day	60.00	56.20	58.00	**58.07**	63.80	62.70	64.00	**63.50**
28 Day	76.20	80.00	79.00	**78.40**	80.00	78.00	78.00	**78.67**
	35%				45%			
	Sp. 1	Sp. 2	Sp. 3	Average	Sp. 1	Sp. 2	Sp. 3	Average
7 Day	68.00	68.00	64.00	**66.67**	64.30	68.50	68.00	**66.93**
28 Day	78.00	80.10	78.10	**78.73**	84.00	84.10	81.00	**83.03**

Elastic modulus

w:c = 0.45 Laboratory Mix (19 mm Coarse Aggregate) (GPa)								
	0%				25%			
	Sp. 1	Sp. 2	Sp. 3	Average	Sp. 1	Sp. 2	Sp. 3	Average
7 Day	28.00	26.90	32.17	**29.02**	31.93	32.40	32.79	**32.37**
28 Day	42.38		41.62	**42.00**	44.62	41.95	46.68	**44.42**
	35%				45%			
	Sp. 1	Sp. 2	Sp. 3	Average	Sp. 1	Sp. 2	Sp. 3	Average
7 Day	34.03	36.30	34.70	**35.01**	38.58	43.14	32.30	**38.01**
28 Day	50.15	49.08	42.28	**47.17**	45.41	50.70	49.09	**48.40**

w:c = 0.6 Laboratory Mix (19 mm Coarse Aggregate) (GPa)								
	0%				25%			
	Sp. 1	Sp. 2	Sp. 3	Average	Sp. 1	Sp. 2	Sp. 3	Average
7 Day	21.12	21.71	21.62	**21.48**	25.75	24.51	26.05	**25.44**
28 Day	30.58	30.86	26.69	**29.38**	36.64	33.33	31.97	**33.98**
	35%				45%			
	Sp. 1	Sp. 2	Sp. 3	Average	Sp. 1	Sp. 2	Sp. 3	Average
7 Day	28.76	27.43	30.91	**29.03**	30.98	33.46	33.00	**32.48**
28 Day	39.17	34.14	38.80	**37.37**	34.76	41.05	41.69	**39.16**

w:c = 0.6 Laboratory Mix (9.5 mm Coarse Aggregate) (GPa)								
	0%				25%			
	Sp. 1	Sp. 2	Sp. 3	Average	Sp. 1	Sp. 2	Sp. 3	Average
7 Day	21.12	21.71	21.62	**21.48**	16.79	25.14	22.01	**21.31**
28 Day	30.58	30.86	26.69	**29.38**	26.98	28.27	26.23	**27.16**
	35%				45%			
	Sp. 1	Sp. 2	Sp. 3	Average	Sp. 1	Sp. 2	Sp. 3	Average
7 Day		24.73	23.67	**24.20**	27.60	29.05	26.43	**27.69**
28 Day	28.88	31.75	27.36	**29.33**	31.99	33.51	31.53	**32.35**

SikaGrout-212 Commercial Mix (19 mm Coarse Aggregate) (GPa)								
	0%				25%			
	Sp. 1	Sp. 2	Sp. 3	Average	Sp. 1	Sp. 2	Sp. 3	Average
7 Day	34.36	31.95	30.10	**32.14**	36.15	36.33	35.28	**35.92**
28 Day	39.11	36.77	35.29	**37.06**	40.73	40.65	41.55	**40.98**
	35%				45%			
	Sp. 1	Sp. 2	Sp. 3	Average	Sp. 1	Sp. 2	Sp. 3	Average
7 Day	39.31	38.14	39.26	**38.90**	42.75	41.13	43.61	**42.50**
28 Day	41.35	44.52	41.73	**42.53**	43.97	44.12	47.36	**45.15**

Tensile strength

w:c = 0.45 Laboratory Mix (19 mm Coarse Aggregate) (MPa)						
	0%			25%		
	Sp. 1	Sp. 2	Average	Sp. 1	Sp. 2	Average
7 Day	2.78	2.53	**2.65**	2.88	3.04	**2.96**
10 Day	2.50	2.33	**2.42**	2.69	3.23	**2.96**
28 Day	3.14	3.18	**3.16**	3.54	3.31	**3.43**
	35%			45%		
	Sp. 1	Sp. 2	Average	Sp. 1	Sp. 2	Average
7 Day	2.44	2.65	**2.54**	3.01	3.09	**3.05**
10 Day	2.31	2.79	**2.55**	3.25	3.17	**3.21**
28 Day	3.19	3.62	**3.40**	2.68	3.84	**3.26**

w:c = 0.6 Laboratory Mix (19 mm Coarse Aggregate) (MPa)						
	0%			25%		
	Sp. 1	Sp. 2	Average	Sp. 1	Sp. 2	Average
7 Day	2.20	2.14	**2.17**	2.88	2.50	**2.69**
10 Day	2.20	2.17	**2.18**	2.90	2.50	**2.70**
28 Day	2.26	3.34	**2.80**	2.90	3.02	**2.96**
	35%			45%		
	Sp. 1	Sp. 2	Average	Sp. 1	Sp. 2	Average
7 Day	2.66	2.45	**2.55**	3.20	3.39	**3.29**
10 Day	2.46	2.26	**2.36**	2.91	3.33	**3.12**
28 Day	2.83	2.54	**2.68**	3.33	3.36	**3.34**

w:c = 0.6 Laboratory Mix (9.5 mm Coarse Aggregate) (MPa)						
	0%			25%		
	Sp. 1	Sp. 2	Average	Sp. 1	Sp. 2	Average
7 Day	2.20	2.14	**2.17**	2.32	2.63	**2.48**
10 Day	2.20	2.17	**2.18**	2.36	2.35	**2.36**
28 Day	2.26	3.34	**2.80**	3.31	3.82	**3.57**
	35%			45%		
	Sp. 1	Sp. 2	Average	Sp. 1	Sp. 2	Average
7 Day	2.71	2.92	**2.81**	3.45	3.19	**3.32**
10 Day	2.82	2.90	**2.86**	3.05	3.40	**3.23**
28 Day	4.03	3.58	**3.81**	4.15	4.68	**4.41**

SikaGrout-212 Commercial Mix (19 mm Coarse Aggregate) (MPa)						
	0%			25%		
	Sp. 1	Sp. 2	Average	Sp. 1	Sp. 2	Average
7 Day	3.46	3.71	**3.59**	4.57	4.39	**4.48**
10 Day	3.86	3.88	**3.87**	4.61	4.84	**4.72**
28 Day	6.07	5.88	**5.97**	4.66	5.56	**5.11**
	35%			45%		
	Sp. 1	Sp. 2	Average	Sp. 1	Sp. 2	Average
7 Day	4.72	4.38	**4.55**	3.86	4.21	**4.03**
10 Day	4.33	6.07	**5.20**	4.85	5.17	**5.01**
28 Day	5.26	5.48	**5.37**	5.97	5.11	**5.54**

Tensile relaxation

w:c = 0.45 Laboratory Mix (19 mm Coarse Aggregate) (%)						
	0%			25%		
	Sp. 1	Sp. 2	Average	Sp. 1	Sp. 2	Average
7 Day	20.87		**20.87**	22.84	16.04	**19.44**
28 Day		15.52	**15.52**	14.35		**14.35**
	35%			45%		
	Sp. 1	Sp. 2	Average	Sp. 1	Sp. 2	Average
7 Day	14.82	17.94	**16.38**	10.67	14.51	**12.59**
28 Day	11.11		**11.11**	5.75	14.06	**9.90**

w:c = 0.6 Laboratory Mix (19 mm Coarse Aggregate) (%)						
	0%			25%		
	Sp. 1	Sp. 2	Average	Sp. 1	Sp. 2	Average
7 Day	22.28		**22.28**		20.61	**20.61**
28 Day	17.83		**17.83**	15.01	18.39	**16.70**
	35%			45%		
	Sp. 1	Sp. 2	Average	Sp. 1	Sp. 2	Average
7 Day		17.50	**17.50**	15.22	17.48	**16.35**
28 Day	12.58	18.79	**15.68**		13.20	**13.20**

w:c = 0.6 Laboratory Mix (9.5 mm Coarse Aggregate) (%)						
	0%			25%		
	Sp. 1	Sp. 2	Average	Sp. 1	Sp. 2	Average
7 Day	22.28		**22.28**	10.79	18.07	**14.43**
28 Day	17.83		**17.83**	8.87	15.21	**12.04**
	35%			45%		
	Sp. 1	Sp. 2	Average	Sp. 1	Sp. 2	Average
7 Day	12.82		**12.82**	11.23	12.50	**11.86**
28 Day	10.96		**10.96**	7.36	15.71	**11.54**

SikaGrout-212 Commercial Mix (19 mm Coarse Aggregate) (%)						
	0%			25%		
	Sp. 1	Sp. 2	Average	Sp. 1	Sp. 2	Average
7 Day		15.69	**15.69**	13.34		**13.34**
28 Day	12.67		**12.67**	7.75	10.83	**9.29**
	35%			45%		
	Sp. 1	Sp. 2	Average	Sp. 1	Sp. 2	Average
7 Day	8.01	12.29	**10.15**	7.05	8.14	**7.59**
28 Day	7.75	10.83	**9.29**	6.04		**6.04**

Ring test (time to first cracking)

w:c = 0.45 Laboratory Mix (19 mm Coarse Aggregate) (days)					
0%			25%		
Sp. 1	Sp. 2	Average	Sp. 1	Sp. 2	Average
4	2	**3**	6	11	**8.5**
35%			45%		
Sp. 1	Sp. 2	Average	Sp. 1	Sp. 2	Average
19	19	**19**	29	30	**29.5**

w:c = 0.6 Laboratory Mix (19 mm Coarse Aggregate) (days)					
0%			25%		
Sp. 1	Sp. 2	Average	Sp. 1	Sp. 2	Average
4	5	**4.5**	13	18	**15.5**
35%			45%		
Sp. 1	Sp. 2	Average	Sp. 1	Sp. 2	Average
24	24	**24**	33	35	**34.0**

w:c = 0.6 Laboratory Mix (9.5 mm Coarse Aggregate) (days)					
0%			25%		
Sp. 1	Sp. 2	Average	Sp. 1	Sp. 2	Average
4	5	**4.5**	6	8	**7**
35%			45%		
Sp. 1	Sp. 2	Average	Sp. 1	Sp. 2	Average
6	11	**8.5**	14	15	**14.5**

SikaGrout-212 Commercial Mix (19 mm Coarse Aggregate) (days)					
0%			25%		
Sp. 1	Sp. 2	Average	Sp. 1	Sp. 2	Average
1	1	**1**	5	5	**5**
35%			45%		
Sp. 1	Sp. 2	Average	Sp. 1	Sp. 2	Average
10	12	**11**	14	15	**14.5**

Ring test (crack area)

w:c = 0.45 Laboratory Mix (19 mm Coarse Aggregate) (mm^2)					
0%			**25%**		
Sp. 1	**Sp. 2**	**Average**	**Sp. 1**	**Sp. 2**	**Average**
200.96	346.62	**273.79**	150.88	27.36	**89.12**
35%			**45%**		
Sp. 1	**Sp. 2**	**Average**	**Sp. 1**	**Sp. 2**	**Average**
34.40	30.06	**32.23**	8.64	6.42	**7.53**

w:c = 0.6 Laboratory Mix (19 mm Coarse Aggregate) (mm^2)					
0%			**25%**		
Sp. 1	**Sp. 2**	**Average**	**Sp. 1**	**Sp. 2**	**Average**
558.00	596.16	**577.08**	25.28	24.36	**24.82**
35%			**45%**		
Sp. 1	**Sp. 2**	**Average**	**Sp. 1**	**Sp. 2**	**Average**
25.92	26.56	**26.24**	5.64	4.86	**5.25**

w:c = 0.6 Laboratory Mix (9.5 mm Coarse Aggregate) (mm^2)					
0%			**25%**		
Sp. 1	**Sp. 2**	**Average**	**Sp. 1**	**Sp. 2**	**Average**
4	5	**4.5**	34.98	184.08	**109.53**
35%			**45%**		
Sp. 1	**Sp. 2**	**Average**	**Sp. 1**	**Sp. 2**	**Average**
55.42	77.28	**66.35**	13.28	5.4	**9.34**

SikaGrout-212 Commercial Mix (19 mm Coarse Aggregate) (mm^2)					
0%			**25%**		
Sp. 1	**Sp. 2**	**Average**	**Sp. 1**	**Sp. 2**	**Average**
298.98	284.58	**291.78**	55.76	29.34	**42.55**
35%			**45%**		
Sp. 1	**Sp. 2**	**Average**	**Sp. 1**	**Sp. 2**	**Average**
13.6	13.2	**13.4**	5.52	11.48	**8.50**

Appendix B: Analytical model inputs

Material property regression curves

Tensile strength

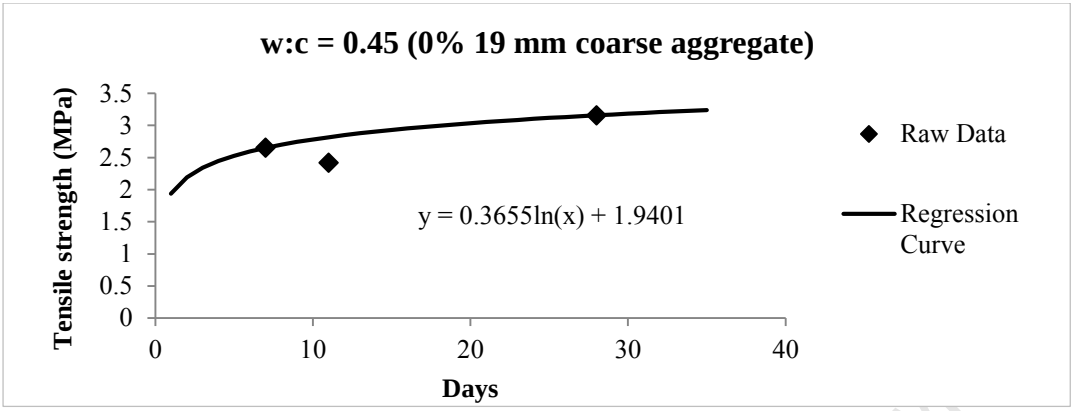

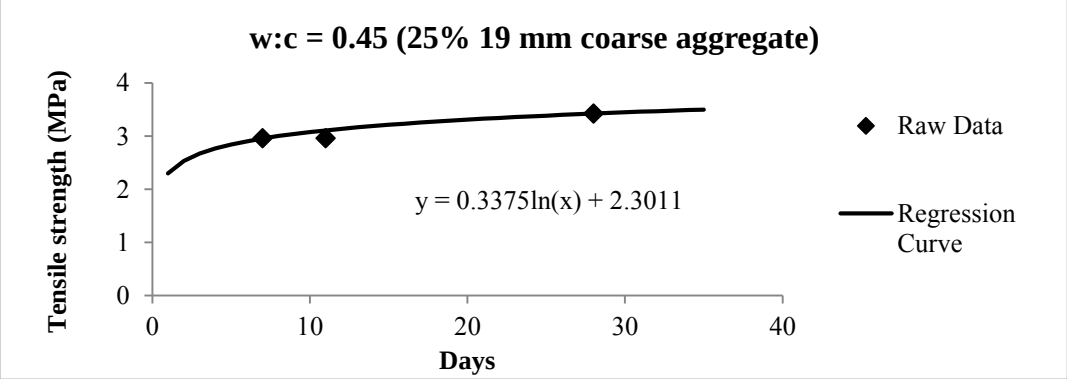

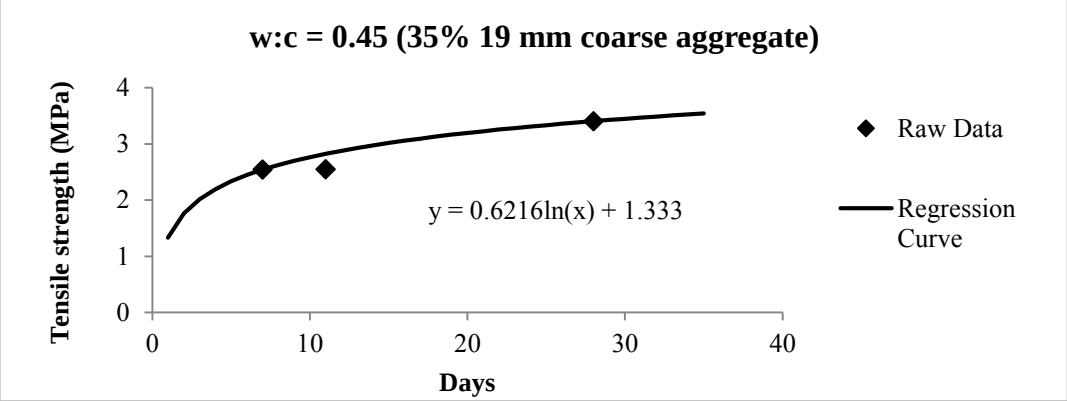

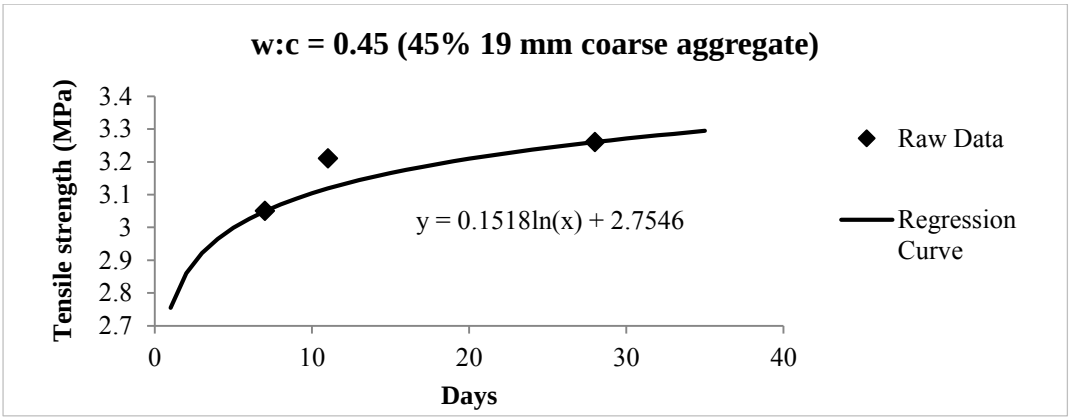

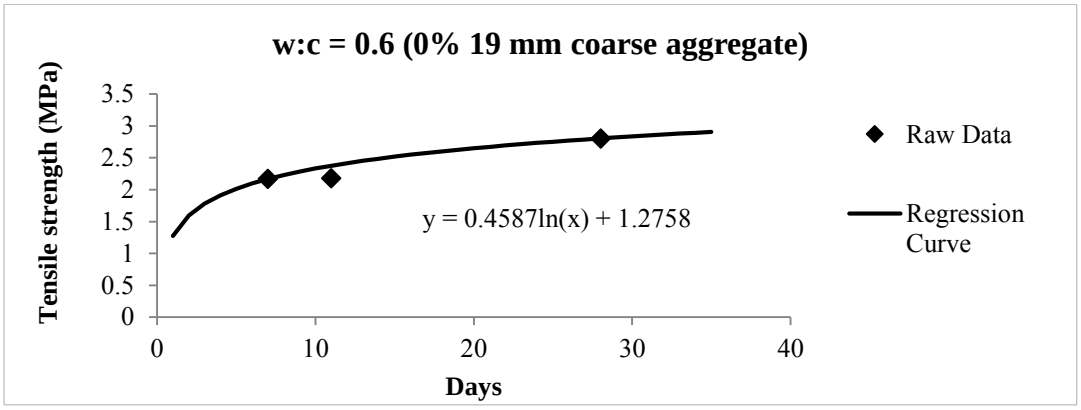
w:c = 0.6 (0% 19 mm coarse aggregate)
Tensile strength (MPa)
3.5
3
2.5
2
1.5
1
0.5
0
0
10
20
30
40
Days
y = 0.4587ln(x) + 1.2758
Raw Data
Regression Curve

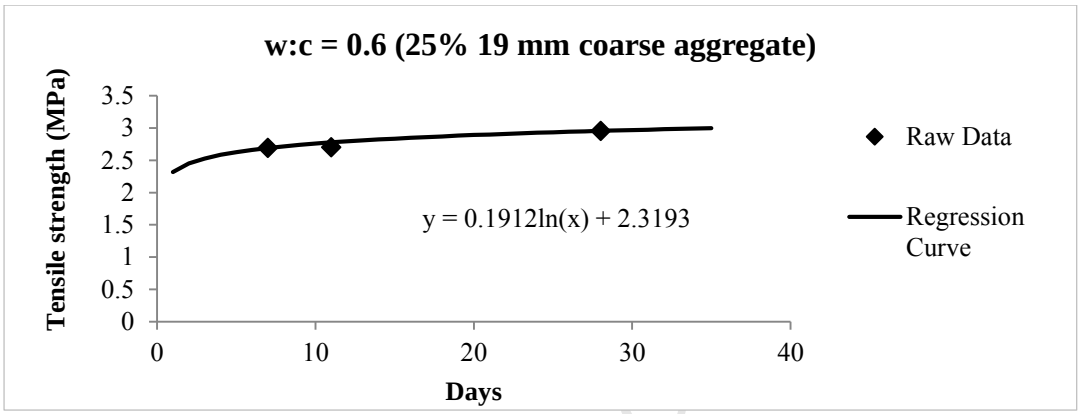
w:c = 0.6 (25% 19 mm coarse aggregate)
Tensile strength (MPa)
3.5
3
2.5
2
1.5
1
0.5
0
0
10
20
30
40
Days
y = 0.1912ln(x) + 2.3193
Raw Data
Regression Curve

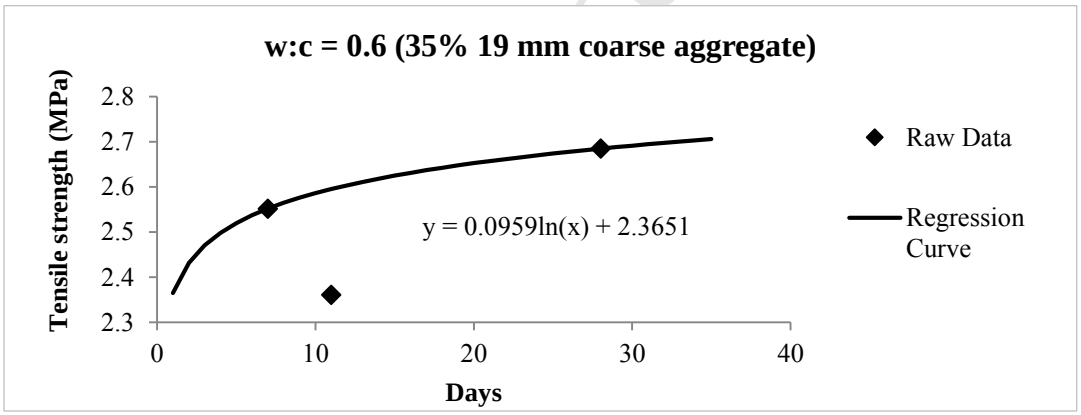
w:c = 0.6 (35% 19 mm coarse aggregate)
Tensile strength (MPa)
2.8
2.7
2.6
2.5
2.4
2.3
0
10
20
30
40
Days
y = 0.0959ln(x) + 2.3651
Raw Data
Regression Curve

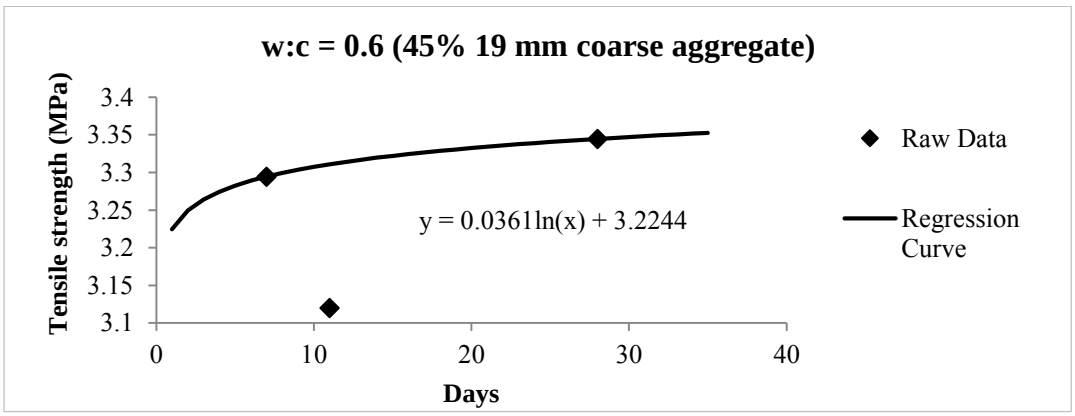
w:c = 0.6 (45% 19 mm coarse aggregate)
Tensile strength (MPa)
3.4
3.35
3.3
3.25
3.2
3.15
3.1
0
10
20
30
40
Days
y = 0.0361ln(x) + 3.2244
Raw Data
Regression Curve

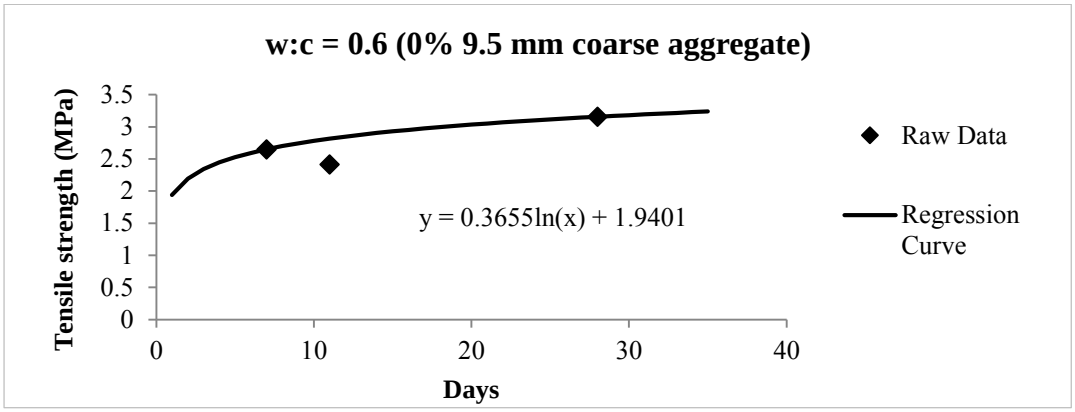
w:c = 0.6 (0% 9.5 mm coarse aggregate)
Tensile strength (MPa)
3.5
3
2.5
2
1.5
1
0.5
0
0
10
20
30
40
Days
y = 0.3655ln(x) + 1.9401
Raw Data
Regression Curve

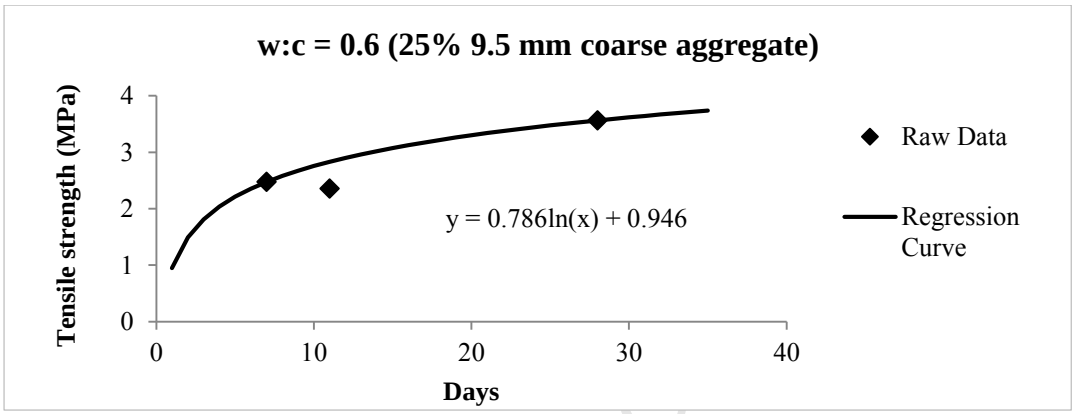
w:c = 0.6 (25% 9.5 mm coarse aggregate)
Tensile strength (MPa)
4
3
2
1
0
0
10
20
30
40
Days
y = 0.786ln(x) + 0.946
Raw Data
Regression Curve

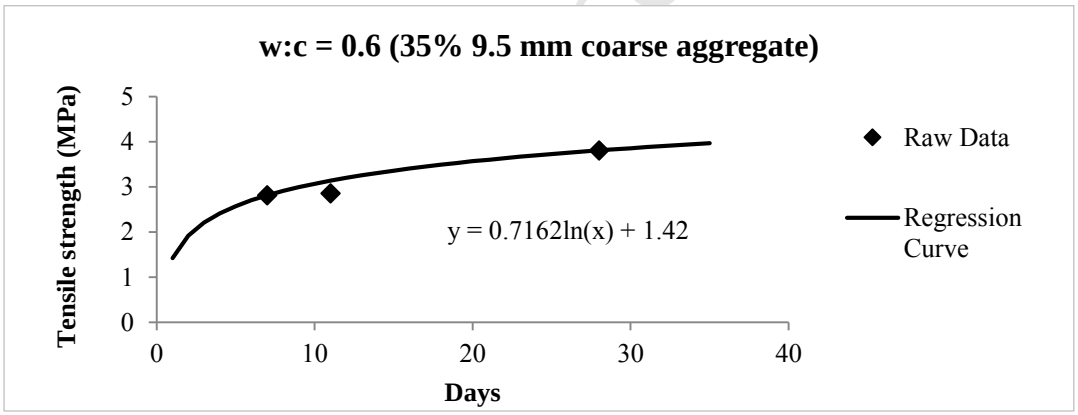
w:c = 0.6 (35% 9.5 mm coarse aggregate)
Tensile strength (MPa)
5
4
3
2
1
0
0
10
20
30
40
Days
y = 0.7162ln(x) + 1.42
Raw Data
Regression Curve

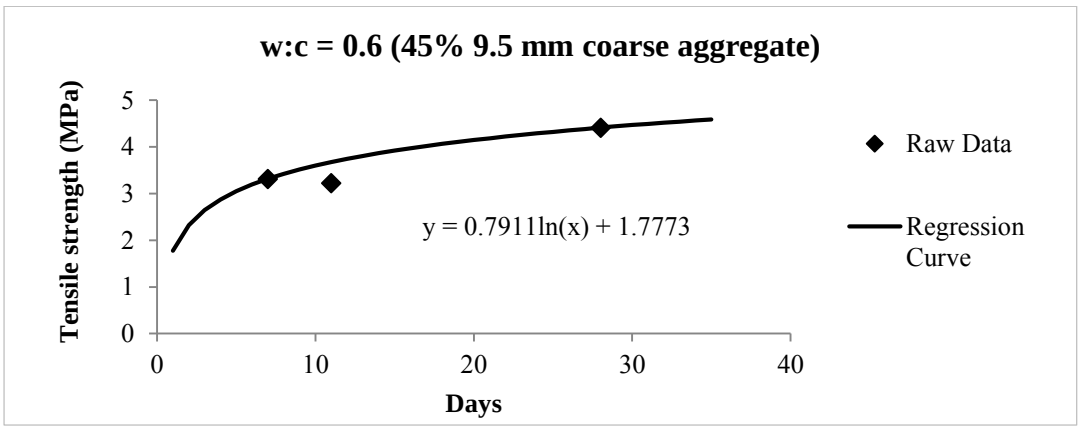
w:c = 0.6 (45% 9.5 mm coarse aggregate)
Tensile strength (MPa)
5
4
3
2
1
0
0
10
20
30
40
Days
y = 0.7911ln(x) + 1.7773
Raw Data
Regression Curve

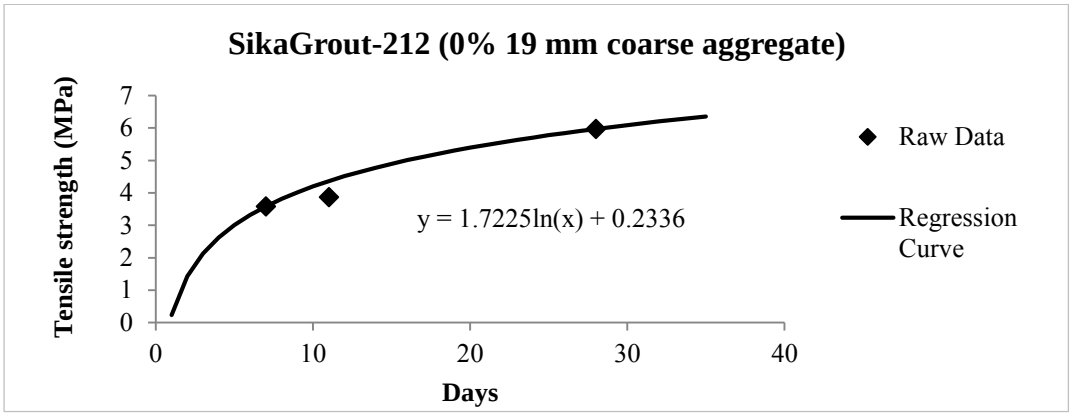
SikaGrout-212 (0% 19 mm coarse aggregate)
Tensile strength (MPa)
Days
y = 1.7225ln(x) + 0.2336
Raw Data
Regression Curve

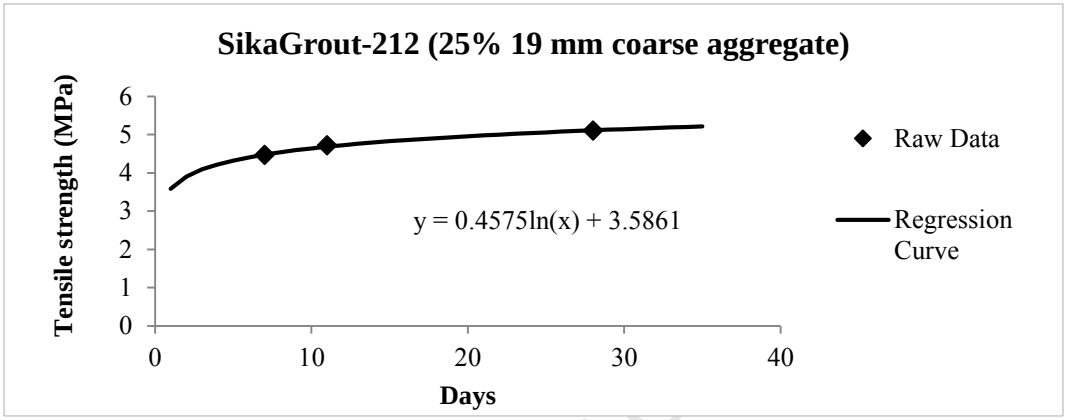
SikaGrout-212 (25% 19 mm coarse aggregate)
Tensile strength (MPa)
Days
y = 0.4575ln(x) + 3.5861
Raw Data
Regression Curve

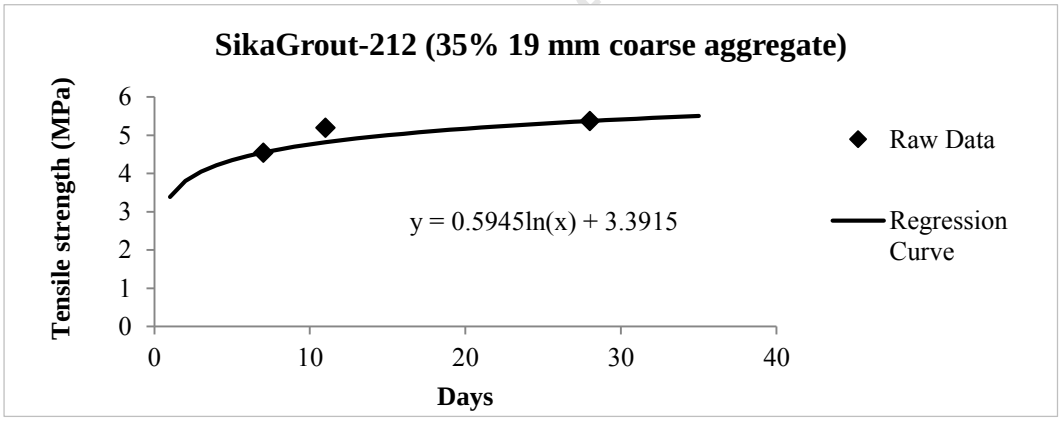
SikaGrout-212 (35% 19 mm coarse aggregate)
Tensile strength (MPa)
Days
y = 0.5945ln(x) + 3.3915
Raw Data
Regression Curve

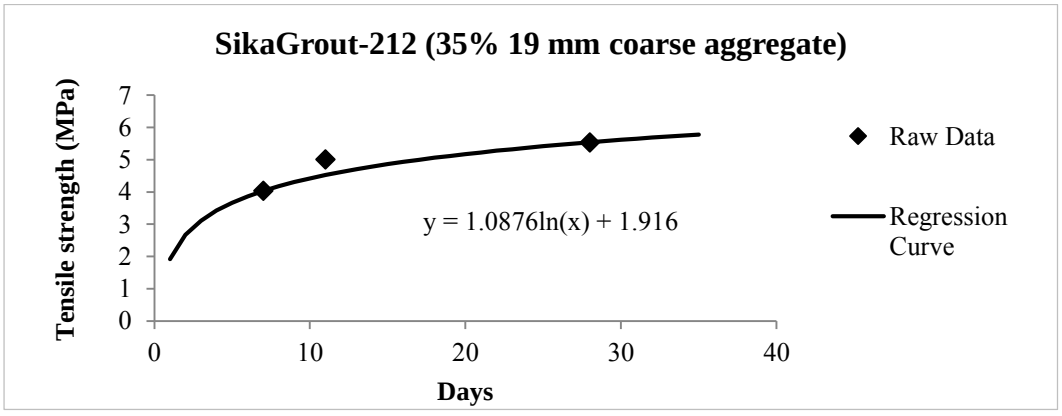
SikaGrout-212 (35% 19 mm coarse aggregate)
Tensile strength (MPa)
Days
y = 1.0876ln(x) + 1.916
Raw Data
Regression Curve

Elastic modulus

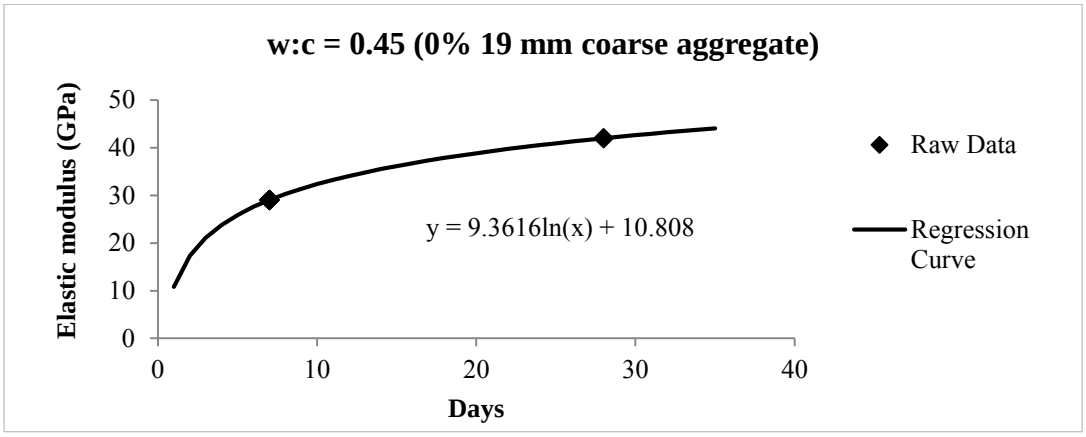

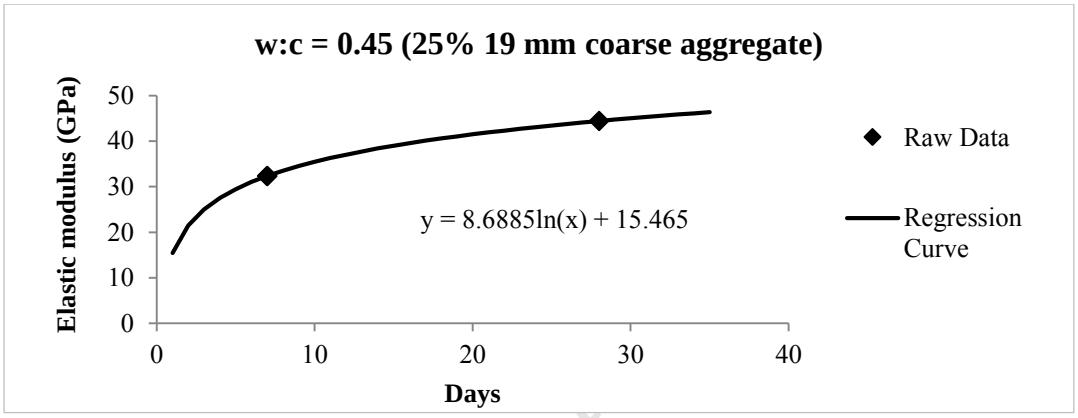

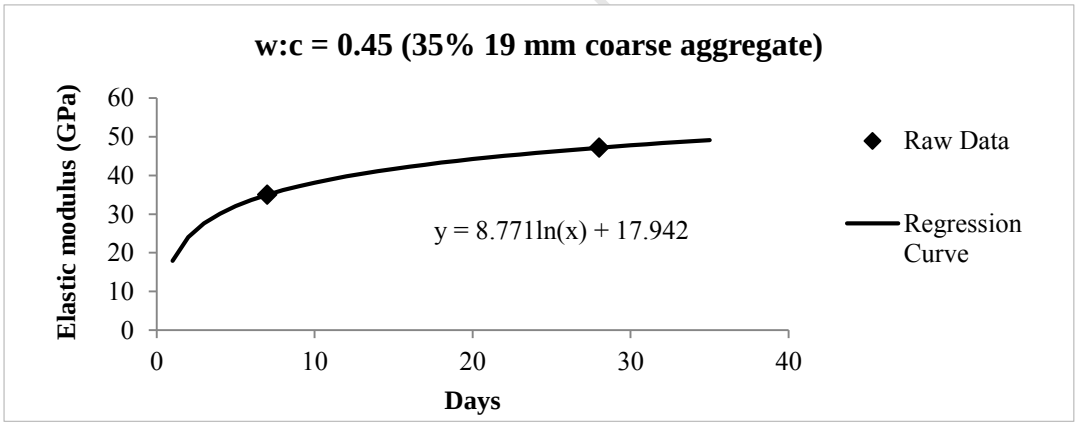

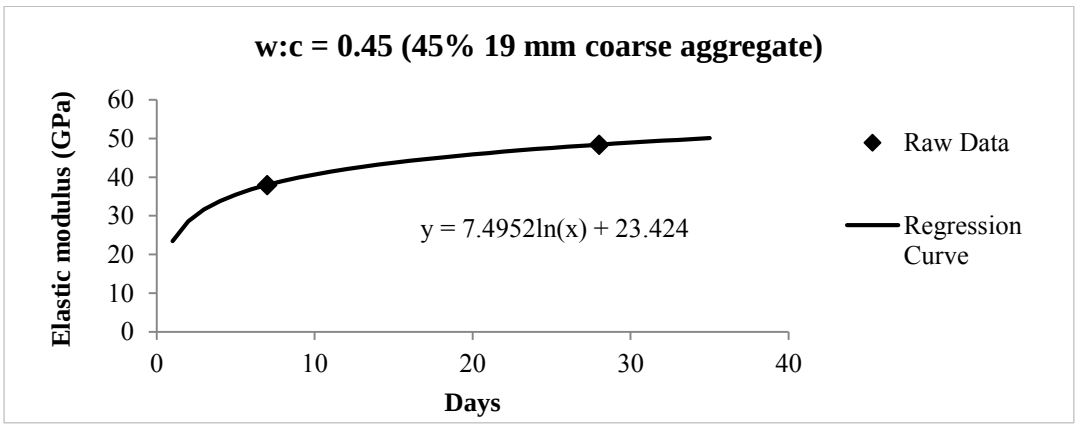

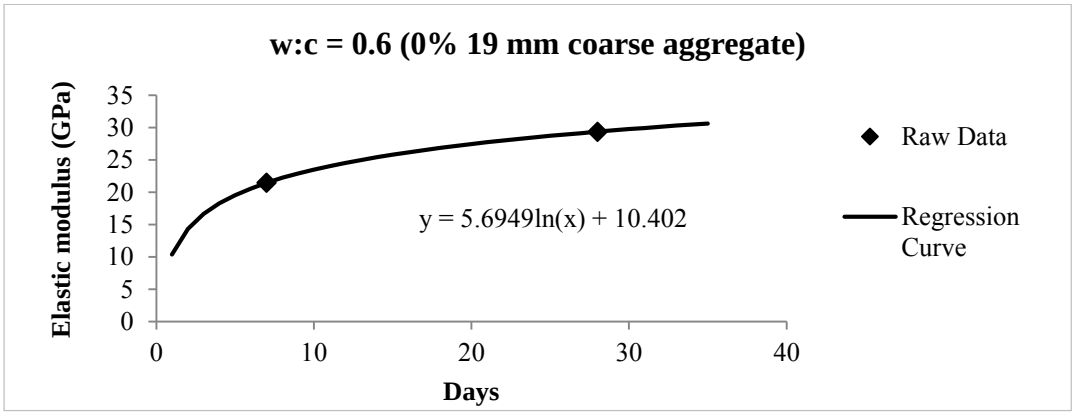
w:c = 0.6 (0% 19 mm coarse aggregate)
Elastic modulus (GPa)
35
30
25
20
15
10
5
0
0
10
20
30
40
Days
y = 5.6949ln(x) + 10.402
Raw Data
Regression Curve

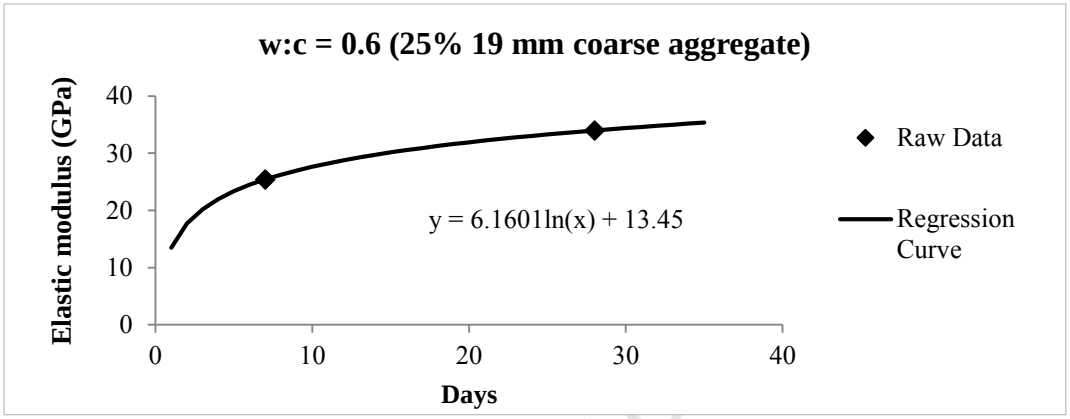
w:c = 0.6 (25% 19 mm coarse aggregate)
Elastic modulus (GPa)
40
30
20
10
0
0
10
20
30
40
Days
y = 6.1601ln(x) + 13.45
Raw Data
Regression Curve

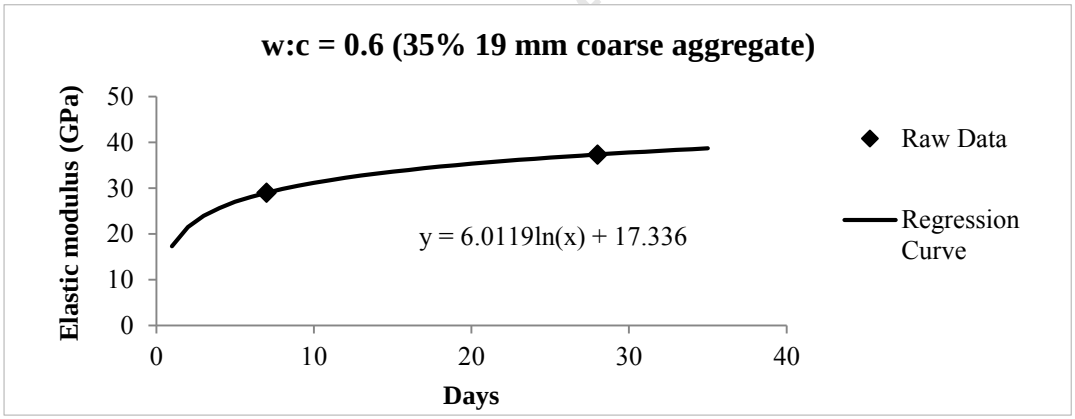
w:c = 0.6 (35% 19 mm coarse aggregate)
Elastic modulus (GPa)
50
40
30
20
10
0
0
10
20
30
40
Days
y = 6.0119ln(x) + 17.336
Raw Data
Regression Curve

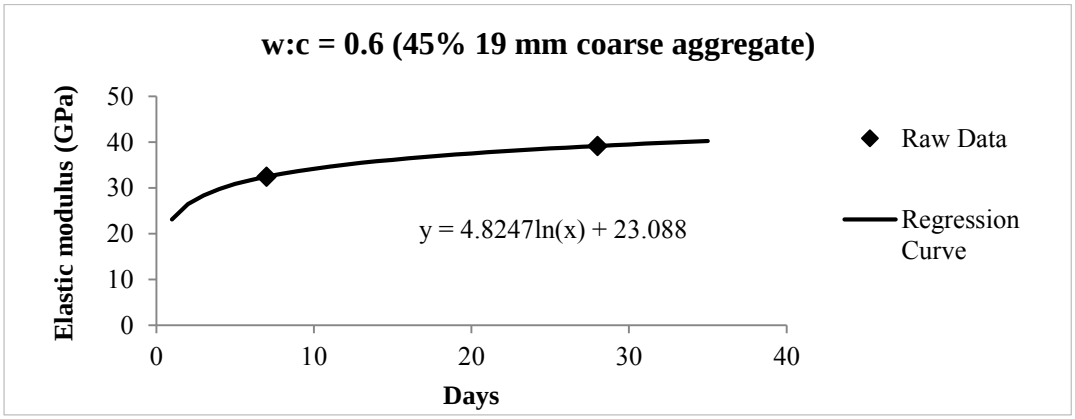
w:c = 0.6 (45% 19 mm coarse aggregate)
Elastic modulus (GPa)
50
40
30
20
10
0
0
10
20
30
40
Days
y = 4.8247ln(x) + 23.088
Raw Data
Regression Curve

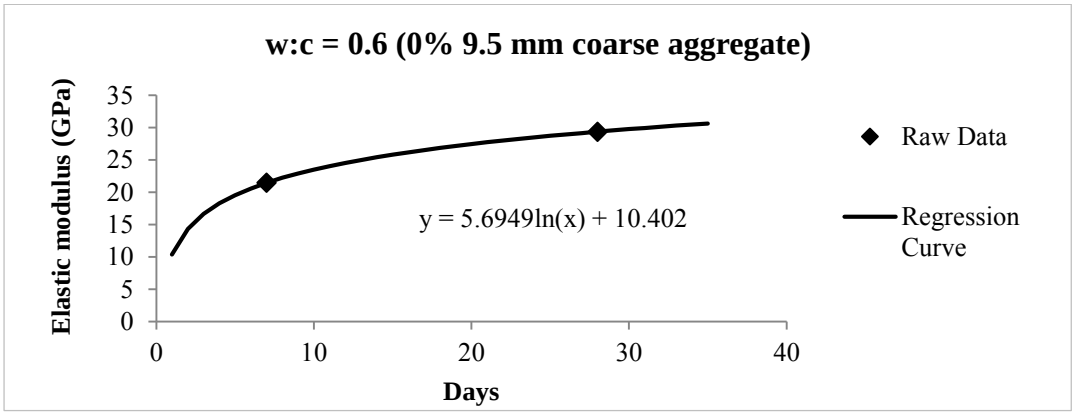
w:c = 0.6 (0% 9.5 mm coarse aggregate)
Elastic modulus (GPa)
Days
y = 5.6949ln(x) + 10.402
Raw Data
Regression Curve

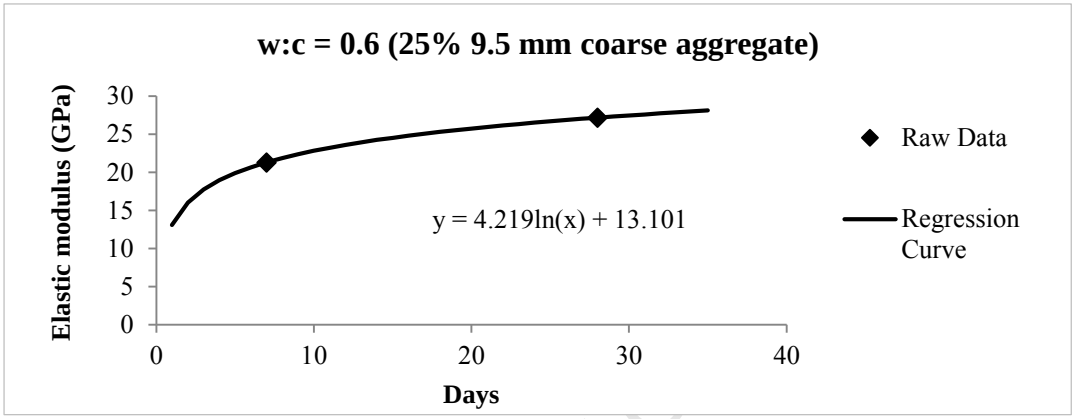
w:c = 0.6 (25% 9.5 mm coarse aggregate)
Elastic modulus (GPa)
Days
y = 4.219ln(x) + 13.101
Raw Data
Regression Curve

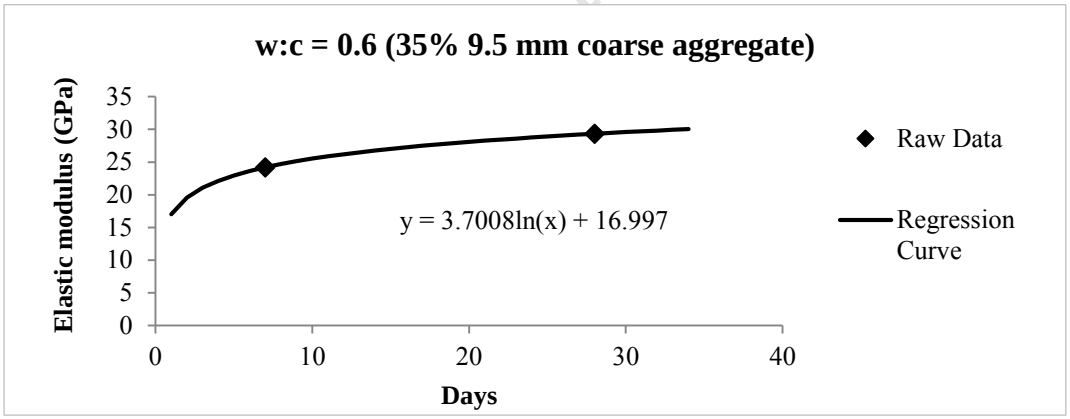
w:c = 0.6 (35% 9.5 mm coarse aggregate)
Elastic modulus (GPa)
Days
y = 3.7008ln(x) + 16.997
Raw Data
Regression Curve

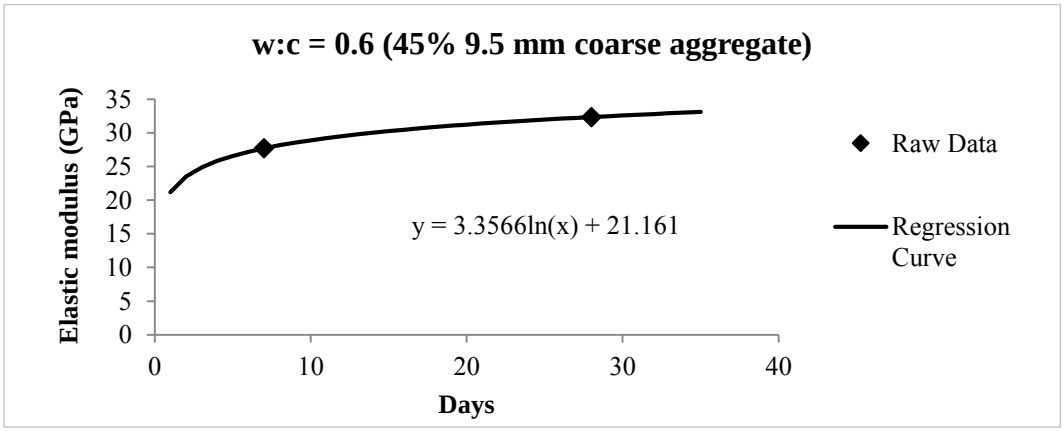
w:c = 0.6 (45% 9.5 mm coarse aggregate)
Elastic modulus (GPa)
Days
y = 3.3566ln(x) + 21.161
Raw Data
Regression Curve

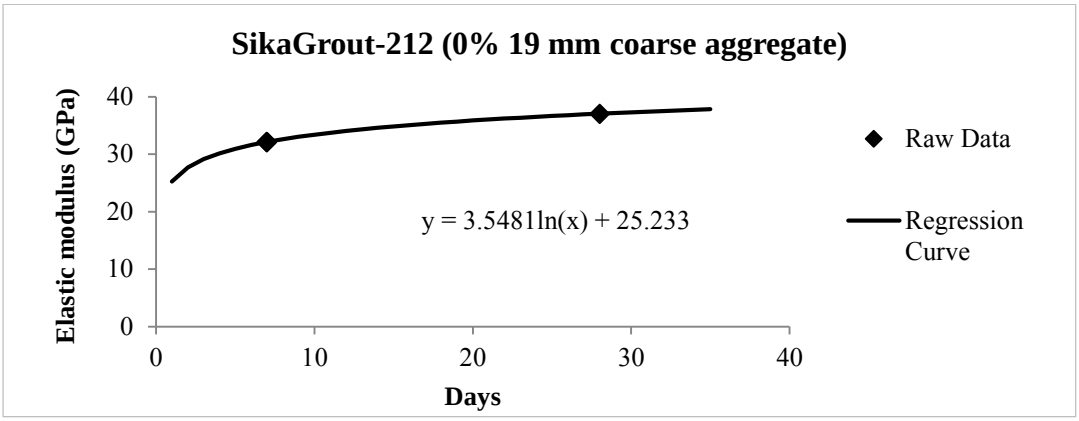
SikaGrout-212 (0% 19 mm coarse aggregate)
Elastic modulus (GPa)
40
30
20
10
0
0
10
20
30
40
Days
y = 3.5481ln(x) + 25.233
Raw Data
Regression Curve

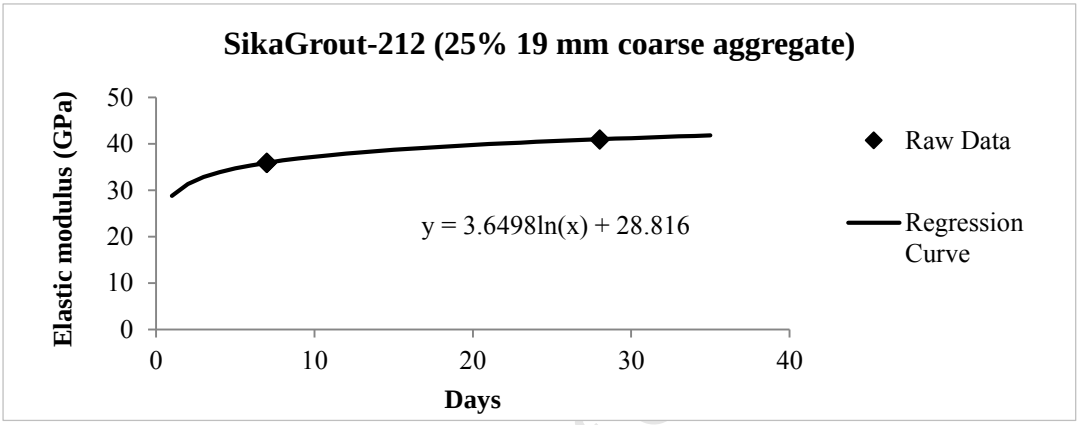
SikaGrout-212 (25% 19 mm coarse aggregate)
Elastic modulus (GPa)
50
40
30
20
10
0
0
10
20
30
40
Days
y = 3.6498ln(x) + 28.816
Raw Data
Regression Curve

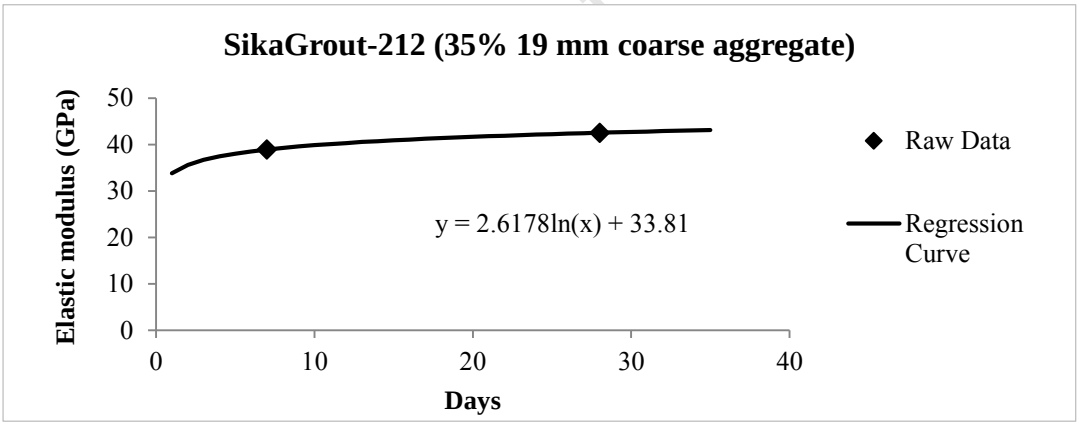
SikaGrout-212 (35% 19 mm coarse aggregate)
Elastic modulus (GPa)
50
40
30
20
10
0
0
10
20
30
40
Days
y = 2.6178ln(x) + 33.81
Raw Data
Regression Curve

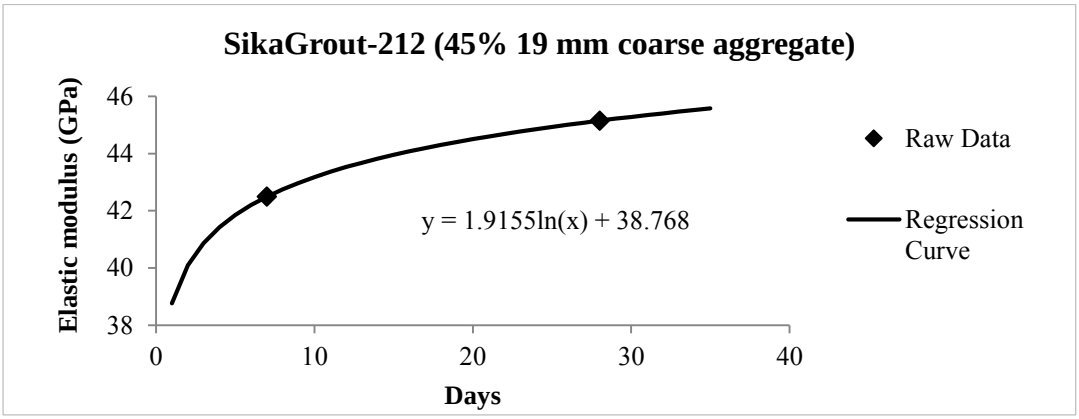
SikaGrout-212 (45% 19 mm coarse aggregate)
Elastic modulus (GPa)
46
44
42
40
38
0
10
20
30
40
Days
y = 1.9155ln(x) + 38.768
Raw Data
Regression Curve

Tensile relaxation

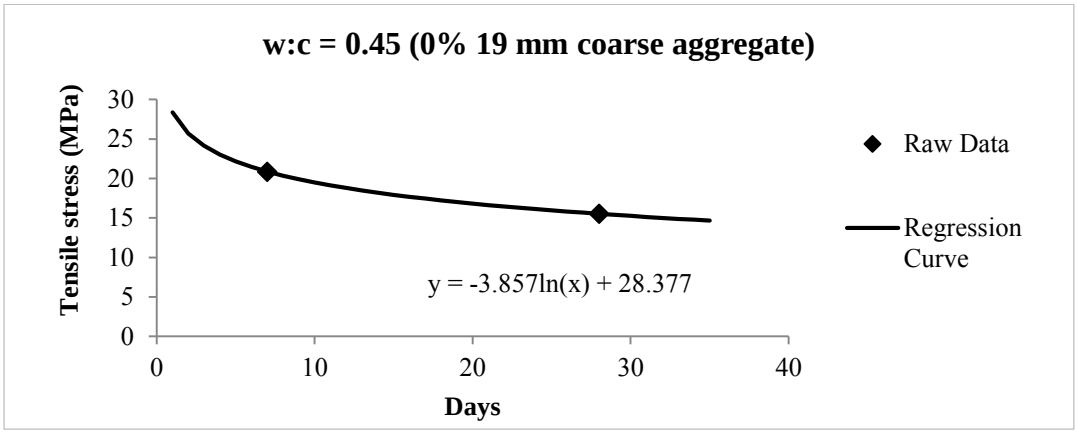

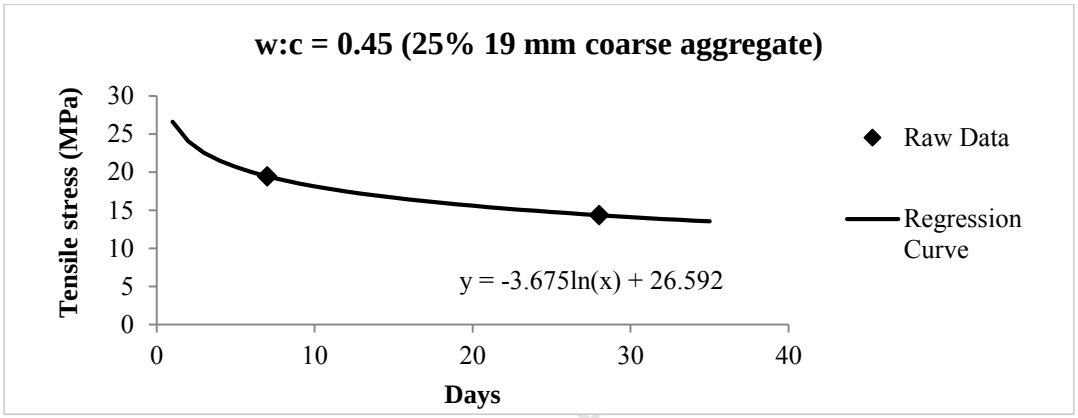

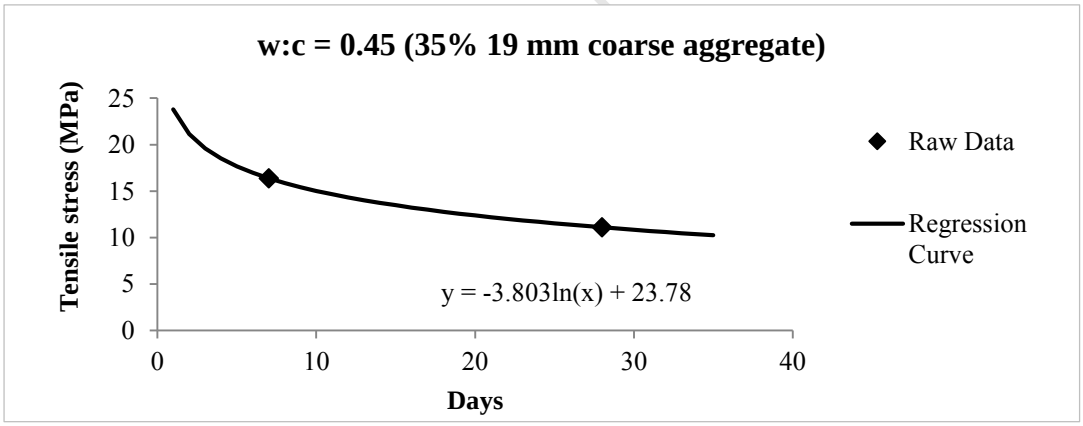

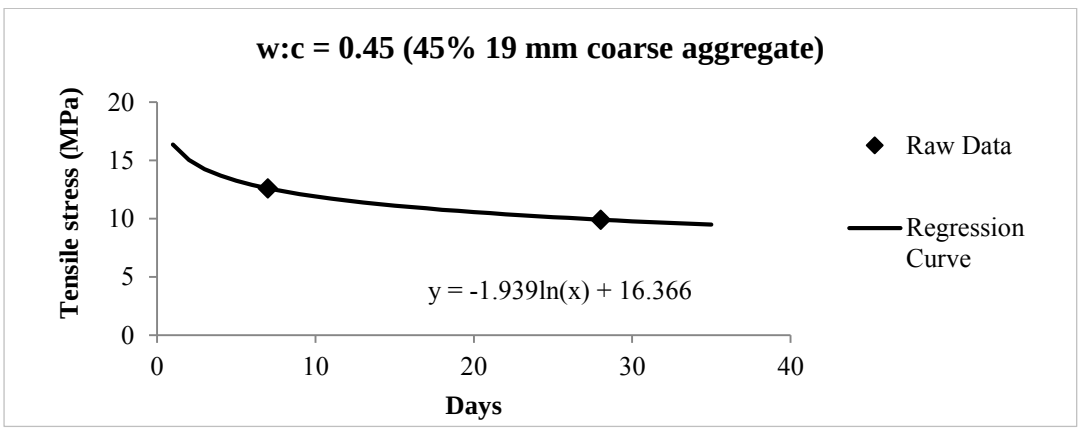

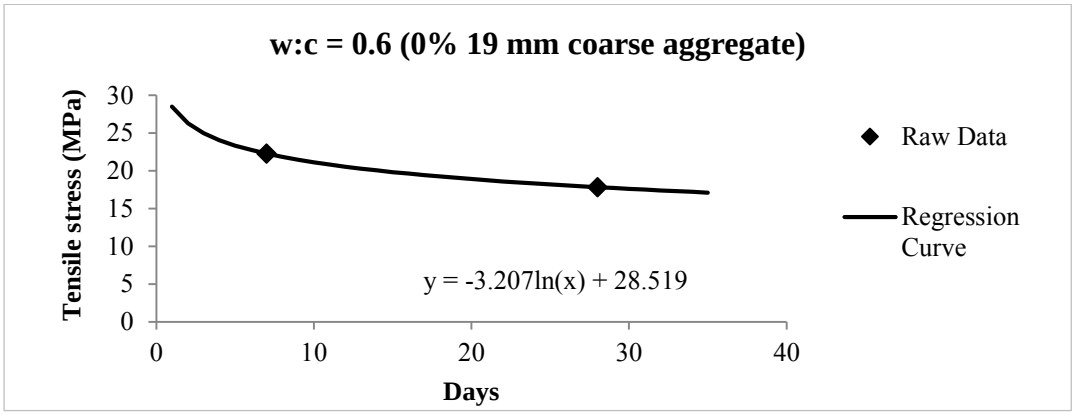
w:c = 0.6 (0% 19 mm coarse aggregate)
Tensile stress (MPa)
Days
y = -3.207ln(x) + 28.519
Raw Data
Regression Curve

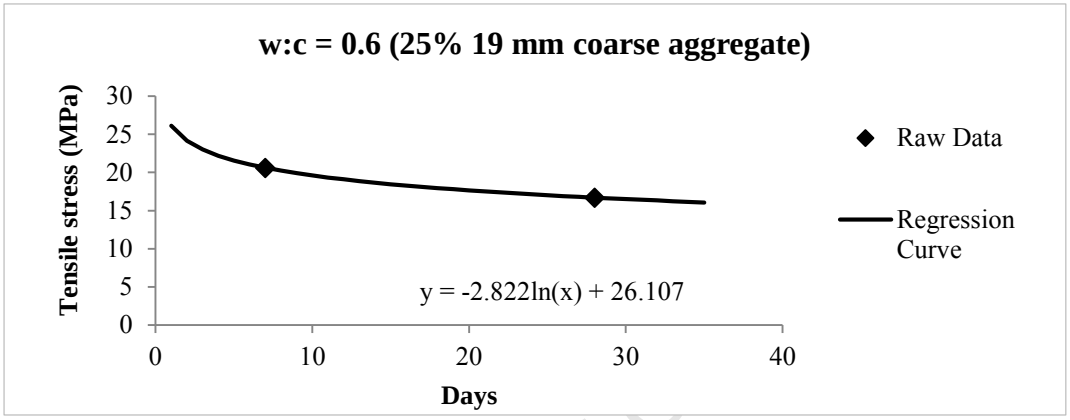
w:c = 0.6 (25% 19 mm coarse aggregate)
Tensile stress (MPa)
Days
y = -2.822ln(x) + 26.107
Raw Data
Regression Curve

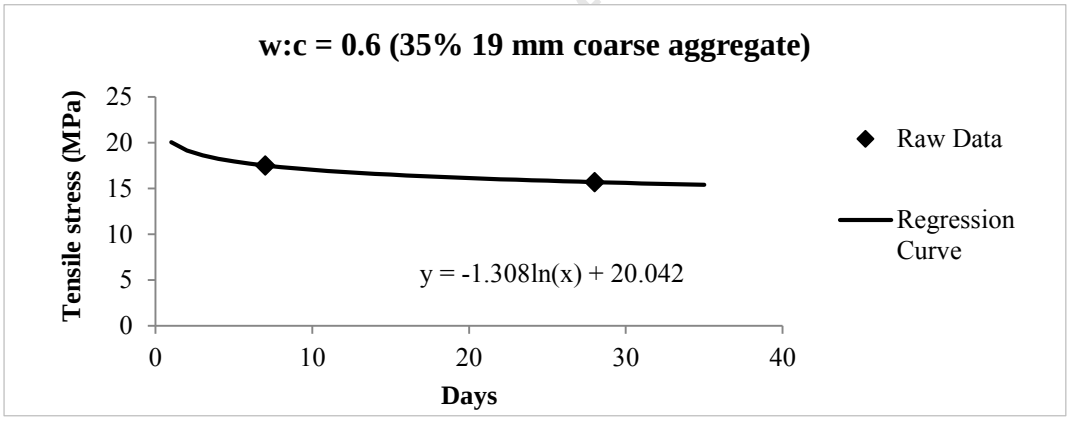
w:c = 0.6 (35% 19 mm coarse aggregate)
Tensile stress (MPa)
Days
y = -1.308ln(x) + 20.042
Raw Data
Regression Curve

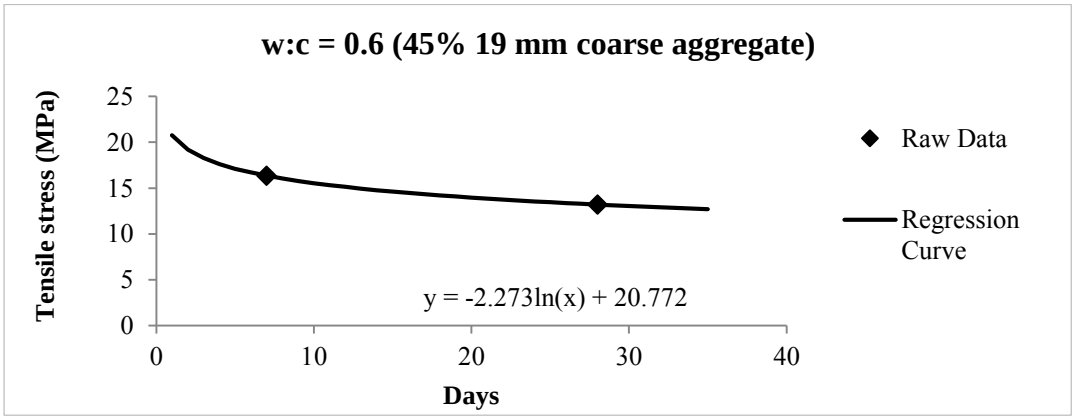
w:c = 0.6 (45% 19 mm coarse aggregate)
Tensile stress (MPa)
Days
y = -2.273ln(x) + 20.772
Raw Data
Regression Curve

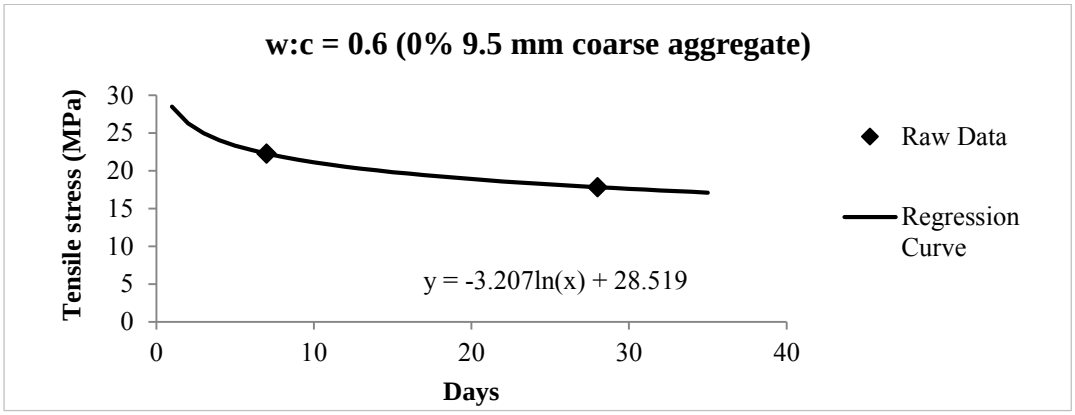
w:c = 0.6 (0% 9.5 mm coarse aggregate)
Tensile stress (MPa)
Days
y = -3.207ln(x) + 28.519
Raw Data
Regression Curve

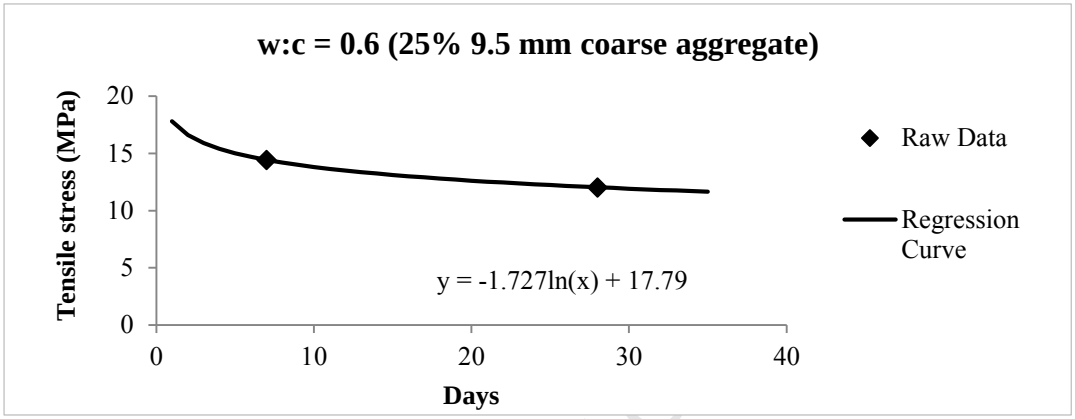
w:c = 0.6 (25% 9.5 mm coarse aggregate)
Tensile stress (MPa)
Days
y = -1.727ln(x) + 17.79
Raw Data
Regression Curve

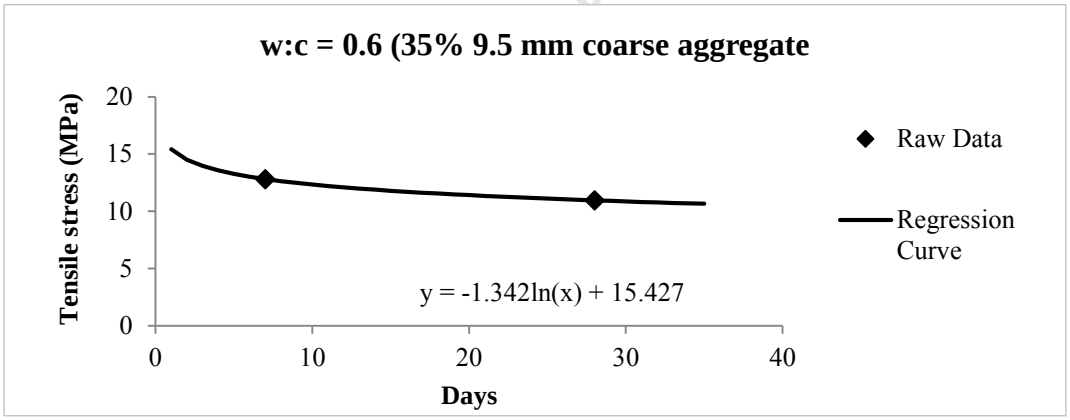
w:c = 0.6 (35% 9.5 mm coarse aggregate
Tensile stress (MPa)
Days
y = -1.342ln(x) + 15.427
Raw Data
Regression Curve

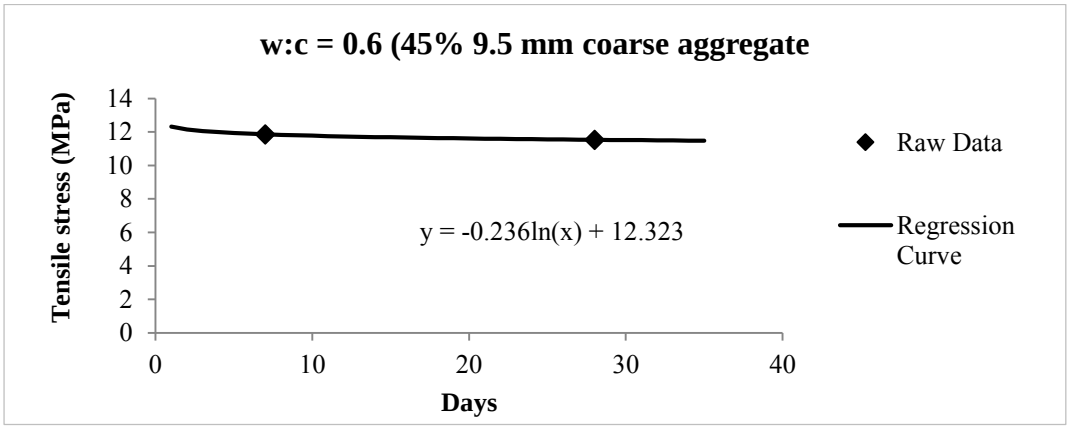
w:c = 0.6 (45% 9.5 mm coarse aggregate
Tensile stress (MPa)
Days
y = -0.236ln(x) + 12.323
Raw Data
Regression Curve

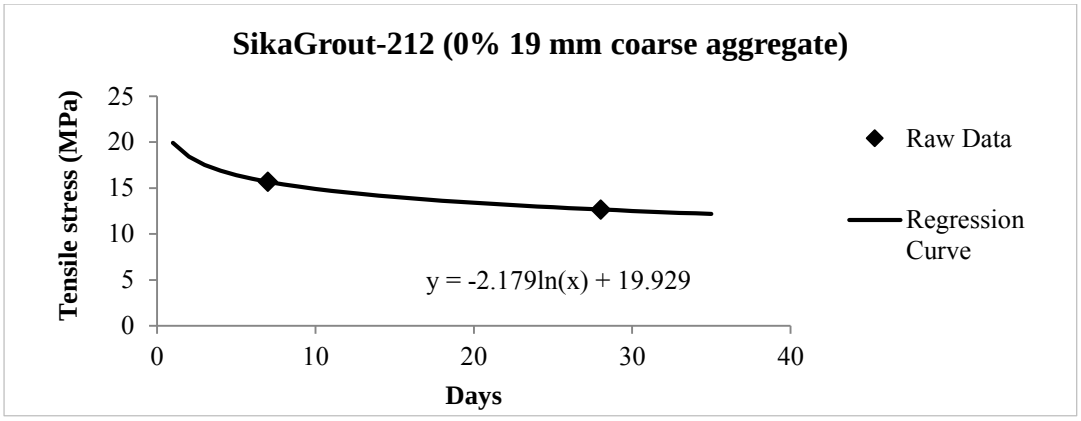

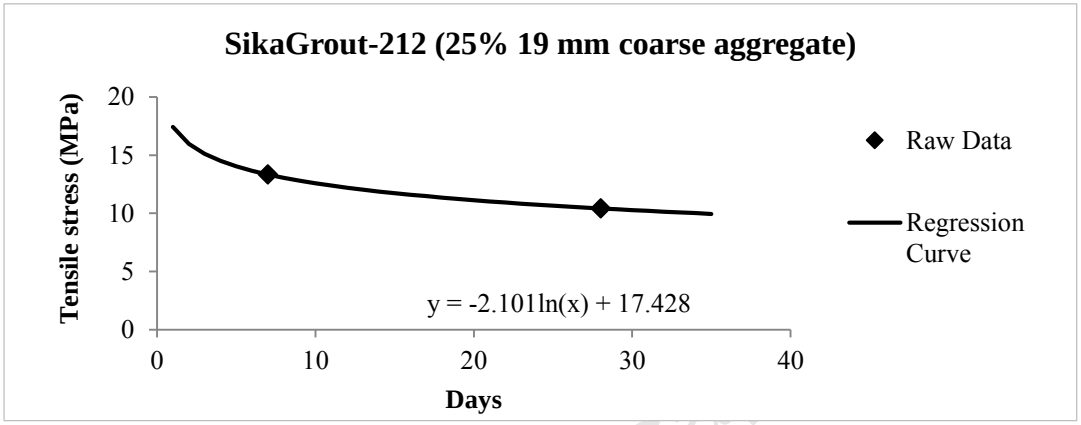

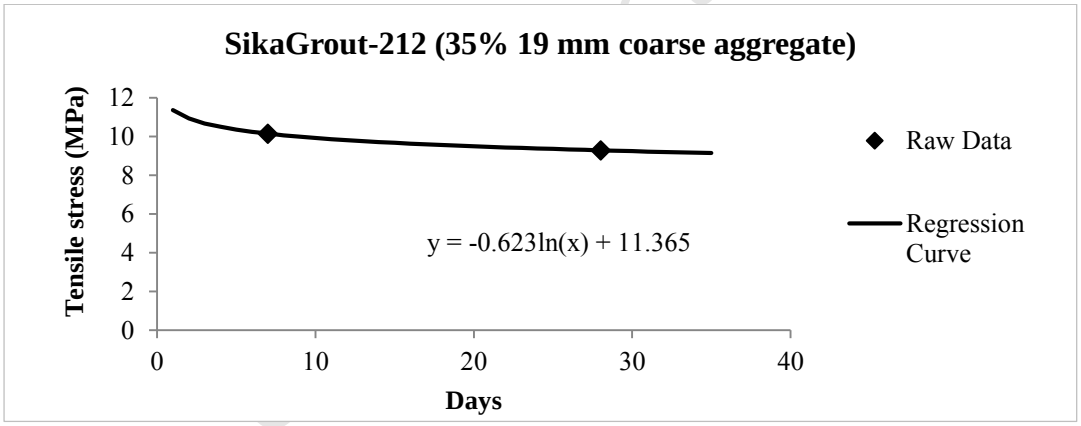

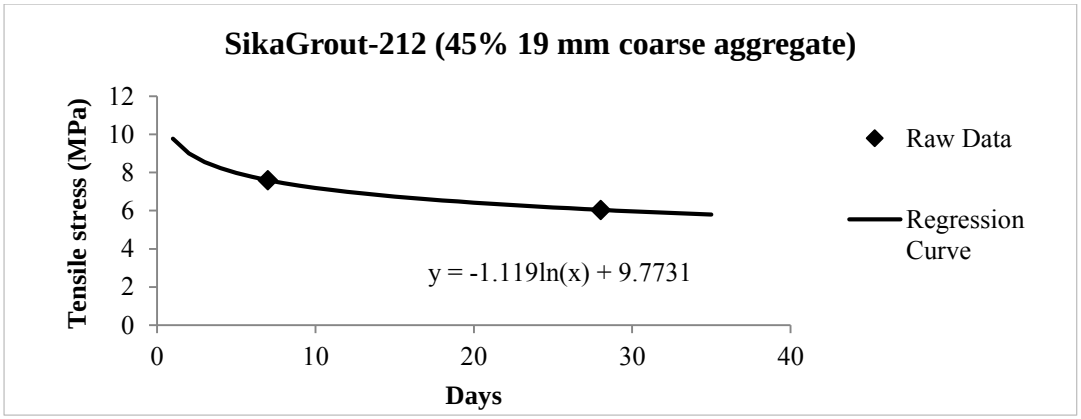

Material property inputs

Table B.1: Material property inputs for w:c = 0.45 laboratory mix (0% 19 mm coarse aggregate content)

Period (days)	Change in restrained shrinkage strain	Mean elastic modulus (GPa)	Tensile strength (MPa)	Relaxation function	Elastic stress (MPa)	Remaining stress (MPa)
Curing (0 to 7)	0	27.6	2.6	0.79	0	0
7 to 8	17.0	29.0	2.7	0.79	0.5	0.4
8 to 9	21.0	30.3	2.7	0.80	1.1	0.9
9 to 10	11.0	31.4	2.7	0.80	1.5	1.2
10 to 11	15.0	32.4	2.8	0.81	2.0	1.6
11 to 12	14.0	33.3	2.8	0.81	2.4	2.0
12 to 13	7.2	34.1	2.8	0.81	2.7	2.2
13 to 14	6.8	34.8	2.9	0.82	2.9	2.4
14 to 15	11.0	35.5	2.9	0.82	3.3	2.7
15 to 16	11.0	36.2	2.9	0.82	3.7	3.0
16 to 17	13.2	36.8	3.0	0.82	4.2	3.4
17 to 18	12.8	37.3	3.0	0.83	4.7	3.8
18 to 19	6.4	37.9	3.0	0.83	4.9	4.1
19 to 20	3.6	38.4	3.0	0.83	5.0	4.2
20 to 21	12.0	38.9	3.0	0.83	5.5	4.6
21 to 22	12.0	39.3	3.1	0.83	6.0	5.0
22 to 23	3.5	39.7	3.1	0.84	6.1	5.1
23 to 24	3.5	40.2	3.1	0.84	6.3	5.2
24 to 25	4.5	40.6	3.1	0.84	6.4	5.4
25 to 26	4.5	40.9	3.1	0.84	6.6	5.6
26 to 27	5.7	41.3	3.1	0.84	6.9	5.8
27 to 28	5.7	41.7	3.1	0.84	7.1	6.0
28 to 29	5.7	42.0	3.2	0.84	7.3	6.2
29 to 30	8.5	42.3	3.2	0.85	7.7	6.5
30 to 31	4.4	42.6	3.2	0.85	7.9	6.7
31 to 32	4.1	43.0	3.2	0.85	8.1	6.8
32 to 33	3.0	43.3	3.2	0.85	8.2	7.0
33 to 34	3.0	43.5	3.2	0.85	8.3	7.1
34 to 35	3.0	43.8	3.2	0.85	8.4	7.2

Table B.2: Material property inputs for w:c = 0.45 laboratory mix (25% 19 mm coarse aggregate content)

Period (days)	Change in restrained shrinkage strain	Mean elastic modulus (GPa)	Tensile strength (MPa)	Relaxation function	Elastic stress (MPa)	Remaining stress (MPa)
Curing (0 to 7)	0	32.4	3.0	0.81	0	0
7 to 8	9.3	33.5	3.0	0.81	0.3	0.2
8 to 9	9.3	34.6	3.0	0.81	0.6	0.5

9 to 10	9.3	35.5	3.1	0.82	0.9	0.8
10 to 11	16.4	36.3	3.1	0.82	1.5	1.2
11 to 12	13.2	37.1	3.1	0.83	2.0	1.6
12 to 13	14.4	37.8	3.2	0.83	2.5	2.1
13 to 14	6.0	38.4	3.2	0.83	2.8	2.3
14 to 15	6.0	39.0	3.2	0.83	3.0	2.5
15 to 16	6.0	39.6	3.2	0.84	3.2	2.7
16 to 17	6.0	40.1	3.3	0.84	3.5	2.9
17 to 18	2.0	40.6	3.3	0.84	3.5	3.0
18 to 19	7.0	41.0	3.3	0.84	3.8	3.2
19 to 20	10.0	41.5	3.3	0.84	4.2	3.6
20 to 21	5.5	41.9	3.3	0.85	4.5	3.8
21 to 22	5.5	42.3	3.3	0.85	4.7	4.0
22 to 23	4.7	42.7	3.4	0.85	4.9	4.1
23 to 24	4.7	43.1	3.4	0.85	5.1	4.3
24 to 25	4.7	43.4	3.4	0.85	5.3	4.5
25 to 26	4.0	43.8	3.4	0.85	5.5	4.7
26 to 27	4.0	44.1	3.4	0.86	5.6	4.8
27 to 28	4.0	44.4	3.4	0.86	5.8	5.0
28 to 29	1.3	44.7	3.4	0.86	5.9	5.0
29 to 30	1.3	45.0	3.4	0.86	5.9	5.1
30 to 31	1.3	45.3	3.5	0.86	6.0	5.2
31 to 32	4.0	45.6	3.5	0.86	6.2	5.3
32 to 33	4.0	45.8	3.5	0.86	6.4	5.5
33 to 34	4.0	46.1	3.5	0.86	6.5	5.6
34 to 35	2.4	46.4	3.5	0.86	6.7	5.7

Table B.3: Material property inputs for w:c = 0.45 laboratory mix (35% 19 mm coarse aggregate content)

Period (days)	Change in restrained shrinkage strain	Mean elastic modulus (GPa)	Tensile strength (MPa)	Relaxation function	Elastic stress (MPa)	Remaining stress (MPa)
Curing (0 to 7)	0	35.0	2.5	0.84	0	0
7 to 8	13.0	36.2	2.6	0.84	0.5	0.4
8 to 9	15.0	37.2	2.7	0.85	1.0	0.8
9 to 10	12.0	38.1	2.8	0.85	1.4	1.2
10 to 11	12.0	39.0	2.8	0.85	1.9	1.6
11 to 12	12.0	39.7	2.9	0.86	2.4	2.0
12 to 13	12.0	40.4	2.9	0.86	2.8	2.4
13 to 14	5.0	41.1	3.0	0.86	3.0	2.6
14 to 15	11.0	41.7	3.0	0.87	3.5	3.0
15 to 16	5.6	42.3	3.1	0.87	3.7	3.2
16 to 17	5.6	42.8	3.1	0.87	4.0	3.4
17 to 18	3.9	43.3	3.1	0.87	4.1	3.6

18 to 19	3.9	43.8	3.2	0.87	4.3	3.8
19 to 20	6.0	44.2	3.2	0.88	4.6	4.0
20 to 21	5.0	44.6	3.2	0.88	4.8	4.2
21 to 22	6.5	45.1	3.3	0.88	5.1	4.5
22 to 23	6.5	45.4	3.3	0.88	5.4	4.7
23 to 24	4.0	45.8	3.3	0.88	5.6	4.9
24 to 25	4.0	46.2	3.3	0.88	5.7	5.1
25 to 26	2.2	46.5	3.4	0.89	5.8	5.2
26 to 27	2.2	46.8	3.4	0.89	5.9	5.3
27 to 28	2.2	47.2	3.4	0.89	6.0	5.4
28 to 29	2.2	47.5	3.4	0.89	6.1	5.5
29 to 30	2.2	47.8	3.4	0.89	6.3	5.6
30 to 31	2.2	48.1	3.5	0.89	6.4	5.7
31 to 32	2.4	48.3	3.5	0.89	6.5	5.8
32 to 33	2.4	48.6	3.5	0.90	6.6	5.9
33 to 34	2.4	48.9	3.5	0.90	6.7	6.0
34 to 35	2.4	49.1	3.5	0.90	6.8	6.1

Table B.4: Material property inputs for w:c = 0.45 laboratory mix (45% 19 mm coarse aggregate content)

Period (days)	Change in restrained shrinkage strain	Mean elastic modulus (GPa)	Tensile strength (MPa)	Relaxation function	Elastic stress (MPa)	Remaining stress (MPa)
Curing (0 to 7)	0	38.0	3.1	0.87	0	0
7 to 8	16.2	39.0	3.1	0.88	0.6	0.5
8 to 9	16.2	39.9	3.1	0.88	1.2	1.1
9 to 10	3.6	40.7	3.1	0.88	1.4	1.2
10 to 11	13.0	41.4	3.1	0.88	1.9	1.7
11 to 12	7.4	42.0	3.1	0.88	2.2	2.0
12 to 13	10.8	42.6	3.1	0.89	2.7	2.4
13 to 14	10.8	43.2	3.2	0.89	3.1	2.8
14 to 15	4.8	43.7	3.2	0.89	3.3	3.0
15 to 16	9.2	44.2	3.2	0.89	3.8	3.3
16 to 17	4.0	44.7	3.2	0.89	3.9	3.5
17 to 18	1.5	45.1	3.2	0.89	4.0	3.6
18 to 19	1.5	45.5	3.2	0.89	4.1	3.6
19 to 20	4.5	45.9	3.2	0.89	4.3	3.8
20 to 21	4.5	46.2	3.2	0.90	4.5	4.0
21 to 22	5.0	46.6	3.2	0.90	4.7	4.2
22 to 23	3.0	46.9	3.2	0.90	4.8	4.3
23 to 24	5.0	47.2	3.2	0.90	5.1	4.6
24 to 25	5.0	47.6	3.2	0.90	5.3	4.8
25 to 26	3.0	47.8	3.2	0.90	5.5	4.9
26 to 27	3.0	48.1	3.3	0.90	5.6	5.0

27 to 28	3.6	48.4	3.3	0.90	5.8	5.2
28 to 29	3.6	48.7	3.3	0.90	5.9	5.4
29 to 30	3.6	48.9	3.3	0.90	6.1	5.5
30 to 31	3.6	49.2	3.3	0.90	6.3	5.7
31 to 32	3.6	49.4	3.3	0.90	6.5	5.8
32 to 33	3.6	49.6	3.3	0.90	6.6	6.0
33 to 34	3.6	49.9	3.3	0.90	6.8	6.2
34 to 35	3.6	50.1	3.3	0.91	7.0	6.3

Table B.5: Material property inputs for w:c = 0.6 laboratory mix (0% 19 mm coarse aggregate content)

Period (days)	Change in restrained shrinkage strain	Mean elastic modulus (GPa)	Tensile strength (MPa)	Relaxation function	Elastic stress (MPa)	Remaining stress (MPa)
Curing (0 to 7)	0	21.5	2.2	0.78	0	0
7 to 8	14.0	22.2	2.2	0.78	0.3	0.2
8 to 9	25.0	22.9	2.3	0.79	0.9	0.7
9 to 10	15.6	23.5	2.3	0.79	1.2	1.0
10 to 11	25.4	24.1	2.4	0.79	1.8	1.4
11 to 12	10.0	24.6	2.4	0.79	2.1	1.6
12 to 13	6.0	25.0	2.5	0.80	2.2	1.7
13 to 14	11.0	25.4	2.5	0.80	2.5	2.0
14 to 15	8.0	25.8	2.5	0.80	2.7	2.1
15 to 16	5.0	26.2	2.5	0.80	2.8	2.3
16 to 17	6.0	26.5	2.6	0.81	3.0	2.4
17 to 18	6.0	26.9	2.6	0.81	3.1	2.5
18 to 19	6.5	27.2	2.6	0.81	3.3	2.7
19 to 20	6.5	27.5	2.6	0.81	3.5	2.8
20 to 21	11.0	27.7	2.7	0.81	3.8	3.1
21 to 22	6.0	28.0	2.7	0.81	3.9	3.2
22 to 23	6.0	28.3	2.7	0.82	4.1	3.3
23 to 24	6.0	28.5	2.7	0.82	4.3	3.5
24 to 25	6.5	28.7	2.8	0.82	4.5	3.6
25 to 26	6.5	29.0	2.8	0.82	4.7	3.8
26 to 27	4.0	29.2	2.8	0.82	4.8	3.9
27 to 28	4.0	29.4	2.8	0.82	4.9	4.0
28 to 29	6.0	29.6	2.8	0.82	5.1	4.2
29 to 30	6.0	29.8	2.8	0.82	5.2	4.3
30 to 31	3.7	30.0	2.9	0.82	5.3	4.4
31 to 32	4.3	30.1	2.9	0.83	5.5	4.5
32 to 33	4.3	30.3	2.9	0.83	5.6	4.6
33 to 34	4.3	30.5	2.9	0.83	5.7	4.7
34 to 35	4.3	30.6	2.9	0.83	5.9	4.9

Table B.6: Material property inputs for w:c = 0.6 laboratory mix (25% 19 mm coarse aggregate content)

Period (days)	Change in restrained shrinkage strain	Mean elastic modulus (GPa)	Tensile strength (MPa)	Relaxation function	Elastic stress (MPa)	Remaining stress (MPa)
Curing (0 to 7)	0	25.4	2.7	0.79	0	0
7 to 8	15.5	26.3	2.7	0.80	0.4	0.3
8 to 9	15.5	27.0	2.7	0.80	0.8	0.6
9 to 10	10.0	27.6	2.8	0.80	1.1	0.9
10 to 11	8.0	28.2	2.8	0.81	1.3	1.0
11 to 12	12.0	28.8	2.8	0.81	1.6	1.3
12 to 13	11.0	29.3	2.8	0.81	1.9	1.6
13 to 14	7.0	29.7	2.8	0.81	2.2	1.7
14 to 15	8.0	30.1	2.8	0.82	2.4	1.9
15 to 16	6.0	30.5	2.8	0.82	2.6	2.1
16 to 17	4.2	30.9	2.9	0.82	2.7	2.2
17 to 18	4.2	31.3	2.9	0.82	2.8	2.3
18 to 19	4.2	31.6	2.9	0.82	3.0	2.4
19 to 20	4.2	31.9	2.9	0.82	3.1	2.5
20 to 21	4.2	32.2	2.9	0.82	3.2	2.7
21 to 22	4.2	32.5	2.9	0.83	3.4	2.8
22 to 23	4.2	32.8	2.9	0.83	3.5	2.9
23 to 24	4.2	33.0	2.9	0.83	3.6	3.0
24 to 25	4.2	33.3	2.9	0.83	3.8	3.1
25 to 26	2.0	33.5	2.9	0.83	3.8	3.2
26 to 27	2.0	33.8	2.9	0.83	3.9	3.3
27 to 28	2.0	34.0	3.0	0.83	4.0	3.3
28 to 29	6.0	34.2	3.0	0.83	4.2	3.5
29 to 30	6.0	34.4	3.0	0.83	4.4	3.7
30 to 31	7.0	34.6	3.0	0.84	4.6	3.9
31 to 32	7.0	34.8	3.0	0.84	4.9	4.1
32 to 33	1.5	35.0	3.0	0.84	4.9	4.1
33 to 34	1.5	35.2	3.0	0.84	5.0	4.2
34 to 35	2.5	35.4	3.0	0.84	5.1	4.2

Table B.7: Material property inputs for w:c = 0.6 laboratory mix (35% 19 mm coarse aggregate content)

Period (days)	Change in restrained shrinkage strain	Mean elastic modulus (GPa)	Tensile strength (MPa)	Relaxation function	Elastic stress (MPa)	Remaining stress (MPa)
Curing (0 to 7)	0	29.0	2.6	0.83	0	0
7 to 8	17.0	29.8	2.6	0.83	0.5	0.4
8 to 9	5.0	30.5	2.6	0.83	0.6	0.5
9 to 10	14.0	31.2	2.6	0.83	1.1	0.9
10 to 11	7.0	31.8	2.6	0.83	1.3	1.1

11 to 12	8.0	32.3	2.6	0.83	1.5	1.3
12 to 13	7.8	32.8	2.6	0.83	1.8	1.5
13 to 14	4.2	33.2	2.6	0.83	1.9	1.6
14 to 15	5.0	33.6	2.6	0.84	2.1	1.7
15 to 16	6.0	34.0	2.6	0.84	2.3	1.9
16 to 17	7.0	34.4	2.6	0.84	2.5	2.1
17 to 18	10.0	34.7	2.6	0.84	2.9	2.4
18 to 19	4.3	35.0	2.6	0.84	3.0	2.5
19 to 20	4.2	35.3	2.7	0.84	3.2	2.7
20 to 21	4.3	35.6	2.7	0.84	3.3	2.8
21 to 22	4.3	35.9	2.7	0.84	3.5	2.9
22 to 23	2.0	36.2	2.7	0.84	3.6	3.0
23 to 24	2.0	36.4	2.7	0.84	3.6	3.0
24 to 25	6.0	36.7	2.7	0.84	3.8	3.2
25 to 26	6.0	36.9	2.7	0.84	4.1	3.4
26 to 27	3.5	37.2	2.7	0.84	4.2	3.5
27 to 28	3.5	37.4	2.7	0.84	4.3	3.6
28 to 29	4.3	37.6	2.7	0.84	4.5	3.8
29 to 30	4.3	37.8	2.7	0.84	4.6	3.9
30 to 31	4.3	38.0	2.7	0.84	4.8	4.1
31 to 32	4.2	38.2	2.7	0.84	5.0	4.2
32 to 33	4.2	38.4	2.7	0.85	5.1	4.3
33 to 34	4.2	38.5	2.7	0.85	5.3	4.5
34 to 35	4.2	38.7	2.7	0.85	5.5	4.6

Table B.8: Material property inputs for w:c = 0.6 laboratory mix (45% 19 mm coarse aggregate content)

Period (days)	Change in restrained shrinkage strain	Mean elastic modulus (GPa)	Tensile strength (MPa)	Relaxation function	Elastic stress (MPa)	Remaining stress (MPa)
Curing (0 to 7)	0	32.5	3.3	0.84	0	0
7 to 8	16.0	33.1	3.3	0.84	0.5	0.4
8 to 9	17.0	33.7	3.3	0.84	1.1	0.9
9 to 10	14.0	34.2	3.3	0.84	1.6	1.3
10 to 11	9.0	34.7	3.3	0.85	1.9	1.6
11 to 12	5.0	35.1	3.3	0.85	2.0	1.7
12 to 13	7.0	35.5	3.3	0.85	2.3	1.9
13 to 14	6.0	35.8	3.3	0.85	2.5	2.1
14 to 15	11.0	36.2	3.3	0.85	2.9	2.5
15 to 16	4.0	36.5	3.3	0.86	3.0	2.6
16 to 17	4.0	36.8	3.3	0.86	3.2	2.7
17 to 18	7.0	37.0	3.3	0.86	3.4	2.9
18 to 19	5.0	37.3	3.3	0.86	3.6	3.1
19 to 20	12.0	37.5	3.3	0.86	4.1	3.5

20 to 21	5.5	37.8	3.3	0.86	4.3	3.7
21 to 22	5.5	38.0	3.3	0.86	4.5	3.9
22 to 23	3.0	38.2	3.3	0.86	4.6	4.0
23 to 24	3.0	38.4	3.3	0.86	4.7	4.1
24 to 25	3.0	38.6	3.3	0.87	4.8	4.2
25 to 26	3.0	38.8	3.3	0.87	4.9	4.3
26 to 27	1.5	39.0	3.3	0.87	5.0	4.3
27 to 28	1.5	39.2	3.3	0.87	5.1	4.4
28 to 29	3.5	39.3	3.3	0.87	5.2	4.5
29 to 30	3.5	39.5	3.3	0.87	5.3	4.6
30 to 31	1.7	39.7	3.3	0.87	5.4	4.7
31 to 32	1.7	39.8	3.3	0.87	5.5	4.8
32 to 33	1.7	40.0	3.4	0.87	5.5	4.8
33 to 34	1.7	40.1	3.4	0.87	5.6	4.9
34 to 35	1.7	40.2	3.4	0.87	5.7	4.9

Table B.9: Material property inputs for w:c = 0.6 laboratory mix (0% 9.5 mm coarse aggregate content)

Period (days)	Change in restrained shrinkage strain	Mean elastic modulus (GPa)	Tensile strength (MPa)	Relaxation function	Elastic stress (MPa)	Remaining stress (MPa)
Curing (0 to 7)	0	21.5	2.2	0.78	0	0
7 to 8	14.0	22.2	2.2	0.78	0.3	0.2
8 to 9	25.0	22.9	2.3	0.79	0.9	0.7
9 to 10	15.6	23.5	2.3	0.79	1.2	1.0
10 to 11	25.4	24.1	2.4	0.79	1.8	1.4
11 to 12	10.0	24.6	2.4	0.79	2.1	1.6
12 to 13	6.0	25.0	2.5	0.80	2.2	1.7
13 to 14	11.0	25.4	2.5	0.80	2.5	2.0
14 to 15	8.0	25.8	2.5	0.80	2.7	2.1
15 to 16	5.0	26.2	2.5	0.80	2.8	2.3
16 to 17	6.0	26.5	2.6	0.81	3.0	2.4
17 to 18	6.0	26.9	2.6	0.81	3.1	2.5
18 to 19	6.5	27.2	2.6	0.81	3.3	2.7
19 to 20	6.5	27.5	2.6	0.81	3.5	2.8
20 to 21	11.0	27.7	2.7	0.81	3.8	3.1
21 to 22	6.0	28.0	2.7	0.81	3.9	3.2
22 to 23	6.0	28.3	2.7	0.82	4.1	3.3
23 to 24	6.0	28.5	2.7	0.82	4.3	3.5
24 to 25	6.5	28.7	2.8	0.82	4.5	3.6
25 to 26	6.5	29.0	2.8	0.82	4.7	3.8
26 to 27	4.0	29.2	2.8	0.82	4.8	3.9
27 to 28	4.0	29.4	2.8	0.82	4.9	4.0
28 to 29	6.0	29.6	2.8	0.82	5.1	4.2

29 to 30	6.0	29.8	2.8	0.82	5.2	4.3
30 to 31	3.7	30.0	2.9	0.82	5.3	4.4
31 to 32	4.3	30.1	2.9	0.83	5.5	4.5
32 to 33	4.3	30.3	2.9	0.83	5.6	4.6
33 to 34	4.3	30.5	2.9	0.83	5.7	4.7
34 to 35	4.3	30.6	2.9	0.83	5.9	4.9

Table B.10: Material property inputs for w:c = 0.6 laboratory mix (25% 9.5 mm coarse aggregate content)

Period (days)	Change in restrained shrinkage strain	Mean elastic modulus (GPa)	Tensile strength (MPa)	Relaxation function	Elastic stress (MPa)	Remaining stress (MPa)
Curing (0 to 7)	0	21.3	2.5	0.86	0	0
7 to 8	15.0	21.9	2.6	0.86	0.3	0.3
8 to 9	15.0	22.4	2.7	0.86	0.6	0.6
9 to 10	19.0	22.8	2.8	0.86	1.1	0.9
10 to 11	16.0	23.2	2.8	0.86	1.4	1.2
11 to 12	10.0	23.6	2.9	0.87	1.7	1.4
12 to 13	10.0	23.9	3.0	0.87	1.9	1.6
13 to 14	5.0	24.2	3.0	0.87	2.0	1.8
14 to 15	5.0	24.5	3.1	0.87	2.1	1.9
15 to 16	9.0	24.8	3.1	0.87	2.4	2.1
16 to 17	7.5	25.1	3.2	0.87	2.6	2.2
17 to 18	7.5	25.3	3.2	0.87	2.7	2.4
18 to 19	7.0	25.5	3.3	0.87	2.9	2.5
19 to 20	7.0	25.7	3.3	0.87	3.1	2.7
20 to 21	6.7	25.9	3.3	0.87	3.3	2.9
21 to 22	6.7	26.1	3.4	0.88	3.4	3.0
22 to 23	6.7	26.3	3.4	0.88	3.6	3.2
23 to 24	5.5	26.5	3.4	0.88	3.8	3.3
24 to 25	5.5	26.7	3.5	0.88	3.9	3.4
25 to 26	5.5	26.8	3.5	0.88	4.1	3.6
26 to 27	5.5	27.0	3.5	0.88	4.2	3.7
27 to 28	5.5	27.2	3.6	0.88	4.3	3.8
28 to 29	5.5	27.3	3.6	0.88	4.5	4.0
29 to 30	5.5	27.5	3.6	0.88	4.6	4.1
30 to 31	5.5	27.6	3.6	0.88	4.8	4.2
31 to 32	6.2	27.7	3.7	0.88	5.0	4.4
32 to 33	6.2	27.9	3.7	0.88	5.1	4.5
33 to 34	6.2	28.0	3.7	0.88	5.3	4.7
34 to 35	6.2	28.1	3.7	0.88	5.5	4.8

Table B.11: Material property inputs for w:c = 0.6 laboratory mix (35% 9.5 mm coarse aggregate content)

Period (days)	Change in restrained shrinkage strain	Mean elastic modulus (GPa)	Tensile strength (MPa)	Relaxation function	Elastic stress (MPa)	Remaining stress (MPa)
Curing (0 to 7)	0	24.2	2.8	0.87	0	0
7 to 8	20.0	24.7	2.9	0.87	0.5	0.4
8 to 9	9.0	25.1	3.0	0.88	0.7	0.6
9 to 10	9.5	25.5	3.1	0.88	0.9	0.8
10 to 11	9.5	25.9	3.1	0.88	1.2	1.0
11 to 12	13.0	26.2	3.2	0.88	1.5	1.3
12 to 13	11.0	26.5	3.3	0.88	1.8	1.6
13 to 14	6.5	26.8	3.3	0.88	2.0	1.7
14 to 15	6.5	27.0	3.4	0.88	2.2	1.9
15 to 16	4.0	27.3	3.4	0.88	2.3	2.0
16 to 17	4.0	27.5	3.4	0.88	2.4	2.1
17 to 18	7.0	27.7	3.5	0.88	2.6	2.3
18 to 19	5.0	27.9	3.5	0.89	2.7	2.4
19 to 20	5.0	28.1	3.6	0.89	2.8	2.5
20 to 21	7.0	28.3	3.6	0.89	3.0	2.7
21 to 22	7.0	28.4	3.6	0.89	3.2	2.9
22 to 23	4.0	28.6	3.7	0.89	3.4	3.0
23 to 24	4.0	28.8	3.7	0.89	3.5	3.1
24 to 25	4.0	28.9	3.7	0.89	3.6	3.2
25 to 26	1.3	29.1	3.8	0.89	3.6	3.2
26 to 27	1.2	29.2	3.8	0.89	3.7	3.3
27 to 28	1.3	29.3	3.8	0.89	3.7	3.3
28 to 29	1.3	29.5	3.8	0.89	3.7	3.3
29 to 30	5.7	29.6	3.9	0.89	3.9	3.5
30 to 31	5.8	29.7	3.9	0.89	4.1	3.6
31 to 32	5.7	29.8	3.9	0.89	4.2	3.8
32 to 33	5.7	29.9	3.9	0.89	4.4	3.9
33 to 34	4.7	30.0	3.9	0.89	4.6	4.1
34 to 35	4.7	30.2	4.0	0.89	4.7	4.2

Table B.12: Material property inputs for w:c = 0.6 laboratory mix (45% 9.5 mm coarse aggregate content)

Period (days)	Change in restrained shrinkage strain	Mean elastic modulus (GPa)	Tensile strength (MPa)	Relaxation function	Elastic stress (MPa)	Remaining stress (MPa)
Curing (0 to 7)	0	27.7	3.3	0.88	0	0
7 to 8	21.0	28.1	3.4	0.88	0.6	0.5
8 to 9	17.0	28.5	3.5	0.88	1.1	0.9
9 to 10	6.0	28.9	3.6	0.88	1.2	1.1
10 to 11	8.0	29.2	3.7	0.88	1.5	1.3

11 to 12	8.5	29.5	3.7	0.88	1.7	1.5
12 to 13	8.5	29.8	3.8	0.88	2.0	1.7
13 to 14	14.0	30.0	3.9	0.88	2.4	2.1
14 to 15	7.0	30.3	3.9	0.88	2.6	2.3
15 to 16	5.3	30.5	4.0	0.88	2.7	2.4
16 to 17	5.3	30.7	4.0	0.88	2.9	2.6
17 to 18	5.3	30.9	4.1	0.88	3.1	2.7
18 to 19	5.3	31.0	4.1	0.88	3.2	2.9
19 to 20	1.8	31.2	4.1	0.88	3.3	2.9
20 to 21	4.1	31.4	4.2	0.88	3.4	3.0
21 to 22	4.1	31.5	4.2	0.88	3.5	3.1
22 to 23	5.5	31.7	4.3	0.88	3.7	3.3
23 to 24	5.5	31.8	4.3	0.88	3.9	3.4
24 to 25	3.0	32.0	4.3	0.88	4.0	3.5
25 to 26	3.0	32.1	4.4	0.88	4.1	3.6
26 to 27	3.0	32.2	4.4	0.88	4.2	3.7
27 to 28	4.8	32.3	4.4	0.88	4.3	3.8
28 to 29	4.8	32.5	4.4	0.88	4.5	4.0
29 to 30	4.8	32.6	4.5	0.88	4.6	4.1
30 to 31	4.8	32.7	4.5	0.88	4.8	4.2
31 to 32	8.0	32.8	4.5	0.88	5.1	4.5
32 to 33	3.0	32.9	4.5	0.89	5.2	4.6
33 to 34	5.5	33.0	4.6	0.89	5.3	4.7
34 to 35	5.5	33.1	4.6	0.89	5.5	4.9

Table B.13: Material property inputs for SikaGrout-212 commercial mix (0% 19 mm coarse aggregate content)

Period (days)	Change in restrained shrinkage strain	Mean elastic modulus (GPa)	Tensile strength (MPa)	Relaxation function	Elastic stress (MPa)	Remaining stress (MPa)
Curing (0 to 7)	0	32.1	3.6	0.84	0	0
7 to 8	38.0	32.6	3.8	0.85	1.2	1.0
8 to 9	35.0	33.0	4.0	0.85	2.4	2.0
9 to 10	22.0	33.4	4.2	0.85	3.1	2.6
10 to 11	10.3	33.7	4.4	0.85	3.4	2.9
11 to 12	10.3	34.0	4.5	0.85	3.8	3.2
12 to 13	10.3	34.3	4.7	0.86	4.1	3.5
13 to 14	10.3	34.6	4.8	0.86	4.5	3.8
14 to 15	22.0	34.8	4.9	0.86	5.2	4.5
15 to 16	10.0	35.1	5.0	0.86	5.6	4.8
16 to 17	9.0	35.3	5.1	0.86	5.9	5.1
17 to 18	5.5	35.5	5.2	0.86	6.1	5.3
18 to 19	5.5	35.7	5.3	0.86	6.3	5.4
19 to 20	12.0	35.9	5.4	0.87	6.7	5.8

20 to 21	12.0	36.0	5.5	0.87	7.2	6.2
21 to 22	12.0	36.2	5.6	0.87	7.6	6.6
22 to 23	3.7	36.4	5.6	0.87	7.7	6.7
23 to 24	3.7	36.5	5.7	0.87	7.8	6.8
24 to 25	3.7	36.7	5.8	0.87	8.0	6.9
25 to 26	7.0	36.8	5.8	0.87	8.2	7.2
26 to 27	5.5	36.9	5.9	0.87	8.4	7.4
27 to 28	5.5	37.1	6.0	0.87	8.6	7.5
28 to 29	5.5	37.2	6.0	0.87	8.8	7.7
29 to 30	5.5	37.3	6.1	0.87	9.1	7.9
30 to 31	0.5	37.4	6.1	0.88	9.1	7.9
31 to 32	0.5	37.5	6.2	0.88	9.1	8.0
32 to 33	0.5	37.6	6.3	0.88	9.1	8.0
33 to 34	0.5	37.7	6.3	0.88	9.1	8.0
34 to 35	0.5	37.8	6.4	0.88	9.1	8.0

Table B.14: Material property inputs for SikaGrout-212 commercial mix (25% 19 mm coarse aggregate content)

Period (days)	Change in restrained shrinkage strain	Mean elastic modulus (GPa)	Tensile strength (MPa)	Relaxation function	Elastic stress (MPa)	Remaining stress (MPa)
Curing (0 to 7)	0	35.9	4.5	0.87	0	0
7 to 8	14.0	36.4	4.5	0.87	0.5	0.4
8 to 9	25.0	36.8	4.6	0.87	1.4	1.2
9 to 10	11.0	37.2	4.6	0.87	1.8	1.6
10 to 11	27.0	37.6	4.7	0.88	2.8	2.5
11 to 12	8.0	37.9	4.7	0.88	3.1	2.7
12 to 13	6.3	38.2	4.8	0.88	3.4	3.0
13 to 14	4.7	38.4	4.8	0.88	3.5	3.1
14 to 15	4.7	38.7	4.8	0.88	3.7	3.3
15 to 16	9.4	38.9	4.9	0.88	4.1	3.6
16 to 17	4.0	39.2	4.9	0.89	4.2	3.7
17 to 18	8.0	39.4	4.9	0.89	4.6	4.0
18 to 19	4.3	39.6	4.9	0.89	4.7	4.2
19 to 20	4.3	39.8	5.0	0.89	4.9	4.3
20 to 21	4.3	39.9	5.0	0.89	5.1	4.5
21 to 22	6.7	40.1	5.0	0.89	5.3	4.7
22 to 23	6.7	40.3	5.0	0.89	5.6	5.0
23 to 24	6.7	40.4	5.0	0.89	5.9	5.2
24 to 25	3.3	40.6	5.1	0.89	6.0	5.4
25 to 26	3.2	40.7	5.1	0.89	6.1	5.5
26 to 27	3.3	40.8	5.1	0.89	6.3	5.6
27 to 28	3.3	41.0	5.1	0.90	6.4	5.7
28 to 29	4.5	41.1	5.1	0.90	6.6	5.9

29 to 30	4.5	41.2	5.1	0.90	6.8	6.1
30 to 31	4.5	41.3	5.2	0.90	7.0	6.2
31 to 32	5.1	41.5	5.2	0.90	7.2	6.4
32 to 33	0.2	41.6	5.2	0.90	7.2	6.4
33 to 34	0.2	41.7	5.2	0.90	7.2	6.5
34 to 35	0.2	41.8	5.2	0.90	7.2	6.5

Table B.15: Material property inputs for SikaGrout-212 commercial mix (35% 19 mm coarse aggregate content)

Period (days)	Change in restrained shrinkage strain	Mean elastic modulus (GPa)	Tensile strength (MPa)	Relaxation function	Elastic stress (MPa)	Remaining stress (MPa)
Curing (0 to 7)	0	38.9	4.5	0.90	0	0
7 to 8	25.8	39.3	4.6	0.90	1.0	0.9
8 to 9	25.8	39.6	4.7	0.90	2.0	1.8
9 to 10	14.2	39.8	4.8	0.90	2.6	2.3
10 to 11	14.2	40.1	4.8	0.90	3.1	2.8
11 to 12	7.7	40.3	4.9	0.90	3.5	3.1
12 to 13	7.7	40.5	4.9	0.90	3.8	3.4
13 to 14	7.7	40.7	5.0	0.90	4.1	3.7
14 to 15	6.0	40.9	5.0	0.90	4.3	3.9
15 to 16	5.0	41.1	5.0	0.90	4.5	4.1
16 to 17	4.5	41.2	5.1	0.90	4.7	4.3
17 to 18	4.5	41.4	5.1	0.90	4.9	4.4
18 to 19	4.5	41.5	5.1	0.90	5.1	4.6
19 to 20	4.5	41.7	5.2	0.91	5.3	4.8
20 to 21	3.0	41.8	5.2	0.91	5.4	4.9
21 to 22	3.0	41.9	5.2	0.91	5.5	5.0
22 to 23	4.8	42.0	5.3	0.91	5.7	5.2
23 to 24	4.2	42.1	5.3	0.91	5.9	5.3
24 to 25	3.0	42.2	5.3	0.91	6.0	5.5
25 to 26	3.6	42.3	5.3	0.91	6.2	5.6
26 to 27	2.7	42.4	5.4	0.91	6.3	5.7
27 to 28	2.7	42.5	5.4	0.91	6.4	5.8
28 to 29	2.8	42.6	5.4	0.91	6.5	5.9
29 to 30	2.8	42.7	5.4	0.91	6.6	6.0
30 to 31	2.7	42.8	5.4	0.91	6.8	6.1
31 to 32	2.7	42.9	5.5	0.91	6.9	6.2
32 to 33	2.7	43.0	5.5	0.91	7.0	6.3
33 to 34	2.7	43.0	5.5	0.91	7.1	6.5
34 to 35	0.8	43.1	5.5	0.91	7.1	6.5

Table B.16: Material property inputs for SikaGrout-212 commercial mix (45% 19 mm coarse aggregate content)

Period (days)	Change in restrained shrinkage strain	Mean elastic modulus (GPa)	Tensile strength (MPa)	Relaxation function	Elastic stress (MPa)	Remaining stress (MPa)
Curing (0 to 7)	0	42.5	4.0	0.92	0	0
7 to 8	30.0	42.8	4.2	0.93	1.3	1.2
8 to 9	16.0	43.0	4.3	0.93	2.0	1.8
9 to 10	12.2	43.2	4.4	0.93	2.5	2.3
10 to 11	12.2	43.4	4.5	0.93	3.0	2.8
11 to 12	12.2	43.5	4.6	0.93	3.5	3.3
12 to 13	12.2	43.7	4.7	0.93	4.1	3.8
13 to 14	6.2	43.8	4.8	0.93	4.3	4.0
14 to 15	4.0	44.0	4.9	0.93	4.5	4.2
15 to 16	5.0	44.1	4.9	0.93	4.7	4.4
16 to 17	5.0	44.2	5.0	0.93	5.0	4.6
17 to 18	6.2	44.3	5.1	0.93	5.2	4.9
18 to 19	4.7	44.4	5.1	0.94	5.4	5.1
19 to 20	4.7	44.5	5.2	0.94	5.6	5.3
20 to 21	4.7	44.6	5.2	0.94	5.9	5.5
21 to 22	4.7	44.7	5.3	0.94	6.1	5.7
22 to 23	1.0	44.8	5.3	0.94	6.1	5.7
23 to 24	1.0	44.9	5.4	0.94	6.2	5.8
24 to 25	3.3	44.9	5.4	0.94	6.3	5.9
25 to 26	3.3	45.0	5.5	0.94	6.5	6.1
26 to 27	3.3	45.1	5.5	0.94	6.6	6.2
27 to 28	3.3	45.2	5.5	0.94	6.8	6.3
28 to 29	3.3	45.2	5.6	0.94	6.9	6.5
29 to 30	3.3	45.3	5.6	0.94	7.1	6.6
30 to 31	2.0	45.3	5.7	0.94	7.1	6.7
31 to 32	2.0	45.4	5.7	0.94	7.2	6.8
32 to 33	2.0	45.5	5.7	0.94	7.3	6.9
33 to 34	2.0	45.5	5.8	0.94	7.4	7.0
34 to 35	2.0	45.6	5.8	0.94	7.5	7.1